DYNAMIC FEATURES OF THE MATURE RETINAL PIGMENT EPITHELIUM

GOLNAZ SHAHABI

Submitted for the degree of Doctor of Philosophy

Institute of Ophthalmology

University College London

2012

Declaration

I declare that this thesis, submitted for the degree of Doctor of Philosophy, is of my own composition, and the data presented herein is my own original work, unless otherwise stated.

A list of collaborations, with details of experiments undertaken in conjunction with others, is provided on the following page.

List of collaborations

(1) Electroretinogram recordings were carried out with the help of Rebecca Longbottom and Magella Neveu.

(2) The in vivo imaging and laser photocoagulation procedures were carried out with the help of Eva Lenassi.

(3) Preparation of the BrdU antibody was carried out with the help of Marcus Fruttiger.

Abstract

The retinal pigment epithelium (RPE) is a monolayer of cells that are vital for visual function and play a key role in the maintenance of the photoreceptors. Within RPE cells are melanin granules which absorb stray light and minimise scatter within the eye, therefore, protecting the RPE from damage. Albinos lack this protective capacity of melanin as a result of mutations of the tyrosinase gene. The first half of this thesis investigates heterogeneity within the RPE in both pigmentation phenotypes. Furthermore, the effect of ageing on the RPE is examined. Immunohistochemistry highlighted the molecular heterogeneity of the RPE and how this varies with pigmentation phenotype. In aged animals, SEM revealed abnormalities occurring within the photoreceptor outer segments of albinos, while ERGs and QRT-PCR illustrated that albinos show the signs of an age-related decline in visual function much sooner than pigmented animals. These studies revealed that in the outer retina, albinism is a progressive disease and not simply a congenital abnormality. The second half of this thesis investigates migration and proliferation of RPE cells in healthy pigmented animals. Using BrdU and DiI it was established that individual RPE cells have the ability to migrate. In addition, the effect of inducing lesions in different retinal locations was studied to determine whether this affects the response of RPE cells to the damaged area. The results conveyed that a single unilateral lesion in the RPE caused an upregulation of proliferating cells not only in the lasered eye, but also the contralateral unlasered eye in a quadrant specific manner. An additional experiment investigated the effect of treating rats with Glatiramer Acetate and found that it elevates levels of cell proliferation in the RPE of treated animals. Together,

the data presented in this thesis demonstrate that the mature RPE is a dynamic heterogeneous epithelial cell layer.

Dedicated to my parents and Lillie …

Acknowledgements

First I would like to thank my wonderful family to whom I cannot even begin to express the extent of my gratitude. My mother, Marjaneh, for without her constant encouragement and belief in me throughout my life I would have never been able to achieve the things that I have. My father, Younes, who from the moment I was born always believed that I would achieve great things. My sister, Lillie, who has been an inspiration and has shown me how one can deal with even the hardest things that life throws at you.

I am especially grateful to my amazing friends who have been my support throughout all the ups and downs that doing a PhD provides. I thank them for listening to me ramble on about my experiments and ideas for the last four years and particularly for the encouragement that they have provided in the last couple of months while I've been writing this thesis.

Finally, I would like to thank my supervisors Glen Jeffery and John Greenwood for their constant support throughout all stages of this project. I am equally grateful to all the staff in the BRU who have always been so helpful whenever I have needed anything, to Matthew Golding for his generous ideas and to Ma'ayan Semo for all the help that she has provided and for waking up at 5am to help me set up an experiment!

Table of Contents

List of Figures

List of Tables

Table 4.3.1: A table showing the number of animals used in the experiments undertaken to investigate RPE cell migration in healthy and lasered rat eyes.

Abbreviations used

Aβ	Amyloid beta
A2E	*N*-retinylidene-*N*-retinylethanolamine
AD	Alzheimer's disease
AMD	Age-related macular degeneration
BrdU	5-bromo-2'-deoxyuridine
bp	Base pairs
CNV	Choroidal neovascularization
CO_2	Carbon dioxide gas
CRALBP	Cellular retinaldehyde binding protein
cSLO	Confocal scanning laser ophthalmoscope
DA	Dark Agouti
DAPI	4',6-diamidino-2-phenylindole
DOPA	Dihydroxyphenylalanine
EAE	Experimental Autoimmune Encephalomyelitis
ECM	Extracellular matrix
EFs	Electric fields
ERG	Electroretinogram
FCS	Fetal calf serum
GA	Glatiramer acetate
i.p.	Intraperitoneal injection
LCA	Leber's congenital amaurosis
MBP	Myelin basic protein
MS	Multiple sclerosis
NTC	No template control

OA	Ocular albinism
OCA	Oculocutaneous albinism
P	Postnatal day
PBS	Phosphate buffer saline
PCNA	Proliferating cell nuclear antigen
PCR	polymerase chain reaction
PDE	Phosphodiesterase
POS	Photoreceptor outer segments
QRT-PCR	Quantitative Real Time PCR
ROS	Reactive oxygen species
RPE	Retinal pigment epithelium
RPE65	Retinal pigment epithelium-specific 65 kDa protein
SAC	Spindle assembly checkpoint
SD	Standard deviation
SD-OCT	Spectral domain optical coherence tomography
SEM	Scanning electron microscope
Th	Tyrosine hydroxylase
ZO-1	Zonula occludens 1

Chapter 1

General Introduction

1.1 The Mammalian Eye

The globe of the eye consists of three coats enclosing the transparent refractive media (Davson, 1990). The outermost coat is made up of the *sclera* and the *cornea*. The white opaque sclera accounts for most of the eye's outer coat, whereas the transparent cornea makes up 16% of it. Both tissues have protective functions in the eye and so consist mainly of collagen fibres which make the tissues rigid and resistant to penetration – this prevents damage to the delicate inner layers. In addition to this, the cornea functions as the eye's principle refractive element (Oyster, 1999).

By comparison, the middle layer is more vascular and consists of the *choroid*, the *iris* and the *ciliary body*. These three structures form the *uveal tract* which is where most of the blood vessels of the eye are located. The iris, which is most accessible to direct inspection, is not a complete layer as it has a hole in its centre, the *pupil*. Light can only enter the posterior portion of the eye through the pupil as the iris is opaque. The iris regulates the amount of light entering the eye by varying the size of the pupil with the use of its two muscles – the sphincter and the dilator. Adjacent to and continuous with the iris is the ciliary body (Oyster 1999). This circular muscle surrounds the anterior portion of the eye inside the sclera, and is responsible for altering the refractive power of the lens. It also contains a set of highly vascular folds on the inner side of the muscular ring – these are the ciliary processes and are the site where the *aqueous humour* forms. The rest of the

uveal tract is made up of the choroid which consists of mainly the blood vessels (including the choriocapillaris – the capillary bed) and dense melanin pigment.

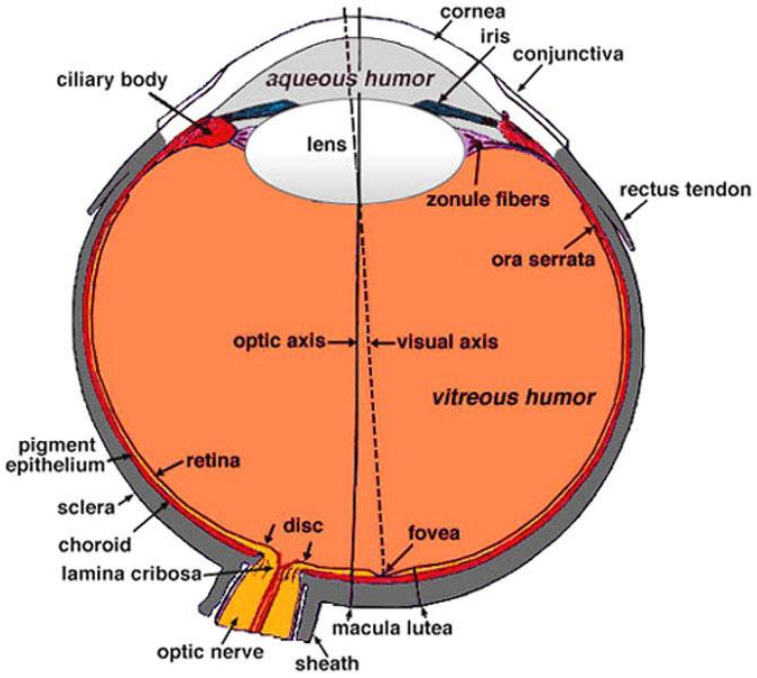

Figure 1.1.1: Sagittal horizontal section of the human eye (from http://webvision.med.utah.edu/imageswv/draweye.jpeg).

Finally, the innermost layer is the *retina*. This is the most complex structure of the eye and it is where the initial processing of an image takes place.

1.2 The Retina

The retina, the light-sensitive part of the eye, is a tissue layer that is responsible for converting light into visual signals that are transmitted to the brain (Mustafi et al., 2009). The retinae of all vertebrates are composed of three layers, consisting of nerve cell bodies, and two layers of synapses (Figure 1.2.1). It consists of five major classes of neurons, these are the:

- Photoreceptors
- Bipolar cells
- Horizontal cells
- Amacrine cells
- Ganglion cells

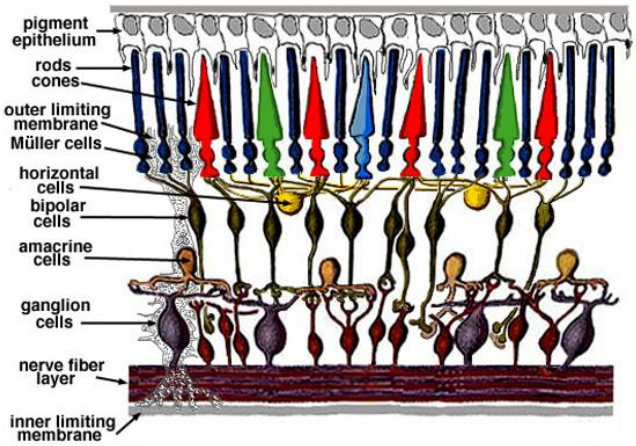

Figure 1.2.1: Simple organisation of the retina (from http://webvision.med.utah.edu/imageswv/schem.jpeg)

The outer most layer, the *outer nuclear layer*, consists of the cell bodies of the photoreceptors – the rods and cones. The *inner nuclear layer* contains the cell bodies of the amacrine, bipolar and horizontal cells, whilst the *ganglion cell layer* is made up of the cell bodies of the ganglion cells as well as displaced amacrine cells. Between these nerve cell layers are two synaptic layers – the *outer plexiform layer*, where the photoreceptors make synaptic connections with the bipolar and horizontal cells and the *inner plexiform*

layer, where the bipolar cells connect to the ganglion cells (Rodieck, 1998). The precise wiring amongst these cells is essential for vision.

Depending on the location within the retina, different cell types are more dominant. Whilst the peripheral retina is rod dominated, the very central retina is cone dominated. Also, the central retina is considerably thicker than the peripheral retina as a result of increased packing density of the photoreceptors, especially the cone photoreceptors, as well as their associated ganglion and bipolar cells (Webvision). The inner nuclear layer is also thicker in the central region of the retina compared to the periphery.

When light enters the eye, it must pass through all the layers of the retina until it reaches the photoreceptors. The transmission of a visual signal through the retina is from the photoreceptors which convert the photons captured from the light into a neural/electrical signal which is then passed to a number of bipolar cells. These signals are relayed from the bipolar cells to the ganglion cells which in turn generate transient responses that are conveyed to the retinorecipient regions of the brain via the optic nerve (Lagnado, 1998). In contrast to the majority of neurons in the brain which generate action potentials, photoreceptors and bipolar cells do not. Instead they produce a graded potential, these are controlled voltage changes that are graded with the intensity of the light (Lagnado, 1998).

The Photoreceptors

In the mammalian retina there are two types of classical photoreceptors present – the rods and the cones. These are distinguished by their shape, retinal distribution, pattern of synaptic connections and the type of photopigment that they contain (Mustafi et al., 2009). In most mammalian species, rods outnumber cones by approximately 20-fold (Mustafi et al., 2009).

There are three types of cone photoreceptors present in man and primates, L, M and S, which are distinguished by the wavelength of light to which they are sensitive, whilst there is only a single type of rod photoreceptor. Rods and cones also differ with their response to light. Rods are very sensitive to light and are adapted to operate in dim light. As a result of this they have low spatial resolution and are required for scotopic vision. In contrast, cones mediate daylight vision. They have a high spatial resolution and are specialised for visual acuity and, therefore, photopic vision. Each rod responds to a single photon of light, whereas, more than a hundred photons are required to generate a similar response in a cone (Mustafi et al., 2009).

Both rods and cones consist of two parts, an outer and inner segment. The nuclei of the cells along with the other cellular organelles required for cell metabolism are contained within the inner segment while the role of the outer segments is to detect a photon signal (Kawamura and Tachibanaki, 2008). The morphology of the outer segments differs

between rods and cones – in rods they are stacks of disc membranes surrounded by a plasma membrane, whilst, in cones the plasma membrane invaginates repeatedly forming a tightly stacked lamellae structure (Figure 1.2.2)

Figure 1.2.2: Interaction between the photoreceptor outer segments and RPE cells. Graphical representation of rod and cone structures by EM images of rod and cone outer segments that display the bands and invaginations of these photoreceptors (Kevany and Palczewki, 2009).

The outer segments are produced from the base of the cilium where membrane evaginations and invaginations occur. The outer segments of the photoreceptors arise from outpouching of the photoreceptor cell plasma membrane (Steinberg et al., 1980). In rods, these expanding membranes become detached as free floating discs inside the outer segment membrane. In cones, however, they remain attached to the membrane (Steinberg et al., 1980). As a result of this, the outer segments become entirely filled with discs of folded double membranes where the light sensitive visual pigment molecules are embedded (Webvision).

These stacks of discs containing the visual pigment molecules are constantly renewed. New discs are added at the base of the outer segment cilium while old discs are displaced up the outer segment and are removed at the tips by the retinal pigment epithelium (RPE) (Steinberg et al., 1977). This phagocytosis of the outer segment discs by the RPE is under circadian control (Marmor and Wolfensberger, 1998).

Visual transduction

The molecular mechanisms of the generation and recovery of a light response are well understood, particularly in rods. In rods, the light sensing molecule is rhodopsin. Once a rhodopsin molecule absorbs a photon of light, it triggers the biochemical cascade that results in photoreceptor activation – phototransduction (Figure 1.2.3). The photoactivated rhodopsin molecule becomes enzymatically active (R*) and activates the G protein, transducin, which in turn activates the effector, phosphodiesterase (PDE). PDE hydrolises cGMP, a diffusible messenger, resulting in a decrease in the levels of cGMP in the cytoplasm of the photoreceptor (Neves and Lagnado, 1999, Kawamura and Tachibanaki, 2008, Yau, 1994). This leads to the closure of the cGMP-gated channels on the plasma membrane prohibiting the inward current flow causing membrane hyperpolarisation which in turn decreases the release of glutamate, the neurotransmitter, from the photoreceptors. Following the cessation of light, the activated components in the phototransduction cascade must be inactivated.

Figure 1.2.3: The second messenger cascade of phototransduction. Light stimulation of rhodopsin in the receptor disks leads to the activation of a G-protein (transducin), which in turn activates a phosphodiesterase (PDE). The phosphodiesterase hydrolyses cGMP, reducing its concentration in the outer segment and leading to the closure of sodium channels in the outer segment membrane (Purves et al., 2001).

1.3 The Retinal Pigment Epithelium

The retinal pigment epithelium (RPE) is a monolayer of cells that are vital for visual function. It has many complex functions and plays a key role in the maintenance of the overlying photoreceptors. These critical functions include the regulation of transepithelial transport, the phagocytosis of the photoreceptor outer segments, the storage and transport of retinoids and protection of the outer retina from light generated reactive oxygen species. These functions are illustrated in the diagram shown below (Figure 1.3.1).

Figure 1.3.1: An illustration showing the functions of the RPE (Strauss, 2005)

Structure of the RPE

The RPE is a hexanocuboidal layer of cells located between the photoreceptors and Bruch's membrane (Boulton, 1991, Hogan et al., 1971). The shape, appearance and size of the cells differ depending on retinal location (Marshall, 1987, Streeten, 1969). In humans, in the macula the cells are small (10-14μm in diameter), however, in the

direction of the periphery, they become flatter and broader (up to 60μm in diameter) (Hogan et al. 1971).

Within each RPE cell there is an abundance of organelles, which reflects the high metabolic rate of the RPE (Boulton and Dayhaw-Barker, 2001). Distributed throughout the cell are the smooth endoplasmic reticulum and lysosomes, while, the numerous mitochondria are found towards the base of the cell (Boulton and Dayhaw-Barker, 2001). Within the apical and midportions of the cell are the melanin granules. These pigment molecules absorb stray light and minimise scatter within the eye (Marmor and Wolfensberger, 1998). This is an important feature for the maintenance of visual function as it helps to protect the RPE from damage. Melanin also acts as a free-radical stabiliser and an antioxidant by binding many toxins. The other pigment found in the RPE is lipofuscin. This accumulates in the RPE throughout life and in older eyes it seems to reach a concentration that is toxic for the RPE.

RPE cells have an apical membrane (facing the photoreceptors) which contains two types of microvilli:

1. Long thin microvilli which cover the majority of the apical surface and increase the surface area of the membrane for transepithelial transport.

2. More specialised microvilli, called photoreceptor sheaths. These extend into the interphotoreceptor matrix in order to reach the photoreceptor outer segments.

The RPE cells near the apical side are all joined by tight junctions which form the outer blood-retinal barrier (Cunha-Vaz, 1976). These tight junctions, zonula occludens, block the free movement of water and ions. RPE cells also have numerous intercellular gap junctions which assist the transport of fluid and metabolites from cell to cell (Stalmans and Himpens, 1997).

Similar to the apical membrane, the basal membrane (facing Bruch's membrane) increases its surface area for the absorption of nutrients and secretion of waste products by containing numerous invaginations, the basal infoldings. This membrane also forms the innermost layer of Bruch's membrane.

1.4 RPE development

The RPE, which derives from the anterior neural plate, shares its origin with the neural retina (Martinez-Morales et al., 2004, Bharti et al., 2006). The correct development of the RPE is vital as it plays an important role during embryogenesis. During this period the RPE influences retinal neurogenesis and ganglion cell projections (Cayouette et al., 2001, Jensen et al., 2001); controls closure of the optic fissure (Chow and Lang, 2001); participates in ciliary body and iris formation (Martinez-Morales et al., 2004) and is implicated in the regulation of choroidal vasculature (Martinez-Morales et al., 2004).

The eyes arise as bilateral evaginations of the diencephalon. Once specified, the optic progenitors begin to evaginate at each side of the forebrain, forming two bulges, known as the optic vesicles (Varga et al., 1999). With the folding of these optic vesicles, the RPE progenitors change their appearance becoming cuboidal and then move to occupy the dorsal aspect of the outer layer of the cup. As morphogenesis continues, the presumptive RPE spreads and completely surrounds the neural retina, therefore, inhabiting the original position of the ventral optic stalk precursors (Figure 1.4.1). As these are now invaginated, it allows for the closure of the ventral fissure (Chow and Lang, 2001).

As the cells that form the early optic vesicle are derived from the same neuroepithelium, the cells are capable of giving rise to any of its subdomains – the cells are all competent to originate RPE, neural retina or optic stalk (Martinez-Morales et al., 2004, Moshiri et al.,

2004). In mammals, this is limited to early development, however, urodeles and anurans, have the capacity to switch their cell fate in the eye late into adulthood (Bharti et al., 2006, Del Rio-Tsonis and Tsonis, 2003).

Figure 1.4.1: Schematic representation of the transition from un-patterned (1) to patterned optic vesicle (2) and to optic cup (3) (Martinez-Morales et al., 2004).

To drive the differentiation of cells in their established direction, exogenous signals coordinate the expression of transcriptional regulators which modify the identity of the cells. The transcription factors that are essential for RPE specification are *Mitf, Otx1/Otx2 and Pax6* (Martinez-Morales et al., 2004).

Microphthalmia-associated transcription factor (Mitf)

Mitf plays a central role in the development of melanin producing cells such as the RPE and the neural crest derived melanocytes (Goding, 2000). Mitf is expressed throughout the development of the RPE and its functional inactivation during this period has been found to impair the development of the presumptive RPE in both mice and quails (Mochii et al., 1998, Nakayama et al., 1998, Nguyen and Arnheiter, 2000). This results in a

hyperproliferating, unpigmented RPE which assumes a neuro-retinal fate and effectively becomes an additional neural retina (Bharti et al., 2006, Martinez-Morales et al., 2004).

Orthodenticle-related transcription factors (Otx1 and Otx2)

Otx1 and Otx2 play a vital role in anterior head formation – in the vertebrate eye, they are initially expressed throughout the entire optic vesicle however, they then become most prominent in the RPE (Martinez-Morales et al., 2003, Martinez-Morales et al., 2001). Interestingly, they are maintained within the RPE throughout adulthood (Bovolenta et al., 1997, Martinez-Morales et al., 2001, Simeone et al., 2002). Whilst the overexpression of Otx2 in retinal cells results in a pigmented phenotype (Martinez-Morales et al., 2003), mice deficient in both Otx1 and Otx2 present with defects in the patterning of their RPE (Martinez-Morales et al., 2001).

It seems that Mitf and Otx2 are not mutually exclusive. They both co-localise in the nuclei of RPE cells where they are involved in the mutual regulation of factors that drive RPE differentiation. Together they activate downstream pigmentation target genes such as *tyrosinase* and *tyrosinase-related protein (Tyrp1)* (Bharti et al., 2006, Martinez-Morales et al., 2004). Until recently the exact mechanism controlling the expression of Otx2 and Mitf was unknown, however, a study now shows that Wnt/β-catenin signalling is necessary for the differentiation of the RPE by directly regulating the expression of these genes (Westenskow et al., 2009).

Although the RPE and neural retina simultaneously differentiate from the neuroectodermal cells of the optic cup, the differentiation of the RPE precedes that of the retina (Streeten, 1969). For this reason the correct development of the RPE is necessary for the proper development of the retina. Many studies have shown the importance of the presence of the RPE during development. First, genetic ablation experiments in mice have shown that ablation of the undifferentiated outer layer of the optic cup causes the entire eye to fail to develop (Raymond and Jackson, 1995). Also, in the adult when the RPE is ablated after differentiation, abnormalities are seen in the retina resulting in severe microphthalmia (very small eyes) (Raymond and Jackson, 1995). Second, interruptions in the melanin biosynthesis pathway result in retinal abnormalities (Strauss, 2005) such as those seen in albino animals. They present with an underdeveloped central retina and abnormal chiasmatic projections (Jeffery, 1997).

1.5 Functions of the RPE

Phagocytosis

Photoreceptors are continually exposed to intense levels of light and oxygen (from the choroid). Both of these cause the production and accumulation of free radicals which leads to an increase in the concentration of light-induced toxic substances within the photoreceptors. To prevent the toxic effects of accumulated photo-oxidative products (Kevany and Palczewski, 2010) and to maintain the excitability of photoreceptors, the photoreceptor outer segments (POS) are constantly shed and renewed. During this daily renewal process, the POS shed approximately 10% of their volume which is subsequently phagocytosed by the adjacent RPE cells (Kevany and Palczewski, 2010). To maintain a constant POS length, roughly the same volume of cellular material is generated basally each day (Kevany and Palczewski, 2010). In humans, each RPE cell on average is adjacent to approximately 45 photoreceptor outer segments (Boulton and Dayhaw-Barker, 2001) and the estimated turnover rate for one entire photoreceptor outer segment is ten days (Strauss, 2005).

This close interaction between the RPE and the retina is crucial for maintaining the structural integrity of photoreceptors and, therefore, for visual function. Not only would a failure of this regulation between the photoreceptors and the RPE result in POS that are of incorrect length (causing conditions such as retinitis pigmentosa, where it appears that the outer segments are shortened), the failure of RPE cells to efficiently dispose of this

material would also result with damaging consequences due to the detrimental effects of POS component build up.

Photoreceptor outer segments contain the highest concentration of free radicals, photo-damaged proteins, and lipids at their tips. It is these tips which are shed and phagocytosed by the RPE. During the phagocytosis of the POS, important molecules such as retinal and docosahexaenoic acid are recycled from the digested POS and redelivered to the photoreceptors in a way which is comparable with the visual cycle (Bok, 1993). The exact substance that permits communication between the POS and the RPE cells has not yet been identified. The molecules involved in the different steps of phagocytosis have, however, been identified (Figure 1.5.1).

Phagocytosis of shed OS occurs in 3 steps:

1. **OS recognition and binding**

   Once a RPE cell recognises a shed POS, it binds to it through a receptor based mechanism. Finnemann et al. (1997) showed that the αvβ5 integrin is required for POS binding to the RPE, although, it does not bind the substrate directly. The milk fat globule-EGF-factor 8 (MFG-E8) was subsequently found to be an essential ligand for αvβ5 during RPE phagocytosis (Kevany and Palczewski, 2010). Another important player in POS recognition and binding is CD36, a scavenger receptor (Ryeom et al., 1996).

2. RPE signalling leading to engulfment and OS internalisation

The binding of the POS to the RPE is not sufficient enough to stimulate phagocytosis – the bound particles must be engulfed and internalised. Once the specific binding of the POS to the RPE has occurred, the receptor tyrosine kinase c-*mer* (MerTK) activates a second messenger cascade that initialises the internalisation of the POS (Feng et al., 2002, Strauss, 2005). MerTK is vital for the ingestion phase as cells lacking MerTK are able to successfully bind to the POS but are unable to ingest them (Feng et al., 2002, Strauss, 2005).

3. Phagosomal degradation of OS

Once internalised, the RPE begins the degradation of the proteins and lipids contained within the POS (Kevany and Palczewski, 2010). The phagosome fuses with a lysosome forming a phagolysosome (Boulton and Dayhaw-Barker, 2001, Kevany and Palczewski, 2010). The ingested POS are then digested by a combination of lysosomal enzymes, the main one being cathepsin D. These are capable of degrading lipids, nucleic acids, proteins and polysaccharides (Boulton and Dayhaw-Barker, 2001). The end products of this process are then recycled or vacated via the choroidal capillaries.

Figure 1.5.1: Photoreceptor phagocytosis components. Components are categorised by their involvement in photoreceptor recognition, engulfment, and degradation separated by their involvement in different stages of the renewal process (adapted from Kevany and Palczewski, 2010).

This daily renewal of POS by phagocytosis is under circadian control (Strauss, 2005) - at the onset of light in the morning, rods tend to shed discs most vigorously, while cones shed their discs more vigorously at the onset of darkness (Marmor and Wolfensberger, 1998). Also, depending on the location within the retina, both the phagocytic load and lysosomal activity varies (Dorey et al., 1989). In humans, lysosomal enzyme activity is highest in the central retina and lowest in the periphery (Boulton et al., 1994). RPE cells in the macula also have a higher ratio of photoreceptors per RPE cell suggesting a higher rate of phagocytosis in the macula (Strauss, 2005).

Retinoid Metabolism and the Visual cycle

The RPE has a fundamental role in the visual/retinoid cycle. The function of this cycle is to regenerate the 11-*cis*-retinal required by photoreceptors for the transduction of light energy into electrical impulses (Baehr et al., 2003). The absorption of light by rhodopsin (Rh) initiates light transduction by changing the conformation of 11-*cis*-retinal into all-*trans*-retinal which in turn forms active rhodopsin (Rh*) (Baehr et al., 2003). The active rhodopsin is able to activate transducin for the next step of the phototransduction cascade (Strauss, 2005) (Figure 1.5.2).

Photoreceptors lack *cis*-*trans* isomerase function, making them unable to convert all-*trans*-retinal into 11-*cis*-retinal. The all-*trans*-retinal in the photoreceptors is, therefore, metabolised into all-*trans*-retinol and translocated to the RPE (Simo et al., 2010, Strauss, 2005) via the interphotoreceptor retinol binding protein (IRBP). Here, the all-*trans*-retinol binds to cellular retinol binding protein (CRBP) initiating an esterification step which is catalysed by lecithin:retinol acyltransferase (LRAT) (Baehr et al., 2003, Strauss, 2005). This ester is converted to 11-*cis*-retinol which undergoes an oxidation step producing 11-*cis*-retinal (Baehr et al., 2003). Cellular retinaldehyde-binding protein aids this reaction (Strauss, 2005). The regenerated 11-*cis*-retinal is transported back to the photoreceptor via the IRBP where it combines with opsin to form rhodopsin, completing the cycle (Simo et al., 2010).

Figure 1.5.2: Diagram of the visual cycle. Absorption of light by rhodopsin (Rh) changes the conformation of 11-cis retinal to all-trans-retinal and activates rhodopsin (Rh*). All-trans-retinol is then transported to the RPE where it is reisomerized into 11-cis-retinal. Following this, 11-cis retinal is transported back to the photoreceptor via an interphotoreceptor matrix-binding protein (IRBP) (www.bumc.bu.edu/www/busm/by/images/carter.jpg).

A vital component of this cycle is RPE65 (retinal pigment epithelium-specific protein 65kDa), which functions as the rate limiting step for the visual cycle (Gollapalli and Rando, 2004). RPE65 can increase or decrease the production of 11-cis-retinal and can, therefore, adapt the visual cycle depending on the different retinoid requirements needed in the light and dark (Gollapalli and Rando, 2004).

Transepithelial Transport

As part of the blood-retina barrier the RPE is responsible for transporting nutrients, ions and water between the photoreceptors and the choriocapillaris (Rizzolo, 1997, Strauss, 2005, Wimmers et al., 2007). For this reason, it has the structural properties of an ion

transporting epithelium where its tight junctions form a barrier between the subretinal space and choriocapillaris (Rizzolo, 1997, Kniesel and Wolburg, 1993, Konari et al., 1995, Ban and Rizzolo, 2000a). The RPE regulates the transportation of ions and water from the subretinal space on the apical side to the blood on the basolateral side, while also transporting nutrients such as glucose or vitamin A, from the blood to the photoreceptors (Wimmers et al., 2007, Strauss, 2005).

Both the apical and basal membranes contain pumps, facilitative transport systems and passive ion channels such as the electrogenic sodium-potassium pump on the apical membrane and the chloride-bicarbonate exchange transporter on the basal membrane. The net effect of these is to move water across the RPE in the apical to basal direction. The retina produces large amounts of water mainly from the large metabolic turnover in neurons and photoreceptors (Strauss, 2005). However, intraocular pressure also causes the movement of water from the vitreous body into the retina (Hamann, 2002). For this reason the continuous removal of water from the retina by the RPE is vital as it establishes an adhesive force between the RPE and the retina (Strauss, 2005). This transport of water is mainly regulated by the transepithelial transport of Cl^- and K^+ (Wimmers et al., 2007, Strauss, 2005). The RPE also regulates the transport of other ions such as Na^+ and HCO_3^- to and from the retina. This is essential for the regulation of pH and the polarisation/hyperpolarisation of cell membranes (Boulton and Dayhaw-Barker, 2001).

Figure 1.5.3: Drawing of an RPE cell showing the major anatomic and physiologic features (Marmor, 1998).

Additionally, metabolites and nutrients such as glucose and vitamin A are transported from the blood to the photoreceptors via the RPE (Strauss, 2005, Wimmers et al., 2007). First, both the apical and the basolateral membranes of the RPE contain a vast amount of glucose transporters (GLUT1 and GLUT3) which allow glucose to be passively transported across both membranes (Harik et al., 1990, Ban and Rizzolo, 2000b). Second, the transport of vitamin A to the photoreceptors is vital for initiating the phototransduction cascade (Baehr et al., 2003). Any alterations in transepithelial transport can result in several pathologies such as macular edema (Marmor, 1999), retinitis pigmentosa, Best's vitelliform macular degeneration (Musarella, 2001) and age-related macular degeneration (Strauss, 2005).

Secretion

The RPE produces and secretes a variety of growth factors as well as factors that are required for the survival of photoreceptors and for maintaining the structural integrity of the choriocapillaris (Simo et al., 2010). These factors include pigment epithelium-derived factor (PEDF) (Cao et al., 1999), fibroblast growth factors (FGF-1, FGF-2, FGF-5) (Bost et al., 1992), vascular endothelial growth factor (VEGF) (Adamis et al., 1993), transforming growth factor-β (TGF-β) (Kvanta, 1994) and insulin-like growth factor-I (IGF-I) (Martin et al., 1992). Recently, additional molecules synthesised in the RPE have been discovered. These include somatostatin, erythropoietin and ApoA1 (Simo et al., 2010).

The two most significant growth factors secreted by the RPE are *PEDF* and *VEGF* (Simo et al., 2010). In the healthy eye, PEDF acts a neuroprotective and antiangiogenic factor in order to help maintain the retinal and choriocapillaris structure (Dawson et al., 1999, King and Suzuma, 2000, Steele et al., 1993). VEGF, on the other hand, is required for the prevention of endothelial cell apoptosis and is vital for an intact choroidal endothelium (Burns and Hartz, 1992). Any changes in the secretory activity of the RPE can lead to various forms of proliferative retinal diseases (Campochiaro, 2000, Frank, 1997, Witmer et al., 2003).

Protection against light and free radicals

The retina is frequently exposed to visible light which is mostly absorbed by the RPE and is surrounded by an oxygen-rich environment (Strauss, 2005, Simo et al., 2010). This, together with the high metabolic activity of the RPE causes the formation of reactive

oxygen species (ROS) which cause oxidative damage to cells by harming proteins, DNA and lipids (Boulton and Dayhaw-Barker, 2001). The phagocytosis of the photoreceptor outer segments also produces large amounts of reactive oxygen species (Miceli et al., 1994). In order to reduce this oxidative damage the RPE has three lines of defence. These are:

First defence: The absorption and filtering of light by pigments in the RPE such as melanin, found throughout the RPE, and the carotenoids which are found only in the macula. Melanin which is found in melanosomes in the RPE is responsible for reducing the levels of light entering the RPE by acting as a neutral filter. The carotenoids, such as lutein and zeaxanthin, however, filter out reactive blue light (Beatty et al., 2000). Blue light seems to be the most damaging to the RPE cells of adult eyes as it enables the photo-oxidation of lipofuscin components into cell toxic substances (Ben-Shabat et al., 2001, Rozanowska et al., 1995, Sparrow and Cai, 2001).

Second defence: The RPE contains antioxidants which reduce the rate of oxidation reactions by neutralising ROS (Simo et al., 2010). This reduces the damage that is caused by ROS to cellular macromolecules (Beatty et al., 2000). There are two types of antioxidants found in the RPE; *enzymatic* and *nonenzymatic* antioxidants. The enzymatic antioxidants are superoxide dismutase and catalase, both of which are found in high concentrations in the RPE (Miceli et al., 1994). The nonenzymatic antioxidants which accumulate in the RPE include ascorbate, α-tocopherol, carotenoids, glutathione and melanin (Beatty et al., 2000).

Third defence: RPE cells are able to repair damaged lipids, DNA and proteins (Strauss, 2005).

Even with these controls some oxidative damage is inevitable. With increasing age, the RPE begins to lose its capability to absorb light which leads to the progression of age related pathologies (Strauss, 2005).

1.6 The Ageing RPE and Retina

Ageing is the 'progressive accumulation of changes with time that are associated with or responsible for the ever-increasing susceptibility to disease and death which accompanies advancing age' (Harman, 1981). The process of ageing in the eye is accompanied by reduced visual performance and an increasing incidence of disorders affecting most tissues in the eye (Marshall, 1987). With increasing age, the RPE undergoes structural changes, loses melanin, accumulates lipofuscin, decreases its antioxidant capacity and progressively accumulates deposits on, or within, the underlying Bruch's membrane (Boulton and Dayhaw-Barker, 2001). These age related changes are thought to contribute to the pathogenesis of AMD, a major cause of blindness in developed countries as well as other pathologies of the eye (Kornzweig et al., 1957, Sarks, 1975).

There is considerable change in the pigmentation of the RPE with age. First, within the RPE, there is an accumulation of lipofuscin with increasing age. Lipofuscin is a lipid/protein aggregate that progressively builds up in RPE cells throughout life and eventually, by 80 years of age (in humans), it occupies up to 19% of the cytoplasmic volume (Boulton and Dayhaw-Barker, 2001). The lipofuscin granules are produced as a by-product from the phagocytosis of the photoreceptor outer segments. After phagocytosis, they are degraded by up to forty enzymes (Shamsi and Boulton, 2001) from the comprehensive lysosomal system present within the cells of the RPE. However, despite this extensive lysosomal

system, undegradable material still accumulates within the lysosomes to form lipofuscin granules (Boulton et al., 2004).

This age-related accumulation of lipofuscin granules appears to be damaging to RPE cell function. First, lipofuscin may have the ability to produce ROS (Boulton *et al.,* 2003). Studies have shown that it is a photoinducible generator of many reactive oxygen species, such as hydrogen peroxide, singlet oxygen and superoxide anion (Sparrow and Boulton, 2005). Second, it causes the inactivation of lysosomes. This leads to an accumulation of non-degradable material and cellular congestion (Shamsi and Boulton, 2001), which ultimately causes cellular dysfunction. Third, it results in the inhibition of antioxidant enzymes, extragranular lipid peroxidation, cytoplasmic vacuolation and membrane blebbing (Sparrow and Boulton, 2005).

A minor constituent of lipofuscin, A2E, also has adverse effects on the RPE cells (Sparrow et al., 2003). A2E is a pyridinium bisretinoid and is found within the chloroform soluble fraction of lipofuscin. Studies using RPE cell cultures have shown that A2E can induce damage to cells of the RPE and cause RPE dysfunction (Boulton et al., 2004). A2E-loaded cells exposed to blue light have the ability to induce apoptosis by generating reactive oxygen species, especially singlet oxygen (Sparrow *et al*. 2003), which can potentially cause DNA damage. Another way in which A2E initiates apoptosis is by releasing cytochrome C and AIF (apoptosis-inducing factor) into the cytoplasm of the cell (Delori et al., 2001).

The exact role of A2E in lipofuscin toxicity is unclear, but A2E has been shown to have the capacity to act like a detergent which can cause lysosomal membrane leakage. This can eventually result in cell death. It has been suggested that the number of lipofuscin granules may in fact be less important than the actual concentration of A2E within each granule (Marmor and Wolfensberger, 1998). A2E may build up throughout life and eventually reach a critical concentration which causes it to leak from the lysosomes (Marmor and Wolfensberger, 1998).

In contrast to lipofuscin and A2E, the melanin content in the RPE decreases with age (Sarna et al., 2003 , Boulton, 1991). RPE melanin is formed during development and there is little turnover afterwards (Weiter et al., 1986). The distribution of melanin granules, therefore, remains constant throughout life. Melanin has an important role as a cellular antioxidant (Sarna et al., 2003) and is also responsible for reducing the levels of light entering the RPE by acting as a neutral filter. The age-related decrease in melanin granules, therefore, results in a decrease in the cells' antioxidant potential as well as increasing the amount of light entering the RPE. Additionally, it appears that whilst melanin granules have a photoprotective role in young eyes, they are highly photoreactive in aged eyes (Boulton and Dayhaw-Barker, 2001), which exacerbates the consequences of melanin loss in terms of oxidative stress. For this reason, experiments carried out in this thesis (Chapters 2 and 3) closely compare the differences between pigmented and albino animals, the latter of which do not contain melanin in their RPE.

A combination of the accumulation of lipofuscin and A2E together with the decrease in melanin leads to increased oxidative stress within these cells, leading to an increased presence of DNA damage with age, resulting in a decline in cellular function, responses and survival (Wang et al., 2008). The important role of the RPE in maintaining retinal integrity suggests that any damage or impairment to these cells would lead to degenerative changes in the retina. With age, there is significant neuronal cell loss in the retina, with rods appearing to be more affected than cones (Curcio et al., 1993). Approximately 50% of all rods are lost between the second and ninth decades from the peripheral retina in humans, while 30% are lost from the central retina (Curcio et al., 1993, Gao and Hollyfield, 1992). Despite the widespread loss of rods in the central retina, the photoreceptor mosaic remains qualitatively normal, as approximately only two rod/mm^2 are lost each day (Curcio et al., 1993). The loss of the rod photoreceptors is preceded by the loss of the cones (Curcio et al., 2000). Other retinal neurones affected by ageing are the ganglion cells and the inter-neurons. In humans, a loss of ganglion cells occurs in the fovea and peripheral retina with age, with approximately 16% of ganglion cells decreasing in the fovea from the second to the sixth decade (Gao and Hollyfield, 1992).

1.7 Albinism

Albinism is a genetic disease that results in a deficiency of melanin pigment in the eyes and often hypopigmentation in the hair and skin (Summers, 1996, Oetting and King, 1999). There are various types of albinism but all are caused as a result of mutations in the genes involved in melanin biosynthesis – in albinism the biosynthesis of melanin is either reduced or absent (Summers, 2009). The number and structure of melanocytes, the cells responsible for pigment formation, however, is normal.

The lack of melanin pigment in albino mammals has many effects on the developing eye. It is associated with abnormal routing of the optic nerves, causing an excessive crossing of the fibres in the optic chiasm as well as foveal hypoplasia (Oetting and King, 1999, Oetting, 2000, Gronskov et al., 2007). This results in several ophthalmic features common to all types of albinism. These include: reduced visual acuity, photosensitivity, strabismus (a squint), iris transillumination and nystagmus (involuntary eye movements). These ocular changes are a direct result of a reduction in melanin in the developing eye and not due to 'a pleiotropic effect of mutations in any specific gene associated with melanin biosynthesis' (Oetting, 2000). This is due to the fact that these changes are seen in all types of albinism, regardless of the genetic mechanism (Jeffery, 1997).

The two main types of albinism are *oculocutaneous albinism* (OCA), affecting the hair, skin and eyes, and *ocular albinism* (OA), which is only limited to the eyes. Mutations in several

different genes are responsible for albinism, however, the most commonly affected genes are the *tyrosinase* and *P* gene. Mutations on these genes causes oculocutaneous albinism type 1 (OCA1) and oculocutaneous albinism type 2 (OCA2), respectively.

Albinism is not targeted towards a particular ethnic group and affects people worldwide. Approximately one in 17 000 people suffer from one of the types of albinism (Gronskov et al., 2007). The prevalence of the type of albinism, however, depends on racial background (Table 1.7.1).

Types of albinism:

Oculocutaneous albinism (OCA)

OCA is inherited in an autosomal recessive manner and is expressed in both females and males (Summers, 2009). There are four different types of OCA:

- *OCA1* (further subdivided into OCA1A and OCA1B)
- *OCA2*
- *OCA3*
- *OCA4*

OCA is characterised by reduced levels of pigmentation in the eyes, skin and hair, however, the clinical spectrum of these differs depending on the type. OCA1A presents as the most severe due to the complete absence of pigmentation throughout life, while the other

forms develop some melanin pigment over time (Gronskov et al., 2007, Summers, 2009). At least four genes are responsible for these different forms of OCA (Table 1.7.1).

Table 1.7.1. The four known types of OCA (fom Gronskov et al., 2007).

Ocular albinism (OA)

There are two types of OA, both of which are characterised by normal to slightly reduced levels of skin pigmentation and a varying degree of ocular hypopigmentation. Autosomal recessive OA occurs in males and females whilst X-linked OA (OA1) occurs only in men (Summers, 1996). The *GPR143* (*OA1*) is the only gene known to be associated with X-linked ocular albinism. This G-protein coupled receptor is expressed only in the RPE and the iris pigment epithelium as well as in the melanocytes of the skin (Schiaffino et al., 1996). The exact function of the GPR143 gene is unclear, however, it may regulate melanin biogenesis through signal transduction from the lumen of the organelle to the cytosol (Riley and Borovansky, 2011).

Other types of albinism that also occur, albeit more infrequently, are *Hermansky-Pudlak Syndrome* and *Chédiak Higashi Syndrome*.

What happens in the melanin biosynthesis pathway to cause albinism?

Melanins are synthesised by a small population of pigment cells, the melanocytes and the retinal pigment epithelium (RPE) (King et al., 1995, Schiaffino, 2010). Melanocytes of the skin, hair and uveal tract derive from the neural crest in embryonic development where they then migrate to several organs and tissues (Kinnear et al., 1985, Summers, 1996). Those in the RPE and iris, however, derive from the neuroectoderm. Melanogenesis occurs early in the RPE and is evident by the fifth week of fetal life (Kinnear et al., 1985). Unlike the melanocytes derived from the neural crest, the neuroectodermally derived melanocytes of the eye do not transfer their pigment to neighbouring cells (Summers, 1996) and do not seem to be capable of resuming melanogenesis after birth (Summers, 1996, Kinnear et al., 1985).

Despite these differences, they are both able to produce melanin pigments from within specialised subcellular organelles, the melanosomes (Schiaffino, 2010, Kinnear et al., 1985). Melanosomes undergo a series of maturation stages. In the early stages they lack pigment (stages I and II), however, they are progressively filled with enzymes and membranous structures (stage III) until eventually the internal structure of the mature organelle becomes completely melanised (stage IV) (Schiaffino, 2010, Marks and Seabra,

2001). Melanogenesis occurs within these matured organelles. Here, tyrosine is converted to either eumelanin (black-brown pigment) or pheomelanin (yellow-red pigment). Tyrosinase is the key enzyme involved and catalyses the rate limiting step – the hydroxylation of tyrosine to dopaquinone (Oetting, 2000, Summers, 1996) (Figure 1.7.1).

Figure 1.7.1: The melanin synthetic pathway and the involvement of melanogenic enzymes. Initial melanin synthesis is catalysed by tyrosinase and is then divided into eumelanogenesis or pheomelanogenesis. The other melanogenic enzymes, that is, I-3,4-dihydroxyphenylalanine (DOPA) chrome tautomerase (DCT) and tyrosinase-related protein 1 (TYRP1), are involved in eumelanogenesis, and no specific enzymes have been found that are involved in pheomelanogenesis so far (Ando et al., 2007).

Any mutations of the tyrosinase gene would result in reduced or absent tyrosinase activity, therefore, preventing synthesis of melanin. The resulting melanosomes would therefore contain either no melanin or a reduced amount of melanin causing oculocutaneous albinism.

The effect of a lack of melanin in retinal development

The developing albino neural retina differs from that of pigmented mammals (Jeffery, 1997, Ilia and Jeffery, 1999, Kralj-Hans et al., 2006). In albino mammals, there is a misrouting of the temporal retinal axons – ganglion cells from the temporal regions which usually remain uncrossed at the optic chiasm, cross the chiasmatic midline resulting in the incorrect innervation of the contralateral hemisphere (Lund, 1965, Stone et al., 1978a). Also, albino mammals present with an underdeveloped central retina (Jeffery et al., 1994a, Stone et al., 1978b). Human albino patients lack a fovea and have an underdeveloped macula (Neveu et al., 2005, Kriss et al., 1992 ,Elschnig, 1913). Individual cell layers of the retina are also affected in a broad range of mammals. The ganglion cell layer is underdeveloped (Jeffery and Kinsella, 1992, Kinnear et al., 1985, Stone et al., 1978b), and the inner and outer nuclear layers are abnormally thin. In the outer nuclear layer this is caused by a deficit in the rod population, where there is a 30% decrease of rods (Jeffery, 1997, Kinnear et al., 1985). Interestingly, the cone population remains unaffected (Jeffery et al., 1994a). This could explain why albino animals with cone dominated retinae, such as birds and squirrels, do not present with the retinal abnormalities present in other albinos (Jeffery and Williams, 1994).

The absence of melanin seems to cause a delay in the pattern of retinal maturation in the albino (Jeffery, 1997). There is a temporal lag in the differentiation of the outer plexiform layer (Jeffery, 1997), as well as delayed cell death in the ganglion cell layer and inner nuclear layer (Webster and Rowe, 1991). The normal centre to periphery gradient of

retinal development also appears to be delayed (Webster and Rowe, 1991). This may explain the difference in cell density in the central retina of the albino as spatio-temporal gradients in cell production are required for the mature gradient in the ganglion cell layer (Jeffery, 1997).

These deficits in the albino visual system are regulated by the tyrosinase gene as the introduction of a functional tyrosinase gene to albino mouse embryos prevents the developmental abnormalities seen in the chiasmatic pathways and retina (Jeffery et al., 1994b). This information raises the question as to which compound in the biosynthesis of melanin disrupts the patterns of retinal neurogenesis?

The DOPA theory

Alongside being a biologically active agent which plays a key role in the synthesis of melanin, I-3,4-dihydroxyphenylalanine (DOPA), is also a regulator of retinal mitosis (Ilia and Jeffery, 1999). This has been shown in studies where the application of DOPA to cultured RPE cells, increases the length of the cell cycle from 19 hours to 27 hours (Akeo et al., 1994).

During development the number of mitotic figures differs greatly between albino and pigmented animals. In rats the number of mitotic figures is much greater in the albino retina and RPE between postconceptional days 14 to 28 (Ilia and Jeffery, 1999, Jeffery,

1997) (Figure 1.7.2). This is the main period of cell production and results with an abnormal thickening of the albino retina late in prenatal development. This increased cell production causes an increase in cell death in order to normalise the retinal thickness. This excessive proliferation followed by excessive cell death occurs before the presence of melanin in the RPE (Jeffery, 1997).

Figure 1.7.2: The number of mitotic figures in the retina of pigmented and albino rats. The numbers of mitotic profiles were counted along the horizontal meridian in the retinae of pigmented (filled circles) and albino (open circles) rats at progressive postconceptional days. B marks the day of birth. From postconceptional day 14-28 there are many more mitotic figures in the retinae of albino animals. The blue line shows the period of peak rod production (Ilia and Jeffery, 1999).

Neural retinal generation is biphasic with the formation of ganglion cells and cone photoreceptors in the first phase followed by the generation of the rod photoreceptors and the bipolar cells in the second phase (Harman and Beazley, 1989). It is in this latter phase where there is a significant difference in the number of mitotic and pyknotic nuclei (Ilia and Jeffery, 1999, Jeffery, 1997). Due to the lack of DOPA in albino animals in phase 2,

cell proliferation is not regulated resulting in increased cell production causing a highly congested retina which eventually leads to excessive cell death (Ilia and Jeffery, 1999). A study by Heintz et al. (1993) reinforces this theory as they showed that cells that are forced to stay in the cell cycle for abnormally long periods die. The accumulated effects of excess mitosis that mostly take place during this second phase where rods are generated explains the deficit in the number of rods in albinism (Jeffery and Kinsella, 1992, Jeffery and Williams, 1994).

The majority of cells affected in albinism are the cells that are generated in this second phase of retinal neurogenesis, however, ganglion cells are also affected showing central retinal abnormalities resulting in abnormal chiasmatic pathways. Although ganglion cells are produced in the first phase, the problem of chiasmatic misrouting may arise due to the fact that chiasm development is time dependent with crossed and uncrossed cells being born at different times. Uncrossed cells in the temporal retina are born before those with a crossed projection (Drager, 1985, Reese and Colello, 1992). The delay in spatiotemporal patterns of cell production in the ganglion cell layer could explain the reduction in uncrossed pathways in albinos (Ilia and Jeffery, 1996, Ilia and Jeffery, 1999).

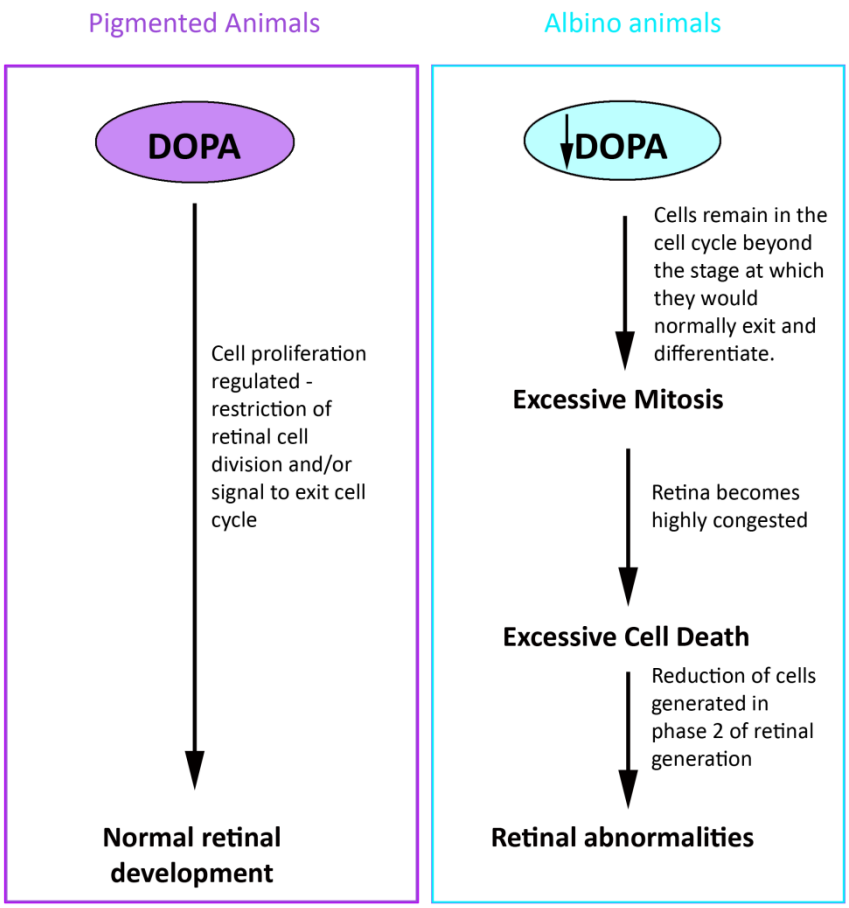

Figure 1.7.3: The effect of a lack of DOPA on retinal development. Decreased DOPA leads to excessive mitosis, which is followed by excessive cell death, resulting in the retinal abnormalities seen in albino mammals.

Studies have demonstrated that the visual deficits that occur in albinism arise as a result of decreased levels of DOPA or its metabolic derivatives rather than as a result of reduced levels of melanin in the RPE. A recent study using transgenic mice expressing tyrosine hydroxylase (*Th*) ectopically in the RPE shows the importance of DOPA for the appropriate development of the mammalian retina (Lavado et al., 2006). *Th* is an enzyme which can convert tyrosine to DOPA but cannot further oxidise this to dopaquinone, therefore, it cannot be involved in the synthesis of melanin. The results showed that the transgenic

mice, although phenotypically albino, displayed the correct number of photoreceptors and also normal chiasmatic pathways proving the vitality of DOPA for normal retinal development.

The question still remains as to how DOPA regulates the mitotic activity of cells during retinal development? It seems that the RPE plays a part in this regulation – during retinal mitosis, the retina forms transitory gap junctions with the RPE (Fujisawa et al., 1976, Hayes, 1976). In the mature retina, many gap junctions are gated by dopamine which restricts junction permeability (Vaney, 1994). This suggests that DOPA may influence the cell cycle by playing a role in gating junctional connections between mitotic profiles and RPE cells (Ilia and Jeffery, 1999). The reduced DOPA levels in the albino may cause junctions to remain more permeable, therefore, failing to restrict mitosis to a level that is necessary for normal development, whilst in pigmented animals the junctions are becoming progressively restricted during this period (Ilia and Jeffery, 1999).

Aims of the thesis

1. To determine whether the RPE is a heterogeneous monolayer of cells by looking at the differences in the expression of certain markers in different regions of the eye. In addition, to identify differences in the RPE of pigmented versus albino animals.

2. To investigate the effect of ageing on pigmented and albino rats to determine whether the lack of melanin would impact the structural and functional relationship between the RPE and photoreceptors more severely in the albinos.

3. To examine migration within the RPE of healthy young pigmented rats. Additionally, to study the effect of inducing laser lesions in either the periphery or the central region of the RPE to determine whether retinal location affects the response of RPE cells to the damaged area.

4. To investigate the effect on the RPE after treating animals with the drug, Glatiramer Acetate, in order to establish whether it impacts RPE cell production in mature rats.

Chapter 2

Heterogeneity in the RPE

2.1 Abstract

Retinal pigment epithelium cells are morphologically similar but show marked regional differences between the centre and periphery. Cell division occurs in peripheral regions throughout life, marking this region out as distinct. In this study, the regional molecular diversity in the RPE of mature pigmented and albino rats is examined. The RPE was examined in whole mounts. Quantitative analysis was undertaken of key morphological features. The whole mounts were also labelled with antibodies known to be markers of the RPE – otx2, CRALBP and RPE65. Antibodies against cell proliferation and RPE tight junctions were also used, Ki67 and ZO-1, respectively. The results show that a high level of heterogeneity was present in the architecture of the RPE sheet. Levels of RPE65, a key element in the visual cycle, are expressed at lower levels in the periphery of the pigmented rats compared to the centre. In albinos, however, the expression of RPE65 appears to be uniformly distributed throughout the entire RPE sheet. Otx2, a transcription factor thought to be ubiquitous to the RPE, is not expressed in some central/equatorial regions, independent of pigmentation phenotype. CRALBP, another element in the cell cycle is expressed in a patchy manner in both the albino and pigmented rats. ZO-1 labelling showed a significant difference in junctional regularity between the different regions of the DA and albino rat with cells appearing more regular in the central region compared to the periphery. These results demonstrate molecular diversity within a homogenous RPE matrix, particularly between the centre and periphery.

2.2 Introduction

The retinal pigment epithelium (RPE) is a monolayer of cuboidal cells which have apical microvilli and parallel lateral membranes joined near the cell apices by junctional complexes of occluden and adherens junctions (Burke and Hjelmeland, 2005). The basal membranes of the RPE are in contact with Bruch's membrane, separating the RPE from the underlying choroid. The apical domain, however, is associated with the outer retina where the RPE is closely associated with the outer segments of the rod and cone photoreceptor cells. This close interaction with the neural retina is vital for the RPE to carry out its function to support the survival and normal functioning of the photoreceptors. The importance of this interaction is demonstrated by the fact that damage to the RPE or separation of the RPE from the photoreceptors leads to retinal degeneration.

When viewed as a flat mount, the RPE appears as a monolayer of hexagonal, phenotypically similar cells (Figure 2.2.1). This uniformity gives a misimpression of the cells, as close inspection of these cells reveals both topographical and cell-cell heterogeneity within this monolayer, showing that the RPE is a mosaic of structurally and functionally heterogeneous cells that interact in various patterns. This can be seen both in situ and in vitro (Burke and Hjelmeland, 2005).

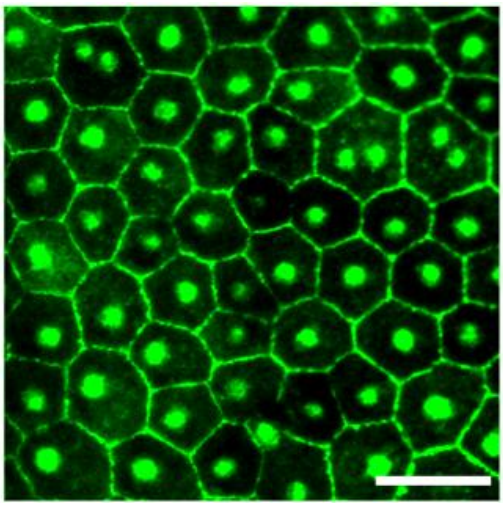

Figure 2.2.1: A microscope image taken from the peripheral RPE of a pigmented rat. The tissue has been stained with ZO-1 to show the RPE junctions. The RPE cells all appear to be hexagonal and phenotypically similar. Scale bar - 50µm

Understanding RPE cell heterogeneity is important to gain an insight into why certain diseases target specific RPE regions, especially with the deleterious effects of ageing. Although many retinal degenerative diseases may have genetic origins, they do not affect all regions in the same way - specific regions appear to be affected earlier than others. Retinitis pigmentosa, for instance, is initiated at the equator and progresses towards the periphery and the posterior pole (Dryja et al., 1990, Merin and Auerbach, 1976). Age-related macular degeneration (AMD), on the other hand, is characterised by the breakdown of the macula, an area in the central retina responsible for high-acuity vision. AMD is one of the leading causes of blindness in the elderly population of developed countries. With increasing life expectancies it is becoming a growing health problem as more of the population are reaching the age when AMD becomes prevalent (Crabb et al., 2002, Bylsma and Guymer, 2005, de Jong, 2006, Friedman et al., 2004). The RPE is a central element in the pathogenesis of AMD (de Jong, 2006), with growing evidence suggesting that age-related RPE dysfunction is an underlying cause. For this reason, an

understanding of regional variations within the RPE are important as the heterogeneity of this tissue may reflect underlying differences in cell biochemistry, kinetics and metabolism (Harman et al., 1997).

The greater predisposition to the effects of ageing seen in the macular region provides strong evidence for topographic heterogeneity in the RPE. This has been demonstrated in studies where morphometric analyses have proven that topographical differences occur in RPE cell size and density with age (Feeney-Burns et al., 1984, Harman et al., 1997, Watzke et al., 1993). Furthermore, regional functional differences have also been verified in the RPE. First, in both bovine and human eyes the Na/K ATPase pump density is lower in the posterior RPE cells (Burke et al., 1991). This may be due to a regional difference in the requirements for ionic regulation (Burke et al., 1991). Second, posterior RPE cells have lower activities of cytochrome oxidase (Burke, 1993) and γ-glutamyltranspeptidase (Frohlich and Klessen, 2001). These topographic variations coincide with regional variations seen in the overlying retina. Depending on the location within the retina, both the phagocytic load and lysosomal activity varies (Boulton and Dayhaw-Barker, 2001). For instance, in humans, the macula is a cone-rich environment in comparison to the periphery. The greater density of photoreceptors found here results in a greater metabolic load for the RPE in this region (Strauss, 2005) .

In addition to these topographical changes, RPE cells also exhibit regional differences among individual cells or clusters of cells. First, there are dramatic differences of some

neighbouring RPE cells in melanin content. RPE melanin is formed during development and there appears to be little turnover of either the melanin or of the cells themselves later, as the RPE is mainly non-mitotic (Marmor, 1998). A high or low melanosome number is, therefore, likely to be an inherent property of each RPE cell throughout its lifetime (Burke and Hjelmeland, 2005). As melanin plays an important photoprotective role in the RPE, differences in melanin granule content suggests that some cells may be more protected from insults than others (Figure 2.2.2).

Second, there are differences in the expression of many specific proteins within individual cells in the RPE. Burke et al. (1996) demonstrated that bovine RPE cells in situ have varied expression of the intermediate filament protein, vimentin, among individual cells. Furthermore, experiments by Burke et al. (2000) showed that the proteins E-cadherin, ankyrin and Na/K ATPase also showed heterogeneity within the RPE of bovine RPE cells in situ. This has also been demonstrated in other species; in humans Miyamura et al. (2004) showed that the expression of the antioxidant enzymes, catalase and heme oxygenase-1 (HO-1), differed significantly between the macula and the periphery. More recently, studies have applied microarray technology to discern the relative differences in gene expression between the posterior and peripheral human RPE. Although significant differences in gene expression have been detected, the biological significance of this phenomenon remains to be determined (Bowes Rickman et al., 2006, Ishibashi et al., 2004, van Soest et al., 2007). This shows that individual cells of this monolayer have the potential to exhibit a diverse spectrum of protein expression levels (Burke et al., 2000).

Figure 2.2.2: Adjacent RPE cells with differing properties, and their overlying photoreceptors. The left RPE cell might be at greater risk for oxidative damage over time because of its lower abundance of photoprotective melanosomes and lower levels of antioxidant enzymes, catalase and HO-1 (Burke and Hjemeland, 2005).

RPE heterogeneity can also be seen in terms of the proliferative capacity of this monolayer in specific regions. First, in rodents, the majority of RPE cells at central locations are binucleated, while in the periphery such cells remain in the minority (Ershov and Stroeva, 1989, Stroeva and Panova, 1983). In the rat, binucleated cells are formed after birth as a result of a postnatal wave of acytokinetic mitoses (Stroeva and Panova, 1983). The majority of mononucleated cells pass through the cell cycle once, becoming binucleated. If these mononucleated or binucleated cells were to enter the cell cycle more than once, but were somehow prevented from passing through mitosis, polyploidal cells would be formed.

Closer inspection of this peripheral region by Al-Hussaini et al. (2008) showed that the mature mammalian RPE has the capacity to proliferate, where cells in the peripheral and equatorial regions, express the proliferation marker, Ki67. Cells positive for Ki67 were never found in the central region of the RPE.

To further examine the heterogeneity and proliferative potential of the RPE, I have quantified the key morphological features of the RPE population and investigated the expression patterns of a range of molecular markers that are thought to be RPE specific. Furthermore, the molecular markers listed below are believed to be expressed uniformly throughout the RPE. Here, the expression patterns of these markers will be investigated in all retinal regions. In addition, the following markers will be examined in both pigmented and albino animals as a study by Al-Hussaini et al. (2008) noted that the number of cells positive for the cell cycle marker, Ki67, varied markedly depending on the pigmentation phenotype of the animal.

Markers of the RPE:

1. *Otx2*

OTX2 regulates the differentiation of the RPE. The *otx* genes, *Otx1* and *Otx2*, are homeodomain-containing transcription factors which have been detected at early and later stages of eye and retinal development. Their expression is first seen in the entire optic vesicle but soon becomes restricted to the presumptive RPE, where it is

maintained throughout adulthood. These genes play an important role in anterior head formation. Otx2 alongside another transcription factor, Mitf, are responsible for the development of the RPE (Martinez-Morales et al., 2003), and it is their early expression that allows for the identification of the presumptive RPE during eye development- a deficiency in the otx genes causes clear defects in the patterning of the RPE in mice.

2. RPE65

RPE65 is a microsomal membrane-associated protein which is abundantly expressed in the RPE and is a key element in normal RPE function. RPE65 has an important role in the visual cycle, a process where 11-*cis*-retinal, is regenerated. Although its exact function is unknown, it appears to play a vital role in the physiology of vision as mutations in the human RPE65 gene cause severe blindness from birth or early childhood in pathologies such as Leber's congenital amaurosis (LCA), autosomal recessive childhood-onset severe retinal dystrophy and some forms of retinitis pigmentosa (Gu et al., 1997, Marlhens et al., 1997). This indicates that defects in RPE65 expression dramatically affect photoreceptor survival and furthermore, highlights the critical role of RPE65 in RPE physiology (Manes et al., 1998). In mice, the homozygous RPE65 knockout has shown photoreceptor degeneration and a decreased rod response in ERGs (Redmond et al., 1998).

3. Cellular retinaldehyde-binding protein (CRALBP)

CRALBP is a water soluble protein which has a high affinity binding pocket for 11-*cis*-retinal and 11-*cis*-retinol, key components of the retinoid visual cycle. It is mostly expressed in the RPE, where the rod visual cycle takes place, however it is also expressed in the cornea, iris, ciliary body, pineal gland, optic nerve, brain and in Müller cells (Deeg et al., 2007). Its function is only known in the RPE, where it is an acceptor of 11-*cis*-retinol in the isomerisation step of the visual cycle (Wu et al., 2004). In humans, defects in the CRALBP gene have been found to cause retinal pathologies such as retinitis pigmentosa (Saari and Crabb, 2005), bothnia dystrophy and retinitis punctata albescens. In mice, targeted disruption of the CRALBP gene impairs regeneration of both rod and cone visual pigments (Wu et al., 2004). CRALBP is commonly used a marker for RPE and Müller glial cells (Saari et al., 2001, Thompson and Gal, 2003).

The following markers, Ki67, ZO-1 and caspase 3 are not markers of the RPE but are found in the RPE in proliferating cells, cell junctions and apoptotic cells, respectively.

4. Ki67

The Ki67 protein is a nuclear protein which is strictly associated with cell proliferation. Ki67 is a large nuclear protein with a molecular mass of 395 K which is endogenously and differentially expressed during different phases of the cell cycle (Wojtowicz and

Kee, 2006). Ki67 expression can be seen in the nuclei of cells during all the phases of the cell cycle (G_1, S, M, G_2) (Figure 2.2.3), quiescent cells, however, which are in the G_0 phase do not express Ki67. Ki67 undergoes phosphorylation and dephosphorylation during mitosis, it is believed that its expression is regulated by proteolytic pathways as it is susceptible to proteases (Brown and Gatter, 2002, Endl and Gerdes, 2000).

Figure 2.2.3: Diagram of the cell cycle which demonstrates the complete series of events from one cell division to the next. Ki67 labels cells in all stages of the cell cycle except for G_0 (from http://www.daviddarling.info/encyclopedia/C/cell_cycle.html).

Characterisation of the Ki67 antibody showed that the antibody was reactive in all proliferating cells, normal and tumour cells. For this reason, the Ki67 antigen is a useful marker for assessing the growth fraction of a given cell population. The absence of Ki67 causes the prevention of cell proliferation, indicating that the expression of this protein is required for progression through the cell cycle.

5. *Tight junction marker: ZO-1*

Epithelial tight junctions regulate paracellular permeability and prevent the intermixing of apical and basolateral membrane components (Cereijido et al., 1998). Tight junctions have a molecular architecture similar to other adhesion complexes and consist of transmembrane proteins such as occludin, claudins and JAMS. These mediate adhesion and barrier function as well as selective paracellular diffusion (Matter et al., 2005). Junctional adapters such as the ZO proteins interact with these membrane proteins in a cytoplasmic plaque containing many protein-protein interaction domains (Matter et al., 2005). Furthermore, tight junctions have been proposed to participate in the regulation of epithelial cell proliferation and differentiation (Balda et al., 2003). The junctional adapters appear to form a protein network, linking the junction to the actin cytoskeleton allowing the recruitment of different types of signalling proteins. These regulate junction assembly and function as well as epithelial proliferation and differentiation (Matter et al., 2005, Balda et al., 2003).

ZO-1, a tight junction-associated cytosolic protein, is a founding member of the membrane-associated guanylate kinases (MAGUK) family of proteins (Katsuno et al., 2008). It is composed of three postsynaptic density 95/disc-large/ZO-1 (PDZ) domains, a Src homology 3 domain, a guanylate kinase (GUK) domain, an acidic domain, and an actin binding region (Haskins et al., 1998, Itoh et al., 1993, Willott et al., 1993). ZO-1 is exclusively located at tight junctions in epithelial cells (Stevenson et al., 1986),

however, when tight junctions are not formed they are concentrated in adherens junctions (Bazzoni et al., 2000, Fanning et al., 1998, Furuse et al., 1994, Itoh et al., 1993). Furthermore, ZO-1 also appears in the nucleus during proliferation (Gottardi et al., 1996). A ZO-1 deficiency in mice causes an embryonic lethal phenotype associated with defected yolk sac angiogenesis and apoptosis of embryonic cells (Katsuno et al., 2008).

The expression levels of ZO-1 are related to the proliferation state of epithelial cells, and in a recent study by Georgiadis et al. (2010) the downregulation of ZO-1 induced RPE proliferation and de-differentiation in vivo. This eventually led to cell loss and retinal degeneration.

In this study, the expression patterns of RPE specific markers will be investigated in different regions of the RPE. In addition, cell death within the RPE will be examined to determine whether cell death within the RPE is location specific. Here, the molecular marker activated caspase 3 will be used.

6. Activated Caspase 3

Apoptosis is a highly regulated and conserved form of cell suicide that is characterised by DNA fragmentation, membrane blebbing, chromatin condensation, cell shrinkage and disassembly into membrane-enclosed vesicles (Duan et al., 2003, Kohler et al.,

2002). Apoptosis is mediated by a proteolytic cascade, in which the caspases, a family of cysteine proteases play an important role. The caspases are involved in the initiation, regulation and execution of the downstream proteolytic events that occur during apoptosis (Cryns and Yuan, 1998, Thornberry, 1999, Thornberry and Lazebnik, 1998). Studies have demonstrated the importance of caspases for the apoptotic process as they have shown that knockout animals lacking certain caspases show profound defects in apoptosis, furthermore, the overexpression of caspases efficiently kills cells (Chang and Yang, 2000, Zheng and Flavell, 2000).

Upon activation through proteolytic processing, caspases trigger substrate proteolysis and other changes that result in the apoptotic phenotype (Goyal, 2001, Thornberry and Lazebnik, 1998). Caspase-3 is necessary for the cleavage of a large number of proteins and for the DNA fragmentation and nuclear collapse during apoptosis, making it one of the primary executioners of apoptosis (Slee et al., 2001). For this reason, caspase-3 activation is one of the most specific indicators of the apoptotic process.

2.3 Methods

Animals

Twenty Dark Agouti (DA) pigmented rats and seventeen Wistar albino rats were used in this study. All were aged between 3 – 4 months. All procedures were performed under the UK government (Home Office) and local animal ethics committee approval. The animals were housed with a 12hour light/dark cycle in a temperature controlled environment and were fed ad libitum. The table below shows the number of animals used in each procedure:

Experiment	DA	Albino
ZO-1 and Ki67 whole mount labelling	6	6
Otx2 whole mount labelling	6	6
RPE65 and Ki67 whole mount labelling	6	6
CRALBP and otx2 whole mount labelling	6	6
Markers for apoptosis	6	6
Markers for apoptosis	6	6

Table 2.3.1: A table showing the experiments carried out to determine whether the RPE is a heterogeneous monolayer of cells alongside the number of pigmented (DA) and albino rats used for each one.

Tissue processing for immunohistochemistry

Following euthanasia with CO_2, a stich was placed on the dorsal aspect of the eye for orientation. Eyes were removed and fixed in 4% paraformaldehyde for 1 hour at room temperature (RT). Following this, the eyes were washed with 0.1M Phosphate Buffered Saline (PBS) and prepared for dissection using a dissecting microscope. First, all the excess

fatty tissue was removed from the back of the eye cup. Then, using a 27 gauge needle a small hole was placed in the cornea and using microsurgical scissors, the cornea and iris were removed. In order to flatten the tissue, radial incisions were made and the ciliary body was removed using a 10 blade scalpel. The retina was easily removed exposing the underlying RPE and attached choroid (Figure 2.3.1).

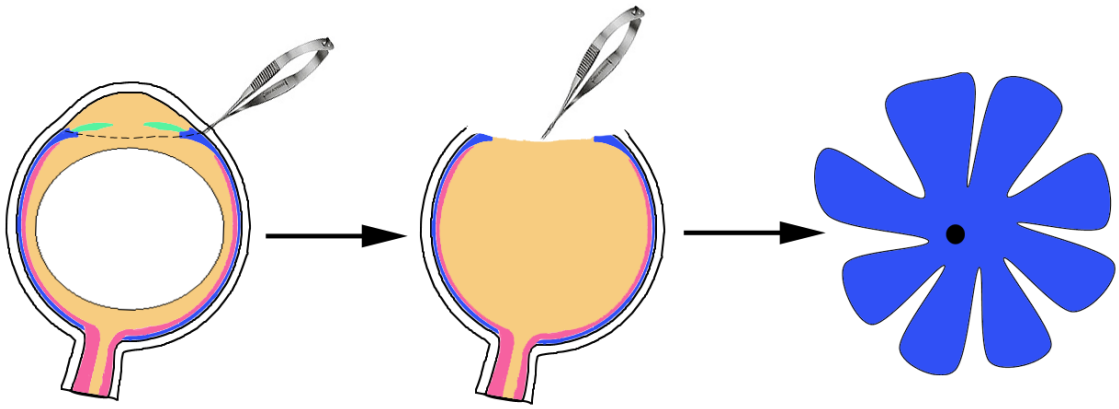

Figure 2.3.1: Diagram illustrating the method used to flatmount the eyecups containing the RPE.

The whole mounts were each placed into a well from a 16 well plate and blocked for 2 hours in 5% normal donkey serum (Jackson Laboratories) in PBS with 3% Triton X-100 (VWR) at RT. After blocking, the eye cups were briefly washed with PBS and then incubated with the primary antibodies overnight, all of which were diluted in 1% normal donkey serum in PBS with 3% Triton X-100. Table 2.3.2 shows the primary antibodies used and their dilutions.

Table 2.3.2: A list of the primary antibodies used to distinguish the differences between central and peripheral RPE regions.

Antibody name	Dilution	Manufacturer	Catalogue number	Species raised	Tissue specificity	Target
Otx2	1:1000	Millipore	ab9566	Rabbit	-	Nuclear transcription factor
Ki67	1:1000	Vector laboratories	VP-K451	Rabbit	All proliferating cells	Nuclei
RPE65	1:500	Millipore	MAB5428	Mouse	RPE	RPE microsomal membranes
CRALBP	1:1000	Affinity Bioreagents	MA1-813	Mouse	Müller glia & RPE cells	cellular retinaldehyde-binding protein
ZO-1	1:100	Abcam	ab59720	Rabbit	Epithelial cells	Tight junctions
Active Caspase 3	1:50	Abcam	ab2302	Rabbit	-	Cytoplasm

The following day, the eyecups were washed several time in PBS and then incubated in the appropriate secondary antibodies for 2 hours in 1% normal donkey serum in PBS with 0.3% Triton X-100. The 16 well plate was covered with aluminium foil as the secondary antibodies are light sensitive. Nuclei were subsequently stained with 4_,6-diamidino-2-phenylindole (DAPI) (Sigma-Aldrich, UK). Specimens were washed three times in PBS followed by three washes in Tris buffer saline (pH 7.4) before being mounted with Vectashield (Vector Laboratories, UK) which prevents the tissue from drying and maintains fluorescence. Table 2.3.3 shows the secondary antibodies used and their dilutions.

Table 2.3.3: A list of the secondary antibodies used to distinguish the differences between central and peripheral RPE regions.

Antibody name	Dilution	Manufacturer	Catalogue number
Alexa Fluor 488 fragment of goat anti mouse IgG (H+L)	1:2000	Invitrogen	A11017
Alexa Fluor 568 Donkey anti-Rabbit IgG (H+L)	1:2000	Invitrogen	A10042
Alexa Fluor 488 Donkey anti Rabbit IgG (H+L)	1:2000	Invitrogen	A21206

Wholemounts were viewed and images captured using two microscopes. Either an Epi-fluorescence bright field microscope (Olympus BX50F4,Olympus, Japan) where images were captured as 24-bit colour images at 3840 x 3072 pixel resolution using a Nikon DXM1200 (Nikon, Tokyo, Japan) digital camera or with a laser scanning confocal microscope (Leica TCS_SP2 AOBS).

Tests to determine apoptotic cells in the RPE

To determine the pattern of cell death within the RPE monolayer and to see whether regional differences exist, three independent methods were used:

1. *The antibody active caspase 3:* once the eyes were removed and processed the protocol for immunohistochemistry described above was used using active caspase 3 as the primary antibody, followed by Alexa Fluor 488 Donkey anti Rabbit as the secondary antibody.

2. *A TUNEL staining kit:* the TUNEL Apoptosis Detection Kit (Millipore, UK) was used. This kit enables the detection of the endonucleolytic cleavage of chromatin, characteristic of apoptosis. The protocol provided by the manufacturer was followed accurately.

3. *Acradine orange:* This dye specifically labels cells dying from programmed cell death. It is a quick and simple method for detecting cell death, however, the tissue must be living and the preparations are not permanent. For this reason, the tissue cannot be fixed and must be viewed under a fluorescence microscope as quickly as possible. In this experiment, following euthanasia with CO_2, the eyes were removed and placed into culture medium. Once dissected, the flatmounts were incubated with the dye for 25 minutes at 37°C. The specimens were washed with PBS and were immediately viewed under the microscope, taking images when necessary.

Analysis

Morphological analysis – measuring the cell size, regularity and % binucleation of RPE cells

Consecutive digital images were taken along a strip of the RPE, starting from the periphery and moving towards the centre, at 400µm intervals using a motorised microscopic stage. From each retina, images were taken from three radially separated equidistant strips using a 400x objective lens in JPEG format using the Epi-fluorescence bright field

microscope described above. Analysis of these images was carried out using a program in MATLAB which allowed for the cell size and the relative regularity index to be measured. This program was adapted from an algorithm designed to distinguish differences in the characteristics of type I and type II muscle fibers. This adapted version, allowed for the cell size and cell regularity to be measured by simply uploading each image onto the programme. The centre of each cell was selected and recorded as an array of coordinates from which a lattice of triangles was constructed (Figure 2.3.2).

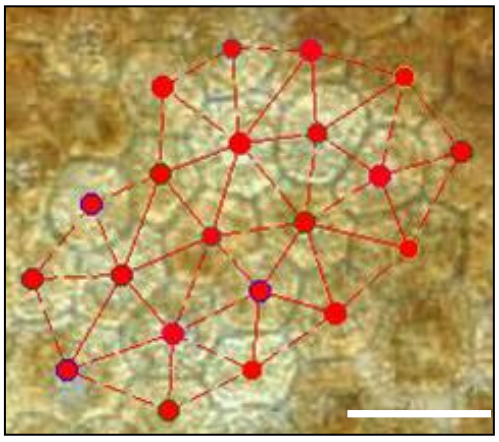

Figure 2.3.2: Triangulation pattern applied to the image of retina from a human RPE. The digital image was acquired with light microscopy. The central points of the RPE cells were marked by a mouse click and then the lattice of triangles was constructed. A MatLab programme was then used to calculate RPE cell diameter and regularity. Scale bar - 50µm.

This morphometric data regarding the regularity of the RPE matrix was derived using a Delaunay triangulation analysis. The method was implemented as a semi-automatic algorithm (Matlab, Mathworks, Natick, MA) where cell size and regulation were derived from the triangulation data. The mean value from the three strips was calculated for each

RPE sheet and an ANOVA was carried out to determine whether there was a significant difference between the different locations of the eye.

In order to calculate the percentage of mononucleated and binucleated cells, every cell within a 520 x 520 µm area was analysed and the type of nuclei they contained was recorded and calculated as a percentage of the total number of cells.

Comparing the expression of Ki67, RPE65 and CRALBP in both pigmentation phenotypes

Digital images were taken using a laser scanning confocal microscope. For the Ki67 positive cells, every cell within the RPE monolayer was imaged and counted. To analyse the regional differences in CRALBP and RPE65 expression, consecutive digital images were taken in strips of the RPE starting from the periphery and moving towards the centre.

Quantifying the number of cells not expressing otx2

RPE regions were standardised such that the centre was an area of a 2mm radius from the optic nerve and the 2mm radius distal to this region was the equator. The periphery was the most distal 1mm radius (Figure 2.3.3). The entire RPE flatmount was analysed under an epi-fluorescent microscope and every cell that lacked otx2 expression was mapped and recorded.

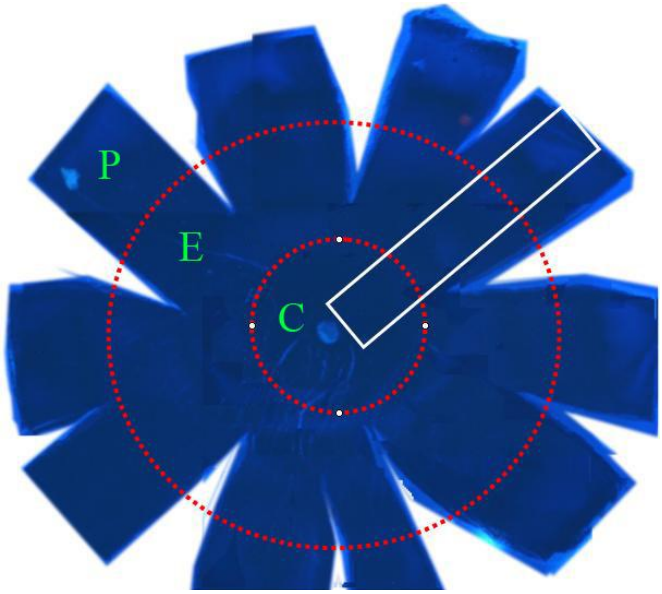

Figure 2.3.3: Image showing how the RPE was divided into 3 regions, the periphery (P), equator (E) and centre (C). The white box demonstrates how strips from periphery to the centre were analysed.

Quantifying the regularity of RPE junctions

Digital images were taken from all three regions of the RPE at x400 magnification. These images were uploaded into Photoshop CS4 where they were analysed. Using the line tool, a straight line was drawn from the corner of one junction to another. This was carried out for every single junction within a 520µm x 520µm area. The number of times the cellular junction did not sit on the drawn line was counted and recorded.

Statistical Analysis

Unless otherwise stated, a non parametric two tailed Mann-Whitney U-Test was used as the sample sizes were relatively small and a normal distribution could not be assumed.

2.4 Results

Morphological features of the RPE in both pigmented and albino rats

Pigmented and albino rat RPE cells showed a high degree of morphometric consistency (Figure 2.4.1). First, there was no significant difference in RPE cell size between the central retina and the retinal margin and across the different quadrants. The average cell size for both pigmentation phenotypes was 27µm in the periphery. In the albino the cell size appeared to increase slightly towards the centre to 29µm, however, this was not significant. Second, the regularity of their mosaic distribution revealed an overall pattern of consistency from the periphery towards the centre. There was no significant difference between the two pigmentation phenotypes. A feature that did vary across the centre to periphery axis was the proportion of cells that are binucleated. As shown by Stroeva and Panova (2008), rodents contain binucleated RPE cells. In the peripheral RPE, pigmented animals had 20% binucleated cells whilst in the centre this number rose to 80%. Similarly, albino rats had 10% binucleated cells in the periphery and 70% towards the centre.

Comparisons of the morphological features between the pigmented and the albino phenotypes demonstrated a largely similar pattern between the two. To determine whether RPE cells are homogenous, the cells were looked into on a molecular level.

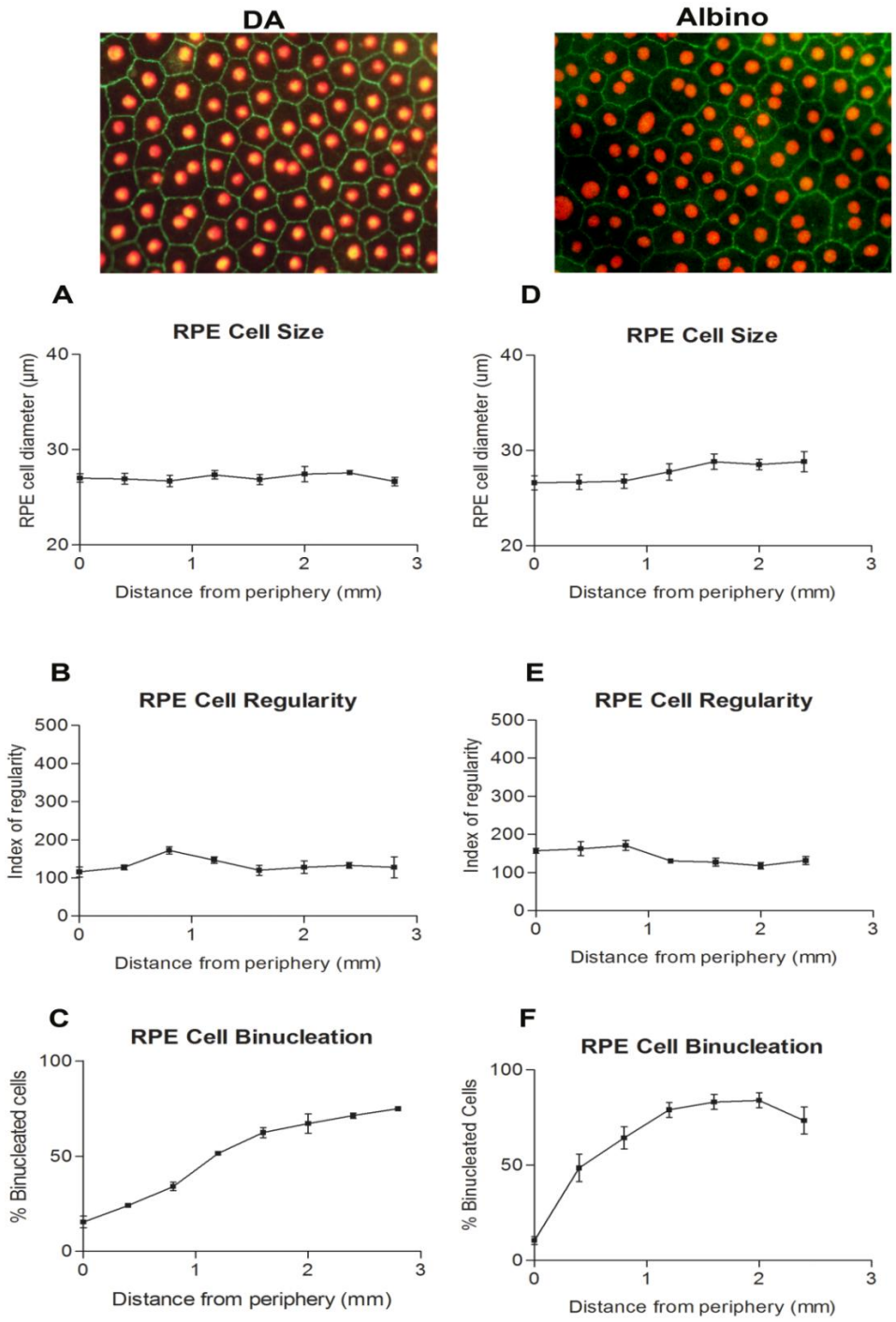

Figure 2.4.1: The comparison of the morphological features of the RPE in terms of cell size, cell regularity and the percentage of cells that are binucleated in pigmented DA and albino Wistar rats. The top photomicrographs are taken from the equatorial retina – the RPE has been labelled with otx2 (red) to show nuclear morphology and ZO-1 (green) to highlight the cell junctions. **Cell size**: In both pigmentation phenotypes there was no significant difference in cell size across the retina or between the two pigmentation phenotypes (A,D). **Matrix regularity**: There were no significant changes in the regularity of RPE cells across the retina in DA rats (B). Regularity in the albinos, however, did decline significantly towards the centre ($p=0.0184$). Differences between the two phenotypes were not significant. **Binucleation:** Both pigmentation phenotypes showed a significant increase in the number of binucleated cells towards the centre of the RPE ($p<0.001$).

Lack of otx2 expression in the equatorial region of the RPE

Otx2 regulates the differentiation of the RPE. Otx2 is present in the nuclei of all cells except for a small population of cells in the equatorial region (Figure 2.4.2). To ensure that the lack of a nuclear label was due to the absence of otx2 and not damage to the cell, the RPE was co-stained with DAPI which binds to nuclear material. From approximately 40 000 cells in the RPE, 400 cells in the equator and 100 cells in the centre did not express otx2. The albino showed a similar pattern with approximately 300 cells in the equator and 90 cells in the centre not expressing otx2.

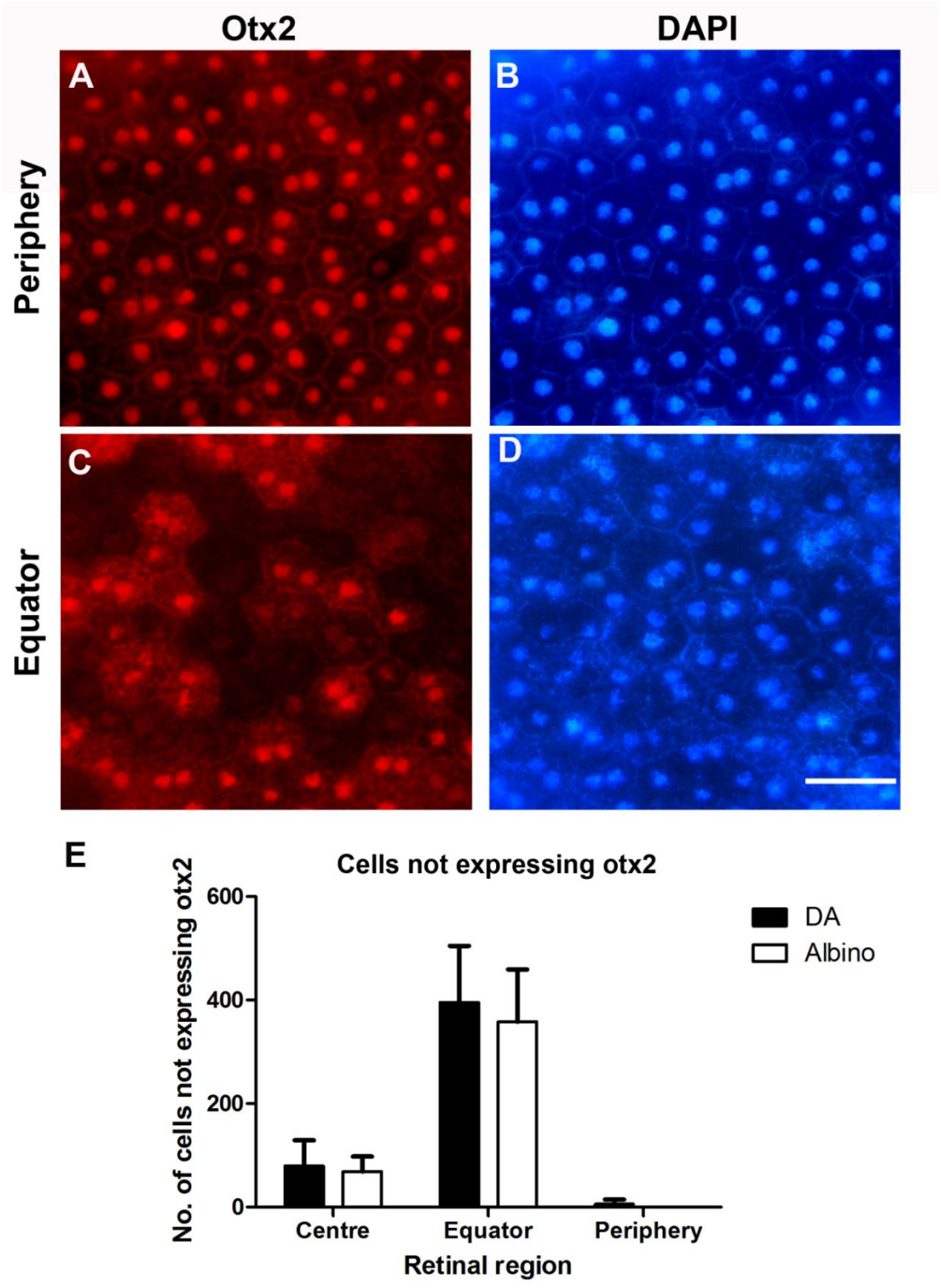

Figure 2.4.2: Otx2 expression in the RPE. (A) is taken from the peripheral retina where all cells are otx2 positive. (B) is the corresponding area stained with DAPI. In the equatorial and central regions of the RPE, patches of cells were found to be negative for otx2 (C). This was not as a result of tissue damage to the RPE as the corresponding DAPI image reveals the presence of the cells (D). Both pigmentation phenotypes showed similar patterns in the expression of otx2 in the RPE. (E) shows the geographic distribution of the cells failing to express otx2. Scale bar - 50um.

Differences in Ki67 and RPE65 expression between the two pigmentation phenotypes

The mature RPE contains a proportion of cells that have the capacity to enter into the cell cycle and divide in the peripheral and equatorial retinal regions (Al-Hussaini et al., 2008). The number of these cells is significantly elevated when pigment is absent as in albino animals. In the DA RPE, an average of 15 Ki67 positive cells are found throughout the peripheral and equatorial regions, whereas in the albinos this number increases to approximately 150 (Figure 2.4.3G). Ki67 is a cell-cycle associated protein that is absent in quiescent cells and is not detectable during DNA repair, therefore, its presence in the RPE cells is strictly associated with the cell cycle. It is confined to the nucleus suggesting it has an important role in the maintenance and/or regulation of the cell division cycle.

RPE65 is a RPE specific protein located in the cells cytoplasm. It is responsible for the conversion of all-trans retinol to 11-cis retinal during phototransduction. The pattern of cellular labelling for RPE65 showed marked regional variations across the centre to periphery axis in pigmented animals (Figure 2.4.3E). Cells in the central retina were clearly positive for RPE65 (Figure 2.4.3A), however, with movement towards the periphery, the intensity of RPE65 expression appeared to decline in individual cells (Figure 2.4.3C). This was a consistent feature in all of the pigmented retinae that were examined. The albino phenotype did not follow this pattern (Figure 2.4.3F), here, the cells were uniformly labelled with RPE65 irrespective of location (Figures 2.4.3B and 2.4.3D). While the difference in the overall label between the pigmentation phenotypes could be due to the presence of melanin granules in the DA RPE partially masking the intensity of the

cytoplasmic label, this would not explain the differences in regional patterning found within the pigmented animals.

Another finding that became apparent while closely looking at the cells in the periphery of the albino RPE was that within the albino peripheral RPE, a population of cells appear to have large distorted nuclei (Figure 2.4.4). The RPE cells in the centre of the albino RPE appeared normal, however, few could be seen with more than 2 nuclei. These cells appear to be polyploidal and may have arisen due to errors in cell division. Such cells were not seen in any region of the pigmented RPE.

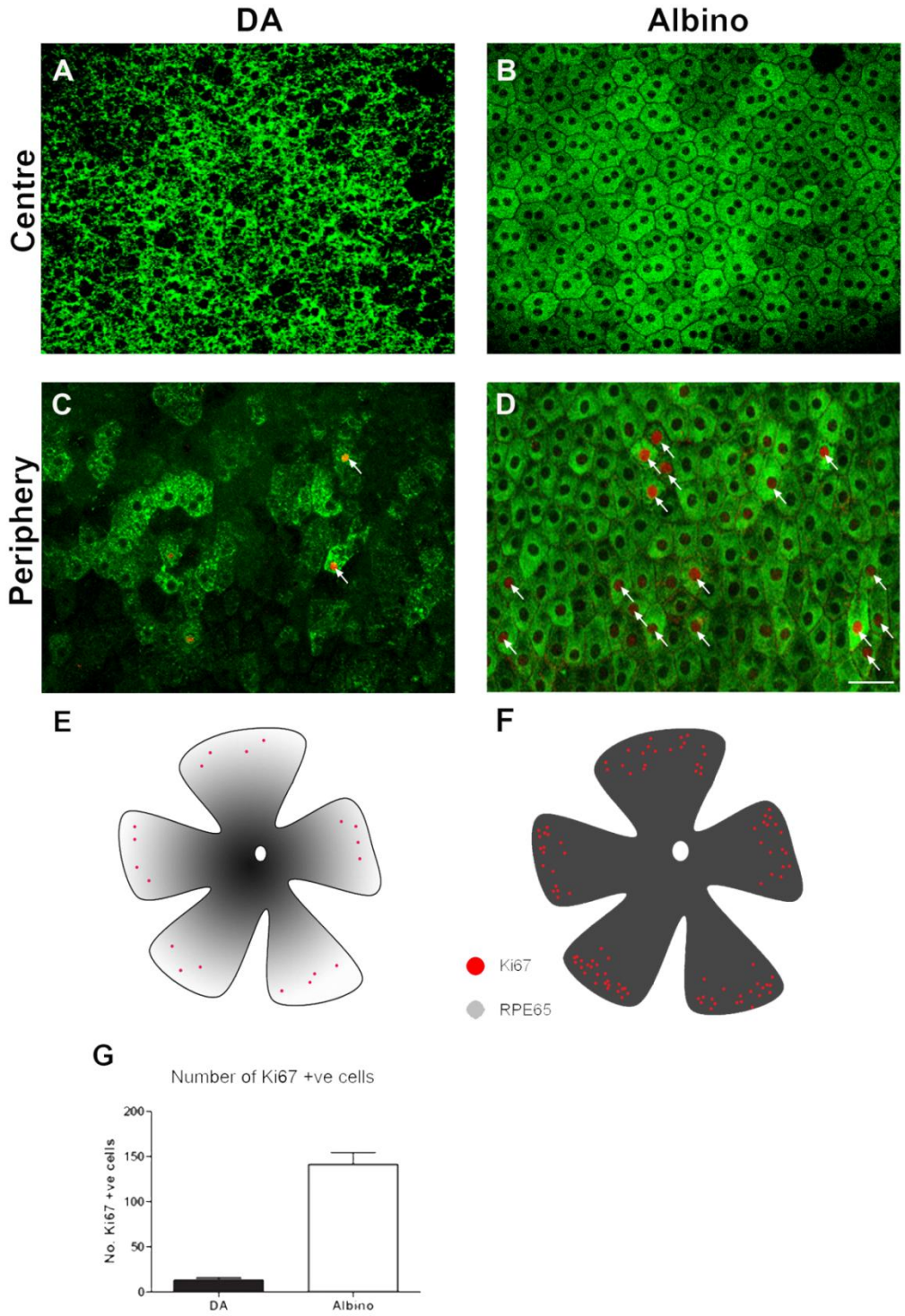

Figure 2.4.3: Expression of RPE65 (green) and Ki67 (red, arrows) in the centre (A,B) and the periphery (C,D) of the RPE in both DA (A,C) and albino (B,D) rats. RPE65 expression declines in the periphery of the pigmented rat but not in the albino. The peripheral RPE of the albino contains almost ten times more Ki67 positive cells than the pigmented DA. The configuration of these markers is shown schematically in (E) and (F), where the red dots represent the location of the Ki67+ve cells and the grey scale shows the relative level of RPE65 expression. (G) shows the quantification of the total number of Ki67+ve cells in both pigmentation phenotypes. Scale bar - 50µm.

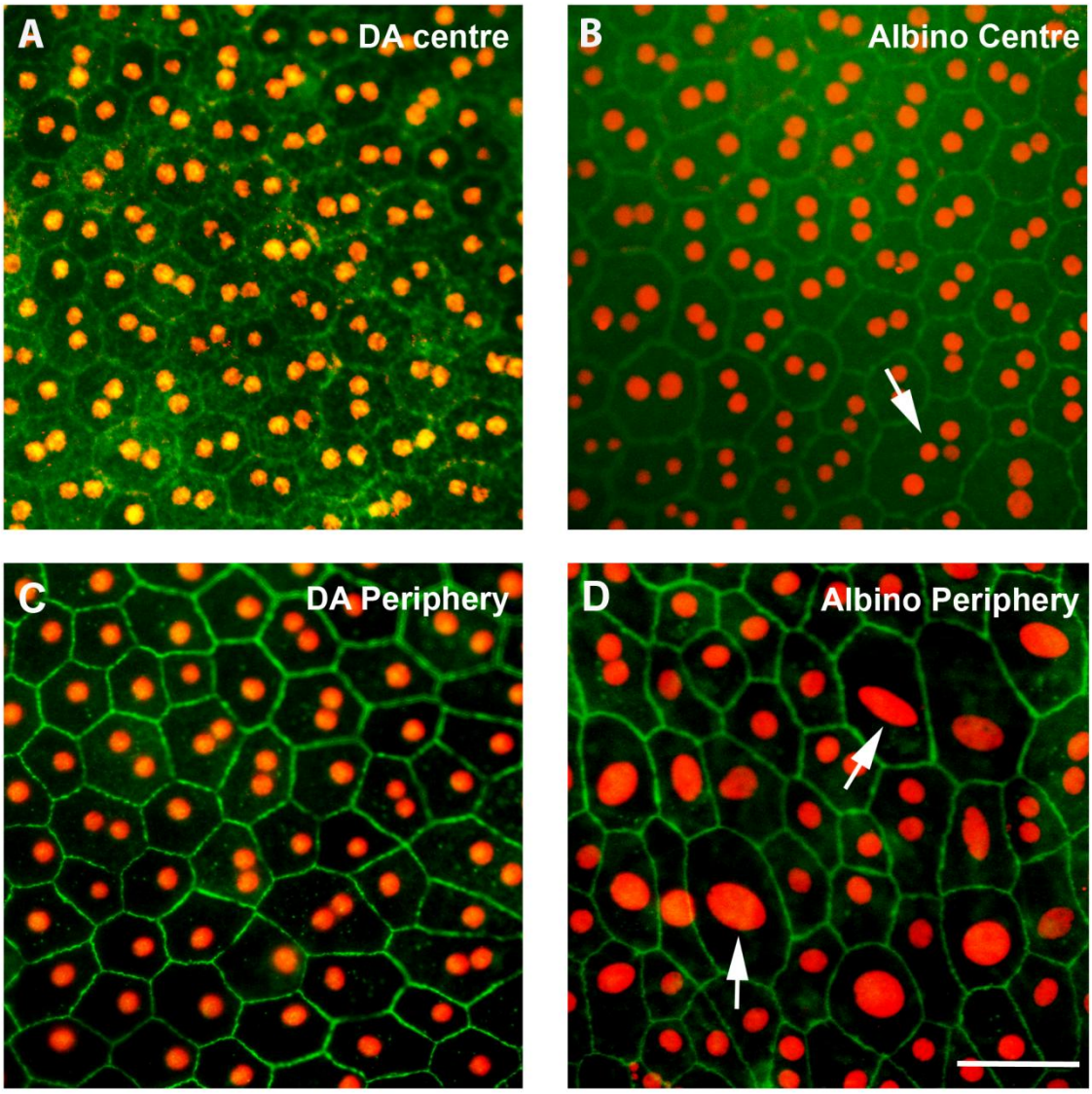

Figure 2.4.4: Immunohistochemistry using ZO-1 (green) to highlight the RPE cell junctions and otx2 (red) to show nuclear morphologies in pigmented and albino rats. (A) and (C) show images from the pigmented animal, from the central and peripheral region, respectively. There appears to be no difference in nuclear morphology between these 2 regions. (B) shows an image from the centre of the albino RPE, where again, nuclear morphology appears normal. Some cells do, however, appear to have more than 2 nuclei present within the cell. (D) shows an image from the periphery, where, some cells appear to have abnormal nuclear morphologies, with large distorted nuclei. Scale bar - 50µm.

CRALBP expression occurs in clusters throughout the RPE

CRALBP is commonly used as a marker for RPE cells as it is an abundant amino acid retinoid-binding protein present in the RPE and Müller cells, where it interacts specifically with 11-*cis* retinol and 11-*cis* retinal (Thompson and Gal, 2003). It has multiple functions in the RPE – first, as a major acceptor of 11-*cis*-retinol in the isomerisation step of the rod visual cycle. Second, as a facilitator of oxidation of 11-*cis*-retinol to 11-*cis*-retinal by 11-*cis*-retinol dehydrogenase (Wu et al., 2004).

Here, it can be seen that CRALBP is not uniformly expressed throughout the RPE as would be expected, in fact, its expression appeared to be in small clusters in varying regions of the RPE (Figures 2.4.5A and 2.4.5B). There was no apparent topographic variability (Figure 2.4.5C). Both pigmentation phenotypes demonstrated the same pattern of CRALBP expression throughout the RPE.

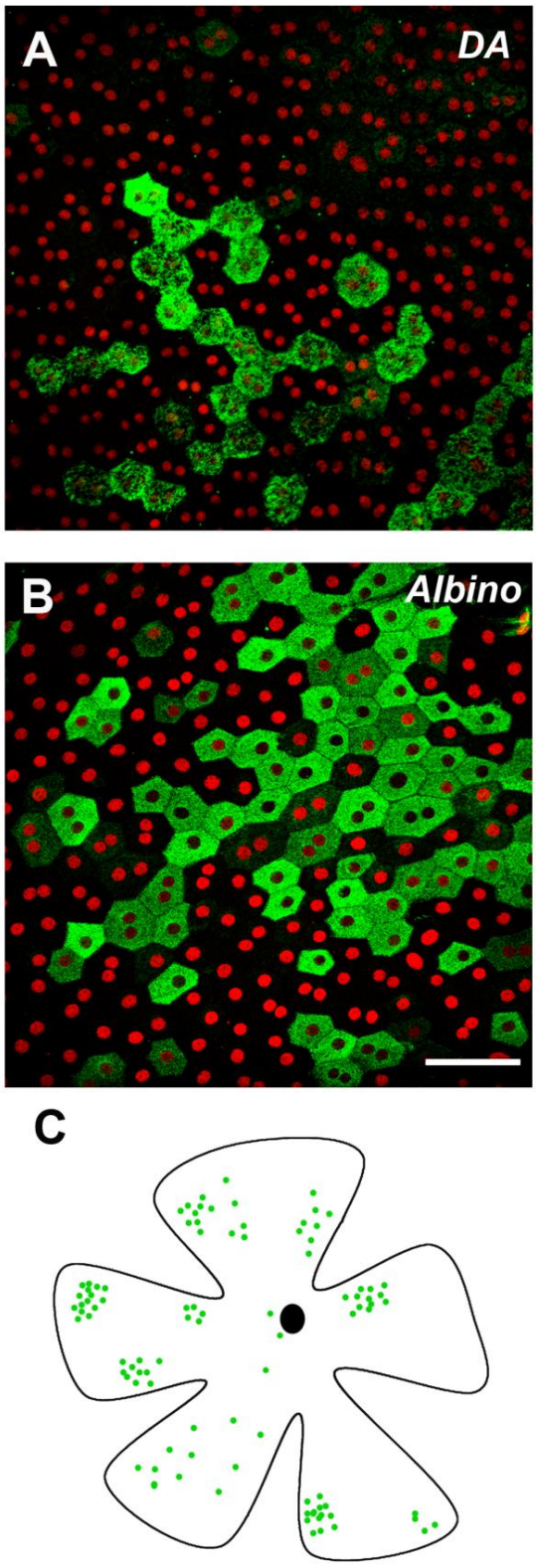

Figure 2.4.5: CRALBP (green) and otx2 (red) expression in the RPE of a pigmented (A) and albino (B) rat. The patterns of labelling were very similar between the two groups. CRALBP expression seemed to occur in clusters of cells, however, isolated individual cells were also present. There did not seem to be any obvious geographic distribution of the labelled cells as shown in the schematic diagram from a DA rat (C). Scale bar - 50um

Differences in junctional morphology depending on location in the RPE

Correlations between junctional modification and cell proliferation have been reported in a variety of epithelial tissues suggesting that these events are related. Here, ki67 and ZO-1 were co-labelled on RPE flatmounts in both pigmented and albino rats. Initially the junctions around the Ki67 positive cells found in the periphery of the RPE were examined to determine whether proliferating cells would have a less regular junctional phenotype (Figure 2.4.6A). The results showed that ZO-1 expression is irregular and ruffled in appearance, not only in these cells, but also in the entire peripheral zone of the RPE (Figure 2.4.6B). Moving towards the centre, ZO-1 expression showed that the junctions of the cells became far more regular and straight, characteristic of RPE cells (Figure 2.4.6C). This pattern was similar for both pigmentation phenotypes. Figures 2.4.6D and 2.4.6E show a significant difference in junctional regularity between the different regions of the DA and albino rat RPE, respectively.

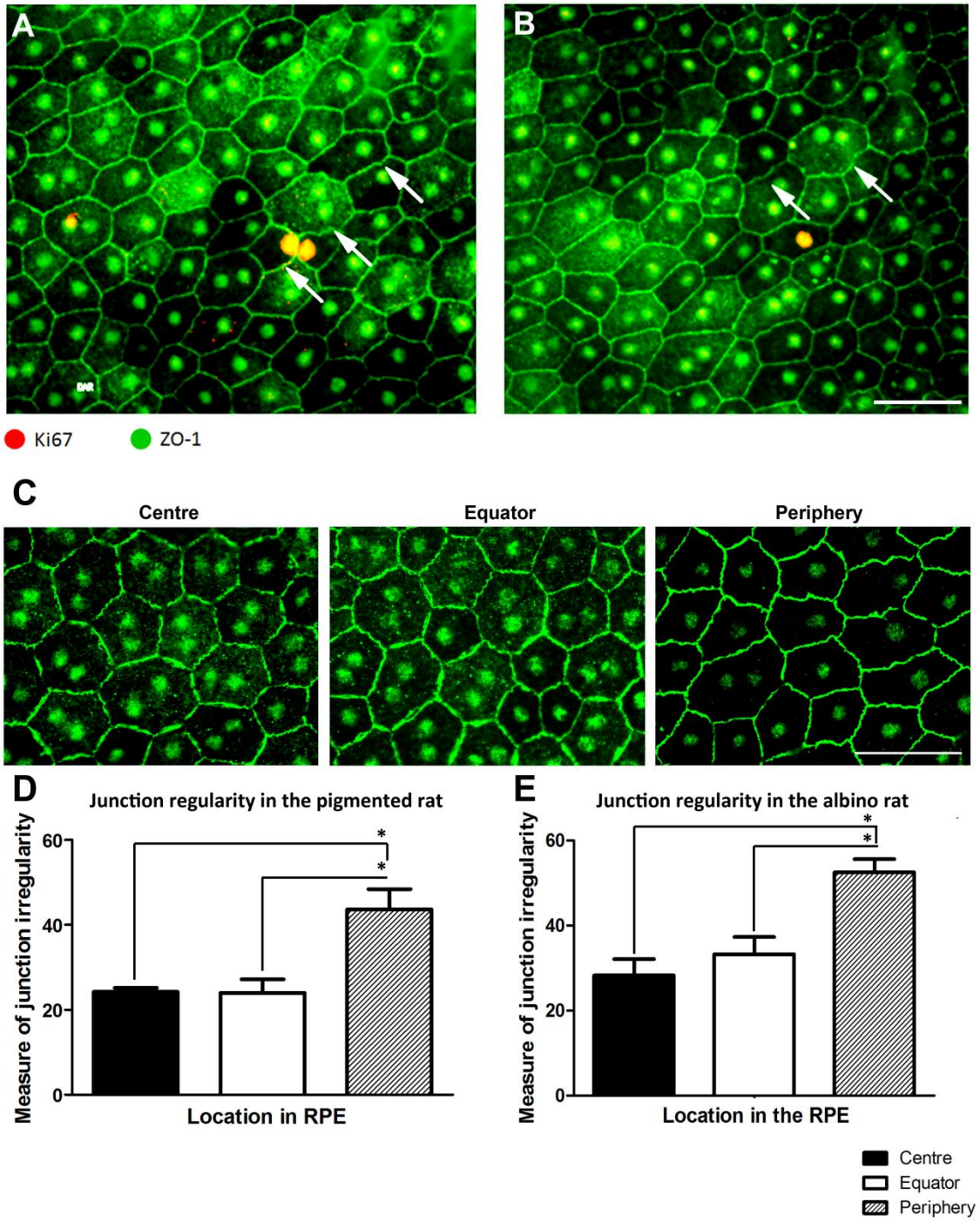

Figure 2.4.6: Cell junctions in the RPE. (A,B) show Ki67 (red) and ZO-1 (green) expression in the periphery of the RPE in a pigmented DA rat. ZO-1 expression is irregular and ruffled in appearance, not only in the Ki67 positive cells (A) but also throughout the peripheral zone of the RPE (B). (C) shows that the tight junctions of the RPE increase in irregularity towards the periphery, with cells in the central and equatorial regions appearing far more regular and straight in appearance. (D) and (E) show a significant increase in irregularity between the periphery and central/equatorial regions ($p<0.05$) of the pigmented and albino rat, respectively. Images from the albino rat are not show as they are similar to that demonstrated in the pigmented rat. Scale bar -50µm.

Cell death in the RPE

Unfortunately, in this study several methods were used to determine cell death in the RPE but all were unsuccessful. This could be due to the fast rate in which apoptosis occurs and the rate in which dead cells are cleared or it could suggest that significant cell death does not occur within the RPE.

2.5 Discussion

Despite the RPE sheet being morphologically homogenous, this study reveals that molecular markers of this tissue demonstrate distinct regional patterns showing RPE cell heterogeneity. Heterogeneity of epithelial cells is an expected outcome of normal development and organogenesis (Iannaccone, 1987). During development, the RPE develops in tandem with the sensory retina, with the periphery being embryologically the last to mature. This gives rise to the differences between the posterior pole and the peripheral regions (Burke and Hjelmeland, 2005). The RPE arises from the neuroectoderm-derived optic vesicle, which collapses to form the bilayered optic cup. Whilst the inner layer of cells give rise to the sensory retina, the outer layer develops into the RPE (Bharti et al., 2006, Martinez-Morales et al., 2004). Subsequently, the RPE undergoes a period of cell proliferation which is followed by growth quiescence and then differentiation in a topographical pattern. First, the cells at the posterior pole stop dividing. Second, is the radial entry of RPE cells into quiescence. As a result of this, the peripheral and posterior RPE undergo differentiation at different times as well as in different locations causing differences within the tissue related to topography.

RPE cells are uniform in size and mosaic regularity irrespective of their pigmentation phenotype or location. In the rat, they show regional binucleation, similar to that previously reported (Ershov and Stroeva, 1989, Stroeva and Panova, 1983). Binucleation in RPE cells is rare and appears to mainly be a rodent specific feature, however, it is also

seen in rabbits (Ts'o and Friedman, 1967). In humans, the presence of binucleated cells is associated with the far retinal periphery and local pathological situations (Al-Hussaini et al., 2009).

Not only do the molecular markers used here demonstrate differences in geographic distribution within the RPE, but also, in some cases, this is associated with different pigmentation phenotypes. RPE65 shows a marked reduction in staining intensity in the periphery of the pigmented animals but not in the albinos, where RPE65 was uniformly expressed throughout the whole eye cup. Ki67 expression, although confined to the peripheral/equatorial region of the RPE in both pigmentation phenotypes, was ten times higher in the albinos compared with the pigmented rats (similar to data shown by Al-Hussaini et al. (2008)). Differences in pigmentation phenotype, however, were not associated with the differences in the staining patterns seen with otx2, CRALBP and ZO-1 expression. In the equatorial regions of the RPE, otx2 expression was relatively sparse, while CRALBP expression was relatively patchy in its distribution. ZO-1 staining revealed that the tight junctions of the peripheral RPE appeared to be very irregular with increasing regularity towards the centre.

RPE65 is critical for the regeneration of 11-*cis*-retinal in the visual cycle and defects in its expression dramatically affect photoreceptor survival (Manes et al., 1998, Redmond et al., 1998). The reduced intensity of RPE65 expression seen in the periphery of the pigmented rats RPE may be associated with the reduced photoreceptor densities at these

eccentricities. In DA rats, the density gradients for outer nuclear layer cells are 25-30% lower in the periphery in comparison to the centre (Ilia and Jeffery, 2000). Although plausible, this seems to be disproportionally small compared to the decline in RPE65 expression demonstrated in the periphery. Also, differences in photoreceptor density do not explain the difference in labelling patterns between the two pigmentation phenotypes. The albino RPE showed a uniform expression of RPE65 in all regions, consistent with the findings from Huang et al. (2009). Albinos have a 25-30% reduction in their rod population across the retina, but retain a centre to periphery gradient within this population (Ilia and Jeffery, 2000). For this reason, it is unlikely that the differences in photoreceptor numbers are directly linked to the level of RPE65 expression alone.

The intensity of RPE65 expression between the two pigmentation phenotypes could not accurately be quantified as for a cytoplasmic label the masking effect of melanin content in the pigmented rats must be taken into account. The effects of melanin, however, do not provide suitable grounds for arguing the differential distribution of RPE65 between the centre and the periphery of the pigmented animals. All images were taken using the same settings on the confocal microscope ensuring that only the true expression of RPE65 was revealed. Another factor that is likely to affect RPE65 expression is the time of day that animals were sacrificed. RPE65 is the rate limiting step for the visual cycle (Gollapalli and Rando, 2004) and can increase or decrease the production of 11-*cis*-retinal and can, therefore, adapt the visual cycle depending on the different retinoid requirements needed in the light and dark (Gollapalli and Rando, 2004). However, as all animals were killed

midmorning and were housed under the same 12hour light/dark cycle, the differences between the pigmentation phenotypes were not due to different circadian time points. Furthermore, to ensure that the expression of RPE65 does not differ at different time points, animals were sacrificed late in the day – these results demonstrated the same results. This is also supported by Huang et al. (2009), who also failed to find any differences in albino mice that were dark or light adapted for 16 hours.

One of the motivations of this study was from an earlier finding by Al-Hussaini et al. (2008) showing that the peripheral RPE supports cell proliferation while the central region does not, therefore, highlighting an interest in the regional differences found here. Also, a study by Ishibashi et al. (2004) where 50 of the most highly expressed retinal genes were analysed, showed that 11 genes presented with a differential expression between the central and peripheral regions in the human RPE. Further, 2 of these were cell cycle genes, fragile histidine triad gene and c-KIT (Stem cell factor receptor), which were found to be downregulated in the central retina compared to the periphery. Kokkinopoulos et al. (2011) also recently showed that the central RPE in vivo in mice has significantly elevated gene expression levels of the cell cycle inhibitor $p27^{Kip1}$.

The marked differences between the pigmentation phenotypes in the number of Ki67 positive cells could be due to the differences that occur during development in the albino. Albinos have a diverse series of visual abnormalities in terms of their overall retinal architecture, cell numbers and pathways into the brain (Jeffery, 1997). These result from a

fundamental difference in the development of the albino retina compared to that of the pigmented animal. During development, albino retinas are more proliferative than the pigmented due to a lack of DOPA, an upstream element in the synthetic pathway of melanin, which has been shown to encourage cell cycle exit (Ilia and Jeffery, 1999, Tibber et al., 2006). The absence of normal DOPA levels disrupts retinal development causing the failure of many cells to leave the cell cycle appropriately leading to excessive proliferation followed by elevated cell death (Ilia and Jeffery, 1999, Tibber et al., 2006). The impact of reduced DOPA levels may not only be confined to development and may persist until maturity, influencing the proliferative capacity of the RPE. Differences between the rats other than pigmentation phenotype could also influence their proliferative capacity. These include variation in genetic background and ocular light experience.

Furthermore, on close inspection of the cells in the periphery of the pigmented and albino rats, it became evident that a population of cells in the periphery of the albino RPE contained large, distorted nuclei. These were not visible in the pigmented animals. These cells appeared to be polyploidal and will be investigated in detail in the following chapter (Chapter 3).

Consistent with these regional differences in cell proliferation, are the regional differences with the junctional marker ZO-1. Correlations between junctional modification and cell proliferation have been reported in a variety of epithelial tissues. Recent studies have shown that changes in tight junctions are associated with cell proliferation and polarity via

actin cytoskeletal modifications in mammalian tight junctions (Matter et al., 2005), intestinal epithelial cells (Tsukita et al., 2008) and in MDCK cells (Balda et al., 2003). These studies all stated that elevated tight junction density is associated with decreased levels of RPE proliferation. The results presented here are consistent with these studies, the tight junctions appear to be less regular in the periphery where the RPE has the capacity to proliferate. Towards the centre, the tight junctions appear to be straight and regular, an area where Ki67 positive cells are never found. In addition, Kokkinopoulos et al. (2011) show differences in the gene expression of E-cadherin, a transmembrane protein that plays a key role in cell adhesion, and phalloidin, a marker of F-actin which is associated with cell junctions, between peripheral and central regions. Both were significantly decreased in the peripheral regions of the RPE.

The expression levels of ZO-1 are related to the proliferation state of epithelial cells, a recent study by Georgiadis et al. (2010) shows that downregulation of ZO-1 induces RPE proliferation and de-differentiation in vivo. Tight junctions regulate epithelial cell proliferation and density via a ZONAB/ZO-1-based pathway (Balda et al., 2003). ZONAB (ZO-1 associated nucleic-acid-binding protein) is a Y-box transcription factor that binds to the SH3 domain of ZO-1 (Balda et al., 2003, Georgiadis et al., 2010). Y-box transcription factors are multifunctional regulators of gene expression and play a role in promoting proliferation (Matsumoto and Wolffe, 1998). Alterations in the levels of ZO-1 and ZONAB lead to changes in RPE cell differentiation, function and proliferation (Georgiadis et al.,

2010). Reduced ZO-1 expression in RPE cells leads to an increase in ZONAB expression resulting in increased RPE proliferation (Georgiadis et al., 2010).

As a small population of cells are proliferating in the periphery of the RPE, the different regions have different membrane protein characteristics. Cell addition within this established matrix requires established cells to shift to allow for the new cells, therefore, the peripheral cells are more loosely packed and may be adjusting their junctions as a result of cell production in this area. Cell migration within the RPE will be explored in greater detail in chapter 4. Interestingly, Del Priore et al. (2002) found that in humans, age-related RPE cell death occurred mainly in the macula, however, the cell density in this region remained unchanged. Instead, the density of RPE cells decreased in the periphery suggesting that cells are proliferating in the periphery and migrating towards the macula in order to compensate for the continuous loss of foveal RPE cells. Unfortunately, in my study several methods were used to determine cell death in the RPE but all were unsuccessful. This could be due to the fast rate in which apoptosis occurs and the rate in which dead cells are cleared. Rosenblatt et al. (2001) performed a series of experiments in which they demonstrated that a dying cell signals to its neighbouring cells to activate an actin and myosin dependent contractile mechanism that both extrudes the dying cell and also prevents the formation of a gap when the dying cell exits the epithelium. Interestingly, Nagai and Kalnins (1996) showed in chick embryo RPE that apoptotic cells are cleared by a mechanism that looks similar to this extrusion process. By removing the dying cell and repairing the gap that might have formed from the dying cell's exit, the extrusion process

maintains the barrier function of the epithelium. This could explain why it was not possible to detect apoptotic cells in the RPE flatmounts as they may have been extruded from the epithelium by this process. Alternatively, my findings could suggest that significant cell death does not occur within the RPE.

Otx2 is a transcription factor that is present from the earliest stage of development and it persists in the RPE through maturity (Rath et al., 2007, Bovolenta et al., 1997, Martinez-Morales et al., 2001, Simeone et al., 2002). For this reason, it is surprising that a population of cells in the equatorial region of the RPE fail to express this marker in both pigmentation phenotypes. The position of these otx2 negative cells offers little indication as to why some cells in this region fail to express this marker. One possibility could be as a result of a decline in otx2 expression in the neural retina with maturity (Rath et al., 2007). In this respect, the absence of it from the central/equatorial regions may indicate an age related effect as the retina develops with a centre to periphery gradient, and as such the central retina is older than the peripheral regions. To test this potential hypothesis, it would be necessary to examine the RPE sheet in much older animals, however, the RPE of P20 rats were examined and showed no differences between the patterns seen in the 3 month old rat, suggesting that this may not be an age related effect.

CRALBP plays a role in the visual cycle and mutations in this gene are associated with the early onset of autosomal recessive retinitis pigmentosa (arRP) (Saari and Crabb, 2005). The results shown here demonstrate a highly patchy distribution of CRALBP throughout

the RPE in both pigmentation phenotypes. These results differ from that shown by Huang et al. (2009) as they found that CRALBP expression in both albino rats and mice is relatively uniform across the RPE. First of all, the strain of albino rat that they used and the source of the antibody used differed to those used here. Most importantly, their tissue was prepared as frozen sections while the tissue in this experiment was viewed as a whole mount. Sectioned material has proven to be a less accurate method for determining the distribution of certain proteins throughout the entire RPE as it is not possible to get a global view of the tissue, only a sample. Had the RPE flatmounts used in this study been sectioned, it would have produced a consistent band of label across the length of the RPE in both pigmentation phenotypes, similar to the data shown by Huang et al. (2009). Huang et al. (2009) also noted that in some of their labelled sections, CRALBP was not present in the soma but was confined to the neural retina within the apical processes of the RPE, therefore, it is possible that this was lost by the removal of the neural retina in this study. In spite of this, it remains difficult to resolve the results of the two studies as here the clear patchy distribution of CRALBP in the RPE can be seen very clearly.

The data presented here highlights the molecular heterogeneity of the RPE and how this varies with pigmentation phenotype. The normal and widespread nature of RPE mosaicism suggests that it arises through normal and widespread processes that occur during normal development and postnatal ageing. This mosaicism within the RPE monolayer raises the question as to whether this may have functional consequences. For

instance, the environmental factors that occur throughout life that lead to the degeneration of cells, may affect the RPE cells in the mosaic differently. This would result in differing RPE cells differentially impacting the overlying photoreceptors. Understanding that the RPE is a mosaic of variable rather than homogenous cells is important for finding ways to prevent age-related RPE decline as it suggests that not one measure can be universally effective for all cells.

Chapter 3

The ageing albino RPE

3.1 Abstract

The retinal pigment epithelium (RPE) near the retinal margin proliferates slowly throughout life. Newly generated cells may move centrally to replace those lost with age. This is partly regulated by melanin, as in albino animals, this process results in a significant increase in polyploidal cells implying that cell cycle regulation may be abnormal. In this study, the impact of ageing on the RPE and adjacent outer retina is investigated. DA pigmented and albino Wistar rats aged 3 months and 20 months were used. Immunohistochemical analysis determined the RPE cell size, number of polyploidal cells, number of centrosomes and the effect of RPE65 on the RPE. Scanning electron microscopy (SEM) revealed the state of the overlying photoreceptors while ERGs and QRT-PCR showed differences in visual function. The results from this study show that differences in pigmentation phenotype affect the ageing response of animals, with albinos having an accelerated form of ageing. First, albino animals have a greater increase in RPE cell loss. Second, there is a threefold increase in the number of polyploidal cells, whilst less than 2% of DA RPE cells become polyploidal. Third, there is a significant decrease in the expression of RPE65 in the polyploidal cells. Fourth, the increased stress faced by the albino RPE leads to the marked deterioration of the overlying photoreceptor outer segments resulting in a decline in visual function. Overall, it seems that a culmination of factors result in the greater decline of visual function in the outer retina of the aged albino RPE. These results reveal that albinism is a progressive outer retinal disease.

3.2 Introduction

The peripheral RPE maintains the capacity to proliferate throughout life (Al-Hussaini et al., 2008, Ts'o and Friedman, 1967, Burke and Soref, 1988) contrary to the belief that the RPE is a post-mitotic tissue. Ts'o and Friedman (1967) systemically analysed the RPE in flatmounts looking at differences in cell size, density and morphology in a number of vertebrates and found the presence of two mitotic figures in the mature albino rat. More recently, Al-Hussaini et al. (2008) found that a proportion of mature RPE cells in pigmented animals have retained the capacity to enter the cell cycle and divide in peripheral regions. Furthermore, they demonstrated that the number of these cells was significantly elevated in albino animals. Several gene analysis studies have also highlighted the differences between the central and peripheral RPE in terms of proliferative capacity. In these studies they find that the central RPE downregulates cell cycle genes (Ishibashi et al., 2004) and maintains high expression levels of genes responsible for cell cycle inhibition (Kokkinopoulos et al., 2011).

Urodele amphibians such as newts and salamanders, have retained the ability to keep their cells in the cell cycle into adulthood and are able to regenerate the neural retina following injury through transdifferentiation of the proliferating RPE population (Stroeva and Mitashov, 1983, Chiba et al., 2006). This process requires the RPE to dedifferentiate, lose pigment granules and undergo several cycles of cell division (Stroeva and Mitashov, 1983). During transdifferentiation, the RPE cells undergo a transitional state where they

express both neural and RPE markers (Fischer and Reh, 2001, Chiba et al., 2006). This level of regeneration has not been seen in higher mammals, however, Fischer and Reh (2001) reported that mature RPE cells in the periphery of postnatal chicks expressed the transcription factors Pax6 and MITF. These are expressed early during development of the RPE but are downregulated as development proceeds. Moreover, these pigmented cells at the retinal margin expressed high levels of the cell cycle marker, proliferating cell nuclear antigen (PCNA). Data from this study suggests that the postnatal chick RPE retains a proliferative outer border making these RPE cells a potential source of neural regeneration. Most recently, a study carried out by Carr et al. (2011) demonstrated that a mechanism to activate transdifferentiation toward neural cells might exist, at least in part, in human RPE cells.

The capacity of the peripheral mammalian RPE to proliferate may be a vestige of what is found in amphibians as local damage to the RPE or retinal detachment in mammals results in excessive proliferation of the RPE around the retinal margin (Anderson et al., 1981, Kiilgaard et al., 2007). When these events are imposed centrally the same results do not take place or occur to a lesser extent (von Leithner et al., 2010). These differences in the proliferative capacity of the RPE in the periphery may be as a result of RPE development. Both the RPE and the neural retina develop with a centre to periphery gradient, such that the last cells to leave the cell cycle are in the periphery (Young, 1983).

Interest in the peripheral RPE was further elevated by the findings shown in the previous chapter where some cells in this region of the albino RPE contained cells with abnormal nuclear morphologies. These appear to be polyploidal and will be further investigated in this chapter. Polyploidy arises from errors in cell division which leads to a failure of cytokinesis (Ganem and Pellman, 2007) and results in cells containing either an increased number of nuclei, one enlarged nucleus or numerous fragmented micronuclei (Rieder and Maiato, 2004). To determine whether the RPE cells with abnormal nuclear morphologies described in the previous chapter, are in fact polyploidal, the number of centrosomes in each cell needs to be determined.

The centrosome is the main microtubule organising centre of the cell and plays an essential role in cell cycle progression and cell polarity (Mazzorana et al., 2011, Nigg, 2007). By controlling the number, polarity and distribution of microtubules, they coordinate all microtubule related functions including:

- Cell shape
- Cell polarity
- Cell adhesion and motility
- Intracellular transport
- Positioning of organelles

Furthermore, centrosome function is vital for chromosome segregation and cytokinesis (Nigg, 2002).

During the eukaryotic cell cycle, two precise duplication events occur – one is the replication of chromosomes and the other is the duplication of the centrosome (Winey, 1999). During the S phase of the cell cycle, the single centrosome that is present in the G1 phase is duplicated. The two centrosomes move to opposite poles of the cell forming the mitotic spindle. The spindle captures the chromosomes and ultimately serves to segregate one set of chromosomes and one centrosome to each progeny cell (Winey, 1999).

Figure 3.2.1: Centrosomes and the mitotic spindle apparatus. (A) A diagram of two centrosomes at opposite poles of the cell during chromosome segregation. (B) Immunohistochemistry showing centrosomes (red) and the mitotic spindle apparatus. Images taken from http://bio-ggs.blogspot.com/2009/12/fluorescnet-microscopy.html and http://cellstructure.pbworks.com/w/page/14755371/Vesicles%20and%20Centrosomes_3rd%20%20%3AP, respectively.

Maintaining proper centrosome number is necessary for genome stability and survival, therefore, the duplication and segregation cycles of centrosomes need to be coordinated to avoid ploidy changes (Nigg, 2002, Tsou and Stearns, 2006). For this reason, the structure and number of centrosomes are tightly regulated throughout the cell cycle

(Doxsey, 2001, Hinchcliffe and Sluder, 2001). Dysregulation of this organelle strongly correlates to aberrant proliferation and the onset of tumours (Mazzorana et al., 2011). Many human cancer cells show a high incidence of centrosome amplification, furthermore, cells derived from mice lacking the tumour suppressor gene p53, show defects in their centrosome duplication or function (Lengauer et al., 1998).

The cells in the RPE should at any moment in time, have only one or two centrosomes depending on which stage of the cell cycle they are in. The presence of an increased number of centrosomes within these cells would suggest that problems are occurring within the cell cycle of these cells leading to polyploidy (Margolis et al., 2003).

The cells with abnormal nuclear morphologies were only seen in the albino rats and may well be linked to the differences in the proliferative capacity between albinos and pigmented animals. The differences in cell cycle activities between the two pigmentation phenotypes could result from similar effects that a lack of melanin has on the developing eye. The reduction of melanin synthesis in albinos is associated with abnormal routing of the optic nerves, causing an excessive crossing of the fibres in the optic chiasm as well as foveal hypoplasia and cell specific deficits (Oetting and King, 1999, Oetting, 2000, Gronskov et al., 2007). The deficits that occur in the albino retina (described in detail in section 1.7) are regulated by the tyrosinase gene which is the key enzyme involved in melanin synthesis. Tyrosinase is responsible for catalysing the rate-limiting step which involves converting tyrosine to DOPA. DOPA is a well-known cell cycle regulator that slows

the pace of the cell cycle as well as also signalling cell cycle exit during development (Tibber et al., 2007, Tibber et al., 2006). As albinos have mutations in the tyrosinase gene, there is an absence of normal DOPA levels causing the disruption of normal retinal development, as many cells fail to leave the cell cycle at the appropriate time. This in turn results in increased cell production followed by excessive cell death (Ilia and Jeffery, 1999, Tibber et al., 2006). DOPA regulates the mitotic activity of cells during retinal development. During retinal mitosis, the retina forms transitory gap junctions with the RPE (Fujisawa et al., 1976, Hayes, 1976). In the mature retina, many gap junctions are gated by dopamine which restricts junction permeability (Vaney, 1994). This suggests that DOPA may influence the cell cycle by playing a role in gating junctional connections between mitotic profiles and RPE cells (Ilia and Jeffery, 1999). The reduced DOPA levels in the albino may cause junctions to remain more permeable, therefore, failing to restrict mitosis to a level that is necessary for normal development, whilst in pigmented animals the junctions are becoming progressively restricted during this period (Ilia and Jeffery, 1999). The impact of reduced DOPA levels may not only be confined to development and may persist until maturity influencing the proliferative capacity of the RPE.

Gaining an insight into RPE cell cycle mechanisms is vital as the regulation of this process would have significant implications for disease processes where the RPE is damaged, such as in age-related macular degeneration (AMD). The RPE is susceptible to many age-related diseases as it is positioned in an environment exposed to large amounts of oxidative stress (Beatty et al., 2000, Liang and Godley, 2003, Binder et al., 2007). First, its anatomic

location between the retina and choroid exposes the RPE cells to an oxygen-rich environment due to the high oxygen tension from the choriocapillaries (Liang and Godley, 2003). Second, its physiological function of phagocytosing the photoreceptor outer segments is a significant oxidative burden. Third, the strong illumination from focal light induces the generation of ROS.

Ageing has been linked to cumulative damage from oxidative stress (Harman, 1981) and to a continuous decline to mount a protective response to it (Hamilton, 1966, Kritchevsky and Muldoon, 1996, Paolisso et al., 1998, Rondanelli et al., 1997). With age, RPE cells lose their normal, functionally optimal phenotype. There is a decline in the melanin content of the cells, while lipofuscin and other complex granules increase (Boulton et al., 2004). One of the most prevalent of the many theories on ageing is the *mitochondrial theory*. In brief, this theory states that it is the production of reactive oxygen species (ROS) as by-products of respiration in the mitochondria that cause a variety of different forms of molecular damage within the cell leading to a reduced performance of a variety of cellular systems (Liang and Godley, 2003). The accumulation of ROS results in an age related RPE cell loss (Parapuram et al., 2010, Cai et al., 2000). Understanding the mechanisms that lead to RPE dysfunction in ageing is vital as the age related changes that occur in the RPE often lead to pathological tissue damage (Binder et al., 2007).

The RPE has several defences against oxidative damage (Shamsi and Boulton, 2001, Liang and Godley, 2003) to counter these deleterious effects. These include; the absorption and

filtering of light by melanin, the ability of cells to recognize and repair damaged lipids, proteins and nucleic acids, and finally the RPE contains antioxidants which reduce the rate of oxidation reactions by neutralising ROS (Boulton and Dayhaw-Barker, 2001, Miceli et al., 1994).

In this chapter I will investigate the effect of ageing on pigmented and albino rats to determine whether the lack of melanin would impact the structural and functional relationship between the RPE and photoreceptors more severely in the albinos. The hypothesis that albinism is a progressive disease of the mature RPE will be examined by tracing the development of the cells with abnormal nuclear morphologies and the consequent impact these cells will have on the ageing retina.

3.3 Methods

Animals

Dark Agouti (DA) pigmented and Wistar albino rats were used in this study as models for pigmented and albino animals respectively. Young (3 month) and old (20 month) animals were used in this study. To determine whether results from the wistar rats were species specific or applied to albino animals in general, another strain of albino rats were also used, Sprague Dawley (n=3). Three immature age groups were also used to see whether differences seen in the albino RPE exist early on in life. Wistar albino pups were used on postnatal day (P) 0 (n=3), P10 (n=2) and P20 (n=2).

Experiment	3 month DA	3 month albino	20 month DA	20 month albino
ZO-1 and otx2 whole mount labelling	6	6	6	6
Ki67 and BrdU whole mount labelling	6	6	-	-
Pericentrin and tubulin whole mount labelling	6	6	-	-
RPE65 and otx2 whole mount labelling	6	6	6	6
Electroretinography	3	3	3	3
Scanning electron microscopy	3	3	3	3
qPCR	3	3	3	3

Table 3.3.1: A table showing the number and age of animals used for each individual experiment that was designed to investigate the effect of ageing on pigmented and albino rats.

The animals were housed with a 12hour light/dark cycle in a temperature controlled environment and were fed ad libitum. All experimental procedures were carried out under the United Kingdom (Scientific Procedures) Act 1986. The table above provides the number of animals used in each of the procedures.

Histology

Following euthanasia with CO_2, eyes were removed and fixed in 4% paraformaldehyde in phosphate-buffered saline (PBS) for 1 hour at room temperature (RT). After washing in PBS, eyes were either prepared for retinal whole mounts or were cryo-preserved in 30% sucrose overnight at 4^{o}C . The cornea and the lens were removed and the eyecups were embedded and frozen in optimal cutting temperature compound (OCT, Agar Scientific UK). Cryostat sections were cut (10µm) using a Lecia CM3050 cryostat and were thaw mounted onto charged slides. To obtain whole mounts, the RPE and attached choroid were isolated and radial incisions were made with microsurgical scissors to flatten the tissue.

Immunohistochemistry

Retinal sections were blocked for 1 hour in 5% normal donkey serum in 0.1M/L PBS with 0.3% Triton X-100 at room temperature. Sections were then incubated overnight in primary antibodies, diluted in 1% normal donkey serum in 0.3% Triton X-100 (for negative controls, primary antibodies were omitted). After rinsing the slides in PBS, sections were incubated for 1 hour in the secondary antibodies (diluted in 2% normal donkey serum in 0.3% Triton X-100) at RT. Nuclei were subsequently stained with 4_,6-diamidino-2-phenylindole (DAPI) (Sigma-Aldrich, UK). Specimens were washed three times in PBS followed by three washes in Tris buffer saline (pH 7.4) before being mounted with Vectashield (Vector Laboratories, UK).

Wholemounts were processed using a modified protocol to the above. They were blocked for 2 hours in 5% normal donkey serum in PBS with 3% Triton X-100 at RT and incubated overnight in primary antibodies, diluted in 1% normal donkey serum in PBS with 3% Triton X-100. After washing several times in PBS, the eyecups were incubated in the secondary antibodies for 2 hours in 1% normal donkey serum in PBS with 0.3% Triton X-100. As above, the eyecups were then washed and mounted with vectashield. Tables 3.3.2 and 3.3.3 show the primary and secondary antibodies used, respectively.

Table 3.3.2: The primary antibodies used to investigate the nuclear abnormalities found in albino RPE cells; the proliferative differences between the two pigmentation phenotypes; and the differences in visual function.

Antibody name	Dilution	Manufacturer	Catalogue number	Species raised	Tissue specificity	Target
Otx2	1:1000	Millipore	ab9566	Rabbit	-	Nuclear transcription factor
Otx2	1:500	Santa Cruz	sc-30659	Goat	-	Nuclear transcription factor
ZO-1	1:100	Abcam	ab59720	Rabbit	Epithelial cells	Tight junctions
Ki67	1:1000	Vector laboratories	VP-K451	Rabbit	All proliferating cells	Nuclei
BrdU	1:5	Made in the lab	NA	Mouse	Proliferating cells in S phase of cell cycle	Nuclei
RPE65	1:500	Millipore	MAB5428	Mouse	RPE	RPE microsomal membranes
GT335	1:500	Gift	NA	Rabbit	Centrioles	Polyglutamated tubulin

Table 3.3.3: The secondary antibodies used to investigate the nuclear abnormalities found in albino RPE cells; the proliferative differences between the two pigmentation phenotypes; and the differences in visual function

Antibody name	Dilution	Manufacturer	Catalogue number
Alexa Fluor 488 fragment of goat anti mouse IgG (H+L)	1:2000	Invitrogen	A11017
Alexa Fluor 568 Donkey anti-Rabbit IgG (H+L)	1:2000	Invitrogen	A10042
Alexa Fluor 488 Donkey anti Rabbit IgG (H+L)	1:2000	Invitrogen	A21206
Alexa Fluor 488 donkey anti-goat IgG (H+L)	1:2000	Invitrogen	A11055
Alexa Fluor 568 Donkey anti Mouse IgG (H+L)	1:2000	Invitrogen	A10037

Sections and wholemounts were viewed and images captured using two microscopes. Either an Epi-fluorescence bright field microscope (Olympus BX50F4,Olympus, Japan) where images were captured as 24-bit colour images at 3840 x 3072 pixel resolution using a Nikon DXM1200 (Nikon, Tokyo, Japan) digital camera and ACT-1 imaging software (Nikon Instruments Europe B.V) or with a laser scanning confocal microscope (Leica TCS_SP2 AOBS).

BrdU Antibody Preparation

First, the hybridoma cells – b lymphocytes fused with lymphoma cells, were removed from liquid nitrogen and thawed. Before plating, medium F10 was added to wash out the DMSO as this is not good for the cells. The thawed cells were transferred into 10ml of culture medium and spun down for 5 minutes at +4°C at 12 000 rpm. The supernatant was discarded and the pellet was gently resuspended in 10ml of fresh DMEM/F12 medium supplemented with 10% fetal calf serum (FCS) and 1:100 strep (penicillin and streptomycin). The cells were then incubated at 37˚C with 5% CO_2. After 3 days of culture, the cells were then checked for viability under the microscope and split into 3-4 falcon tubes. Hybridoma cells can be removed from the plate by gentle pipetting and do not need to be trypsinized. The tubes were spun down for 5 minutes at 15 000 rpm and the supernatant was removed from each tube. The supernatant is the BrdU antibody that will be used in the experiments.

BrdU Injections and immunohistochemistry

5'-bromo-2'-deoxyuridine (BrdU) is a thymidine analog that is incorporated into dividing cells during DNA synthesis (Wojtowicz and Kee, 2006). Once the BrdU has been incorporated into the new DNA, it remains there and is passed down to daughter cells following cell division.

Animals were injected intraperitoneally (i.p) with BrdU (Sigma, UK) (50mg/kg) every day at the same time (in the morning) for 5 days. They were then left for three weeks and sacrificed using CO_2. Their eyes were removed and processed following a similar protocol as that described above, however, in order to detect the BrdU staining antigen retrieval using 6M HCl diluted in 0.1% triton X-100 must be undertaken.

Eyes were dissected and blocked for 2 hours in 5% normal donkey serum in PBS with 3% Triton X-100 at RT and incubated overnight in the Ki67 primary antibody, diluted in 1% normal donkey serum in PBS with 3% Triton X-100. The following day, the eyes were washed in PBS and placed into the secondary antibody. Following this the eyes were washed and fixed for 10 minutes in 4% paraformaldehyde in PBS. To ensure that the fixative doesn't curl the tissue the eyecups were mounted onto slides and covered with a cover slip. After 10 minutes, the tissue was washed in PBS three times for 5 minutes each. During this time, the 6M HCl was prepared. Again the eyecups were mounted onto slides and the 6M HCl was added and left for 30 minutes. The eyes were washed in PBS and blocked again for 2 hours at RT. The BrdU primary antibody was added and left overnight. The next day the secondary antibody was applied and the same steps as previously were carried out.

Electroretinography (ERGs)

Animals were dark-adapted overnight before ERG on both eyes. Animals were anaesthetised by Ketamine/Dormitor (37.5% Ketamine (Fort Dodge, UK), 25% Dormitor (Pfizer, UK) and 37.5% sterile water at 0.2mL/100g, i.p. supplemented as required). Under

red-light conditions, pupils were dilated using topical atropine and phenylephrine. The animal was placed in a light-tight box and was kept warm on a thermostatically regulated heated platform which was set to 36°C. ERG recordings were carried out via platinum loop electrodes placed on the cornea and a reference platinum electrode was placed on the scalp of the animal alongside a platinum earth electrode placed on the lower back (s.c.) of the animal. The filter settings ranged from 0.312 Hz to 300 Hz with a total sweep time of 270ms (20ms pre stimulus and 250ms post stimulus). Flash stimuli were presented via an LED stimulator, log intensity −6.5 to +3, under scotopic conditions. After scotopic testing was completed, animals were light-adapted to 20 cd/m^2 background for 20 min.

Table 3.3.4: The conditions for the ERGs at the varying light intensities

Intensity Log	Intensity cd.s/m2	step	**Sweeps per result**	Inter sweep delay (ms)
-6.50031	3.16E-07	1	15	1000
-6	1.00E-06	2	15	1000
-5.50004	3.16E-06	3	15	1000
-5.22185	6.00E-06	4	15	1000
-4.69897	2.00E-05	5	15	2000
-4.22185	6.00E-05	6	15	3000
-3.69897	0.0002	7	15	4000
-3.22185	0.0006	8	15	5000
-2.82391	0.0015	9	10	6000
-2.4437	0.0036	10	10	7000
-2.03621	0.0092	11	4	10000
-1.62709	0.0236	12	4	15000
-1.22185	0.06	13	4	20000

-0.81023	0.1548	14	4	20000
-0.41851	0.3815	15	4	20000
-0.01579	0.9643	16	4	20000
0.376029	2.377	17	4	20000
0.884648	7.6674	18	3	25000
1.365312	23.1906	19	3	30000
1.892634	78.097	20	3	40000
2.387514	244.07	21	3	50000
2.858578	722.0671	22	3	60000

Scanning Electron Microscopy (SEM)

Directly after ERGs were carried out on the young and old animals, they were euthanised using CO_2 and the eyes were removed and placed on ice. The retinae of each animal were placed straight into 2% paraformaldehyde and 2% glutaldehyde in PBS for 24 hour fixation. After briefly washing the retinae in PBS, the specimens were post fixed in 1% osmium tetroxide in 0.1M PBS for 2 hours. Specimens were washed in distilled water and dehydrated through a graded series of ethanol. After washing in absolute ethanol, the tissues were dried with a critical dry point apparatus. Once this was achieved they were coated with gold palladium and images were captured using a Carl Zeiss scanning electron microscope. In order to ensure that there was no bias at the time of capturing images, the samples were only labelled as numbers and it was not possible to know which sample was being looked at.

Gene expression methods

To determine the effect of ageing on RPE function in both albino and pigmented rats, gene expression analysis was undertaken using quantitative real-time PCR (QRT-PCR). For each pigmentation phenotype, 3 young animals and 3 old animals were used. Animals were terminated immediately after the ERGs were carried out. Their eyes were enucleated and placed into sterile eppendorf tubes on ice ready for RNA extraction. The RNA extraction was followed straightaway by the first strand cDNA synthesis.

Prior to the RNA extraction, all work benches that were to be used were wiped down with RNase away (Molecular BioProducts). All surgical tools were also soaked in RNase away and wiped down with sterile RNase-free water. Sterile and packed syringes, needles and scalpel knives were used for each RNA extraction.

Total RNA extraction

Previous work has shown that the RPE produces a very low yield of RNA. RNA extraction using TRI Reagent™ was first tested but a very low yield of RNA was retrieved, for this reason the Qiagen RNeasy Micro Kit was used as this is specifically designed to provide a good yield of RNA from tissues in which it is difficult to retrieve RNA from.

Using this kit, only a maximum of 5mg of fresh tissue can be used which is more than enough to pool the RNA from 2 eyes together. Before starting the extraction, several solutions must be prepared:

1. 10µl of β-Mercaptoethanol must be added to 1ml of Buffer RLT
2. The Buffer RPE needs to be diluted with 100% ethanol
3. RNase-free water needs to be diluted with 100% ethanol in order to obtain 70% and 80% ethanol.

The other reagents used for this RNA extraction are listed in the Table 3.3.5.

Table 3.3.5: Reagents used for RNA extraction

Component	Supplier
Buffer RLT	Qiagen
Ethanol	Fisher Scientific
Buffer RW1	Qiagen
Buffer RPE	Qiagen
RNase-free water	Qiagen

Following the removal of the eyes, they were placed on ice and dissected open using a dissecting microscope. After the removal of the cornea, iris and lens, radial incisions were made into the eye cup enabling for it to be flattened. Using a 10 blade scalpel, the ciliary body was removed from the peripheral edge of the eye allowing for the easy removal of the retina. Using forceps, the RPE was gently scraped away from the eye cup and the tissue placed into 350µl of Buffer RLT. With the use of an eppendorf shaped pestle, the RPE was disrupted followed by homogenisation using a 27, 25 and 23 gauge needle fitted to a syringe. Once the RNA from all the eyes had been removed, the individual

microcentrifuge tubes containing the lysate were centrifuged for 3 minutes at full speed (13 000 rpm). The supernatant was transferred to a new tube and 350µl of 70% ethanol was added. The RNeasy MinElute spin columns were removed from the fridge and the samples were transferred into the spin columns. Samples were centrifuged for 15s at 10 000 rpm and the flow through was discarded. To wash the spin column membrane, 700µl of Buffer RW1 was added and the samples were centrifuged for 15s at 10 000 rpm. The spin columns were placed into new collection tubes and 500µl of Buffer RPE was added. After centrifuging, the flow through was discarded and 500µl of 80% ethanol was added. The samples were centrifuged for 2 min at 10 000 rpm and then placed into new collection tubes, where they were then centrifuged with their lids open for 5 minutes at full speed. Finally, the spin columns were placed into 1.5ml collection tubes and 10µl of RNase-free water was added directly to the centre of the spin column membrane. The samples were incubated on the bench top for 10 minutes before they were centrifuged to elute the RNA.

Measuring concentration and purity of extracted RNA

With the eluted RNA samples placed on ice, the concentration of the RNA was measured using the Nano Drop (NanoDrop Technologies, USA).

DNAase treatment

Prior to cDNA synthesis, the RNA samples were treated with DNase to remove genomic DNA contamination. The DNAse I (Invitrogen) kit was used. For each sample, 8µl of the extracted RNA was mixed with 1µl of the 10X DNase buffer and 1µl of the DNase I enzyme. This mixture was incubated at RT for 15 minutes and then 1µl of 25mM EDTA was added. Each sample was then incubated at 65°C for 10 minutes and then chilled on ice for 2 minutes.

First Strand cDNA synthesis

The first strand cDNA synthesis was carried out using the Superscript III (Invitrogen) kit. First a master mix was made, consisting of the 2x RT reaction (10 µl per sample) and the RT Enzyme mix (2 µl per sample). Then 12 µl of the master mix was added per tube and incubated at 25°C for 10 minutes. Following this the samples were incubated at 50°C for 30 minutes and the reaction was then terminated at 85°C for 5 minutes. The samples were chilled on ice and 1µl of RNase H was added to each sample and was further incubated at 37°C for 20 minutes.

Primer Design

The majority of the primers were designed using Perl Primer (http://perlprimer.sourceforge.net/). The following specifications were used in order to obtain primers specific for the genes of interest:

1. Melting temperature between 58 and 60˚C
2. Primer should be 20-30 bp long
3. The product should be 100-400bp
4. The product should span an intron to prevent amplification of genomic DNA

Following the primer design, a BLAST search was carried out to ensure that the primers would be specific only for the target gene (http://blast.ncbi.nlm.nih.gov/Blast.cgi). All primers were synthesised by Eurofins MWG Operon. The primers used for quantitative real-time PCR are shown in table 3.3.6.

Table 3.3.6: Primer sequences for all the genes tested

Target Transcript	Primer Sequence (5' -> 3')	Melting Temp. (°C)
MFG-E8	Forward: CGGAGACAAGGAGTTTATGG Reverse: AGGAATCGTGTTATTCTTCAGG	81.6
MERTK	Forward: AAGCAGCCTGAGAGCGTGAATG Reverse: TGGGGAAGGGATGACTTTGATG	83.0
Beta actin	Forward: TGTCACCAACTGGGACGATA Reverse: GGGGTGTTGAAGGTCTCAA	83.8

Quantitative Real Time PCR (QRT-PCR)

Using fluorescent DNA binding dyes, QRT-PCR allows for the visualisation of PCR product accumulation throughout the PCR. PCR product accumulation is dependent on the concentration of the target sequence present. Therefore, a sample with a high concentration of the target sequence will accumulate a product at a much earlier cycle than a sample with a lower concentration. Once the reaction is complete, amplification

plots are produced enabling the calculation of the relative changes in gene expression of target gene relative to the control gene.

The ABI PRISM™ 7700 Sequence Detection system (Applied Biosystems) was used to carry out the QRT-PCRs. This machine contains a built in thermocycler with 96 well positions, an argon ion continuous wave laser, and a spectrograph with a charge-coupled device camera. During the PCR reaction, fibre optics distribute the laser light among the 96 wells. Following this, the fluorescence between 500 and 660nm is detected and converted into a form appropriate for analysing using the Sequence Detector software (SDS), version 2.2 (Applied Biosystems). SYBR I green dye (Biosystem) was used to carry out these QRT-PCR reactions. It binds specifically to double-stranded DNA, and after each cycle of the PCR as the DNA content increases, the fluorescence intensity of the dye increases proportionally.

Before the samples were tested, the primers were tested using cDNA from a separate animal to preserve using the RNA extracted from the young and old pigmented and albino rats. A Power Sybr Green Master Mix (Applied Biosystems) consisting of an optimised buffer, the Sybr Green I dye, an AmpliTaq Gold DNA polymerase, PCR components and a passive reference dye (ROX) was used for all the QRT-PCR reactions. To this master mix, distilled water and the forward and reverse primers were added in the following volumes:

Power SYBR Green Master Mix	42.5µl
Distilled Water	39.5 µl
Forward Primer	1 µl
Reverse Primer	1 µl

For each primer to be tested this mixture was made up and 25µl aliquots were placed into individual wells on a clean RNase free 96-well plate. 0.5µl of the sample cDNA was added to the first triplicate, 0.5µl of a sample of the DNA where the reverse transcription enzymes was not added during the reaction (NRT cDNA) was added to the second triplicate, followed by 0.5µl of a no template control (NTC) where molecular grade water was added to the mix. The NRT and NTC ensure that the primers are specific and are a good way of ensuring that there is no contamination in the sample and that primer dimers will not form.

The thermocycling conditions used for primer testing were slightly different from a standard PCR, they were carried out on a Techne Progene thermocycler, using the following parameters: 95 °C for 10 minutes to activate the DNA polymerase, then 40 cycles of 95 °C for 15 seconds, and 60 °C for 60 seconds for both primer annealing and product extension.

The 96-well plate containing the primers was loaded into the ABI PRISM™ 7700 Sequence Detection System. The temperature was increased from 60 to 95 °C over 20 minutes and

the fluorescence recorded at each 0.1 °C change in temperature. The fluorescence data was then exported into the Dissociation Curve (version 1.0) software (Applied Biosystems) for analysis. The melting temperatures of the products in the samples were visualized by plotting the rate of change of fluorescence, the first negative derivative (–d(Fluorescence)/d(Temperature) versus temperature). From this data the melting temperature of the product was seen as a peak. The melting temperature is a useful tool for determining the temperature at which the fluorescence should be recorded during the real-time PCR. For optimum results the recording should be made at a temperature that is 2°C below that of the product melting temperature. The dissociation curve also indicates the presence of any primer dimers or other undesired amplified products that would interfere with the true reading.

Once the primers were all tested and the melting temperatures recorded the QRT-PCR reactions could be carried out for each gene to be tested using the samples from the young and old pigmented and albino rats.

Each QRT-PCR was carried out in a reaction volume of 25µl loaded into a 96-well plate. The reactions contained 300 nM of each primer as well as the RPE cDNA templates from the albino and pigmented animals. In order to reduce intra-assay variability, master mixes were made containing both the primers and Power Sybr Green Master Mix, diluted in molecular grade water. An excess was always made to allow for residual loss during pipetting. Each cDNA sample was quantified as a triplicate, enabling a measurement of

intra-assay variance. The master mix was made up to a total volume of 85µl (in excess as only 75µl are needed for each sample) to which 1µl of the cDNA was added and mixed thoroughly. A triplicate no template control was also set up on every plate to check for contamination. After each sample was mixed, triplicates of 25µl were pipetted from each aliquot into a 96 well plate. The optical caps were placed on top of the wells and the plate was loaded into the sequence detection instrument.

Thermocycling and data collection

The sequence detection system was controlled by the SDS 2.2 software. The cycling conditions consisted of an initial *Taq* activation step of 95°C for 10 minutes, followed by 40 cycles of 95°C denaturation for 15 seconds, followed by a 60°C annealing/extension step for 30 seconds. A final data collection step of 30 seconds was added to each cycle (x), with the fluorescence measured at 2°C below the melting temperature of the desired product as determined by melting curve analysis. This ensures that any primer dimers formed, do not contribute to the measured fluorescence. During data collection periods, the system records fluorescence every 7 seconds.

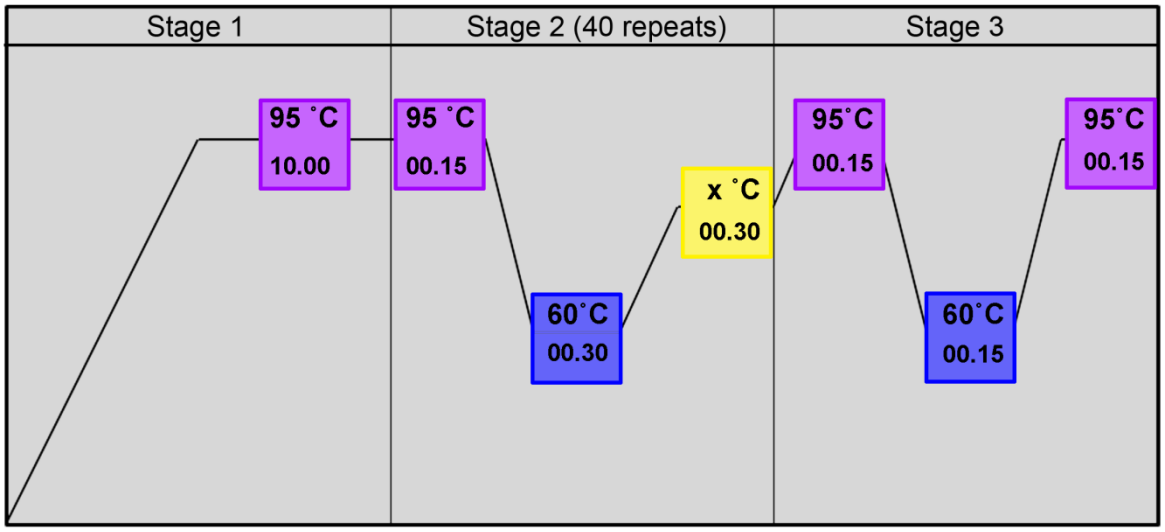

Figure 3.3.1: A diagram showing the cycling conditions for the QRT-PCR.

Data analysis

Two initial corrections were made automatically to the raw fluorescence data by the SDS software. First, the data was corrected to ROX, a passive internal reference dye. ROX is contained within the Sybr Green mix and is used as a control for the amount of reagent in each PCR, therefore, controlling for any pipetting errors and any evaporation within the tubes. For each cycle, the fluorescence is recorded for Sybr Green and is corrected with respect to the reference dye to give a relative fluorescence (R_n) value. Second, R_n values are further modified by the subtraction of the background fluorescence levels. The background fluorescence is calculated as the mean fluorescence during the first 3 to 15 cycles of the PCR – this is before products can be seen to accumulate.

Once recorded, the R_n values were exported to a text file and imported into Excel (Microsoft) where they were further analysed using an automated workbook called Data

Analysis for Real-Time PCR (DART-PCR) (Peirson et al., 2003). This workbook enables the rapid calculation of threshold cycles, amplification efficiency and the resulting R_0 (the theoretical starting fluorescence) values (with the associated error) from the raw data exported from the SDS software. Differences in amplification efficiency were assessed using one way analysis of variance (ANOVA) based on the null hypotheses that:

1. Amplification efficiency is comparable within sample groups
2. Amplification efficiency is comparable between sample groups

The differences between the normalised pigmented and albino MFG-E8 and MERTK expression were assessed using a 2 tailed Student's t-test, assuming unequal variance.

Gel electrophoresis

The PCR products were separated and visualised by agarose gel electrophoresis. Gels were prepared to 1.5% agarose into 1xTAE (Tis/Acetic Acid/EDTA buffer 50x, BIO-RAD). 1.5g of agarose was dissolved into 100ml of 1xTAE by heating in a microwave. After the mixture had completely dissolved and cooled to approximately 50°C, ethidium bromide was added (0.5µl/ml). The gel was poured into a sealed tray and a comb was inserted at the top to make the loading wells. The gel was left to cool and solidify for 30 minutes.

5µl of buffer was added to each PCR product so a total of 25µl of sample was loaded into the gel. 15µl of a 100bp or 1kb ladder was also loaded onto the gel for reference. Once all the samples had been loaded, the gel was submersed in 1xTAE in a gel tank and

electrophoresed to the desired separation at 60–90 V. Once completed, the gel was removed and placed onto a UV transilluminator to view the DNA in a gel documentation system. Here a digital photo of the gel was also taken.

DNA gel extraction

Once viewed on the UV transilliuminator, the products were excised using a sterile scalpel blade. Each band was cut and placed into a 1.5ml eppendorf tube. To each tube 75ul of Buffer QG from the QIAquick Gel Extraction Kit was added. The manufacturer's guidelines were then followed until the end, where the DNA was eluted in 30µl of elution buffer.

Sample sequencing

Once the DNA had been extracted from the gel band, the product was sequenced to ensure that it was the correct product for the gene that had been tested. To sequence the products, the following were mixed together for each sample:

- 4 µl Big Dye
- 2 µl SB buffer
- 8 µl molecular grade water
- 0.5 µl of the 25 µM primer (either the forward or the reverse)

Once these were added, 5.5µl of the purified product was added. The tubes for each sample were put into a Techne Progene thermocycler. The cycling conditions consisted of

3 minutes at 95 ^{o}C for the initial denaturation. This was followed by 35 cycles of 10 seconds at 96 ^{o}C for denaturation, 10 seconds at optimum primer annealing temperature of 50 ^{o}C, followed by 4 minutes at 60 ^{o}C for primer extension. The reaction was then held at 10 ^{o}C overnight.

The following day, the sequencing mix was cleaned up. First, the samples were centrifuged at 4°C at 13 000 rpm. Then in order to precipitate the sequencing reaction, a mixture of 0.5µl of (0.5 M) EDTA, 2µl of (3M, pH5) NaOAc and 50µl Benzene free (96%) EtOH was added. The samples were left for 15 minutes at RT to incubate. The mixture was then centrifuged at 13 000 rpm at 4°C for 30 minutes. The supernatant was removed carefully, making sure not to remove the pellet, and 70µl of 75% EtOH was added to each tube. Again the samples were centrifuged at 13 000rpm for 15 minutes. The supernatant was removed and the pellets were left to air dry for 5-10 minutes at 50°C. To dissolve the pellets, 12µl of Hi Di Formamide was added to each tube just before loading into the ABI automated sequencer. The results were viewed using Ridom TraceEdit.

RPE Cell Analysis

Morphological analysis – measuring cell area, density and nuclear characteristics of the RPE cells in the pigmented and albino rats

Consecutive digital images were taken along a strip of the flat mounted RPE, starting from the periphery and moving towards the centre at 400µm intervals using a motorized

microscopic stage. From each retina, x400 magnification epi-fluorescence images were taken from three radially separated equidistant strips. Separate images were taken from the green channel (ZO-1) and the red channel (otx2) which were later merged using Photoshop CS4.

The RPE was divided into 3 regions: periphery, equator and centre, in the same way as described in chapter 2. To measure cell area, the first most peripheral image was used and every cell in a 520µm x 520µm area was analysed. Using Adobe Photoshop CS4, individual cells were outlined and the cell area measured in μm^2. Statistical comparisons for differences in cell size were undertaken using the Kruskal-Wallis test followed by the Dunn's multiple comparison test.

Cell densities were calculated by counting individual cells within a 170μm^2 area. The total number of cells, the number of cells presenting with a normal nuclear morphology and the number of cells exhibiting abnormal nuclear morphology were counted and recorded.

To assess the number and type of polyploidal cells, the nuclei in every cell in a 520µm x 520µm area was analysed. Large cells with polyploidal nuclei were defined as having a nuclear diameter greater or equal to 2 times the SD of the mean to minimise the potential for producing false positive results. The mean diameter was based on the diameter of nuclei in pigmented rats. Fragmented and multi-nucleated cells were easily distinguishable.

Statistical comparisons for differences in the percentage of polyploidal cells in the young and old pigmented and albinos rats was undertaken using a Mann Whitney U Test.

Centrosome quantification

X400 epi-fluorescence images were taken of RPE flatmounts. Every cell within the image was analysed and the number of centrosomes surrounding the nucleus recorded.

Quantifying the effect of RPE65 on polyploidal cells

X200 epi-fluorescence images were taken of the whole retina. Areas of 1.9mm x 1.3mm were analysed in the periphery of the RPE as this is where the highest percentage of polyploidal cells are seen. Cells within this area where individually assessed for RPE65 expression using the function on Photoshop which measures mean pixel density. Each cell in this area was outlined using the magic wand tool and the mean pixel density was recorded using the record measurements tool.

3.4 Results

Three distinct types of cells with abnormal nuclear morphologies were present in the albino RPE

Immunohistochemical staining using otx2 (red) to show nuclear morpholgy and ZO-1 (green) demonstrating the RPE cell boundaries, revealed 3 distinct cell types with abnormal nuclei in the albino RPE (Figure 3.4.2). These include cells with one very large nuclei (Figure 3.4.2A), cells with multiple fragmented nuclei (Figure 3.4.2B) and cells that were polynuclear containing more than 3 nuclei of a normal size (Figure 3.4.2C). In pigmented animals cells with such features are rarely found (Figure 3.4.1A). Nuclei in pigmented rats with normal RPE cells were approximately 6-7µm in diameter with very little variation. In the albinos, however, cells with normal nuclei had a similar size diameter but the cells with abnormal nuclear morphologies could be as large as 15µm in diameter (Figure 3.4.1B).

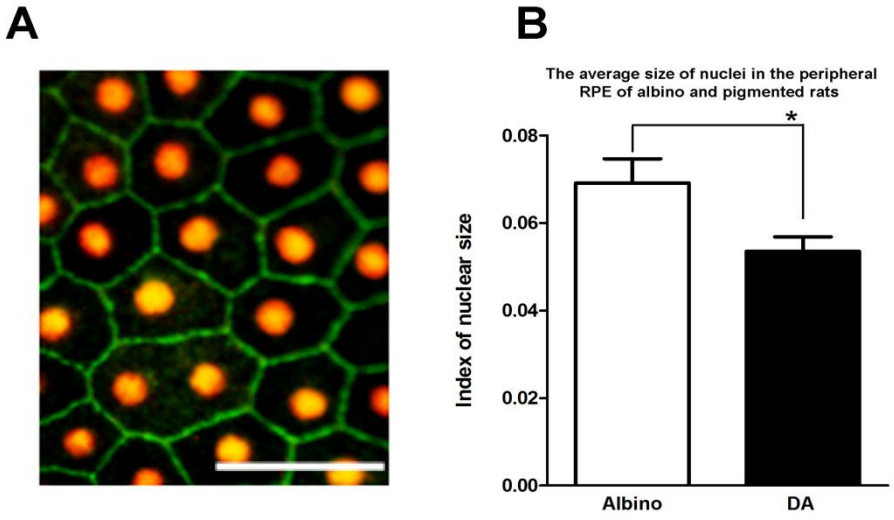

Figure 3.4.1: (A) ZO-1 and otx2 staining showing the morphology of the RPE cells in the periphery of a 3 month young pigmented rat. Cells with an abnormal morphology are not present. (B) Graph showing that the average size of nuclei in the periphery of the albino RPE is significantly larger compared to that of the pigmented DA ($p<0.05$). Scale bar-50µm.

Sprague Dawley albino rats were also tested to determine whether these abnormal cells are strain specific. Immunostaining the RPE of these rats gave the same results – cells with abnormal nuclei could be seen in the periphery of the RPE. For this reason, it appears that these cells are a phenomenon of the albino RPE and not just individual strains.

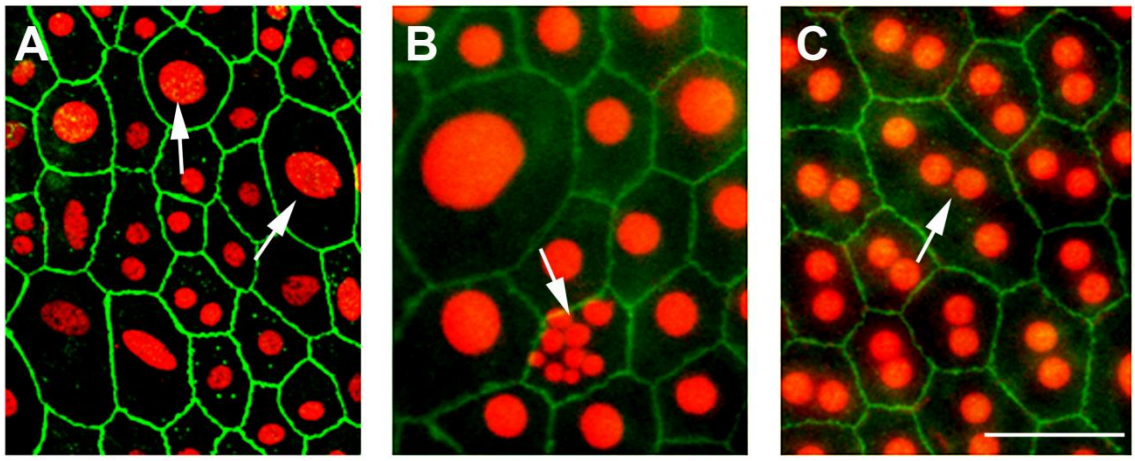

Figure 3.4.2: Three distinct types of cells with abnormal nuclear morphologies were present in the peripheral region of the albino RPE. These cell types were cells with a single enlarged nucleus (A), cells with fragmented nuclear material (B) and cells containing 3 or more normal sized nuclei (C). Immunohistochemical staining was used: otx2 (red) shows the nuclear morphology and ZO-1 (green) shows the RPE junctions. Scale bar - 50µm.

Abnormal nuclear morphology appears from P10

To determine whether the abnormal nuclear morphologies present in the albino RPE are a continuation of the developmental regularities known to occur prenatally in albinos, immunohistochemical staining using ZO-1 (green) and otx2 (red) was again used on flatmounts of rats from PO (the day of birth), P10 and P20 (Figure 3.4.3). The RPE was systematically scanned and appeared normal in the P0 rats, however, from P10 clear nuclear abnormalities became apparent in the peripheral RPE. Enlarged and elliptical nuclei could be seen in both the P10 and P20 albino rats. For this reason, it seems that the development of these cells is a post natal event and not a developmental abnormality.

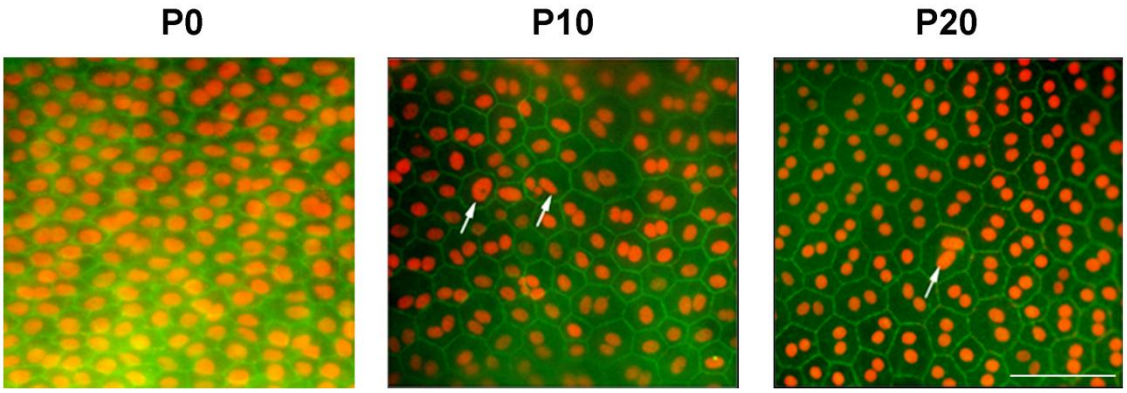

Figure 3.4.3: Cells with an abnormal nuclear morphology appear from post-natal day 10. The development of these abnormal nuclei was traced from P0 to determine when they appeared. They were not present at P0 but were seen from as early as P10. This suggests that the abnormal morphology in the adult albino is not a continuation of developmental irregularities known to occur prenatally. Scale bar - 50µm.

No significant difference in the number of BrdU positive cells between pigmented and albino rats

BrdU is a thymidine analog that is incorporated into DNA only during the S phase of the mitotic process (Kee et al., 2002, Wojtowicz and Kee, 2006). Once incorporated, BrdU will remain in place and be passed down to daughter cells folllowing division. Ki67, on the other hand is a large nuclear protein that is expressed in dividing cells for most of their mitotic process. It is not expressed during the resting phase (G_0) and during the early G1 phase of the cell cycle. The expression of Ki67 begins at the onset of late G1 and ends once the cell exits the cycle and is in the G_0 phase (Wojtowicz and Kee, 2006). Whilst BrdU shows the history of a cell, allowing for tracking the fate of divided cells and their progeny, Ki67 shows the cell cycle state in the moment of time the animal was sacrificed.

Prelimary studies (not shown here) testing the use of BrdU and Ki67 as proliferative markers showed that after one pulse of BrdU, followed by sacrificing the animal 24 hours later, resulted in very few BrdU positive RPE cells being present, with approximately 3-4 cells found within the entire RPE sheet. After pulsing the animals once everyday for 5 days and then leaving them for 3 weeks until sacrifice, the highest number of BrdU positive cells was achieved. After 3 weeks it became evident that BrdU was being diluted out of the cells as the number of BrdU positive cells was significantly reduced at 4 weeks (this data can be seen in Figure 4.4.2 in chapter 4). The number of Ki67 positive cells remained uniform for each experiment. For this reason, in this experiment to obtain the maximum number of proliferating cells, both the pigmented and albino animals were given an intraperitoneal injection everyday for 5 days and were then left for 3 weeks.

As shown previously, the albino rat has ten times more Ki67 positive cells in the RPE compared to the pigmented indicating that at any moment in time, the albino RPE has more proliferating cells (Al-Hussaini et al., 2008). Rats were pulsed with BrdU for 5 days and left for 3 weeks and the number of BrdU positive cells were counted. Interestingly, there was no significant difference in the number of these cells between the two pigmentation phenotypes (Figure 3.4.4). This suggests that in the albino RPE, cells are entering the cell cycle in which they are Ki67 positive but become arrested and are unable to complete cell division and, therefore, do not enter the S phase in which they would become BrdU positive. On the other hand, it is possible that the length of the G1 phase is much longer in the albinos, therefore, at any moment in time, there are more cells in G1

in the albino compared to the pigmented rat resulting in a greater number of Ki67 positive cells.

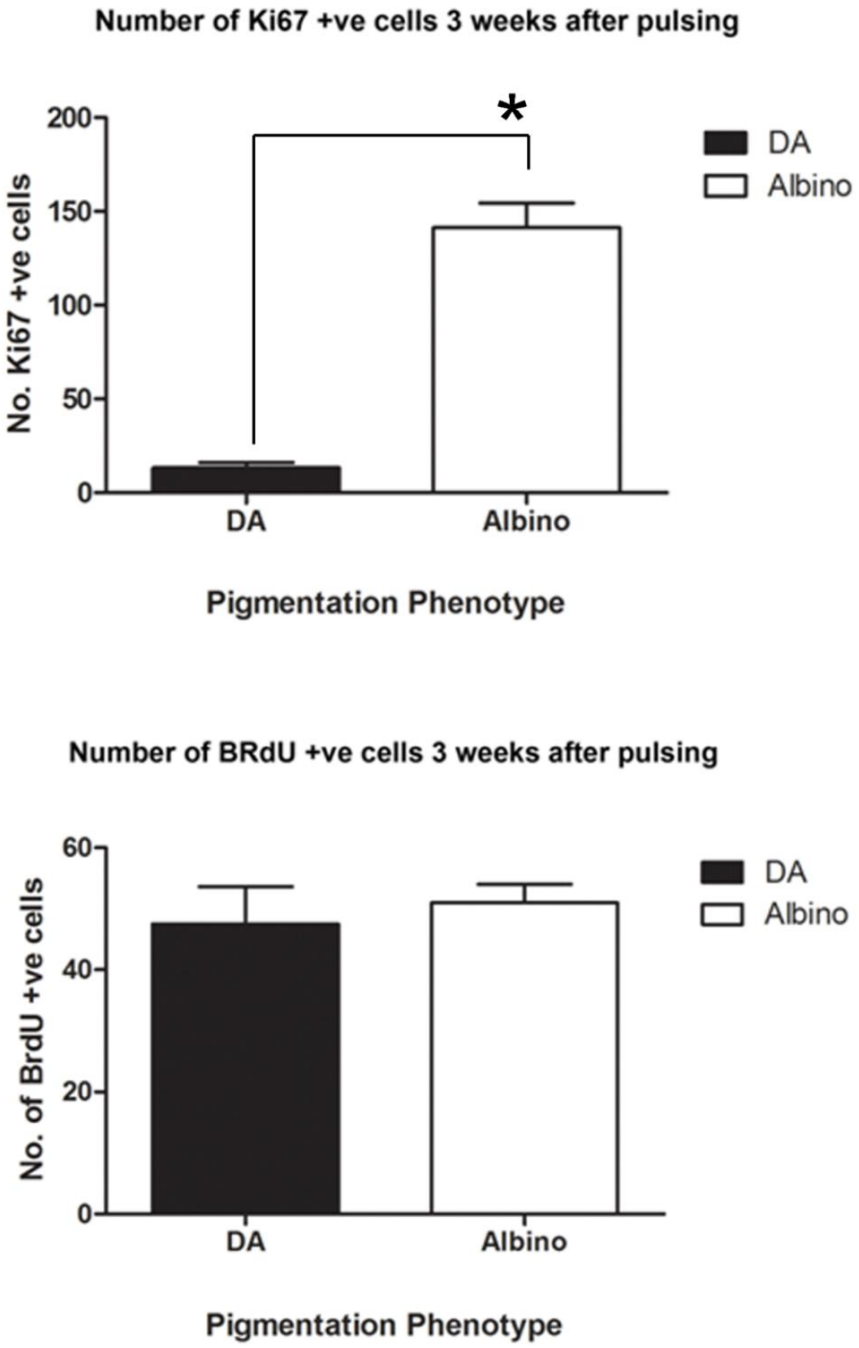

Figure 3.4.4: Differences in the proliferative capacity of the RPE in pigmented DA and albino Wistar rats. Albino rats had approximately ten times more cells that were positive for the cell cycle marker, Ki67, than the pigmented rats ($p<0.001$). When rats were pulsed with BrdU, a marker for cells in the S phase of the cell cycle, for 5 days and then left for 3 weeks there was no significant difference in the numbers of BrdU positive cells between the two pigmentation phenotypes.

Significant increase in centrosome number in polyploidal cells

At any point in time, a cell should have only one or two centrosomes depending on which stage of the cell cycle they are in. During the S phase of the cell cycle, the single centrosome that is present in the G1 phase is duplicated and moves to the opposite end of the cell during spindle formation. Immunofluorescence labelling was carried out using the antibody GT335. This targets polyglutamated tubulin and labels individual centrioles. Immunohistochemistry analysis showed that the RPE cells in 3 month pigmented rats contained either one or two centrosomes (Figure 3.4.5A). The polyploidal cells of the 3 month albino rat, however, contained multiple centrosomes with an average of 17 centrosomes surrounding one cell (Figures 3.4.5B-F), with some cells having as many as 40. The surrounding non-polyploidal cells contained the normal expected number of centrosomes (Figure 3.4.5G).

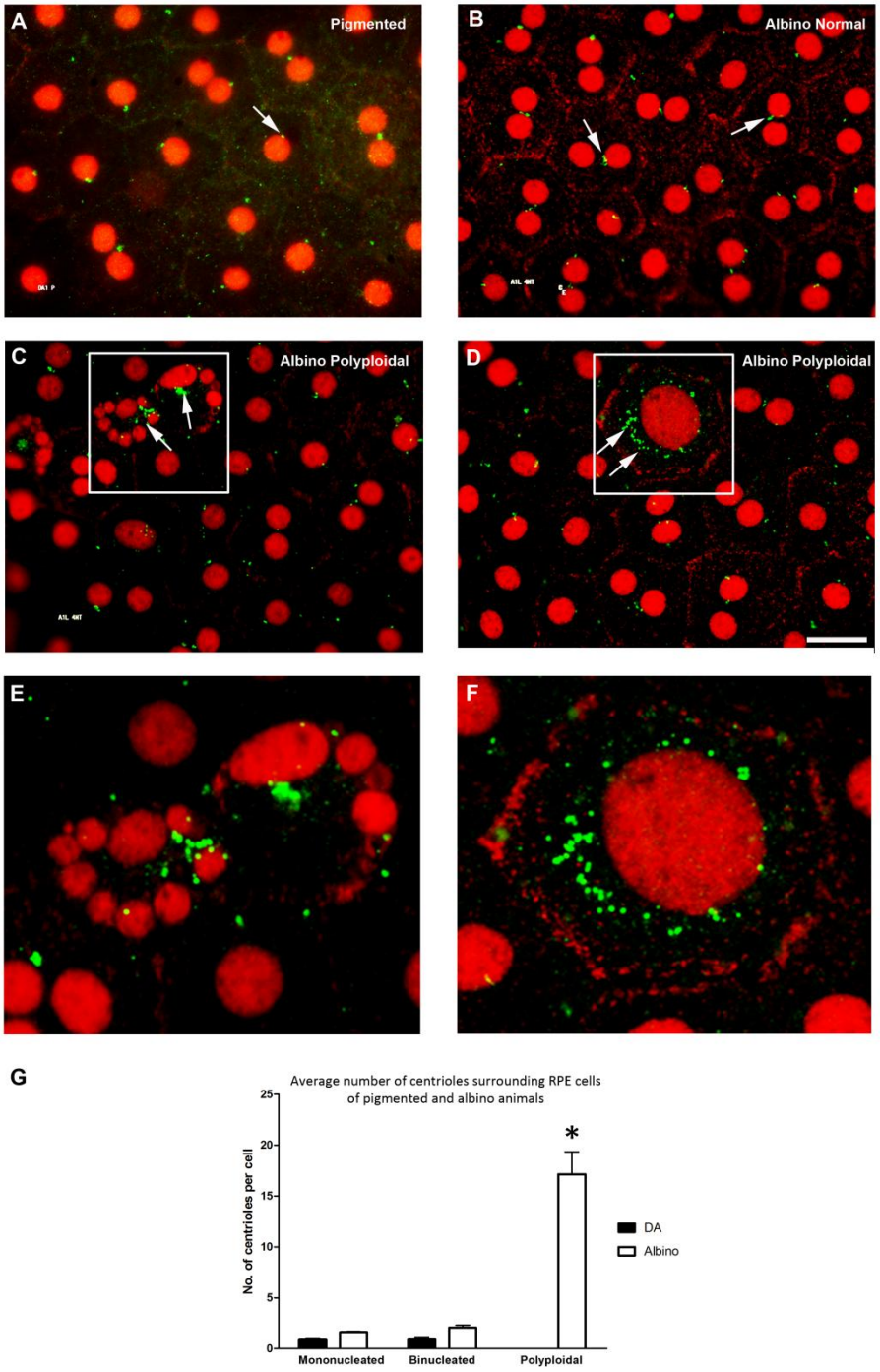

Figure 3.4.5:Polyploidal cells in the albino RPE. (A-F) Immunohistochemistry staining using otx2 (red) to show nuclear morphology and GT335 (green) showing centrioles in the RPE of both young pigmented (A) and albino (B-F) rats. In the pigmented rat, each cell has either 1 or 2 centrioles depending on the stage in the cell cycle with which they are in (white arrows point to centrioles) (A). In the albino, in regions where the nuclei appear normal there are also 1 or 2 centrioles per cell (B). In cells which have abnormal distorted nuclei such as fragmented (C) or large (D), the number of centrioles is significantly increased. The cells in the white box in images C and D are enlarged in in E and F, respectively. (G) shows the average number of centrioles per cell in both pigmentation phenotypes. The young DA rat has no polyploidal cells and therefore, a number of the centrioles could not be counted. On average, each polyploidal cell has 17 centrioles surrounding the nuclei.

Aged albino RPE has abnormal larger cell morphology

The RPE cells of old pigmented rats maintain their hexagonal shape (Figure 3.4.6C), although they do appear to be slightly more elongated and larger than the cells of the young rat (Figure 3.4.6A). The RPE of aged albino rats, however, present with an abnormal morphology in which most cells have lost the characteristic hexagonal shape seen in the younger animals (Figure 3.4.6B and Figure 3.4.6D). The hexagonal shape of the RPE in general is well suited for this monolayer of cells as it allows the best fit for these cells and appears to be an adaptive consequence for maintaining the regularity of the RPE.

Analysis of images taken from the immunofluorescence labelled RPE cells showed that the RPE cell area increases significantly with age ($p<0.0001$; Figure 3.4.6E), with albino rats exhibiting a much greater increase in comparison to pigmented rats. The RPE cells of the pigmented rats show a twofold increase in their mean cell area (from 2900μm^2 to 5600μm^2) between the ages of 3 and 20 months, whilst the albino rats exhibit a fourfold increase in RPE cell area (from 2400μm^2 to 10 100μm^2). Images from the 20 month pigmented rats show that the increase in cell size is due to changes in only a few of the RPE cells, with most surrounding cells maintaining their average size. In the albino, however, this age related increase in cell size is due to changes in all of the cells, with them all losing their hexagonal shape.

Only cells in the periphery of the RPE were analysed as this is where cells maintain their proliferative capacity and where most of the polyploidal cells were found. The periphery was classified as the outermost 20% of the whole RPE sheet. This increase in cell area with age could be due to cells dying and surrounding cells filling their space.

As a consequence of increased cell area, cell density decreases with age in both pigmentation phenotypes (Figure 3.4.6F). This is however, more marked in the albino RPE. Both the pigmented and albino animals show the greatest decrease in cell density in the extreme periphery, which is then followed by a slight increase before the cell density plateaus towards the centre.

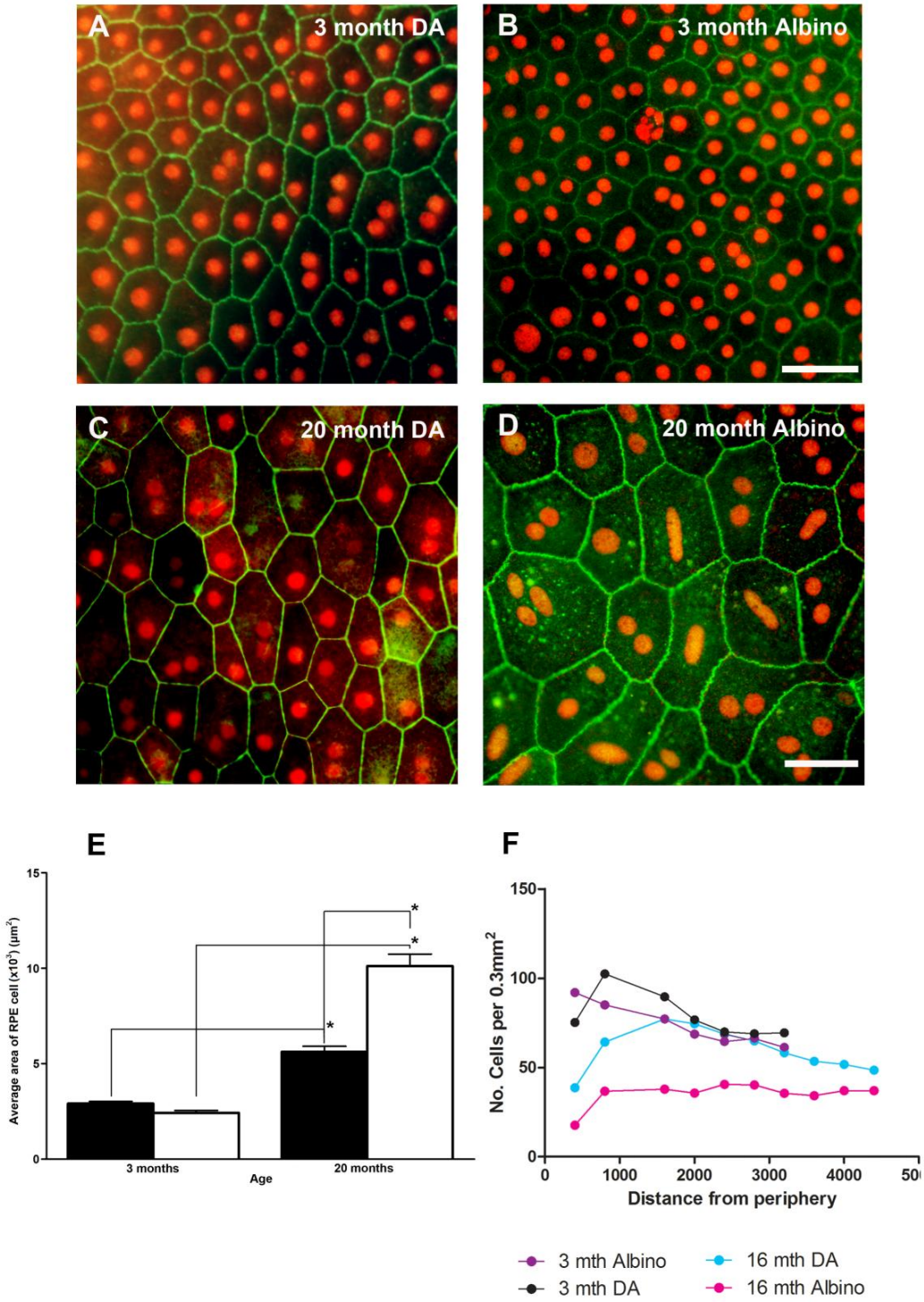

Figure 3.4.6: Cell size and density in young (3 month) and old (20 month) pigmented and albino rats. (A-D) Immunohistochemistry using ZO-1 (green) to show the RPE junctions and otx2 (red) to show nuclear morphology in both pigmentation phenotypes at the RPE periphery. In the young pigmented rat, the RPE cells have their characteristic hexagonal shape and normal mono or binucleated nuclei (A). With age the RPE cells maintain their shape and an increase in cell size is visible (C). In the young albino rat, the RPE cells have a normal hexagonal shape, however, a few cells can be seen containing distorted, polyploidal nuclei (B). With age, the RPE cells completely lose their characteristic morphology and a dramatic increase in cell size is visible (D).

(E) shows that there is a significant increase in cell size with age in both pigmented and albino animals, $p<0.0001$. (F) shows that with age, there is a decrease in the density of RPE cells especially in the periphery of both pigmentation phenotypes. The albino presents with a greater overall decrease in cell density with age. Scale bar - 50μm.

Threefold increase in the number of polyploidal cells with age

Previous studies have shown that there are a population of cells in the peripheral region of the RPE which maintain the capacity to proliferate (Al-Hussaini et al., 2008). Further investigation into this region suggested that the albino RPE contained cells that had not been able to exit the cell cycle and have failed to undergo cytokinesis, resulting in cells with either large, fragmented or multiple nuclei. In young albino animals, these cells are seen mainly in the periphery of the RPE where 10% of the cells are polyploidal (Figure 3.4.7A), although the equatorial and central regions also contain polyploidal cells. This cellular feature was rarely found in young pigmented animals with less than 0.5% of the cells being polyploidal (Figure 3.4.7A). With increasing age, there is a significant increase in the number of polyploidal cells in the RPE of both pigmentation phenotypes ($p<0.001$) (Figure 3.4.7B). In albino animals, the greatest number of polyploidal cells are still found in the periphery (~25%) (Figure 3.4.7D), however, the greatest increase is in the centre where there is a threefold increase in the number of these cells (from 5 to 15%). Pigmented animals also exhibited an increase in polyploidal cells with age, similarly, the greatest increase was found in the centre (Figure 3.4.7C).

Polyploidal cells arise from a failure of a cell to undergo normal mitosis and/or failure to undergo cytokinesis. As shown in previous data, proliferating cells were only found in the

periphery of the RPE (Al-Hussaini et al., 2008). This suggests that the increase in polyploidal cells observed in the centre of the RPE in both pigmentation phenotypes could be due to cells in the periphery proliferating and becoming arrested in the cell cycle – with time, the number of these cells accumulate and they possibly migrate towards the centre.

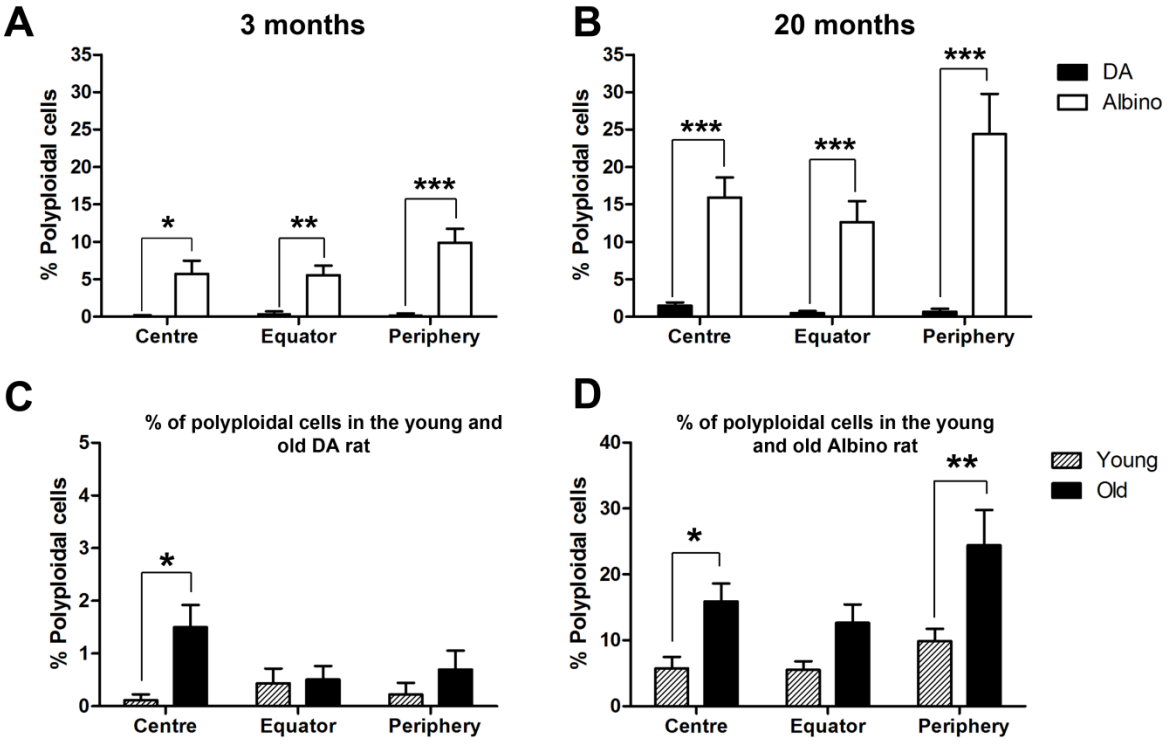

Figure 3.4.7: The effect of ageing on the number of polyploidal cells in the RPE. (A and B) show the percentage of polyploidal cells in the RPE of pigmented and albino rats in separate regions in both young 3 month (A) and old 20 month (B) rats. (C and D) show the difference in the percentage of polyploidal cells with age in each pigmentation phenotype. Young pigmented rats have almost no polyploidal cells throughout the RPE, with less than 0.5% in the equatorial and peripheral regions. Young albinos however, have approximately 25% of their cells showing distorted nuclei, with the majority of these in the peripheral region of the RPE. With age, there is a small increase in the number of polyploidal cells in pigmented animals with approximately 3.5% of the cells appearing to be polyploidal. The largest increase is seen in the centre of the RPE. The old albinos showed a significant increase in the number of polyploidal cells with approximately 53% of the cells appearing to be polyploidal. The largest increase was seen in the peripheral region with an increase of 15%, followed by the central region with an increase of 10%. * $p<0.05$, ** $p<0.01$, *** $p<0.001$.

Significant decrease in RPE65 expression in polyploidal cells suggesting that aged albinos have an affected visual cycle

RPE65 is a vital component of the visual cycle and is involved in retinoid processing. The RPE65 protein is predominantly expressed in the RPE and is a key element in the normal functioning of the RPE. It plays an important role in vitamin A metabolism and is associated with retinol binding protein and 11-*cis*-retinol dehydrogenase (Redmond et al., 1998). Although its exact function is unknown, it appears to play a key role in the physiology of vision as mutations in the human RPE65 gene cause severe blindness from birth or early childhood (Redmond et al., 1998). Immunofluorescence labelling with RPE65 and otx2 shows that a population of polyploidal cells, compared to cells with normal nuclei, do not express RPE65 in both age groups (Figure 3.4.8A and 3.4.8B). Images taken using a confocal microscope show that cells surrounding the polyploidal cells exhibit a bright green cytoplasm, indicating that they are strongly positive for RPE65. The polyploidal cells, however, appear to have a black cytoplasm suggesting a lack of RPE65 in these cells. Figure 3.4.8C shows a snapshot of the periphery of the RPE of a 20 month old albino. The majority of the polyploidal cells show a decrease in the expression of the RPE65, this was quantified by measuring the pixel density of each cell in this area (Figure 3.4.8D). The results show a significant decrease in RPE65 expression in cells containing polyploidal nuclei ($p<0.01$).

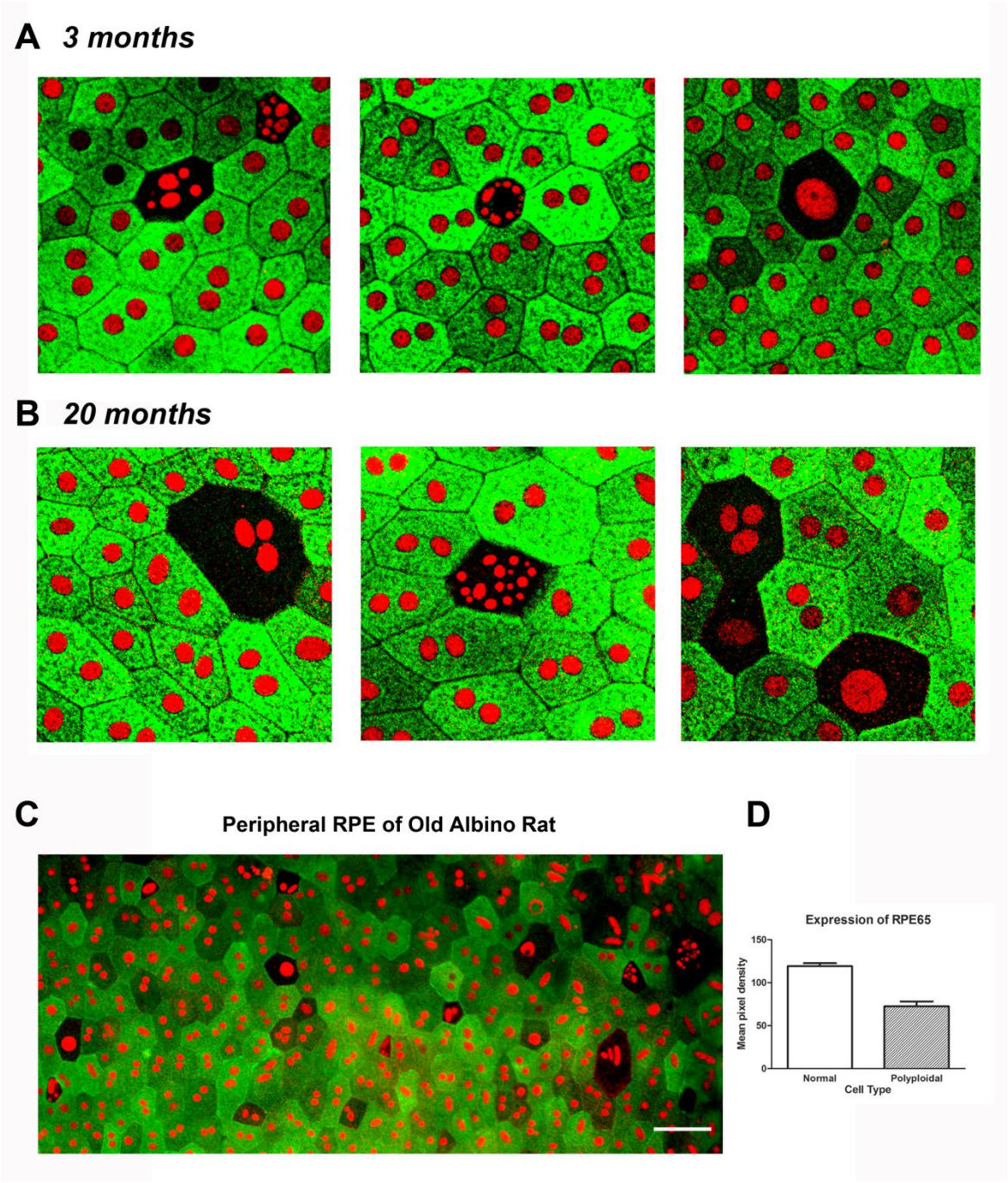

Figure 3.4.8: RPE65 expression in polyploidal cells. Immunohistochemistry using RPE65 (green) and otx2 (red). A decrease in RPE65 expression can be seen in polyploidal cells of both young (A) and old (B) albino rats regardless of whether the cell has large or fragmented nuclei. (C) shows an image taken from the periphery of an old 20 month albino. A large number of the polyploidal cells appear to have downregulated their RPE65 expression. Measuring mean pixel density, there is a significant decrease in the expression of RPE65 in the polyploidal cells in comparison to surrounding cells with normal nuclear morphology ($p=<0.01$) (D).

Increased outer segment length and distorted heads in aged albino photoreceptors

Ageing is a multifaceted biological process influenced by stochastic occurrence of molecular damage over time (Parapuram et al., 2010). The age-related degeneration of the retina is among the most prevalent complications of ageing (Bonnel et al., 2003, Beatty et al., 2000). With age, there is a marked loss of retinal neurons including the photoreceptors (Curcio et al., 1993, Katz and Robison, 1986) and ganglion cells (Curcio and Drucker, 1993, Gao and Hollyfield, 1992). The rod photoreceptors represent the principal retinal cell type in most mammals and are uniquely vulnerable to the effects of ageing (Parapuram et al., 2010). In humans, 30% of central rods are lost between the ages of 34 to 90 years (Curcio et al., 1993), whilst the cone density appears to remain unchanged (Curcio et al., 1993, Gao and Hollyfield, 1992). Studies have reported significant changes in the morphology of photoreceptors with age, with Marshall et al. (1979) showing that in humans, aged rod photoreceptors show extensive convolutions along their major axis, causing an increase in their length. This was countered by a study by Cunea and Jeffery (2007), who showed that aged rods in rodents are significantly shorter than that found in their younger counterparts.

Whilst cones are robust conical-shaped structures, rods are slim rod-shaped structures with their inner and outer segments filling the area between the larger cones in the subretinal space and stretching to the RPE. Here, scanning electron microscopy (SEM) was used to determine whether the abnormalities seen in the albino RPE affected the architecture of the overlying photoreceptors of the neural retina. Images were taken from

the retinae of 3 and 20 month old albino and pigmented rats (Figure 3.4.9). The images revealed that the outer segments of the young pigmented rats are all similar in shape and size and appear to be very uniform in appearance, with the average outer segment length being 12µm. The photoreceptors of the young albino rats, however, are shorter and thicker than those of the pigmented rats, with an average length of 7µm. They also seemed to have a more distinct banding pattern along their length. With age, pigmented rats showed a significant decrease in the length of their outer segments as shown in previous studies. Here, it can be seen that the outer segment length decreases to 10µm in the 20 month pigmented rats. Although there is a difference in outer segment length with age in the pigmented rats, the morphology of the cells appear to remain the same, with the outer segments appearing to be regularly stacked in a uniform manner.

With age, the outer segments of the albino retina, however, show a dramatic increase in length with an average outer segment length of 11µm. The outer segments are also less regularly stacked and present with swollen, globular tips (Figure 3.4.10). This data suggests that they may have less efficient patterns of phagocytosis by the RPE cells. The banding patterns of the discs also appear to be more distinct in the aged outer segments of the albino, with some discs appearing thicker than others. In addition, the inner segments of the aged 20 month albino appear to be shorter than those of the aged pigmented rat. This, however, could not be quantified as during tissue processing the tissue is broken into very small fragments and it was difficult to obtain a significant number of samples containing the full length of the inner and outer segments.

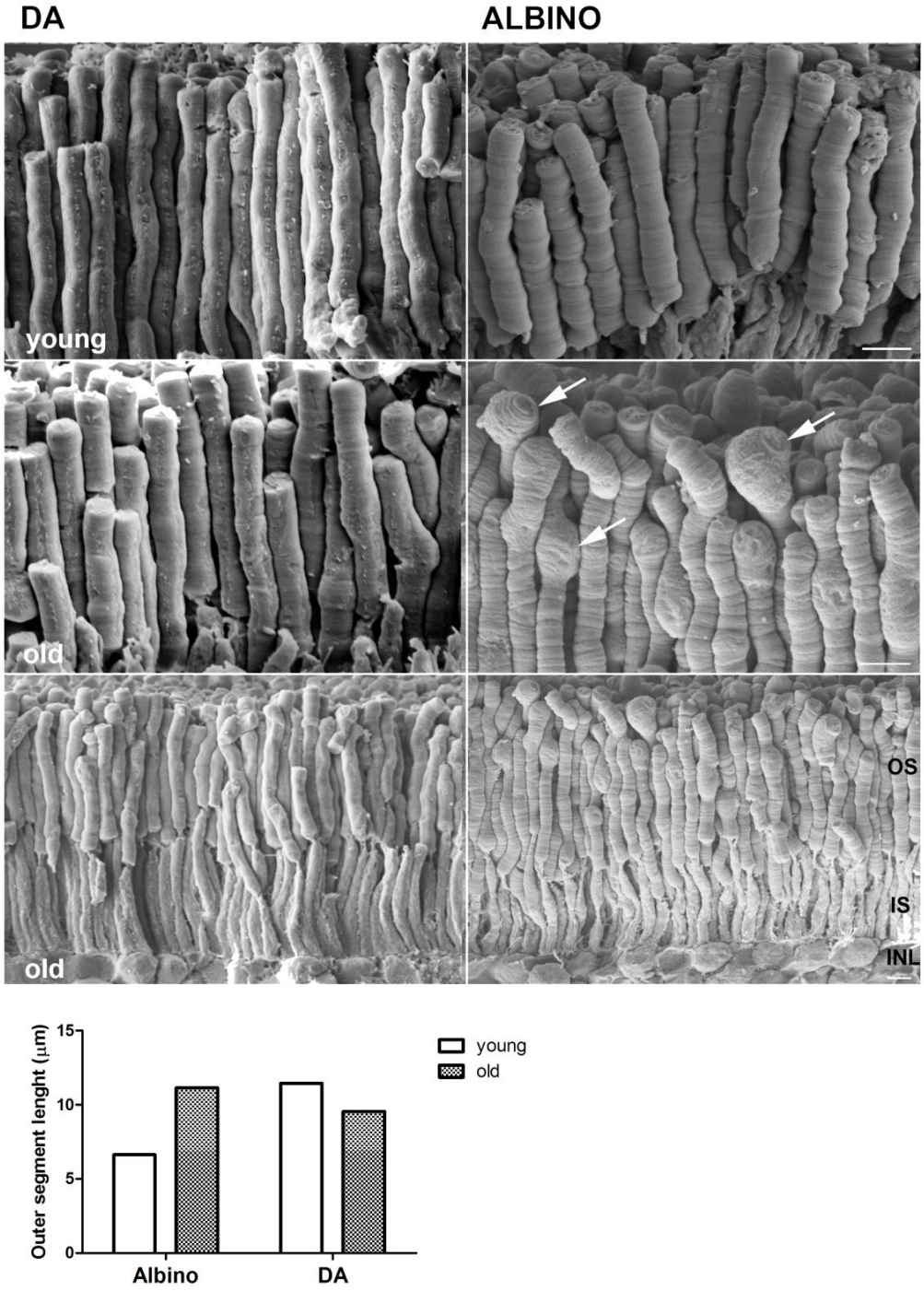

Figure 3.4.9: Scanning electron microscopy images of the outer retina in both 3 month (young) and 20 month (old) pigmented and albino rats. The outer segments (OS) of the young pigmented rat appear to be regularly stacked with a normal morphology. The OS of the albino rat, although regular have a distinct banding pattern and appear to be shorter than those of the pigmented rat. With age, the OS of the pigmented rat decrease in length (as shown by the graph) however, their morphology still remains normal. The aged albino OS segments, however, increase in length and present with distorted globular tips (shown with the white arrows). This distinct morphology can be seen throughout the entire retina. The bottom two images show a lower magnification of the aged rat retina in both pigmentation phenotypes where the difference in OS length distinctly visible. Scale bar - 2µm.

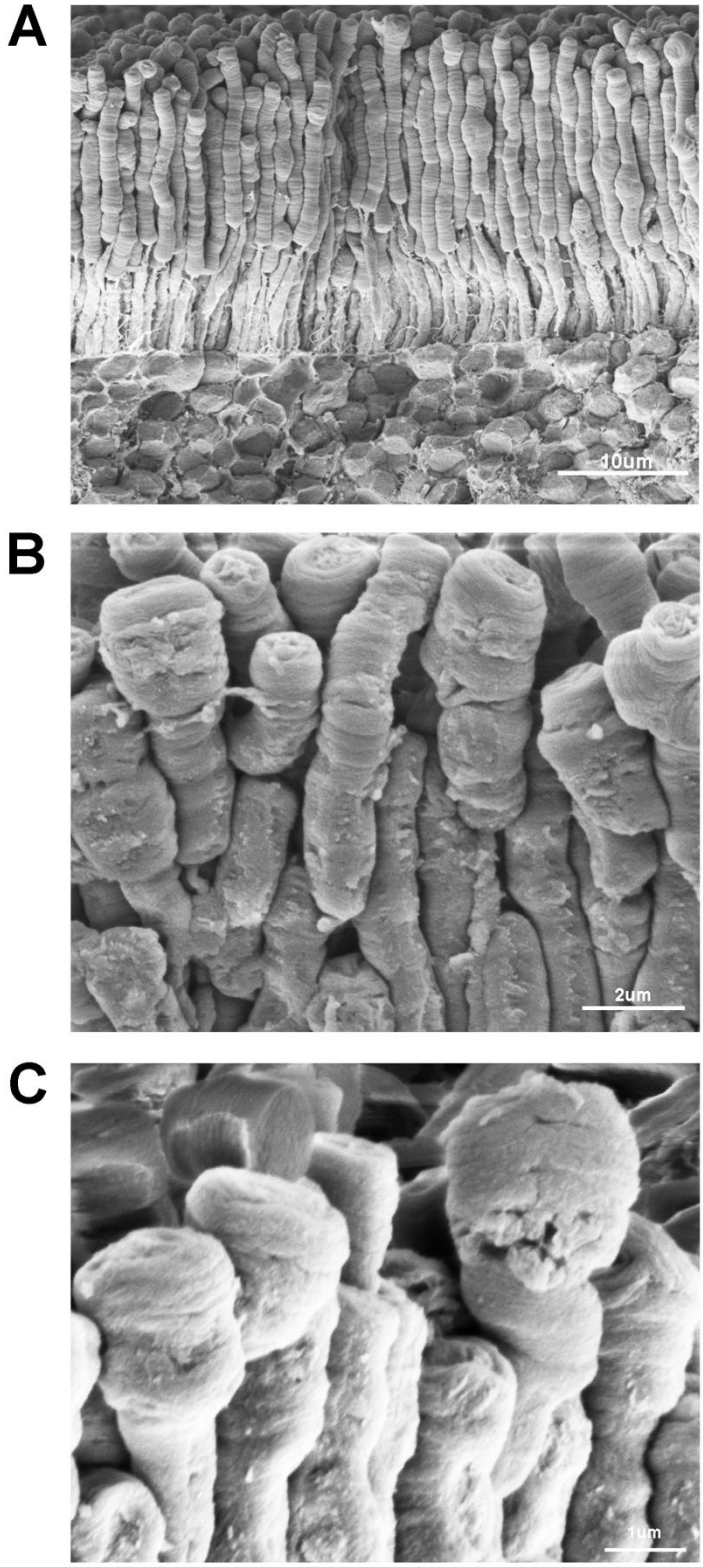

Figure 3.4.10: Ageing albino photoreceptors in a 20 month rat. (A) shows stacks of the elongated outer segments at a low magnification. Swellings are evident at the tips of the outer segments as well as in the middle of them. The banding of the discs is very distinctly visible. The inner segments and the outer nuclear layer are also demonstrated. (B) and (C) show the globular tips of the outer segments at a very high magnification.

Decrease in the expression of MFG-E8 in old albino rats

Both MFG-E8 and MERTK are vital for phagocytosis of the photoreceptor outer segments (POS) (Feng et al., 2002, Kevany and Palczewski, 2010). MFG-E8 is responsible for the initial recognition and binding of the RPE to the POS while MERTK is vital for the ingestion of the POS which occurs once the binding has occurred. Quantitative Real Time PCR (QRT-PCR) was used to show the relative changes in gene expression of target gene relative to the control gene, beta actin (Figure 3.4.11). MFG-E8 expression shows no significant change with age in the pigmented animals. In albinos, however, there is a significant decrease of this gene with age ($p<0.01$). Comparing the two pigmentation phenotypes, the aged albinos showed a significant decrease in MGF-E8 expression compared to the aged pigmented albinos ($p<0.05$). MERTK expression showed no significant change with age in either the pigmented or albino animals. In order to confirm that the correct product for each gene had been tested, the samples were run on a gel, excised and sequenced.

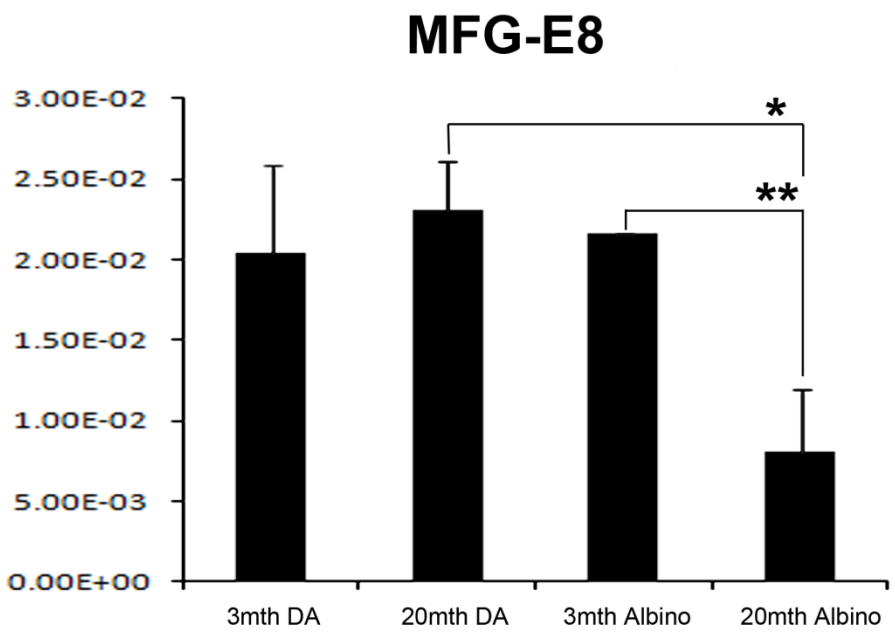

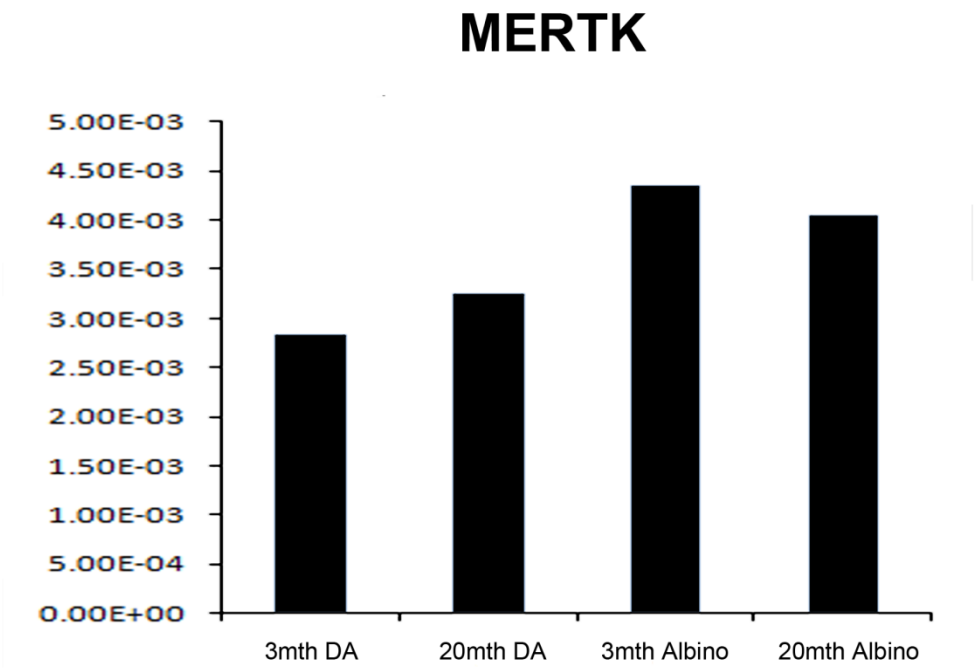

Figure 3.4.11: Quantitative Real Time PCR (QRT-PCR) showing the relative changes in gene expression of the target gene relative to the control gene, beta actin. MFG-E8 expression shows no significant change with age in the pigmented animals. In albinos, however, there is a significant decrease of this gene with age ($p<0.01$). Comparing the two pigmentation phenotypes, the aged albinos showed a significant decrease in MGF-E8 expression compared to the aged pigmented albinos ($p<0.05$). MERTK expression showed no significant change with age in either the pigmented or albino animals.

Decrease in retinal function in old albino rats

The electroretinogram (ERG) records the electrical response of the eye to a flash of light at the cornea. This response is generated by radial currents that arise either directly from retinal neurones or as a result of the effect on retinal glia changes in extracellular K^+ concentration brought about by the activity of these neurons. The ERG is an important tool for measuring retinal function as it can be recorded easily and noninvasively with a corneal electrode under physiological conditions.

The ERG response to a flash of light measured at the cornea is the sum of positive and negative component potentials that originate from different stages of retinal processing and overlap in time. The cornea-negative a-wave is mainly associated with the photoreceptors whilst the cornea-positive b-wave is related primarily to the activity of depolarising (ON) bipolar cells. The dark-adapted a-wave is the initial negative wave that occurs in response to strong stimuli from darkness and is primarily rod-driven (i.e. scotopic). The light-adapted a-wave is the initial negative wave in response to a stimulus presented on an adapting background, and when the background is rod-saturating, the a-wave is cone driven (photopic). Under both dark and light adapted conditions, the a-wave is truncated by the rise of the b-wave.

The magnitude of the a-wave (photoreceptor generated) and the b-wave (post receptoral generated) of the ERG to flash stimuli was measured at both 3 and 20 months in both

pigmentation phenotypes. Retinal function in the pigmented animals does not appear to change with age, with both the a- and b- wave amplitudes appearing to be similar at all in the light intensities (Figure 3.4.12A). In the albino animals, however, at low stimulus intensities both the a- and b- wave amplitudes follow the same pattern. At the higher intensities, however, there is a marked difference between the ages, with the 20 month albinos showing a reduction in both the a- and b-waves compared to the 3 month animals (Figure 3.4.12B). This is also demonstrated in the waveforms from the ERGs, where it is clearly visible that the aged albinos have a decreased reaction to higher light intensities, compared to the younger albinos (Figure 3.4.13). Unfortunately, due to the low number of animals available for the experiment, statistical tests could not be carried out and only a trend could be identified. Furthermore, at both ages, the b-wave amplitude in the albino rats plateaus and then drops. At low light intensities, fewer rods are required, however, the increasing intensity causes damage to the photoreceptors causing them to overload and saturate, resulting in a drop in the b-wave in both the age groups. This plateauing of the b-wave is not seen to this extent in the pigmented animals.

Interestingly, when comparing the young 3 month pigmented animals against the young albinos (Figure 3.4.12C), the results show that the albinos have higher a- and b-wave amplitudes compared to the pigmented animals. When the highest light intensity is reached, however, there is a drop in both the a- and b-wave in the albino. With age, however, at low intensities, the a- wave of both pigmentation phenotypes appears the same, until the higher light intensities are reached where the a-wave of the albinos

decreases markedly in comparison to the pigmented animals (Figure 3.4.12D). In addition, at low intensities, the b-wave of the 20 month albino appears to be greater than that of the pigmented, until once again at high intensities the b-wave drops prominently.

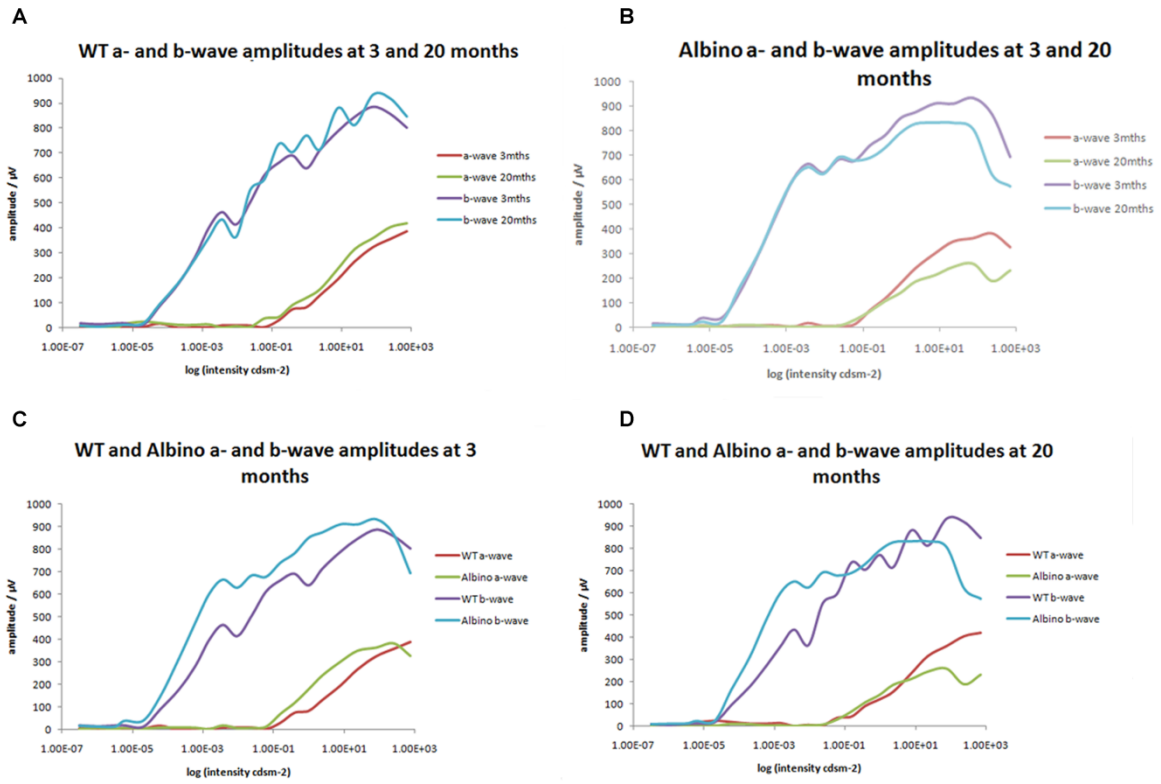

Figure 3.4.12: ERGs showing retinal function in young 3 month and old 20 month pigmented and albino rats. (A) With age there appears to be no difference in the intensity of the a- or b- waves of the pigmented rats. (B) In the albinos, however, especially at the higher light intensities, there is a decrease in retinal function as the response to the flashes of light are greatly reduced in the 20 month rat. Comparing both pigmentation phenotypes shows that at 3 months there is no difference in their response to light with either the a- or b- waves (C), however, at 20 months, there is a difference between the pigmented and albino rats, with the albinos showing a decreased response to increasing light intensities.

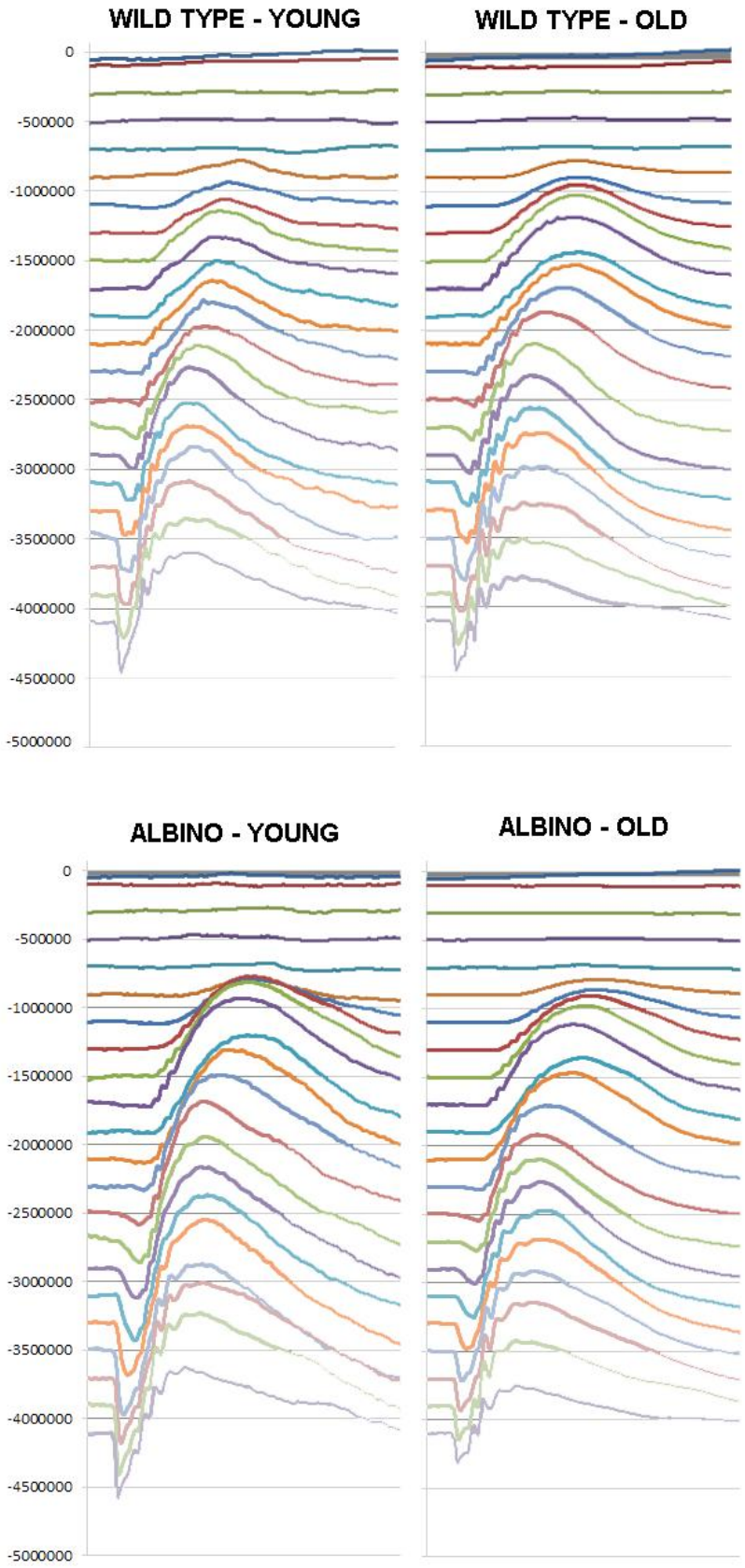

Figure 3.4.13: The waveforms from every ERG recording in the 3 month and 20 month pigmented and albino rats.

3.5 Discussion

The peripheral RPE cells of the albino rat show a less regular, distorted morphology with some cells containing polyploidal nuclei. Three distinct types of polyploidal cells were identified. These were cells with enlarged nuclei, cells with fragmented nuclei, and cells with multiple nuclei of a normal size (more than 3, as binucleation is normal in rodent RPE). The abnormally high number of centrosomes shown in some of the albino RPE cells indicates that these cells are in fact polyploidal. At any moment in time, a cell should have one or two centrosomes depending on which stage of the cell cycle they are in (Nigg, 2002, Winey, 1999). Here, it can be seen that cells with fragmented or enlarged nuclei have an average of 17 centrosomes, clearly demonstrating that they are polyploidal.

Polyploidy arises from errors in cell division which lead to the failure of cytokinesis (Ganem and Pellman, 2007), the final phase of the division cycle, in which the cytoplasm of a single cell is divided to form two daughter cells (Figure 3.5.1). Polyploidal cells contain DNA levels greater than the diploid content and are prevalent in a variety of cells, including those of mammalian origin, most notably in hepatocytes (Ravid et al., 2002, Guidotti et al., 2003). Polyploidy occurs in some cell types as a normal developmental process, while in others as a result of stress (Ravid et al., 2002). Polyploidisation allows an increase in metabolic output, cell size and cell mass, therefore, enabling specialised cells to upregulate the synthesis of proteins (especially in cells with high metabolic and synthetic burden, such as those in the liver) (Guidotti et al., 2003, Ravid et al., 2002). It can,

however, also have deleterious consequences such as genetic instability (Ganem and Pellman, 2007) which can facilitate tumorigenesis (Ganem et al., 2007).

Figure 3.5.1: Errors in mitosis, leading to cells containing more than 2 centrosomes, followed by incorrect spindle formation and uneven chromosome segregation. This results in one cell having gone through nuclear division but not cytokinesis, therefore, instead of producing 2 daughter cells, one cell with a very large nucleus is produced (from Ravid et al., 2002).

Many cell-cycle defects can lead to cytokinesis failure, such as progression past the DNA damage or spindle checkpoints (Ganem and Pellman, 2007). Checkpoint controls were evolved to delay cells from entering and exiting mitosis under conditions which could compromise genome integrity (Rieder and Maiato, 2004). Two major checkpoints are the *DNA damage checkpoint* (at the G2/M transition) which prevents damaged cells from entering mitosis and the *spindle assembly checkpoint (SAC)*. Once in mitosis, exit from mitosis is controlled by the SAC. If spindle assembly is disrupted, a cell can leave mitosis before cytokinesis, leaving mononuclear tetraploidal cells and cells containing numerous

micronuclei (Rieder and Maiato, 2004), similar to those seen in the periphery of the albino RPE. It appears that in some tissues, polyploidy occurs as a result of failed cytokinesis, whilst in others polyploidal cells may be generated through failure to repair DNA damage in G2. Normally, DNA damage results in a p53 dependent pause or arrest in the G1 and G2 phases of the cell cycle (Bunz et al., 1998, Harper et al., 1993), however, failure of DNA repair combined with cell cycle progression in the absence of absolute G2 arrest, will result in the formation of polyploid cells (Margolis et al., 2003) (Figure 3.5.2).

Figure 3.5.2: Diagram showing the proposed process for the generation of cells proliferating with gross aneuploidy. The first event is the failure in mitosis or cleavage generating tetraploidy or gross aneuploidy. The second event is the failure of surveillance by p53 or pRB in tetraploid (or aneuploidy) G1, permitting cell cycle progression (from Margolis et al., 2003).

The defects occurring within the cell cycle of the albino RPE cells may help to explain why the relatively high number of RPE cells in the albino that are positive for Ki67 do not translate into an elevated cell production beyond that found in normally pigmented animals. Although there are ten times more Ki67 positive cells in the RPE of albino animals compared with the pigmented (Al-Hussaini et al., 2008), both pigmentation phenotypes have the same number of BrdU positive cells. Ki67 labels cells in all stages of the cell cycle, whereas, BrdU labels cells specifically in the S phase. This lack of difference in BrdU positive cells between the two pigmentation phenotypes suggests that the RPE cells in the albino enter the cell cycle where they are Ki67 positive, but fail to complete it, therefore, cells are unable to pass through the S phase in which they would have been labelled with BrdU. It is also possible that the length of the G1 phase is much longer in the albinos resulting in a greater number of Ki67 positive cells compared to the pigmented animals.

Having establsihed that polyploidy in the albino RPE is a distinct post natal event (seen in P10 but not P0), I asked whether ageing would exacerbate this condition. This study shows that differences in pigmentation phenotype affect the ageing response of the RPE and photoreceptors, with albino animals appearing to have an accelerated form of ageing. With age, they have a greater increase in RPE cell loss, the cells in the RPE become more polyploidal, there is a decrease in the expression of RPE65 as well as of the expression of genes responsible for phagocytosis and the photoreceptor outer segments develop abnormalities. In general, the RPE of the aged albino rat seems to be under a lot more stress than that of the aged pigmented rat resulting in a decline in retinal function.

The number of polyploidal cells increased by 30% in the aged albino RPE compared with the young animals, over time. This could be a result of cumulative oxidative damage occurring within these cells, therefore, they are less able to prevent polyploidal cells from arising as the cell cycle checkpoints fail to prevent the cell from undergoing mass nuclear division. Many studies have shown that ageing transpires as a result of an accumulation of molecular damage to cells over time (Druzhyna et al., 2008, Golden and Melov, 2001, Jarrett et al., 2008, Sastre et al., 2000), however, the cellular hallmarks of ageing appear to be specific and uniform between individuals and even among species (Parapuram et al., 2010).

A highly-conserved age-related change in neurons and other post mitotic cells, is the decrease in the expression of the mitochondrial electron transport chain gene set (Zahn et al., 2007). This results in a decrease in mitochondrial function and an increase in the formation of ROS. An accumulation of ROS causes oxidative damage to cellular components (Parapuram et al., 2010), which leads to cellular damage and consequent apoptosis (Del Priore et al., 2002, Cai et al., 2000). The lack of the protective antioxidant capacities provided by melanin in the albino seems to result with the albino exhibiting a greater extent of damage to the RPE and the overlying photoreceptors than the pigmented rat. This suggests that the albino RPE ages and degenerates faster than its aged matched pigmented equivalent. O'Steen et al. (1974) noticed that the RPE cells in adult rats exposed to high amounts of light were enlarged and spherical in shape suggesting that these cells could also be polyploidal. It seems that high illuminance levels, like age,

induce a stress response in the albino RPE and that albino animals are particularly susceptible to such light induced damage.

In the RPE, the structural damage that occurs with ageing includes the loss of the characteristic hexagonal shape of the cells, cell loss, hypopigmentation resulting from a loss of melanin granules and an increase in cell diameter as cells spread to fill the spaces left by dead cells (Boulton et al., 2004). Here, it can be seen that during the ageing process, RPE cells become more irregular in both pigmentation phenotypes. The morphological irregularity of the albino RPE is greater than that of the pigmented as a result of the large increase in polyploidal cells and the need to accommodate for the mass increase in nuclear material within individual cells. Also, as cells die, remaining cells have to spread to maintain the integrity of the RPE. Polyploid cells undergo apoptosis at substantially higher rates than diploids (Castedo et al., 2006). This, alongside the decrease in cell density suggests that there is more cell death occurring in the albino RPE. To determine whether or not this was true, the RPE sheet of both pigmentation phenotypes was stained with activated caspase 3, a known marker for apoptosis. Unfortunately, the staining was negative or did not work and no clear answer was given.

The effect that these changes in the albino RPE have on the neurosensory retina was also investigated. Understanding the relationship between the retina and RPE is vital for understanding many age-related pathologies such as AMD. AMD is believed to be caused by progressive deterioration of the RPE, Bruch's membrane and the choroid, which

consequently leads to subsequent damage of the photoreceptor cells (Binder et al., 2007). In this study it can be seen that with age, significant changes occur to the outer segments of both albino and pigmented rats. It is known that the performance of the visual system deteriorates with age (Kolesnikov et al., 2010, Gresh et al., 2003, Jackson et al., 2002) as a result of a 30-40% loss of rod photoreceptors in the retina (Curcio et al., 1993). Studies have also observed that in rodents, the outer segments of rod photoreceptors in aged animals are significantly shorter compared to those of younger animals (Kolesnikov et al., 2010, Cunea and Jeffery, 2007). Surprisingly, here it was observed that the length of the outer segments of the albino rod photoreceptors increased with age. Not only do the outer segments increase in length, but they also appear to have abnormal globular tips as well as a corrugated appearance due to the distinct banding of the discs. This is similar to data from human tissue, in which it was found that the rods in aged healthy human retinae were longer than those found in young eyes (Marshall et al., 1979). Although Cunea and Jeffery (2007) challenged this observation where they reported that aged rods in rodents are significantly shorter than those found in their younger counterparts, Marshall et al. (1979) noted that the rod outer segments in the aged retinae examined, suffered from extensive convolutions and localised swellings. This may be similar to the globular tips seen in the aged albino outer segments.

The significant increase in outer segment length and the globular heads of the outer segments suggest that the RPE of the aged albino retina cannot phagocytose efficiently. Phagocytosis of the outer segments is essential for proper retinal function (Kevany and Palczewski, 2010). The photoreceptor cells maintain their length by continuously

generating new outer segments from their base while simultaneously releasing mature outer segments which are engulfed and phagocytosed by the RPE. It appears that the inability of some of the RPE cells to efficiently phagocytose the outer segments of the aged albino photoreceptors prevents them from shedding their discs and so they culminate at the heads forming these globular swellings. This is further enhanced by the results showing that the 20 month old albinos down-regulate the expression of MFG-E8, a gene responsible for recognition and binding of the RPE to the photoreceptor outer segments (POS). MFG-E8 is a soluble ligand which exhibits high-affinity binding for αVβ5 (Duncan et al., 2003). αVβ5 is involved in recognition and binding of outer segment packets which then activate downstream signalling pathways that set into motion the phagocytic process (Finnemann et al., 1997, Finnemann and Nandrot, 2006, Finnemann and Silverstein, 2001). Nandrot et al. (2004) showed that $\alpha V\beta 5^{-/-}$ mice lacked the daily morning burst in phagosome formation seen in wild type retinas and demonstrated an age-related accumulation in lipid deposits associated with a decline in visual activity. These mice did not, however, exhibit retinal degeneration as seen in $MERTK^{-/-}$ mice (Duncan et al., 2003). Interestingly, here the expression levels of MERTK, which is vital for the ingestion of the POS are the same as those in the aged pigmented animal. This suggests that the globular tips are preventing the RPE from binding to the outer segments (the initial step of phagocytosis) resulting in a failure of the aged albino RPE to phagocytose efficiently.

The failure of efficient phagocytosis as well as the increase in polyploidal cells in the aged albinos compared to their pigmented counterparts results in a decline in retinal function in the aged albinos, as seen in the ERG results. The ERGs show a significant decrease in both the a- and b-waves, with the aged 20 month albinos having a weaker reaction at high stimulus intensities compared to the young 3 month albinos. A significant difference in the ERG responses was also seen between the two pigmentation phenotypes at the higher light intensities, with the aged albinos having decreased a- and b- wave amplitudes compared to the aged pigmented animals. This is similar to data shown by Heiduschka and Schraermeyer (2008), where they show that the scotopic b-waves of the Long-Evans pigmented rats were markedly larger than those in the Wistar albino rats. Most recently, Charng et al. (2011) also showed that ageing results in markedly different outcomes in pigmented and albino strains, with the ageing effect appearing greater in the Sprague Dawley albino rats compared with the Long Evans pigmented rat.

At 3 months, however, the albinos presented with larger a- and b-wave amplitudes in comparison to the pigmented animals. The larger a- and b- wave amplitudes in the 3 month albinos compared to the 3 month pigmented animals could be due to the differences in the passive electrical properties of the albino and pigmented eye. Interestingly, studies on human albinos have shown that albino patients have larger a- and b-wave amplitudes than pigmented individuals (Krill and Lee, 1963, Russell-Eggitt et al., 1990). These higher ERG responses in the albino patients could be as a result of:

- more light entering the albino eye via the translucent iris

- a greater fundal reflectance
- light scatter due to a lack of absorption by the RPE

Similar to humans, albino guinea-pigs also gave significantly larger amplitudes than the pigmented guinea-pigs (Bui et al., 1998). Studies in pigmented and albino rats and mice, however, have not shown this pattern. Heiduschka and Schraermeyer (2008) found that all amplitudes in pigmented animals were larger than those of the albino while Green et al. (1991) and Green et al. (1994) found no significant differences in the ERGs between the two pigmentation phenotypes. Unfortunately, due to the low number used in these experiments, statistical tests could not be carried out, but the results show a clear trend indicating that in the young animals, the albino rats have larger ERG responses compared to the pigmented rats. As described in the humans, this could be due to internal reflection and transmission through the iris and sclera. One of the functions of melanin in the RPE is to absorb light entering the eye, in the albinos, however, where there is a lack of melanin, light can enter the eye not just through the pupil but also the translucent iris and sclera. Although the albinos contain less rods in their retina compared to the pigmented animals, they receive more light, inducing a higher ERG response.

With age, there is a marked difference in the ERG responses between the two pigmentation phenotypes with the aged albinos showing a decrease in both the a- and b-waves at high intensities. The decrease in rod function (as seen by the reduced amplitudes) in the aged albino retina compared to the aged pigmented retina, may be due to the limited availability of 11-*cis*-retinal for rod pigment formation. The polyploidal cells in the

albino RPE expressed a significantly lower amount of RPE65 in the cytoplasm of their cells. RPE65 is a vital component of the visual cycle, which is responsible for retinoid processing and the conversion of all-trans-retinol to 11-*cis*-retinal. According to the retinoid deficiency hypothesis, the localised scarcity of 11-*cis*-retinal caused by either defects in the processing of retinoids in the RPE or within photoreceptors causes an accumulation of intermediates (constitutively active free opsin) in aged rods resulting in desensitization of the retina (Curcio et al., 2000, Jackson et al., 2002). It is possible that age related changes in the RPE-based components of the visual cycle alter precursor uptake, substrate availability and enzyme activity leading to a localised decrease of 11-*cis*-retinal to the photoreceptors and ultimately resulting with reduced rod function. This theory is further strengthened by the study carried out by Redmond et al. (1998) in which they use ERGs to show that rod function is abolished in $Rpe65^{-/-}$ mice, highlighting the importance of RPE65 in visual function. They also show that the outer segment discs of rod photoreceptors of the $Rpe65^{-/-}$ mice are disorganised in comparison to those of $Rpe65^{+/+}$ and $Rpe65^{+/-}$ mice. A lack of RPE65 in the aged albinos may also contribute to the distorted morphology of the photoreceptor outer segments.

Defects in the recycling of 11-*cis*-retinal, combined with the distorted photoreceptor outer segments which appear to make phagocytosis of the outer segments less efficient, seem to cause a reduced rod function as seen in the aged albino. It appears that the primary effects of the aged albino are caused in the photoreceptors (where there is reduced rod

function, and therefore, a-wave amplitudes) and that this is reflected in the inner retina, resulting in decreased b- wave amplitudes.

Another reason for the differences demonstrated could be due to differences in the composition of the extracellular environment, especially with regards to calcium ion concentration during phototransduction, therefore, leading to different photoreceptor responses. Lavalle et al.(2003) found significantly higher Ca^{2+} levels in the retina of albino animals. This could explain the decreased b-wave amplitudes (at high intensities) in the aged albino compared to the pigmented as a Ca^{2+} influx into retinal neurones could lead to a partially excited state with a permanently decreased membrane potential and availability of neurotransmitters. This consequently could result in decreased post-receptoral activity.

A deficit in neurotransmitter levels and impaired retinal development in the albino could also be a reason for the smaller retinal response in the aged albino rats. Albinos have a lack of tyrosinase metabolites such as L-DOPA. They also have reduced levels of the inhibitory neurotransmitter γ-aminobutyric acid (GABA) in their retina and a higher portion of the excitatory neurotransmitter glutamate compared to pigmented animals (Blaszczyk et al., 2004). GABA is assumed to be involved in rod-driven visual signals (Kim et al., 1998) and so enhanced GABA in the pigmented retina could contribute to the higher post-receptoral response seen in the aged pigmented rats compared to the albinos.

Interestingly, when comparing the 3 month and 20 month ERG responses of the albino, a marked decrease in both a- and b-wave amplitudes can be seen at high intensities. At low intensities, however, there appears to be no difference between the a- and b- waves. This could be due to the fact that at low intensities, enough of the rod population is not working to demonstrate a difference. With increasing intensity, however, there is an onslaught of incident light, therefore, photon capture is less efficient.

This is the first study that suggests that albinism could be a progressive retinal condition as opposed to a congenital abnormality. The stress associated with ageing results in a gradual loss in functional efficiency that only over time becomes sufficient to cause significant impairment or cell death. Due to the greater amount of stress the albino RPE is under, the signs of an age-related decline in visual function appear sooner than pigmented animals. If the pigmented animals were able to live longer, it is probable that they would also show the same distorted morphologies seen in the aged albino retina and RPE. It seems that the lack of melanin and its photo-protective and anti-oxidant capabilities exacerbate the effects of ageing in the albino.

Chapter 4

RPE Cell migration

4.1 Abstract

RPE cell migration is required to establish a confluent monolayer during development and also to maintain the integrity of the RPE during cell loss associated with ageing. In this study, migration within the RPE of healthy young pigmented rats will be examined. Furthermore, the effect of inducing laser lesions in either the peripheral or the central region of the RPE will be investigated to determine whether retinal location affects the response of RPE cells to the damaged area. To determine whether individual cells within the RPE of healthy rats migrate, 3 month DA rats were injected with BrdU every day for 5 days, and each week, 3 were sacrificed and the number and location of BrdU and Ki67 positive cells were mapped. In addition, DiI crystals were injected into the far periphery of the RPE and were examined after 3 weeks. To investigate the effects of inducing laser lesions on the migration of RPE cells, laser burns were applied unilaterally. Fundus photographs were taken with a digital camera mounted on a modified confocal laser ophthalmoscope (cSLO). Spectral domain optical coherence tomography imaging was performed in the same session as the cSLO to ensure that only the RPE layer was damaged. Animals were then either injected with BrdU or BrdU was administered through their drinking water. After 3 weeks, animals were sacrificed and the BrdU positive cells were mapped. The findings from this study strongly suggest that RPE cells have the capacity to migrate from the periphery towards the centre. First, the DiI experiment shows that inserting DiI into the far periphery of the RPE results with DiI positive cells in the centre. Second, the BrdU experiment demonstrates that cells in the periphery of the RPE are proliferating, in which they are both Ki67 and BrdU positive, and that the daughter cells

from the proliferating cells, still containing the BrdU, migrate centrally. This study also demonstrated that in situations where a single laser lesion had been placed in either the central or peripheral RPE, movement of cells towards the lesion site occurred. Unexpectedly, lesions placed in only one eye caused an equal and quadrant specific upregulation of BrdU positive cells in the fellow (contralateral) eye. The findings in this study should be considered when future treatments are targeted to just one eye as the paradigm of using the contralateral eye as a control appears to be inappropriate.

4.2 Introduction

The interactions of RPE cells with the Bruch's membrane, the overlying photoreceptors and adjacent RPE cells, are critical for the maintenance of normal retinal function. Dysfunction of the RPE plays a role in the pathogenesis of a wide variety of diseases that cause damage to vision, including AMD. Although many pathologies result in RPE cell loss, cells are also lost as a function of age (Del Priore et al., 2002, Panda-Jonas et al., 1996). Del Priore et al. (2002) showed that in humans age-related RPE cell death occurred mainly in the macula. The cell density in this region, however, remained unchanged. Instead, the density of RPE cells decreased in the periphery suggesting that cells are proliferating in the periphery and migrating towards the macula in order to compensate for the continuous loss of foveal RPE cells.

RPE cell migration is required to establish a confluent monolayer during development and also to maintain the integrity of the RPE during cell loss associated with ageing. The migration of RPE cells can be triggered as a result of a release of chemotactic agents or growth factors (Johnson et al., 2002). Trauma to the eye, such as retinal detachment, or certain pathologic conditions, such as subretinal neovascularisation, can trigger the release of these factors from the blood or the vitreous (Charteris, 1995, Machemer and Laqua, 1975, Miller et al., 1986). Migration of RPE cells can play both a beneficial and detrimental role in the healing process. To aid the healing process, RPE cells may aggregate along injured capillaries in order to slow leakage and therefore inhibit further

neovascular growth. Exuberant migration and proliferation of the RPE, on the other hand, may also result in the accumulation of ectopic RPE cells in the form of epiretinal membranes that result in a severe loss of vision (Verstraeten et al., 1990).

In order for a cell to be able to migrate, specific cellular mechanisms take place to produce coordinated cycles of four basic steps:

1. Protrusion of the leading edge
2. Formation of attachment sites
3. Generation of contractile forces
4. Detachment of the trailing edge

Figure 4.2.1: Steps involved for a single cell to migrate. Migration is initiated at cellular protrusion sites by polymerisation of an actin network along the cell's leading edge. Focal adhesions are composed of complexes of integrin receptors, actin filaments and associated proteins that provide anchor points for actin stress fibres. Movement is initiated by contraction of myosin in association with stress fibres (Horwitz and Parsons, 1999).

To begin with, there is the initial protrusion of the plasma membrane at the leading edge of the cell. These protrusions are driven by the polymerisation of a network of cytoskeletal actin filaments. These are stabilised via the formation of adhesive complexes which are regions of the plasma membrane where integrin receptors, actin filaments and associated proteins cluster together. As the cell migrates, the small emerging adhesive complexes at the front of the cell grow and strengthen into larger, more organised adhesive complexes. These serve as points of traction over which the cell body moves. Following this, there is a release of adhesions at the rear of the cell causing the net displacement of the cell (Horwitz and Parsons, 1999) (Figure 4.2.1).

In the RPE, the factors that regulate these cytoskeletal elements are protein kinase C, which stimulates migration via phosphorylation of integrin (Hergott et al., 1993, Murphy et al., 1995); mitogen-activated protein kinase (Hinton et al., 1998) and the polyamines - spermidine and spermine (Johnson et al., 2002). In addition to these, are other regulatory factors that appear in several epithelial cell types. These include the members of the Rho family of small GTPases, Cdc42, Rac, Rho, as well as the Src family kinases, calpain and focal adhesion kinase (FAK) (Hall, 1998, Huttenlocher et al., 1997, Klinghoffer et al., 1999, Sieg et al., 1999).

In the previous experiments from chapter 3, where Ki67 and BrdU proliferation in the RPE were examined, a strong pattern became evident. Ki67 positive cells were only ever found in the peripheral region of the RPE, whereas, BrdU positive cells were found throughout

the entire RPE sheet. This includes the central region, a region thought to be senescent. This suggested that cells may be proliferating in the periphery and then migrating towards the centre. RPE proliferation and migration is most often affiliated to diseases such as proliferative vitreoretinopathy (PVR), proliferative diabetic retinopathy (PDR) and age-related macular degeneration (AMD). In this study, however, migration within the RPE of healthy young pigmented rats will be investigated. Furthermore, the effect of inducing laser lesions in either the periphery or the central region of the RPE will be investigated to determine whether retinal location affects the response of RPE cells to the damaged area.

Laser induced retinal lesions are widely used in ophthalmology for treatments aimed at restoring vision and postponing blinding processes (Belokopytov et al., 2010, Schuele et al., 2005). They provide a method for the selective destruction of RPE cells, without causing adverse effects to the neural retina and the choroid, allowing for damaged cells to be replaced by proliferation and migration of neighbouring intact RPE cells (Brinkmann et al., 2000). The selective damage of the RPE was first demonstrated by Roider et al. (1992), where Argon-ion laser pulses (5-µs) at 514nm were used on the rabbit RPE. Following the treatment, histological examinations took place demonstrating the selectivity of the damage to the RPE as the photoreceptors were well preserved.

The selectivity of the laser lesions on the RPE occurs due to the fact that the RPE absorbs the highest amount of light in the retina (Birngruber et al., 1985). The melanosomes within these cells are the strongest chromophores for visible light in the fundus

(Schraermeyer and Heimann, 1999), with approximately 60% of incident light being absorbed by the RPE in humans (Hammond and Caruso-Avery, 2000). When the fundus is irradiated with laser pulses at a pulse duration below 5µsec, high temperatures are limited to the RPE cells and only a low sub-lethal temperature increase in the neighbouring tissue structures is obtained (Roider et al., 1993).

Previous studies have shown that laser photocoagulation triggers local (Miller et al., 1986, Pollack and Korte, 1990) and distant RPE proliferation (von Leithner et al., 2010). Here, a single lesion will be placed in either in the centre of the RPE near the optic nerve, or in the far periphery and the proliferative and the migratory responses will be recorded.

4.3 Methods

Three month Dark Agouti rats were used for all the experiments in this study. The animals were housed with a 12h light/dark cycle in a temperature controlled environment. All experimental procedures were carried out under the United Kingdom (Scientific Procedures) Act 1986. The table below shows the number of animals used for each individual experiment.

Experiment	Number of DA rats used
Month long BrdU preliminary experiment	3
Migration experiment (BrdU)	12
Migration experiment (DiI)	5
Laser (BrdU in water)	8
Laser (BrdU injections)	8

Table 4.3.1: A table showing the number of animals used in the experiments undertaken to investigate RPE cell migration in healthy and lasered rat eyes.

A number of procedures were undertaken to provide a comprehensive picture of the migratory and proliferative capacity of RPE cells under normal and laser induced conditions.

BrdU injections and immunohistochemistry

To determine whether individual cells within the RPE monolayer have the capacity to migrate in non-pathological situations, a preliminary experiment was undertaken. Here, animals were given a single pulse of BrdU every day for 5 days, and were then left for a month before they were sacrificed. Once sacrificed, the immunohistochemistry was carried out in the same way as described in the methods section of chapter 3.

Following this experiment, a more extensive study was carried out in which a larger group of 12 animals were injected with BrdU every day for 5 days, and then each week, 3 were sacrificed. As 12 animals were more difficult to handle on a daily basis, the animals were anaesthetised with Isoflurane (2-chloro-2-(difluoromethoxy)-1,1,1-trifluoro-ethane) before they were given the BrdU injections. Again, after sacrificing, the animals were enucleated and immunostaining against the BrdU antibody was carried out in the same was as described in chapter 3.

In vivo imaging

In order to view the condition of the eye before and after laser lesions were induced, in vivo imaging was used. Rats were anaesthetised with 37.5% Ketamine (Fort Dodge, UK), 25% Dormitor (Pfizer, UK) and 37.5% sterile water (Norbrook Laboratories Ltd, UK) at 0.2mL/100g (i.p. supplemented as required). Once they had gone down, their pupils were

dilated using 1% tropicamide (Bausch and Lomb, UK). All animals under anaesthesia were kept warm on a 37°C heating pad.

Fundus photographs were taken with a digital camera mounted on a modified confocal laser ophthalmoscope (cSLO) (Heidelberg Retina Angiograph, Heidelberg Engineering, Germany) where the pinhole diameter had been reduced to 100µm to improve axial resolution, and the laser power increased to improve signal-to-noise ratio. The axial and lateral resolution of cSLO images were 15.7µm and 2.2µm, respectively. The cSLO frame rate was 8.9Hz, and the field of view was 55°. Whilst imaging, to avoid cataract formation and other ocular artifacts, the corneas of the rats were kept moist using 2% hydroxypropylmethylcellulose (Torbay P.M.U, UK).

Spectral domain optical coherence tomography (SD-OCT) (Spectralis, Heidelberg Engineering) imaging was performed in the same session as the cSLO. SD-OCT is a non-invasive method that provides high resolution, cross sectional images of the retina. In order to adapt for the optical qualities of the rat eye, a commercially available LINOS Achromats NIR 80D lens (Linos Photonics, Germany) was mounted directly in front of the camera unit. Imaging was performed using the proprietary software package Eye Explorer version 3.2.1.0 from Heidelberg Engineering. The length of the reference pathway was adjusted manually according to the manufacturer's instructions.

Laser photocoagulation

After taking initial images of the eye using the cSLO, the retinas of the rats were exposed to laser photocoagulation to cause focal RPE lesions. The burns were applied unilaterally using a Novus Spectra (Lumenis, UK) with diode-pumped solid state laser system with 532 wavelength laser pointer mounted on a slit lamp (Haag-Streitt, BQ-900, Switzerland). A glass coverslip was placed over the eye during the laser delivery, fulfilling the role of a contact lens. One individual coagulation lesion was placed either by the optic nerve in the centre of the eye, or out in the periphery of the eye. Lesions of 200µm spot size, 0.1s duration and 100mW power were placed into the right eye of each animal. The left eye was left as an internal control. A reactive bubble was not seen at the retinal surface after laser in any of the treated eyes, indicating that Bruch's membrane had not been ruptured. The region of damage after the lesion was then examined using the cSLO, followed by the SD-OCT. Animals were recovered by an i.p. injection of 20% Antisedan (Orion Pharma, Finland) and 80% sterile water at 0.01ml/150g.

Following laser lesions, 2 different methods of BrdU administration took place:

1. **BrdU in the drinking water of the rats.** By incorporating the BrdU into the drinking water, a continuous uptake of BrdU was presumed. Animals were given one pulse of BrdU immediately after the laser lesions were placed. Then 0.05g BrdU was added to 41.6 ml water and 8.3 ml orange juice (to mask the taste of the BrdU) and placed in an opaque water bottle. BrdU is light sensitive so prior to the experiments, water bottles were painted with a matt black paint to ensure that

light cannot enter. The animals' drinking water was changed every day and the amount of water consumed was recorded (Figure 4.3.1). After 3 weeks, the animals were sacrificed using CO_2 and their eyes were removed and stained for BrdU.

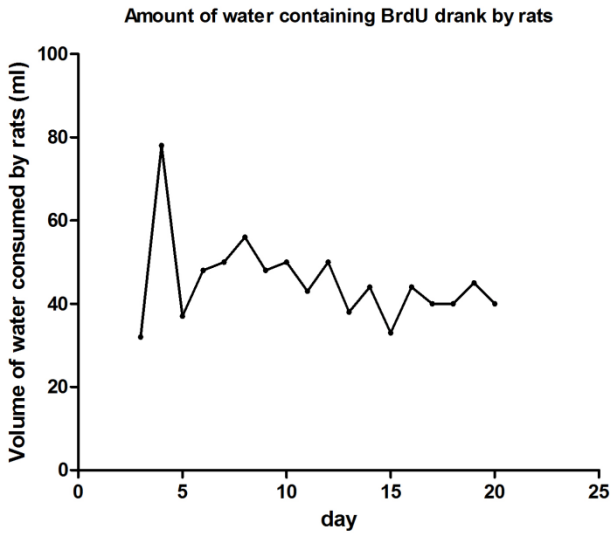

Figure 4.3.1: Volume of water containing BrdU drank by rats in the same cage over the 3 weeks after the lesions were induced.

2. **BrdU given as IP injections following lesions.** Immediately after the laser lesions had been placed, the rats were given an i.p. injection of BrdU and were then recovered. The rats were given another 4 injections, every day at the same time so a total of 5 injections were given, similar to the previous experiments. The animals were then left for 3 weeks until they were sacrificed. Again, the animals were enucleated and their RPE stained for BrdU. Before enucleation, a stitch was placed at the top of the eye for orientation.

DiI application

Another method to determine whether cells in the periphery of the RPE have the capacity to migrate towards the centre was the application DiI. DiI (1,1'-dioctadecyl-3,3,3'3'-tetramethylindocarbocyanine perchlorate) is a lipid-soluble substance that has been used to measure lipid mobility in cell membranes, to assess cell fusion and to study growth cone metabolism (Vidal-Sanz et al., 1988). The dye readily becomes incorporated into the plasma membrane of neurons exposed to it and then diffuses within the plane of the membrane to label the neurons retrogradely and anterogradely. DiI fluoresces bright red when viewed under the microscope and as it labels neurons by diffusion into the membrane rather than by axonal transport, it can be used to trace projections not only in living specimens but also in fixed tissue (Elberger and Honig, 1990).

Animals were anaesthetized with 37.5% Ketamine (Fort Dodge, UK), 25% Dormitor (Pfizer, UK) and 37.5% sterile water (Norbrook Laboratories Ltd, UK) at 0.2mL/100g (i.p. supplemented as required). Once fully anaesthetized, DiI crystals (on the tip of a sterile syringe needle) were placed into the far periphery of the back of the eye using an operating microscope. The DiI crystals were placed in three equidistant locations of the eye in each animal. Immediately after the DiI was applied, the animals were taken and both eyes were imaged using the cSLO. The animals were then left for 3 weeks, when again their eyes were imaged using the cSLO. After imaging, the animals were not recovered and their eyes were enucleated and fixed in 4% paraformaldehyde in phosphate-buffered saline (PBS) for 3 hours at room temperature. The eyes were carefully

dissected in order to expose the RPE sheet and were stained with Alexa Fluor 488 phalloidin (Invitrogen, 1:50,) diluted in PBS, for 1 hour. The RPE flatmounts were washed three times in PBS before being mounted with Vectashield (Vector Laboratories, UK). The RPE sheets were viewed under an epi-fluorescence microscope and images were acquired.

Tissue Analysis

Mapping the BrdU positive cells

For all the experiments in which BrdU proliferation and migration was being assessed, each individual RPE flatmount was carefully mapped and the location of each BrdU positive cell was recorded. Each flatmount was traced around by placing the eye onto a light box (very briefly in order to avoid bleaching the tissue) and the image was scanned into the computer where it was enlarged. Then using an epi-fluorescence microscope to view the BrdU positive cells, the location of the cells was placed onto the drawing of the RPE sheet.

The RPE was divided into three regions, periphery, equator and centre in the same way as described in chapters 2 and 3. The outermost 20% of the RPE was considered to be the periphery, whilst the following 40% was considered to be the equatorial region and the innermost 40% was considered as the central region.

4.4 Results

Increase in number of BrdU positive cells in the centre of the RPE

BrdU is a thymidine analog that is incorporated into DNA only during the S phase of the mitotic process (Kee et al., 2002, Wojtowicz and Kee, 2006). Once incorporated, BrdU will remain in place and be passed down to daughter cells folllowing division. The preliminary experiment, in which the animals were pulsed with BrdU for 5 days and then left for a month, showed BrdU postive cells present in the centre of the RPE (Figure 4.4.1). Ki67 positive cells were only ever present in the periphery suggesting that cells from the periphery had migrated towards the centre.

Following this, a further experiment was carried out in which 12 animals were pulsed with BrdU, everyday for 5 days and each week a group were killed (Figure 4.4.2). The number of BrdU positive cells increased in each retinal region each week until the fourth week (Figure 4.4.2A), where the numbers of BrdU positive cells dropped (Figure 4.4.2C). This is most likely as a result of BrdU being diluted out of the cells rather than a drop in proliferation. Three weeks appears to be the period of peak proliferation, for this reason, for all future experiments, animals were always left for three weeks post-injection, in order to obtain the maximum number of proliferating cells.

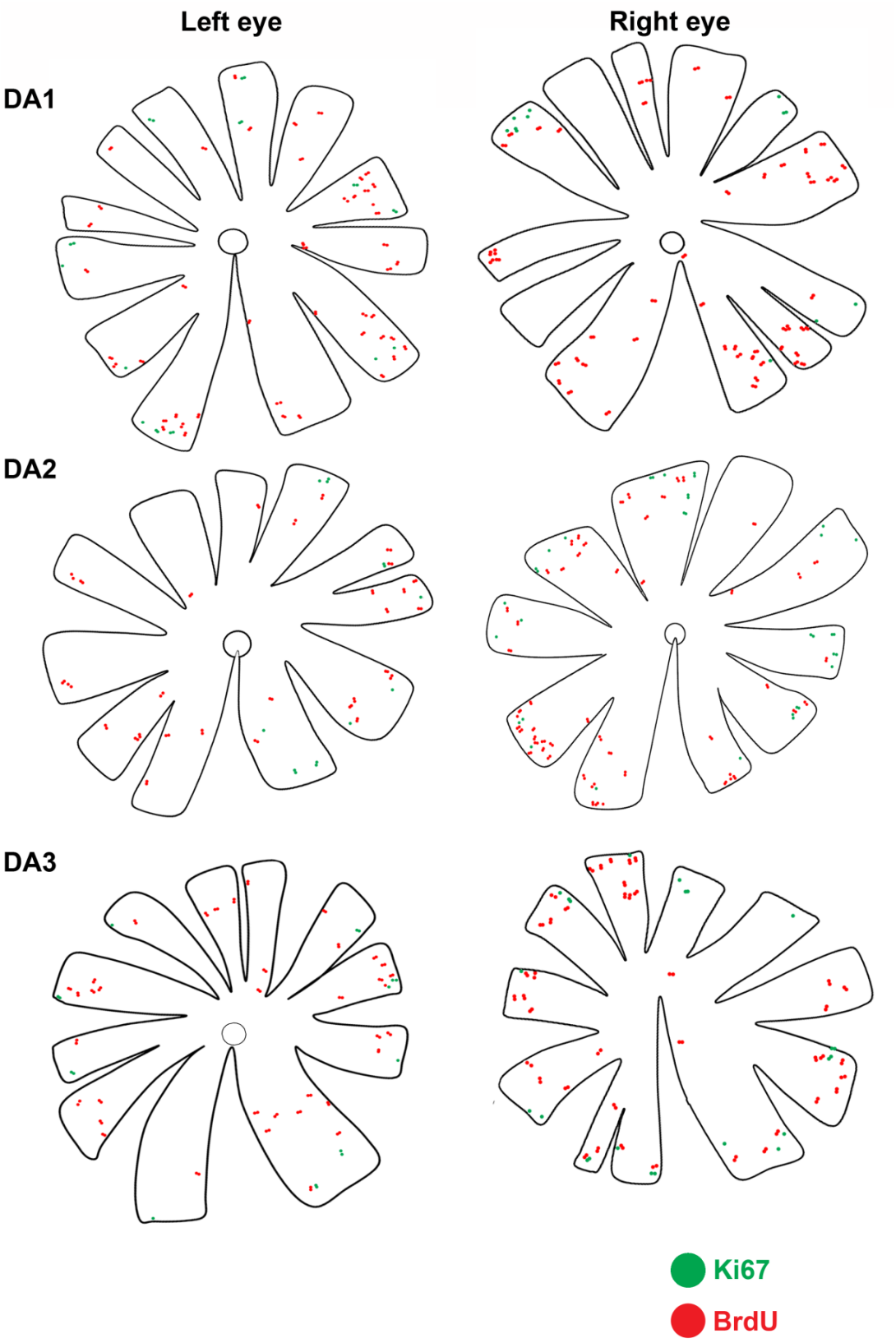

Figure 4.4.1: Maps of the RPE from 3 DA rats showing BrdU +ve cells in the centre of the RPE after a month. After pulsing the animals for 5 days and leaving them for a month, BrdU +ve cells (red) can be seen in all retinal regions of the RPE (periphery, equator and centre). Ki67 +ve cells, however, were only ever found in the periphery of the eye.

The number of BrdU positive cells was always the greatest in the proliferative peripheral region of the RPE, however, a steady increase of BrdU positive cells was demsonstrated in both the equatorial and central regions. There is a significant increase in the number of cells in the centre of the RPE after 3 weeks, compared to the first week ($p<0.001$) (Figure 4.4.2B). This indicates that the cells are being directed to migrate towards the centre to replace those lost. Immunohistochemistry results of BrdU positive cells in the RPE show that a clear trail can be seen where cells are dividing and migrating (Figure 4.4.3).

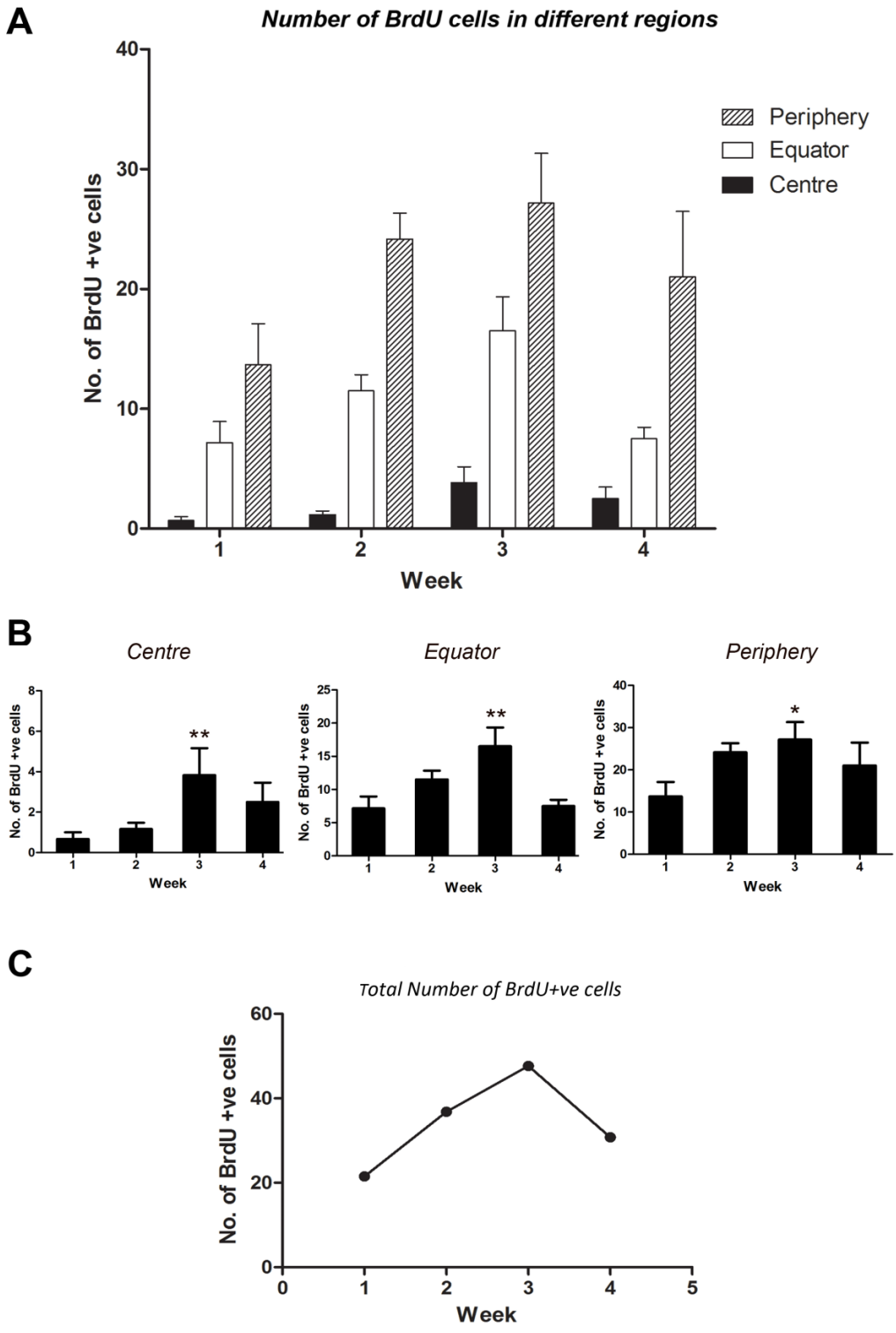

Figure 4.4.2: (A) shows the number of BrdU positive cells in each retinal region over the 4 weeks that animals were examined. The results show that as the number of weeks after the initial BrdU injections increases, the number of BrdU +ve cells increases in all regions until the 4th week, where the cell number decreases (also demonstrated in (C)). More specifically an increase can be seen in the central region (B), a region considered to be senescent, with a significant increase in the number of BrdU +ve cells between week 1 and 3. * $p < 0.05$, ** $p<0.01$.

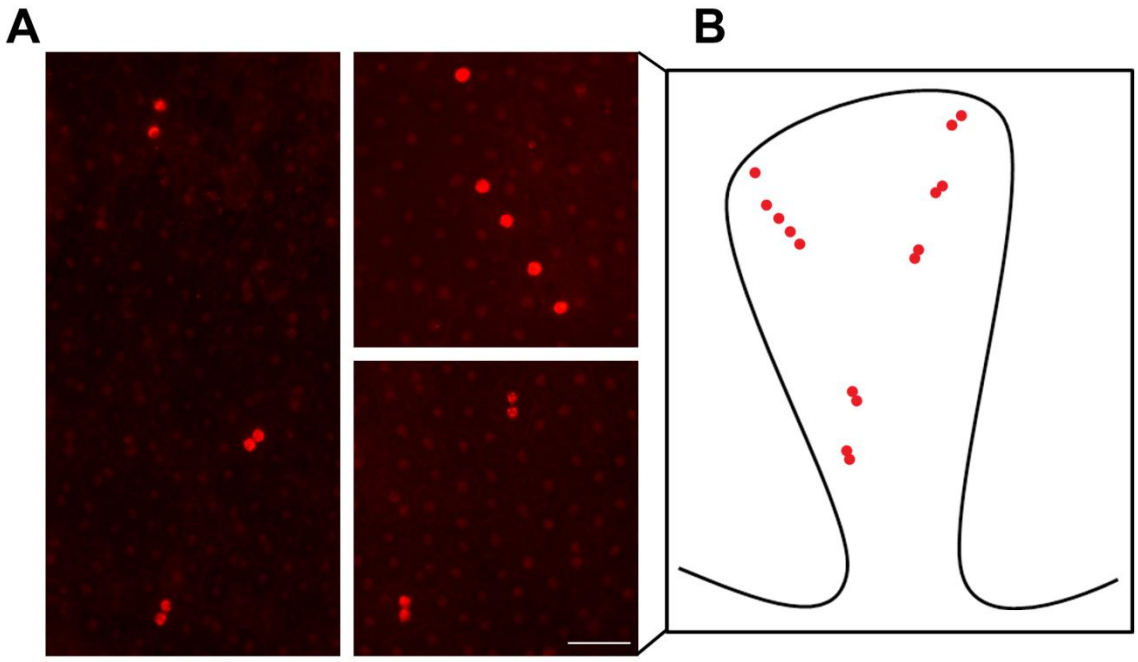

Figure 4.4.3: (A) shows immunofluorescence images of the RPE showing the BrdU +ve cells. A trail of cells can be seen, suggesting that cells are dividing and migrating towards the centre.(B) shows a diagrammatic map of one section of the RPE, indicating where the trails of the BrdU positive cells can be seen on the RPE sheet. Cells are seen forming little trails that appear to be going towards the centre of the RPE. Scale bar - 50µm.

Following DiI application, patterns can be seen that are consistent with cells migrating towards the centre of the RPE in normal healthy rats

DiI was placed into the far periphery of the eye of the DA rats. Immediately after placing the DiI crystals into the eye, in vivo images were taken using the confocal laser ophthalmoscope (cSLO) (Figure 4.4.4A). As a result of the slight trauma caused to the eye, haemorrhaging is visible in the bottom left part of the eye where the DiI was inserted. The rest of the eye appears to be healthy. After 3 weeks, animals were imaged again and a macrophage response to the points of injection was visible (Kam et al., 2010, Luhmann et al., 2009). These are indicated by the white spots seen scattered around the entire eye

(Figure 4.4.4B). The large white area (figure 4.4.4C) appears to be another point in which the needle containing the DiI was placed.

Figure 4.4.4D shows a strip of the RPE spanning from the periphery towards the optic nerve. DiI emission is bright red when viewed under the microscope. The point of entry of the DiI can be seen in the bottom right hand corner, the white arrows in the central/equatorial region of the RPE point to individually labelled RPE cells. DiI diffuses into the membranes of cells, suggesting that cells from the periphery have migrated towards the centre, carrying the label. A magnified image of a DiI labelled cell shows black holes in the centre of the cell (Figure 4.4.4E). This is where the nuclei of the cell are, showing the membrane specific staining of the DiI. The RPE sheets were also stained with phalloidin, a high-affinity filamentous actin (F-actin) probe to highlight the cell junctions, this further proves the specificity of the DiI stain as the DiI labelled RPE cell lies within the RPE cell junctions (Figure 4.4.4F).

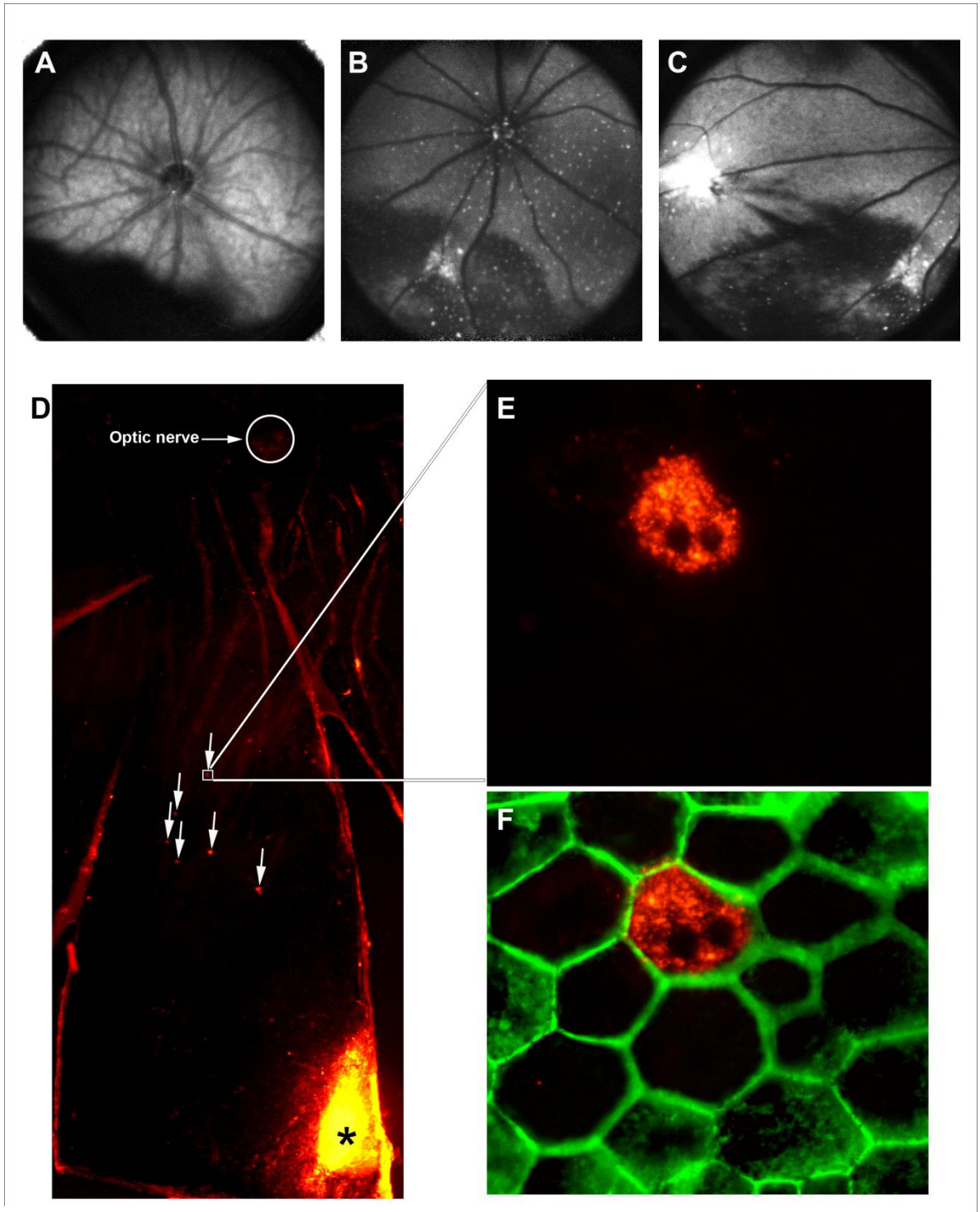

Figure 4.4.4: Incorporation of DiI into the RPE. (A-C) show images from in vivo imaging of the eye. (A) was taken directly after the DiI crystals were placed into the back of the eye, the trauma to the eye has caused haemorrhaging in the eye. (B-C) show the same eye, 3 weeks later, the site where the needle was placed is visible. The white spots indicate macrophage presence. (D) shows an immunofluorescence image of part of the rat RPE, spanning from the optic nerve to the periphery. The asterisk indicates the site where the DiI was placed in the far right peripheral corner, and individually labelled cells can be seen in the equatorial region of the eye. (E) shows a magnified close up of one of these cells, where the RPE is clearly labelled. (F) shows the same cell with a phalloidin stain showing the junctions of the RPE.

After inducing RPE proliferation via laser lesions, in vivo imaging confirmed laser damage was just targeted to the RPE

Before the laser lesions were placed, both eyes of each animal were imaged using the confocal laser ophthalmoscope (cSLO). Immediately after the right eye of each animal had been lesioned, the eye was imaged again to show the location of the lesion. Only one lesion was placed in either the centre or the periphery of the eye (Figures 4.4.5 A and 4.4.5B, respectively). Spectral domain optical coherence tomography (SD-OCT) images were then taken to ensure that CNV had not been induced and that damage was only targeted to the RPE (Figures 4.4.5C and 4.4.5D). This is evident as all the retinal layers seem well-defined surrounding the lesion and at the site of the lesion only RPE thinning could be observed and tissue beneath the RPE was not disrupted. Although all lesions were placed using the same conditions, lesions placed in the far periphery appeared to induce more damage, and seemed to create a greater impact on the retina with complete disruption to the outer segments (Figure 4.4.5D).

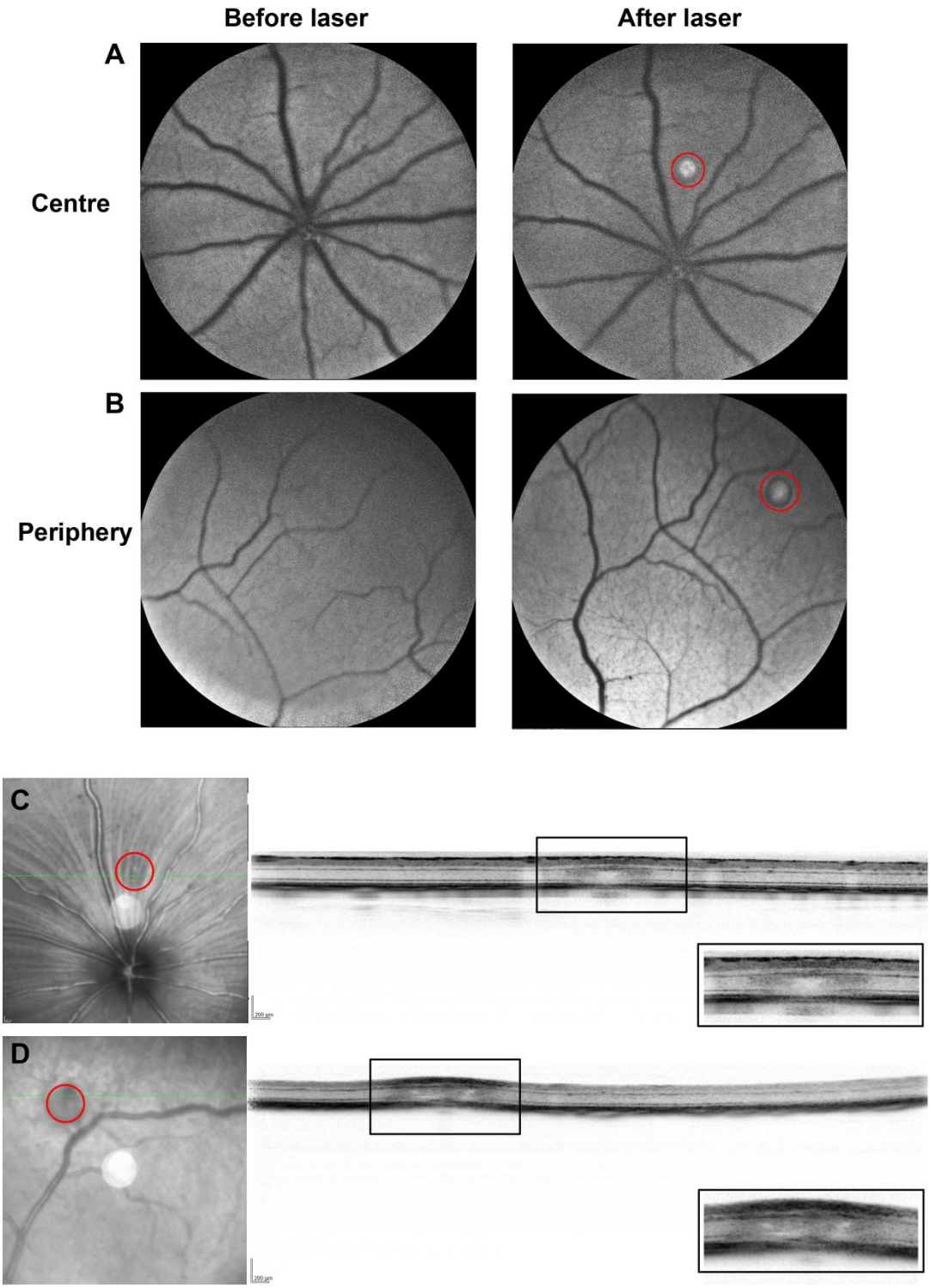

Figure 4.4.5: In vivo imaging before and after laser lesions were placed. (A-B) Confocal laser ophthalmoscope was used to image the eye before the lesion was placed. Immediately afterwards, another image was taken to show the exact retinal location of the lesion. Lesions were placed either centrally, close to the optic nerve (A), or in the far periphery (B). In order to ensure that CNV was not induced and damage was only targeted to the RPE and not the underlying Bruch's membrane, SD-OCT images were also take from both the central (C) and peripheral (D) lesions. The areas in the black box have been enlarged as this is the site of the lesion. The black arrows point towards the RPE layer.

Lesions placed in only one eye cause an equal upregulation of BrdU positive cells in the fellow (contralateral) eye

In this study, BrdU was administered orally for 3 weeks as it can be given continuously in drinking water, therefore, avoiding the stress induced by repeated i.p. injections. Data from the previous experiment (Figure 4.4.2), where animals were not lesioned and BrdU positive cells were counted, showed that the average number of BrdU positive cells in the RPE was approximately 50. Here, however, the number of BrdU positive cells seemed to be quite low, especially since the RPE had been damaged via the laser, with approximately 22 BrdU positive cells found within the lasered eye, and 18 in the non-lasered eye (Figure 4.4.6A). This strongly suggests that the availability of BrdU changed during the experiment, reaching at some point a level that was too low to be detected. As the amount of BrdU taken up by the animals stayed constant during the entire administration period, the lower level of BrdU in the circulation could be due to a change in the metabolism of BrdU during the 3 weeks of administration, leading to a lower level of BrdU in the circulation. BrdU is rapidly dehalogenated in the liver, leaving only a small amount available for incorporation into the DNA (Kriss et al., 1963). The continuous BrdU application may, therefore, lead to enzyme induction in the liver, leading to the more efficient degradation of BrdU. This results in a reduction of BrdU that is available for labelling cells in the S-phase of the cell cycle.

As the oral application of BrdU was not a good method of determining the proliferative capacity of the RPE after laser lesions had been placed, the experiment was repeated and

the animals were pulsed with BrdU once a day, for 5 days and then left for 3 weeks. Lesions placed in the periphery of the RPE appeared to cause more cell proliferation than lesions placed centrally, however, this was not significant. Lesions placed centrally did, however, have a significantly greater number of BrdU positive cells compared to the baseline (Figure 4.4.6B). The baseline indicates the average number of BrdU positive cells in animals that have not been lesioned.

An unexpected finding was that not only do cells in the lesioned eye show increased proliferation, but the contralateral non-lesioned eye also shows increased proliferation compared to the baseline. When lesions were placed centrally, the contralateral eye showed almost an identical response to the lesioned eye. Lesions placed in the already proliferative periphery had a greater number of BrdU positive cells in the lesioned eye, however, the non-lesioned eye also had a significantly greater number of BrdU cells compared to the baseline.

Figure 4.4.6C shows an image of a centrally lasered eye, 4 weeks after the laser was placed. The area in the black square shows the location of the lesion. Immunostaining for BrdU showed the BrdU positive cells in the actual lesion and around the RPE. The image in Figure 4.4.6C shows the BrdU positive cells within the lesion. These were not counted and only cells outside of the lesion site were included.

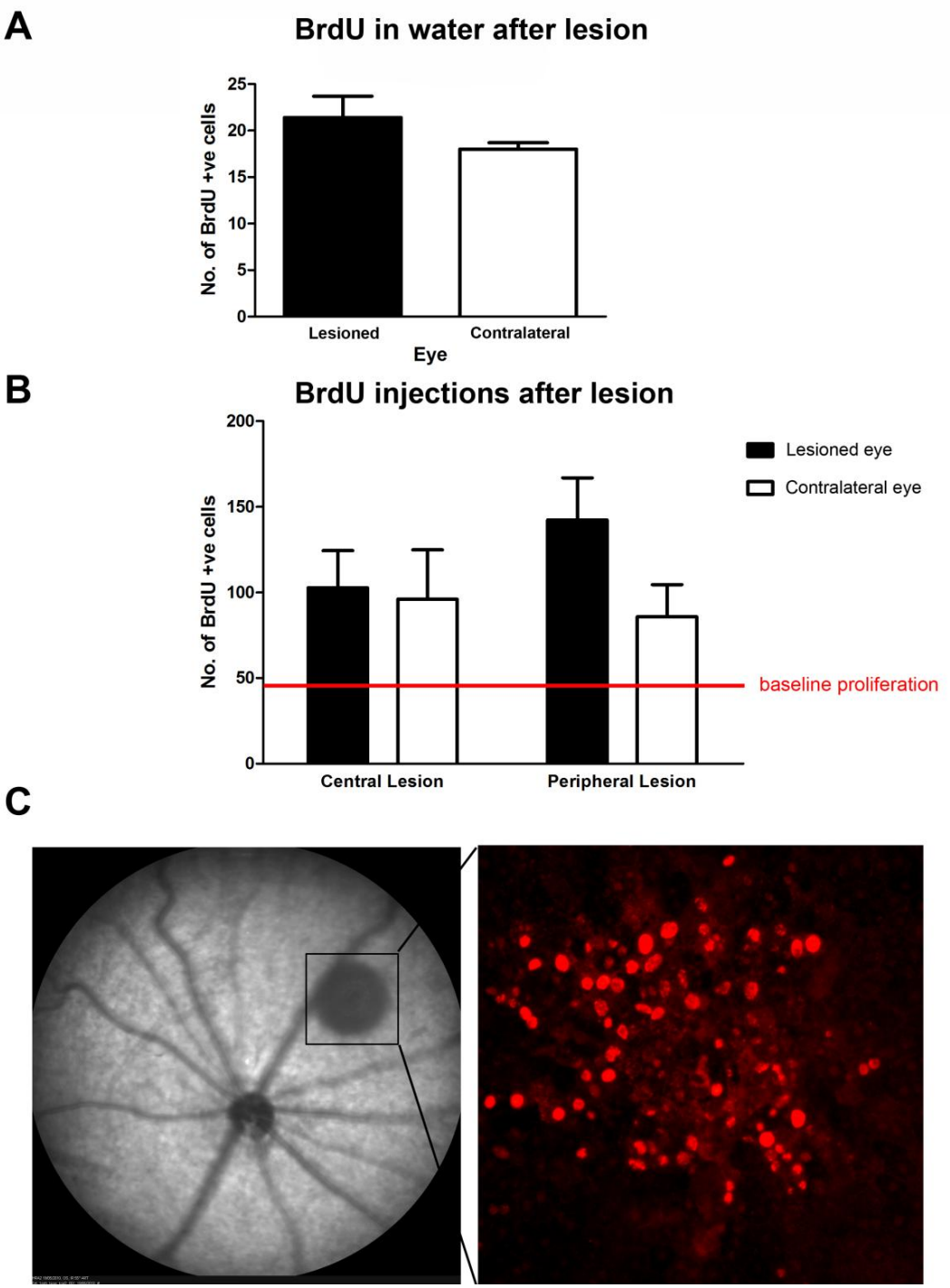

Figure 4.4.6: BrdU proliferation 3 weeks after laser lesion. (A) shows the number of BrdU +ve cells in the lesioned eye and non-lesioned control eye after BrdU had been placed in the rats' drinking water for 3 weeks. Although the number of BrdU +ve cells was low, there appeared to be no difference between the lesioned and contralateral control eye. Both presented with almost the same number of BrdU +ve cells. (B) shows the number of BrdU +ve cells in both the lesioned and control eye after a lesion was placed in either the central or peripheral region of the RPE. The red line indicates the baseline, this is taken from animals in which a lesion was not placed in either eye. Lesions in both regions, induced a response in both the lesioned and contralateral eye. Lesions placed in the central region, induced almost an identical response in the contralateral eye.

Peripheral lesions resulted in a greater number of BrdU positive cells in the lasered eye compared to the control eye as well as the centrally lesioned eye. The contralateral eye, still, however, had a significant more number of BrdU+ cells compared to the baseline. (C) shows a cSLO image of a centrally placed lesion. The small black box indicates the location of the lesion and immunohistochemical results show BrdU +ve cells within the lesion. BrdU +ve cells within the lesion were not counted - only +ve cells outside of this region were included.

Upregulation of BrdU in the contralateral eye appears to be quadrant specific

The non-lesioned "control" eye from each animal has an almost identical response in regards to proliferation within the RPE, as the lesioned eye. The response seemed to be specific to the same retinal location as in the lesioned retina. All BrdU positive cells were mapped for both the lesioned and non-lesioned eye. Although the whole RPE sheet seems to react to the lesion, the highest percentage of BrdU positive cells was always seen in the quadrant where the lesion was placed. Interestingly, this was mirrored in the contralateral eye, where similarly the highest percentage of BrdU positive cells were found in the same area as the site of the lesion in the other eye (Figure 4.4.7 and 4.4.8). This effect was seen regardless of the retinal location of the lesion.

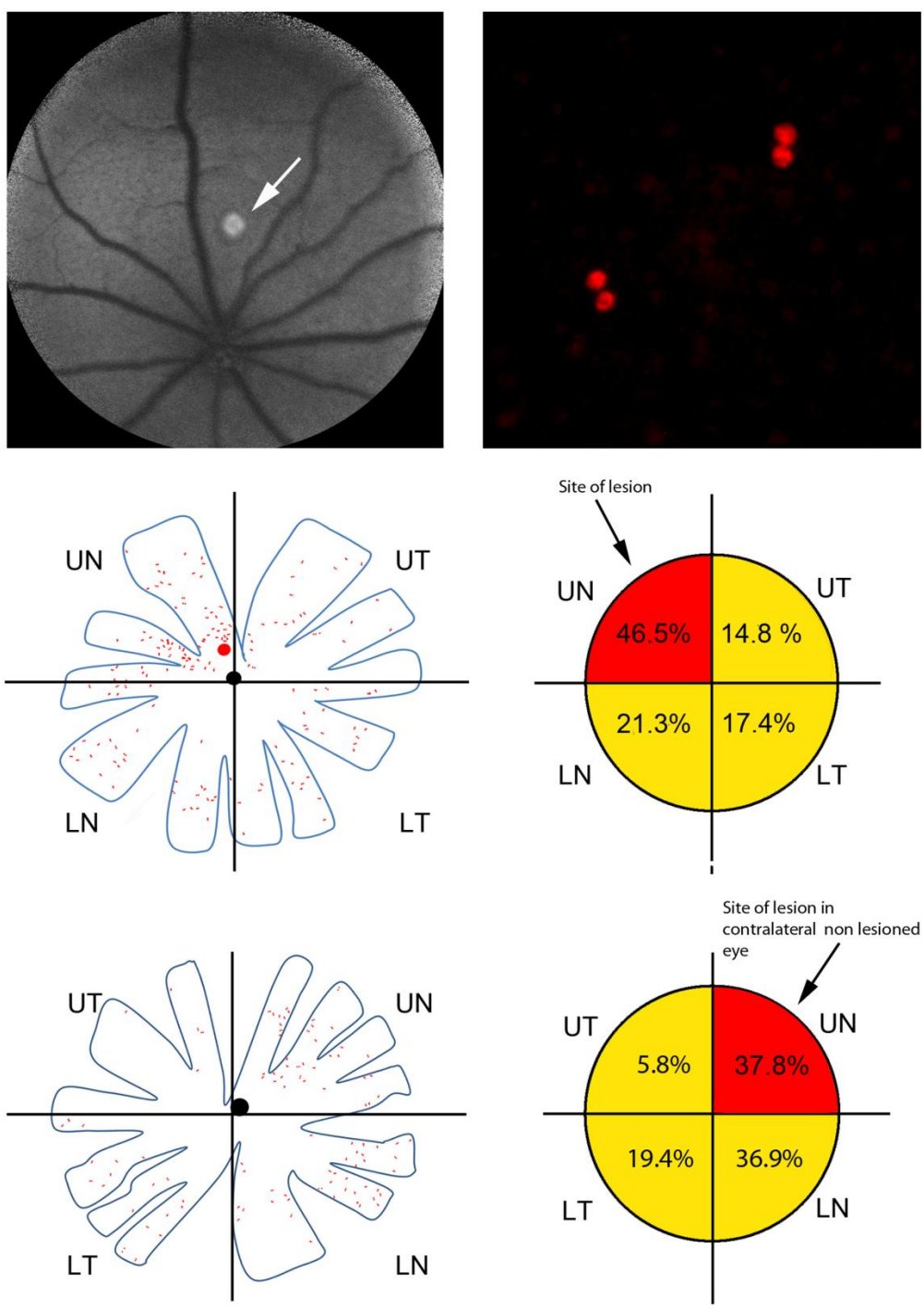

Figure 4.4.7: A cSLO image showing the site of the lesion in the central region of the RPE together with an image showing the BrdU positive cells that were mapped onto a tracing of the RPE flatmount. Here, maps from 1 animal are shown, one from the right (lasered) eye and one from the left (non-lasered) eye. The eye was divided into 4 quadrants [Upper temporal (UT), Lower temporal (LT), Upper nasal (UN), Lower nasal (LN)], and the number of BrdU cells in each region counted. The percentage of BrdU positive cells in each quadrant can be seen in the diagrams beside the maps of the RPE. First, in the lasered eye, it is apparent that the largest number of BrdU +ve cells is in the region where the laser was placed. Interestingly, a quadrant specific upregulation of BrdU can be seen in the control eye which was not lasered.

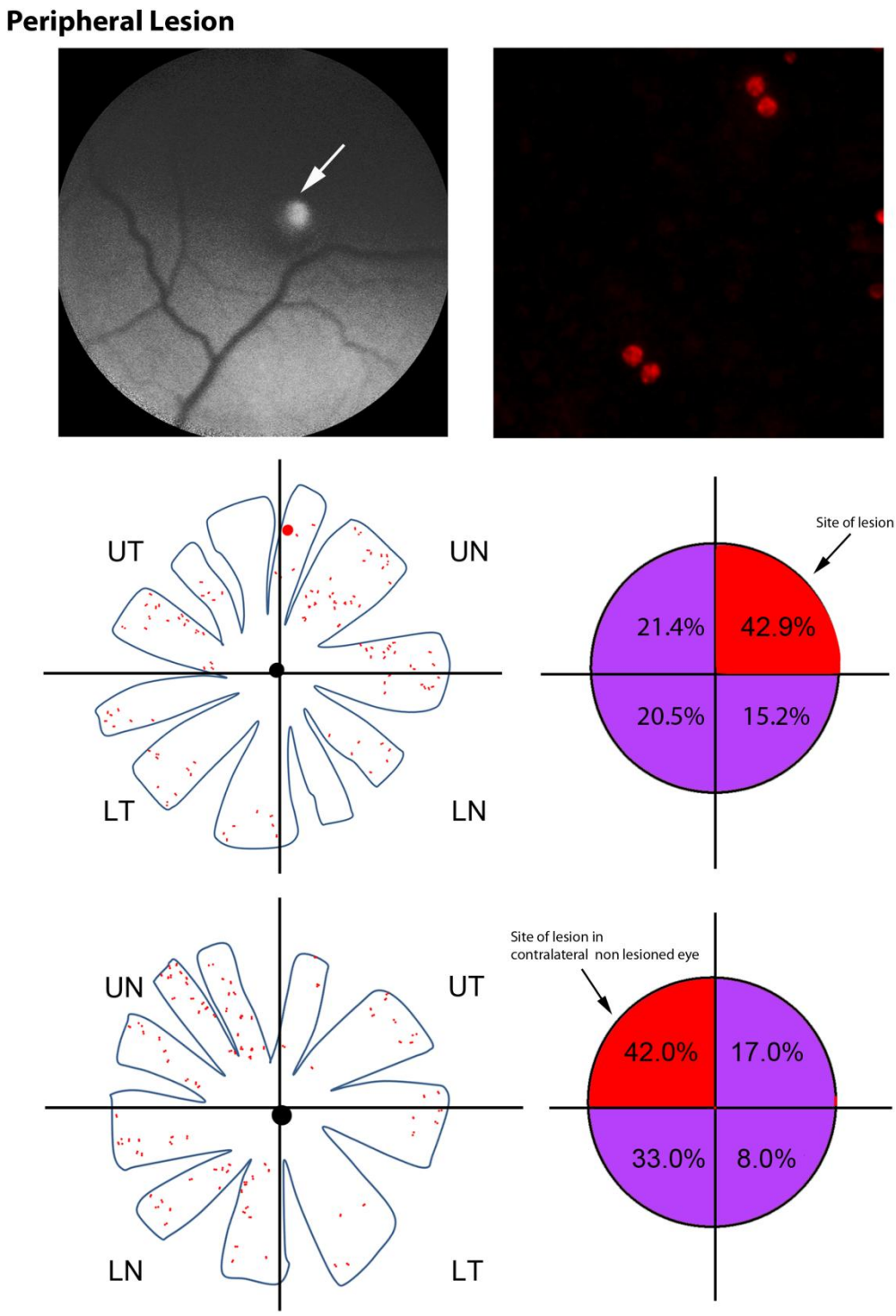

Figure 4.4.8: A cSLO image showing the site of the lesion in the peripheral region of the RPE together with an image showing the BrdU positive cells that were mapped onto a tracing of the RPE flatmount. Here, maps from 1 animal are shown, one from the right (lasered) eye and one from the left (non-lasered) eye. The eye was divided into 4 quadrants [Upper temporal (UT), Lower temporal (LT), Upper nasal (UN), Lower nasal (LN)], and the number of BrdU cells in each region counted. The percentage of BrdU positive cells in each quadrant can be seen in the diagrams beside the maps of the RPE. First, in the lasered eye, it is apparent that largest number of BrdU +ve cells is in the region where the laser was placed. Interestingly, a quadrant specific upregulation of BrdU can be seen in the control eye which was not lasered.

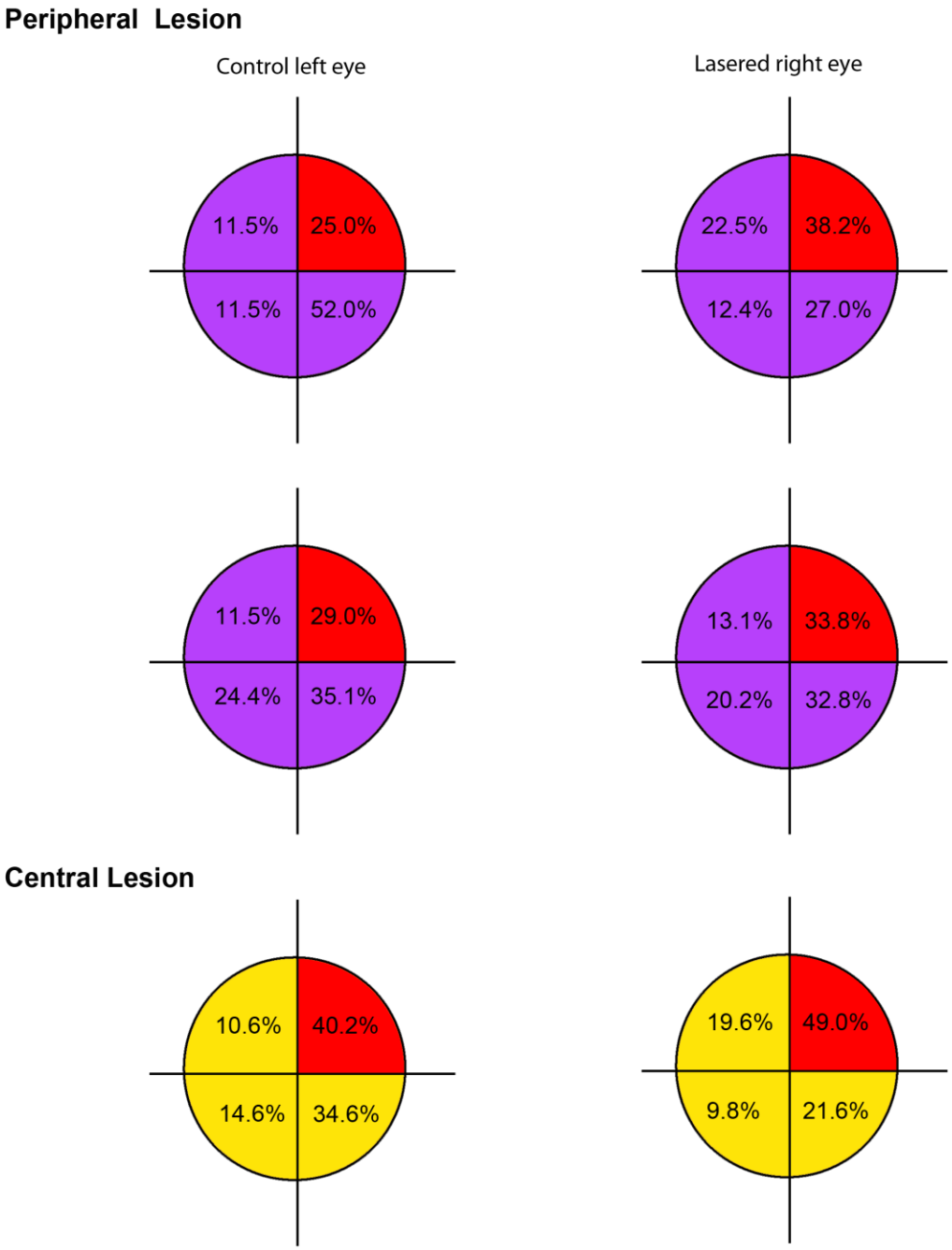

Figure 4.4.9: More diagrams showing that the laser lesion induced in the RPE of one eye causes a quadrant specific upregulation of BrdU +ve cells in the non-lasered contralateral eye. The quadrant marked in red shows the area in which the laser lesion was placed in the right eye and also shows the same region in the fellow eye.

4.5 Discussion

RPE cell migration is a complex process in which the remodelling of the extracellular matrix (ECM) and the secretion of certain growth factors and cytokines by the RPE play a fundamental role (Han et al., 2009, Hiscott et al., 1999). The migration of RPE cells are influenced by the cross talk in cytokines and growth factors such as interleukin (IL)-1β, transforming growth factor (TGF)-β, tumor necrosis factor (TNF)-α, platelet derived growth factor (PDGF) and basic fibroblast growth factor (bFGF) (Nagineni et al., 2005, Spraul et al., 2004). Predominantly, there are three cytokines and growth factors, IL-1β, TNF-α and TGF-β2, which upregulate matrix metalloproteinases (MMPs) in RPE cells. This facilitates the breakdown of the ECM and promotes RPE cell migration (Eichler et al., 2002, Han et al., 2009). Oxidative stress and mechanical stress, such as that generated by ageing, also participate in the migration of RPE cells (Lu et al., 2006).

In this study, RPE cell migration is seen in the RPE of animals in which no damage has been induced. Instead, cell migration has probably occurred to replace cells lost as a result of ageing in order to maintain the integrity of the RPE. Data from this study confirms the theory proposed by Del Priore et al. (2002) that cells from the periphery of the RPE migrate towards the centre to replace those lost with age, rather than the expected decline in macular RPE cell density which is thought to precede cell loss in the macula via apoptosis. Both the DiI and BrdU (in normal animals) experiments suggest strongly that RPE cells have the capacity to migrate towards the centre. First, the DiI experiment shows

that inserting a few crystals into the far periphery of the RPE, results with DiI positive cells in the centre after a few weeks. Second, the BrdU experiment demonstrates that cells in the periphery of the RPE are proliferating, in which they are both Ki67 and BrdU positive, and that the daughter cells from the proliferating cells, still containing the BrdU, migrate centrally.

This study also demonstrated that in situations where a single laser lesion had been placed in either the central or peripheral RPE, movement of cells towards the lesion site occurred. This could be due to the fact that trauma to the eye triggers the release of the necessary growth factors and cytokines required for cell migration from the blood or the vitreous. Wound healing of the RPE is involved in many physiological and pathological processes, as migration of RPE cells plays a fundamental role in the healing process. The wound-induced electric field is one of the earliest signals to initiate directed cell migration and has been proven to play a vital role in wound healing (Nuccitelli, 2003). These electric fields are generated as a consequence of short-circuiting the transepithelial potential difference when a lesion or damage occurs in the epithelial layer (Zhao et al., 2006). Sulik et al. (1992) found that electric fields (EFs), with field strengths of 6 to 10 V/cm, could induce the cathodal migration of RPE cells. They suggested that the endogenous, biologically generated electric fields play a role in the guidance and migration of RPE cells. Although the specific effects and the mechanisms are still unclear, it has been proposed that an important factor of wound healing is that the disruption of an epithelial layer instantaneously generates endogenous electric fields (Zhao et al., 2006). The above draw

to the conclusion that electrical signals are predominant directional cues that guide and stimulate the migration of epithelial cells in wound healing (Zhao et al., 2006).

As wound healing induces directed cell migration to the site of the lesion an understanding of the mechanism is needed. In directed cell migration, acquiring spatial asymmetry is required in establishing polarised leading and trailing edges, and the accumulation of F-actin is a driving force for membrane protrusion during this process (Borisy and Svitkina, 2000). Furthermore, actin filaments selectively accumulate in the cathodal cytoplasm of the cells in EFs (Li and Kolega, 2002). Cell migration also requires cell attachment to the extracellular matrix (ECM), which is mediated by members of the integrin family (Hynes and Lander, 1992). Integrins are heterodimeric transmembrane receptors and the principle cell surface adhesion receptors mediating interactions between the ECM and the actin cytoskeleton. Activation of the integrins, induces integrin clustering, leading to the recruitment of multiple signalling molecules, resulting in the regulation of different signalling pathways. A recent study by Han et al. (2011) shows that EF exposure results in the directed migration of the separated RPE cells and RPE monolayer. In addition, they state that these effects may partially act through the activation of the integrin β1 subunit signalling. Integrins have a strategic cell transmembrane location, therefore, they are good candidates for sensing changes in stress which is exerted by the extracellular current at the cell surface (Han et al., 2011).

Interestingly, regardless of the retinal position of the laser, BrdU upregulation was evident and much higher than the baseline in all the animals tested. This demonstrates that the whole RPE sheet seems to react and become responsive to the damage caused by the laser rather than the specific retinal location.

An unexpected result from the laser study is the indication that a single lesion in one eye, causes an equivalent quadrant specific upregulation of BrdU cells in the contralateral eye. The left eye of each animal in this experiment was initially thought to be used as an internal control. A single lesion was placed in either the centre or periphery of the RPE in the right eye of the animal. In vivo imaging straight after the lesion was placed showed very clearly that damage was only caused to the RPE and not the underlying Bruch's membrane, so the results seen are as not as a result of CNV being induced.

Although the nervous system exhibits a high degree of symmetry, which requires powerful transmedian communication systems to integrate the organism's behaviour (Koltzenburg et al., 1999), some clinical disorders suggest that an extreme point to point bilateral matching of neural function exists (Matthews, 1991, Melzack, 1990). Many studies have shown that unilateral interventions produce bilateral effects. Furthermore, it has been noted that the contralateral effects are qualitatively similar to those occurring at the ipsilateral side (Koltzenburg et al., 1999). The existence of this phenomenon implies the presence of an unrecognised signalling mechanism that links the two sides of the body or a finely orchestrated array of signalling mechanisms.

Studies have shown that following peripheral-nerve lesions, the contralateral non-lesioned structures are also affected. Rotshenker et al. (1979) showed in both the frog and mouse that following unilateral section of a motor nerve and degeneration of ipsilateral neuromuscular junctions, robust signs of sprouting at the junctions of the same, intact, contralateral muscles were evident. Furthermore, the adaptive changes that occur in the ipsilateral motor nucleus following axotomy have also been reported in homonymous neurones on the contralateral side. This includes the increase in peptide levels (Piehl et al., 1991) and mRNA (Linda et al., 1992, Piehl et al., 1991, Booth and Brown, 1993) as well as the proliferation of microglia (Streit et al., 1989).

Axotomy produces a sequence of degenerative events in the sympathetic ganglia and their axons. Damaged sensory neurones issue growth signals that attract sympathetic fibres, the sprouting of these sympathetic fibres not only appear where the damage was caused, but also on the contralateral side. Interestingly, the sprouting on the contralateral side is restricted to homonymous segments of the spinal cord (Chung et al., 1993, McLachlan et al., 1993).

The potential mechanisms of contralateral changes following nerve lesion can be divided into two categories – humoral and neural. Unilateral perturbations result in a number of systemic changes of an organism. These include stress-related changes in endocrine function; circulation of breakdown products from the lesion; and compensatory changes in the behaviour of the animal.

Although these may contribute to the contralateral changes, it seems improbable due to the specificity of the contralateral effects, in terms of the spatial distribution and response type. It is unlikely that these nonspecific mechanisms lead to the precise effects seen. It seems more likely that the response witnessed is due to a neural mechanism and that nerves damaged unilaterally have the capacity to communicate with their contralateral counterpart (Koltzenburg et al., 1999). There are several ways in which this could take place. First, as a result of bilateral peripheral projections to a target and transmedian sprouting. Second, through contralateral communication via the CNS. Third, via communication by commissural interneurons.

There are few studies on the effects that occur to the contralateral eye after induced damage to just one eye. Sympathetic Ophthalmia is a rare, bilateral granulomatous uveitis that occurs following accidental or surgical trauma to one eye which then leads to an inflammatory response not only in the traumatised eye, but also in the fellow eye (Albert and Diaz-Rohena, 1989, Chang and Young, 2011, Damico et al., 2005, Chang and Yang, 2000). The time from ocular injury to onset of sympathetic ophthalmia varies greatly, ranging from a few days to decades, with approximately 80% of patients developing symptoms within 3 months and 90% within a year (Chan et al., 1995, Chang and Young, 2011, Damico et al., 2005). Initially, it was believed that this inflammatory process spreads from one eye to the other via the optic nerve, however, more recent studies have suggested that there appears to be an autoimmune inflammatory response directed against ocular self-antigens found on choroidal melanocytes (Damico et al., 2005). It is

unlikely that the effect being seen in contralateral eye after inducing a laser lesion on the RPE in this study results from Sympathetic Ophthalmia. First, the response seen in the contralateral eye occurs in a short period of time following the laser lesion. Second, it is unlikely that this is an autoimmune response as this would not explain the quadrant specific manner in which the contralateral eye is affected.

Drubaix et al. (1997) performed a study investigating the hyaluronan content during wound healing following excimer laser photoablation in the rabbit. They showed that following the photoablation, the hyaluronan contents of both the wounded and contralateral non-photablated corneas increased in a similar fashion during wound healing. You et al. (1993)and Rask and Jensen (1995) also recorded a similar effect in the contralateral eye after causing corneal damage in rabbits and humans, respectively. You et al. (1993) suggested that the contralateral alterations may reflect a direct or sympathetic response to the laser radiations, or they could be as a result of a systemic factor or hormonal changes induced by the surgery. Fonn et al. (1999) carried out a study in which they compared the central corneal swelling and light scatter after 8 hours of sleep in eyes wearing a certain type of contact lens to the contralateral control eyes. They found that there is a sympathetic swelling response of the control eye to the soft lenses in the other eye. Out of the 20 subjects tested, 16 that exhibited corneal swelling in the tested eye, resulted in corneal swelling in the contralateral eye. Here, the authors did not propose a mechanism for the sympathetic swelling effect.

More recently, Guymer et al. (2011) reported the findings from a clinical trial that they had designed to prevent vision loss from AMD by using a novel nanosecond laser treatment. One eye from each patient was treated with nanosecond retinal regenerative therapy (2RT) laser, whilst the contralateral eye was used as a control. The patients all suffered from bilateral high risk early AMD. Results from this study showed that 6 months after the laser treatment, a large number of treated and untreated eyes were showing some signs of overall retinal function improvement. The fellow untreated eye showed improvements in dark adaptation, flicker, colour thresholds, visual acuity and drusen resolution. The authors suggest that the laser is inducing some long-term systemic effect that is able to affect the contralateral eye, however, as of yet, they have not proposed a possible mechanism for this response.

Until recently, thermal laser photocoagulation was the only well-established and widely accepted treatment for classic choroidal neovascularisation (CNV), secondary to age-related macular degeneration (Bylsma and Guymer, 2005). AMD is now the most common cause of untreatable blindness in the Western world, with a prevalence of 11.8% after the age of 80 (Friedman et al., 2004). The early stages of the disease, early AMD, are characterised by drusen or by small hypopigmentation, without visible choroidal vessels. Drusen are discrete whitish-yellow spots external to the neural retina and the RPE, displacing the RPE inwards (Bylsma and Guymer, 2005). While patients have preserved visual acuity at this stage, they may manifest more abnormalities of visual function such as fading vision in bright light and poor vision in dim light (Steinmetz et al., 1993).

In the late stages of the disease, AMD has two forms – a dry and wet form (de Jong, 2006). Dry AMD, also known as geographic atrophy, starts with a sharply demarcated round or oval hypopigmented spot that is often juxtafoveal and in which large choroidal vessels are visible (de Jong, 2006). Wet AMD, on the other hand, results from hemorrhagic fluid that causes the neuroretina or the RPE to detach from Bruch's membrane. This detachment disturbs the regular arrangement of the photoreceptors and causes metamorphopsia (image distortion) (de Jong, 2006). With continual time, more extensive hemorrhages and scars can appear. Usually a similar type of AMD develops in both eyes, but dry AMD can become wet AMD, and wet AMD can become dry AMD. The prevention and treatment of CNV, resulting from AMD, is the aim of most current and experimental therapeutic interventions. Laser photocoagulation has been widely used and is an accepted treatment for CNV, however, it is beneficial only for a small subset of patients, causes collateral damage to the overlying retina and has a high rate of CNV persistence (Hooper and Guymer, 2003). Other treatments that are currently being used are:

- Photodynamic therapy
- Radiotherapy
- Transpupillary thermotherapy
- Anti-angiogenic drugs
- Macular translocation

Most recently, a nanosecond laser-based treatment has been used in pilot studies to impede the progress of AMD. In the 1970s it was noted that drusen close to retinal laser

burns often disappeared. These findings prompted researchers to investigate the possibility of preventing AMD complications by reducing the drusen with prophylactic laser treatment. Previous studies using laser have shown damage to the surrounding tissue, however, this relatively new nanosecond laser technology (Ellex 2RT ^{TM}) utilises an ultra-fast nanosecond laser pulse that is uniquely different to the current retinal laser treatments. This new technology allows the precise and specific delivery of laser energy to nano-sized targets within the RPE cells, without causing thermal destruction of the retina.

Together with new laser technologies, the results from my study may possibly be able to add some further ideas into the current treatments for AMD. Here, lesions placed both centrally and in the far periphery caused a similar increase in proliferation. The RPE appears to react as a whole, regardless of the location of the lesion, with an up-regulation of proliferating cells observed in the contralateral eye. From these results it is possible to consider lasering the peripheral region of the eye instead of the centre for future trials. The benefits of this are that there is a larger surface area to target and most importantly it is far from the central vision and is, therefore, less risky and CNV secure.

The findings in this study should be considered when future treatments are targeted to just one eye as the paradigm of using the contralateral eye as a control appears to be inappropriate. Studies that have been performed using intrinsic contralateral controls may need to be re-examined. An intrinsic control that is not independent of the treated eye could lead to misinterpretations.

Chapter 5

Glatiramer acetate and the RPE

5.1 Abstract.

The retinal pigmented epithelium (RPE) is critical for visual function. Throughout life central RPE cells are lost, but replenished by cell production in peripheral regions. Glatiramer acetate increases neuronal production in mature brains and is thought to erode age related deposits in the human retina that are risk factors for macular degeneration. Here, we ask whether this agent also elevates RPE production in mature rat eyes. If so, it may be used to replenish these cells in damaged eyes. Glatiramer acetate was given systemically for 14 days combined with Bromodeoxyuridine (BrdU) to mark cell division. One eye was then processed for the cell cycle marker Ki67 and the other for BrdU. Glatiramer acetate significantly elevated RPE cell proliferation, increasing the number of peripheral cells labelled with Ki67. There were also significantly more BrdU labelled cells over the 14 days, confirming that some cells divided. However, while Ki67 positive cell numbers increased by approximately 100% following examination at one time point, BrdU positive cell numbers increased by only 3% when averaged per day. The findings in this study suggest that glatiramer acetate enhances the RPEs natural ability to proliferate and may be a beneficial tool for elevating RPE production, particularly in response to specific RPE damage.

5.2 Introduction

RPE cell production is maintained in the peripheral retina throughout life at a low level (Al-Hussaini et al., 2008) to replace the cells lost with age (Del Priore et al., 2002). Data from the previous chapter suggests that these newly generated RPE cells in the periphery, migrate centrally to compensate for this age related cell loss. This appears to be an important homeostatic mechanism of the RPE.

Whilst the regulators of cell generation in the mature CNS are largely unknown, a recent finding has demonstrated that glatiramer acetate (GA) induces elevated neuronal production in the adult hippocampus (Aharoni et al., 2005). Glatiramer acetate (GA) is the generic name for the drug Copaxone (also called Copolymer or Cop 1). GA is a random polymer of four amino acids; glutamic acid, lysine, tyrosine and alanine, and is the first non-interferon approved treatment for multiple sclerosis (MS) (Kala et al., 2011, Racke et al., 2010, Varkony et al., 2009). Recently, treatment with GA has also been shown to play a role in the reduction of amyloid plaques in patients with Alzheimer's disease. Furthermore, the application of GA to patients suffering from AMD, has shown that GA reduces drusen area – a major risk factor for AMD (Landa et al., 2008, Landa et al., 2011).

Glatiramer acetate and multiple sclerosis

Multiple sclerosis (MS) is a chronic disease of the central nervous system characterised by a complex interplay between inflammation and neurodegeneration (Kala et al., 2011). It is an inflammatory demyelinating disease of the CNS, which is believed to result from an autoimmune reactivity to myelin components (Sela and Teitelbaum, 2001). The pathological hallmark of MS is a multifocal inflammatory attack on the white and gray matter with loss of oligodendrocytes in the chronic stages, significant neuronal cell loss, damage to axons and gliosis with astrocyte proliferation and intensive glial fibre production (Kala et al., 2011). While the functional consequences of demyelination and inflammation are at least part reversible, the deficits that occur as a result of neuronal and axonal loss are irreversible. Current treatments for MS include immunomodulators, such as copaxone and interferon-β, as well as immunosuppressants, such as natalizumab and mitoxantrone.

Initially, glatiramer acetate was developed to induce experimental autoimmune encephalomyelitis (EAE), the animal model of MS, by mimicking the major component of the myelin sheath, the myelin basic protein (MBP). Interestingly, it appeared to inhibit EAE in both rodents and monkeys instead (Sela and Teitelbaum, 2001). Furthermore, it was shown to reduce relapse rates as well as delay the progression of disability in MS patients (Johnson et al., 1995). The mechanism of action of GA is immunomodulatory, studies in MS patients and animals models to date have indicated that GA mediates its suppression of MS/EAE by modulating the function of many different types of immune cells (Kala et al.,

2011). GA appears to modulate inflammation and act in a neuroprotective capacity (Schrempf and Ziemssen, 2007). An important action of GA is to induce a shift in the T lymphocytes, from the pro inflammatory T helper type 1 (TH1) to the anti-inflammatory T helper type 2 (Th2) phenotype (Aharoni et al., 2003, Blanchette and Neuhaus, 2008). These immunoregulatory cells cross into the CNS where they release anti-inflammatory cytokines and growth factors (Aharoni et al., 2003). GA also stimulates the secretion of neurotrophins that protect axons and may promote repair to damaged neurons (Blanchette and Neuhaus, 2008).

Glatiramer acetate and Alzheimer's disease

Alzheimer's disease (AD) is an age-related progressive neurodegenerative disorder characterised by memory loss and sever cognitive decline (Hardy and Selkoe, 2002). The neuropathological features of AD are senile plaques, dystrophic neuritis and neurofibrillary tangles composed of paired helical filaments (Frenkel et al., 2005). The compact senile plaques are manifested by the excessive accumulation of extracellular aggregations of the amyloid β (Aβ) peptide. These plaques are formed within the brain parenchyma, especially in the hippocampus and cerebral cortex, leading to neuronal cell loss (Selkoe, 1991). Aggregated Aβ induces microglia to become cytotoxic and blocks neurogenesis causing deleterious effects.

In AD, the microglia-mediated local immune response does not operate in the optimal way to fight off the adverse conditions that lead to AD progression (Frenkel et al., 2005). Recent studies have shown that autoreactive T cells regulate these microglia in a way that renders them supportive of neural tissue repair and neuronal survival (Butovsky et al., 2001, Butovsky et al., 2005). GA weakly cross reacts with CNS-resident autoantigens and can stimulate the reparative and protective effects of autoreactive T cells (Kipnis et al., 2000, Angelov et al., 2003, Avidan et al., 2004). For this reason Butovsky et al. (2006) injected an AD mouse model with GA over a course of 24 days and found that vaccination with GA resulted in an elimination of plaque formation, a reduction of the naturally occurring cognitive decline and an induction of neuronal survival and neurogenesis. Here, the authors suggest that the beneficial effects of GA on the AD mouse model was as a result of the evoked T cell effect on their microglial phenotype modulating the microglia into a neuroprotective phenotype.

Glatiramer acetate and Age-Related Macular Degeneration (AMD)

Alzheimer's disease and age-related macular degeneration have many characteristics in common. One such characteristic is the presence of amyloid β, found within the senile plaques of the AD brain and in the drusen of AMD patients (Ohno-Matsui, 2011). Due to the similarities in the characteristics of AD and AMD, anti-amyloid agents, similar to those developed for AD, are being investigated to treat AMD (Ohno-Matsui, 2011). Landa et al. (2008) treated patients with intermediate dry AMD with GA and found that GA led to the reduction of total drusen area compared with sham-treated patients. More recently,

Landa et al. (2011) used high resolution spectral domain OCT/SLO (SD-OCT) to evaluate the morphological appearance of drusen in GA-treated and sham-treated dry AMD patients and found that the patients treated with GA showed a reduction in drusen volume.

AMD is characterised by the accumulation of extracellular deposits called drusen in which Aβ is a key constituent. Aβ plays a role in alterations and dysfunction of the RPE as it activates the complement cascade and its deposition is associated with activated macrophages (Hoh Kam et al., 2010). To date, the accumulation of Aβ in the retina has mostly been studied in the transgenic murine models for AD, to determine whether toxic Aβ in the retina would cause visual disturbances in patients suffering from AD. Little data had been compiled to show the accumulation of Aβ in the retina as part of a normal ageing process. Hoh Kam et al. (2010) demonstrated in a comprehensive study that Aβ accumulates in the normal murine retina and is deposited primarily among photoreceptor outer segments and on the RPE/Bruch's membrane interface. Recently, a study undertaken in our lab investigated the effects of GA on reducing Aβ in the Bruch's membrane of aged mice. As GA has also been shown to promote neurogenesis, it was of interest to see whether GA would have any effect on proliferation within the RPE.

Overall, treatment with GA appears to induce a neuroprotective mechanism. Aharoni et al. (2005) showed that GA treatment in EAE mice not only resulted in decreased neuronal damage but also in increased neuronal proliferation. These newborn cells migrated to

injury sites in the brain regions which do not usually undergo neurogenesis, and differentiated into a mature neuronal phenotype. The mature RPE shows a low level of proliferation in its periphery, in this study, the effect of GA treatment on the RPE will be investigated to establish whether it impacts RPE cell production in mature rats.

5.3 Methods

In order to determine which age group of animals should be used for the experiment, five 3 month and five 10 month Lister hooded rats were used and were pulsed with BrdU every day for 5 days and were left for 3 weeks in order to maintain the greatest number of BrdU positive cells (as demonstrated in chapter 4).

Following this, 10 Lister hooded female rats were used at approximately 10 months old. They were housed with a 12h light/dark cycle in a temperature controlled environment and fed ad libitum. All experimental procedures were carried out under local ethical guidance and the United Kingdom (Scientific Procedures) Act 1986. Animals were divided into two groups, the control group or the experimental group, where they were injected with PBS (n=5) or glatiramer acetate (n=5, 500µg/rat) respectively. This was followed by an i.p. injection of Bromodeoxyuridine (5-bromo-2-deoxyuridine, BrdU, Sigma UK. 50mg/kg). Animals were injected every day for fourteen days and were then sacrificed using CO_2. Their eyes and brains were removed and were fixed in 4% paraformaldehyde in phosphate-buffered saline (PBS) for 1 hour (eyes) or 5 hours (brains) at room temperature (RT).

The RPE and attached choroid were isolated and radial incisions made to produce RPE sheet whole-mounts. One eye from each animal was processed for the cell cycle marker Ki67 and one for BrdU to reveal patterns of cell division. For Ki67, wholemounts were

blocked for 2h in 5% normal donkey serum in PBS with 3% Triton X-100 and incubated overnight in Rabbit anti- Ki67 (1:1000, Vector), diluted in 1% normal donkey serum in PBS with 3% Triton X-100. After PBS washing, eyecups were incubated in the secondary antibody, donkey anti-rabbit Alexa Flour 488, for 2h in 1% normal donkey serum in PBS with 0.3% Triton X-100. Nuclei were subsequently stained with 4,6-diamidino-2-phenylindole (Sigma-Aldrich, UK). The tissue was then washed in PBS followed by washing in Tris buffer saline (pH 7.4). They were mounted with Vectashield (Vector Laboratories, UK).

For BrdU, the processing was identical to that described in chapter 3. Briefly, whole mounts were stained with a mouse anti-BrdU primary antibody and a donkey anti-mouse Alexa Flour 568 as the secondary. Before the secondary antibody could be used, antigen retrieval was undertaken by applying 6M hydrochloric acid diluted in 1% Triton-X 100 in PBS for 30 minutes onto the whole mounts. The tissue was washed and mounted as above.

After fixation, the brains were cryo-preserved in 30% sucrose overnight at 4^{o}C. The region containing the hippocampus was blocked out and frozen sections were cut (50 µm) using a Lecia CM3050 cryostat. These free floating sections were processed for BrdU using the same protocol described above.

Data analysis

Each flatmount was analysed and every BrdU/Ki67 positive cell was counted and their location within the RPE noted. These results were plotted and statistical comparisons were undertaken using a Mann-Whitney *U* test. Furthermore, the area of each flatmount was measured so that the number of positive BrdU and Ki67 cells could be counted as a measure of cells per mm^2 in order to correct for inter animal variability. Sequential images were taken of the entire eyecup at a low magnification and were aligned in Photoshop to make a single image of the flatmount. Once this was completed, the flatmount was selected and the area was recorded using the record measurements tool in Photoshop.

5.4 Results

Decrease in number of proliferating cells with age

To determine which age group of animals should be used for the experiment involving GA and its effect on the RPE, young 3 month and old 10 month animals were injected with BrdU for 5 days and left for 3 weeks. A significant decrease in the proliferative capacity of the RPE can be seen with increased age ($p<0.05$), with the number of BrdU positive cells decreasing from an average of 84 to 62 (Figure 5.4.1). This is similar to 1.4 positive cells per mm^2 and 0.9 positive cells per mm^2 of the RPE sheet, respectively. For this reason, old 10 month animals were used in this study. Although the BrdU labelling method was different for the experimental animals (they were given BrdU every day for 14 days and were then sacrificed), it was of interest to see whether levels similar to that of a 3 month old animal could be regained.

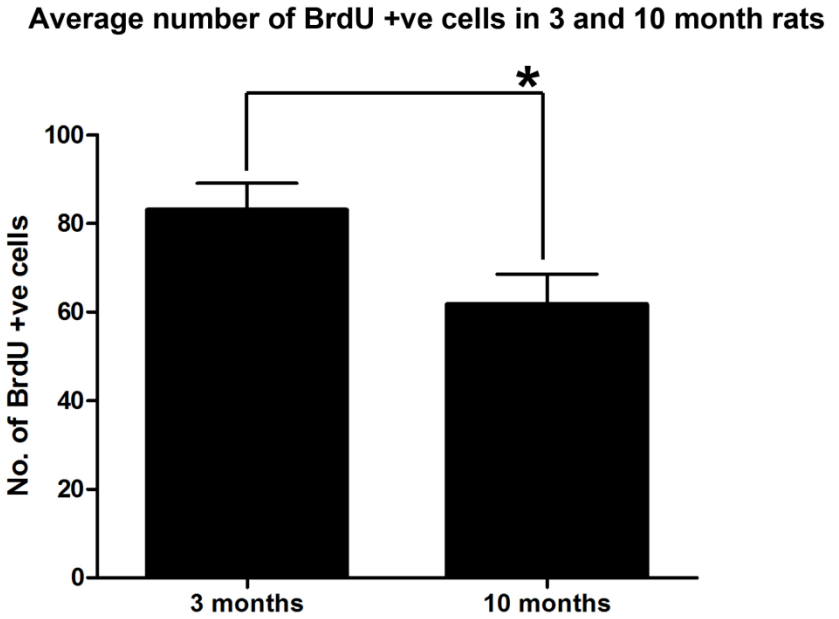

Figure 5.4.1: The difference in the number of BrdU +ve cells between young 3 month and old 10 month Lister hooded rats. The results show a significant decrease in the number of BrdU positive cells with age ($p<0.05$).

Little variability in RPE area between animals

As the numbers of Ki67 and BrdU positive cells are generally low in the mature RPE, it was important to see the level of variability amongst individual animals. There is little variability in the area of the RPE amongst the 10 animals, with the area ranging from 61 to 70 mm^2 (Figure 5.4.2). This was factored into the results and for the experimental animals the number of Ki67/BrdU positive cells was divided by the area to demonstrate the number of positive cells per mm^2.

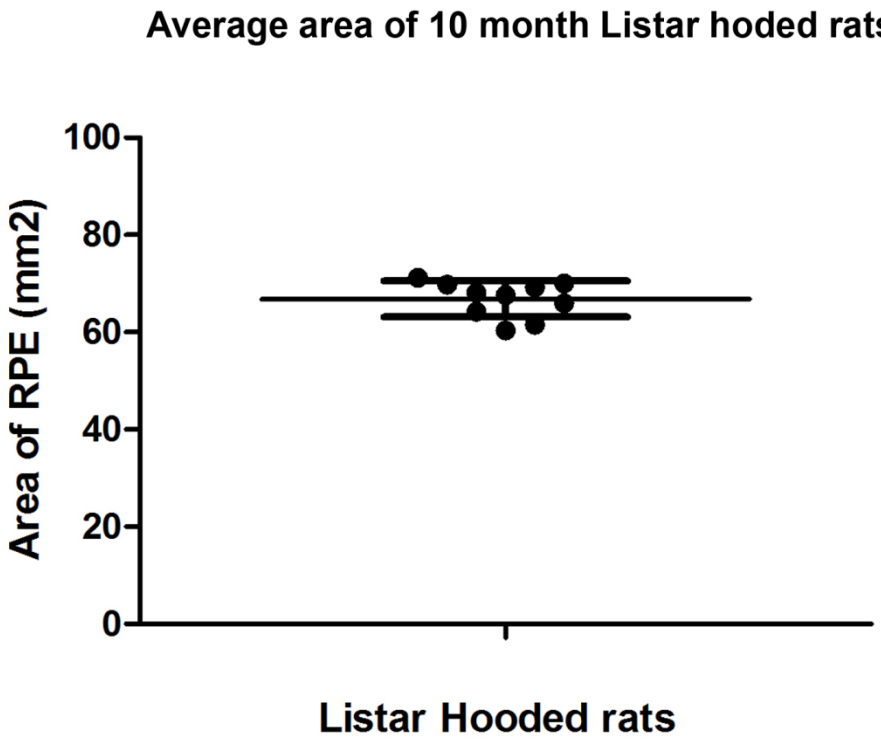

Figure 5.4.2: Area of the RPE sheet of 10 month old Lister Hooded rats. The results show little variability between individual animals.

Increase in the number of proliferating cells in animals treated with Glatiramer Acetate

Ki67 and BrdU positive cells were present in all of the eyes examined (Figure 5.4.3). The number of Ki67 positive cells significantly increased ($p<0.05$) and more than doubled in the drug treated animals compared to those only treated with PBS, with an increase from 0.1 cells per mm^2 to 0.24 cell per mm^2 (Figure 5.4.3A). This indicates that significantly more cells were in the cell cycle in the animals treated with GA compared to those only injected with PBS.

Ki67 does not indicate whether cells are actually dividing, it only determines that cells are in the cell cycle on the day the animal was sacrificed. It cannot be assumed that each cell in the cell cycle continues to complete cell division. Labelling with BrdU, however, gives an indication of a cell's history as once it is incorporated, BrdU will remain in place and be passed down to daughter cells folllowing division. In the animals injected with BrdU for 14 consectutive days followed by PBS, approxiamtely 0.6 positive cells were present per mm^2 of the RPE. In the animals injected with GA, however, this number increased to 0.9 positive cells per mm^2, showing a significant increase in the drug treated animals ($p<0.05$) (Figure 5.4.3B). Although the number of BrdU positive cells increased in the GA treated animals, the increase was not as significant as the increase of Ki67 positive cells.

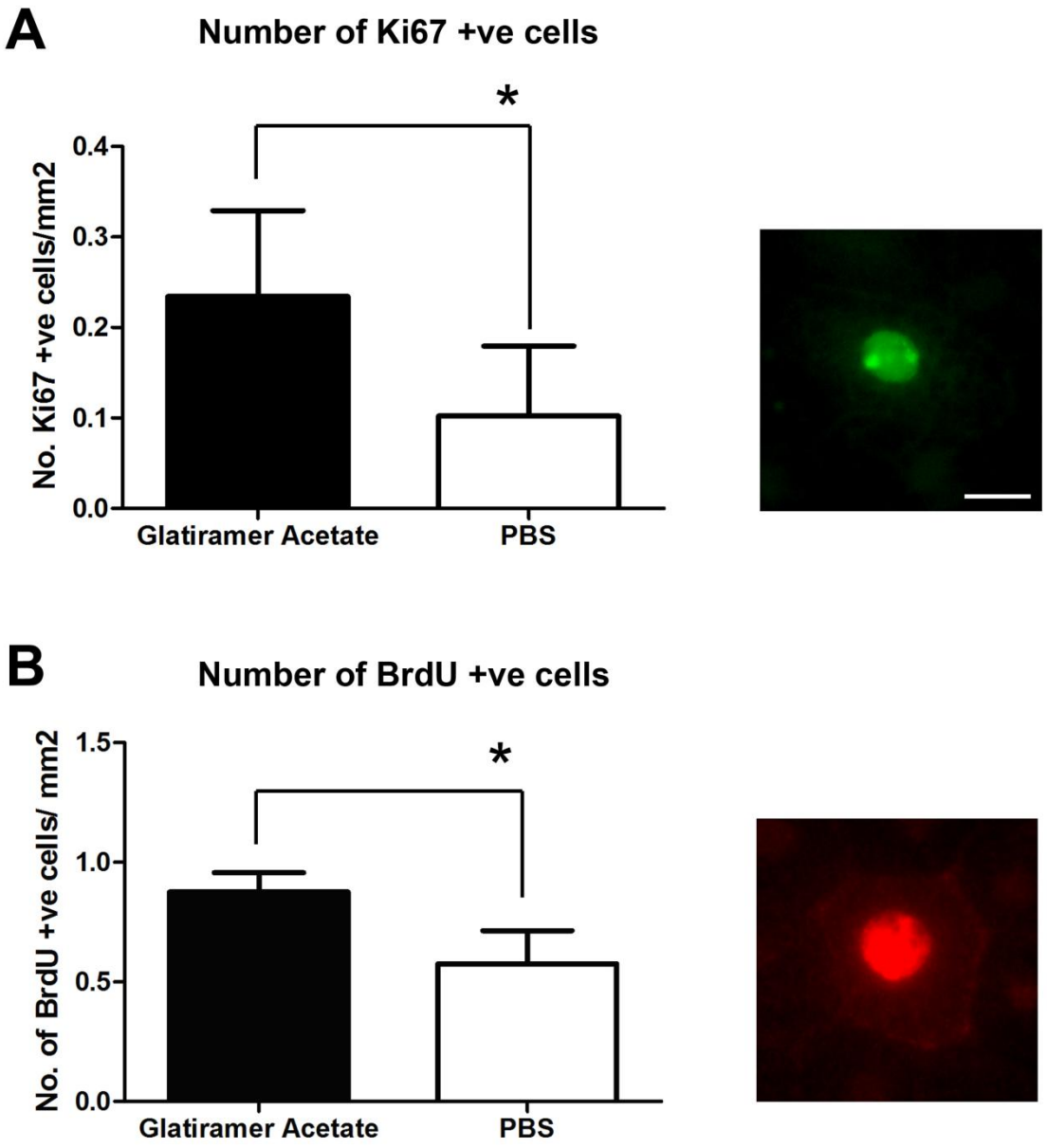

Figure 5.4.3: Number of Ki67 (A) and BrdU (B) positive cells per mm^2 of the RPE. (A) shows a significant increase in the number of Ki67 positive cells in the group treated with glatiramer acetate ($p<0.05$). (B) similarly shows that animals treated with glatiramer acetate had an elevated number of BrdU positive cells compared to those in the control group ($p<0.05$). The microscope images besides the graphs show the immunostaining results and demonstrate the cells that were counted. Scale bar - 25µm.

Cell proliferation by GA significantly affects the peripheral region of the RPE

A proportion of mature RPE cells are retained in or have the capacity to enter into the cell cycle and divide in peripheral regions of the RPE establishing a proliferative zone within this area (Al-Hussaini et al., 2008). Ki67 positive cells are only ever found within this region, however, previous studies and the data from chapter 4 show that BrdU cells can also be located centrally. It is believed that cells are proliferating in the periphery in this proliferative zone and migrating centrally to replace those lost. Here, the labelling methods for BrdU were different to those used in chapter 4, and the animals were sacrificed sooner so very few BrdU positive cells can be seen in the centre of the RPE (Figure 5.4.4) in both the PBS and GA treated animals. It is of interest, however, that GA induced RPE proliferation seemed to only affect the peripheral region. Differences between the control (PBS) and drug treated (GA) group can only be seen in the peripheral region. It appears that GA enhances the RPE's natural capacity to proliferate.

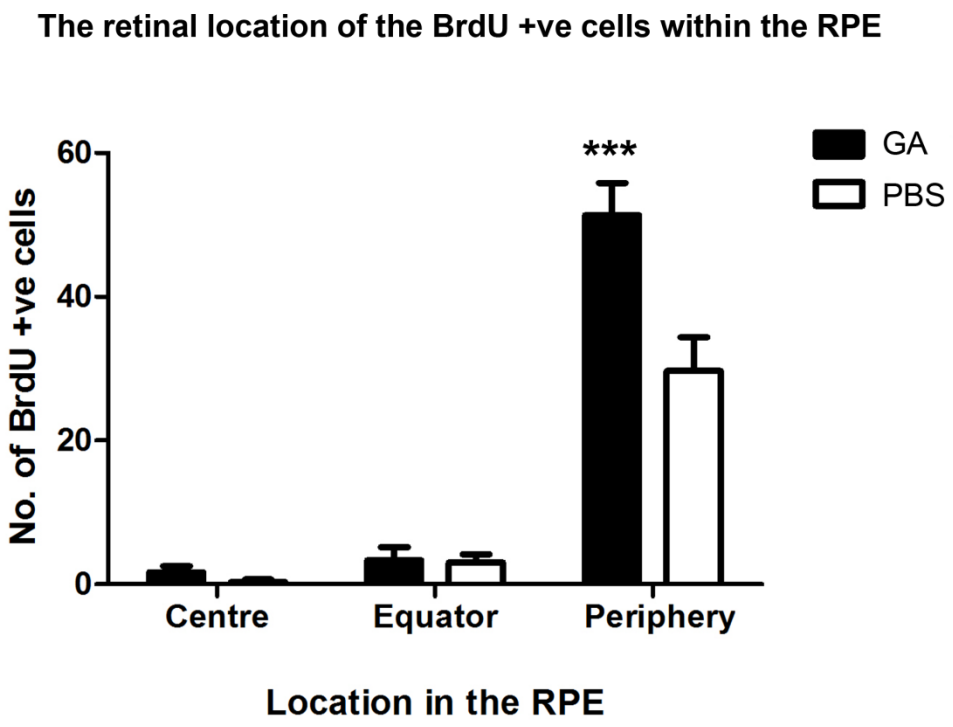

Figure 5.4.4: The graph shows the retinal location of where the BrdU positive cells were found within the RPE. Most of the cells were located within the proliferative peripheral region of the RPE with the GA group showing a significantly higher number ($p<0.001$) of BrdU positive cells than the PBS control group in this region.

5.5 Discussion

Glatiramer acetate (GA) is synthetic copolymer of a pool of peptides composed of four amino acids (Wang et al., 2011). GA was originally synthesised based on the structure of myelin basic protein, an antigen involved in the induction of autoimmunity in MS and experimental autoimmune encephalomyelitis (EAE). Rather than inducing EAE in animal models, however, it inhibited EAE in both rodents and monkeys (Sela and Teitelbaum, 2001). Furthermore, in controlled clinical trials, it significantly reduced the relapse rate and progression of disability in MS patients, showing long term efficacy and remarkable tolerability and safety (Ruggieri et al., 2007).

GA appears to have an effect on neuroprotection and neurogenesis in many other pathologies including Alzheimer's disease, spinal cord injuries (Hauben et al., 2000), CNS trauma (Kipnis et al., 2001) and ALS (Kipnis and Schwartz, 2002). In relation to the eye, neuroprotective immunisation with GA has been found to be beneficial in animal models of glaucoma (Schori et al., 2001, Bakalash et al., 2005) and optic nerve trauma (Fisher et al., 2001). Recently, it has also been shown to help reduce drusen in patients with AMD (Landa et al., 2008, Landa et al., 2011). AMD is characterised by the accumulation of extracellular deposits called drusen in which Aβ is a key constituent. Aβ plays a role in alterations and dysfunction of the RPE as it activates the complement cascade and its deposition is associated with activated macrophages (Hoh Kam et al., 2010). Recently, Hoh Kam et al. (2010) demonstrated that Aβ accumulates in the normal murine retina and is

deposited primarily among photoreceptor outer segments and on the RPE/Bruch's membrane interface. Furthermore, a study undertaken in our lab investigated the effects of GA on reducing Aβ in the Bruch's membrane of aged mice. This, together with the fact that GA has also been shown to promote neurogenesis, led to the question of whether GA would have any effect on proliferation within the RPE. In this study, relatively brief exposure to glatiramer acetate (GA) is shown to elevate cell production in peripheral but not central, RPE cells.

The mechanism of action for how this occurs is unclear, however, many studies have shown that GA promotes neurogenesis in areas which do not normally undergo neurogenesis (Arnon and Aharoni, 2007). The clinical effects of GA are thought to be largely mediated by a T-helper 1 (Th1) to Th2 shift of GA-reactive T lymphocytes (Wang et al., 2011) (Figure 5.5.1). GA may act as a partial agonist and shift adaptive T cell responses from the pro-inflammatory Th1 towards the anti-inflammatory Th2 (Duda et al., 2000, Neuhaus et al., 2000). It has been proposed that the activated GA-reactive Th2 cells penetrate the CNS and release anti-inflammatory cytokines such as interleukin (IL)-4, IL-5 and IL-10, therefore, inhibit nearby inflammatory cells.

Figure 5.5.1: A schematic view of the putative mechanism of action of glatiramer acetate (GA). In the periphery, outside the CNS, GA initially stimulates a population of TH1-like cells. During treatment, the properties of the GA-stimulated T cells change and they become more TH2-like (dotted arrow). The activated GA-specific T cells enter the CNS, where they encounter CNS antigens like MBP bound to MHC class II and presented on the surface of microglia cells. The GA-reactive T cells are stimulated to secrete downmodulatory cytokines like IL-4, which exert a bystander suppressive effect on other T cells (Neuhaus et al., 2001).

In various models of inflammatory and degenerative CNS disorders, it was shown that peripheral GA-induced T cells cross the blood brain barrier where they then secrete various neurotrophins and high levels of anti-inflammatory cytokines leading to a reduction of neuronal and axonal damage (Aharoni et al., 2003, Aharoni et al., 2000, Kipnis et al., 2000). This effect is amplified by a profound bystander effect on astrocytes and microglia, which results in an increased expression of neurotrophins at the site of injury and a reduced release of nitric oxide, pro-inflammatory cytokines and glutamate by these cells (Kipnis et al., 2000, Schori et al., 2001). Furthermore, GA promotes neurogenesis, resulting in proliferation of neuroprogenitor cells and their migration towards injury/lesion sites which normally do not undergo neurogenesis and the eventual

differentiation into mature neurons, thereby, counteracting the neurodegenerative disease course (Arnon and Aharoni, 2007).

Most studies demonstrate the neuroprotective action of GA in models of damage to myelinated neural cells. Belokopytov et al. (2008) were the first to show that GA is also neuroprotective in unmyelinated neural tissue. In their study, they demonstrate that GA is an effective neuroprotectant in laser-induced retinal lesions in rats. Prior to the induction of laser lesions, the rats were immunised with GA for 7 days. The results showed that GA immunisation protected the outer retina from laser-induced injuries and also improved the functional recovery of the injured retina.

In this study, GA induced elevated cell production in the periphery of the RPE of old 10 month rats. Cells proliferating in the periphery of the RPE are important for RPE maintenance as it appears that they move centrally to replace those lost with age (Al-Hussaini et al., 2008, Del Priore et al., 2002). Although there is likely to be a balance between cell production and death over extended periods in the ageing RPE, the data on ageing RPE has provided contradictory results with studies providing evidence for age related cell loss, age related cell increase and for a relatively static state.

Goa and Hollyfield. (1992) found that the equatorial RPE density decreased from the second to the ninth decade in humans. On the other hand, there was no significant

change in foveal RPE cell density. Watzke et al. (1993) also found that the RPE from the fovea was more densely packed than that of the equatorial regions. However, this was only true in young eyes. No correlation of RPE cell density with increasing age in any fundus area was found in their study. In contrast, Harman et al. (1997) found that the central RPE density increases later in life and that there is no significant change in equatorial RPE density, although a slight decrease with increasing age was observed.

The most comprehensive study seems to have been carried out by Panda-Jonas et al. (1996). They found that the RPE cell density decreased significantly by 0.3% per year with increasing age. They also reported that the cell density decreased from the fovea to the retinal periphery. Similarly, Del Priore et al. (2002) showed that age-related RPE cell death occurred mainly in the macula, however, the cell density in this region remained unchanged. Instead, the density of RPE cells decreased in the periphery suggesting that cells are proliferating in the periphery and migrating towards the macula in order to compensate for the continuous loss of foveal RPE cells. This is the only study that has been able to demonstrate cell death in the mature RPE as apoptotic cells are quite difficult to identify due to their rapid rate of clearance. The data from this study supports the findings in chapter 3, in which a general decline in cell density is seen with age in pigmented and albino rats, furthermore, the extreme periphery had a much lower cell density compared to the equatorial and central regions. Del Priore's theory for cell migration from the periphery to the centre to replace those lost with age is also further strengthened by the

results from chapter 4, in which migration of cells towards the centre of the RPE has been demonstrated.

The replacement of dying cells in the RPE is important, in particular with the detrimental effects that accumulate with ageing. With age, the RPE undergoes several structural changes, including the accumulation of the age pigment lipofuscin, the loss of melanin granules, the accumulation of basal deposits on or within Bruch's membrane, thickening of the Bruch's membrane and an increase in the number of residual bodies (Boulton and Dayhaw-Barker, 2001). These factors combined lead to the age-related death of RPE and photoreceptor cells. In humans this results in the elderly suffering from a loss of colour perception (Page and Crognale, 2005), visual acuity (Del Viva and Agostini, 2007, Weale, 1975) and dark-adaption sensitivity (Werner, 2005).

Lipofuscin, a yellow-brown autofluorescent granule, can be detrimental to RPE cell function. In the RPE, the major source of lipofuscin is from phagocytosis of the photoreceptor outer segments (Sparrow and Boulton, 2005). In the young, lipofuscin granules first appear in the basal portions of the RPE cells, however, with age they form into clumps and fill the entire RPE cytoplasm (Wing et al., 1978). The accumulation of lipofuscin within the aged RPE appears to be connected to the functional degradation of the RPE by either clogging of the cytoplasm or by increased oxidative stress in the cell (Bonilha, 2008). Oxidative stress is believed to contribute to the pathogenesis of many diseases as well as ageing (Liang and Godley, 2003). Lipofuscin is a photoinducible

generator of many reactive oxygen species including superoxide anion, hydrogen peroxide and singlet oxygen (Boulton et al., 1993, Rozanowska et al., 1995). The visible light irradiation of lipofuscin granules results in the extra-granular oxidation of lipids and inactivation of lysosomal and antioxidant enzymes (Wassell et al., 1999). The main fluorophore of lipofuscin has been identified as a derivative of vitamin A, pyridinium bis-retinoid, N-retinylidene-N-retinylethanolamine (A2E). In addition to the phototoxic effects of lipofuscin, A2E has also been shown to exhibit phototoxic and detergent properties and is capable of inducing disintegration of membrane-bound organelles in RPE cultures (Bonilha, 2008). Furthermore, lipofuscin interferes with the antioxidant properties of melanin (Boulton et al., 1993, Rozanowska et al., 1995, Wang et al., 2006). The increasing intracellular accumulation of lipofuscin granules in the aged RPE coincides with the depletion of melanin (Han et al., 2007).

Melanin protects the RPE cells from oxidative damage as it is able to scavenge reactive free radicals (Rozanowska et al., 1999), quench electronically excited states (Sarna et al., 1985) and sequester redox-active metal ions (Zareba et al., 1995). With age, not only is there a loss of melanin granules but the remaining granules undergo an age-related change. The granules become increasingly complex, due to the fusion of melanin with lipofuscin, therefore, reducing its photoprotective role (Sarna et al., 2003).

As the RPE accumulates more injury due to age related changes, it seems necessary to replace those lost, for this reason it appears plausible that a homeostatic mechanism

regulates the size of the RPE over life. In this study, two separate cell cycle markers (BrdU and Ki67), revealed that GA increases levels of proliferation in the mature rat RPE. Interestingly, the two makers showed a disparity in the in the number of cells present in the cell cycle with Ki67 showing a doubling in the number of positive cells, whilst the number of BrdU positive cells seemed to increase by only a third. First, it must be taken into account that these markers vary in the type of cells that they label. BrdU is incorporated into DNA only during the S phase of the mitotic process (Kee et al., 2002, Wojtowicz and Kee, 2006), whilst Ki67 is expressed in dividing cells for most of their mitotic process. Once incorporated, BrdU will remain in place and be passed down to daughter cells folllowing division, therefore, BrdU labelling shows the history of a cell, allowing for tracking the fate of divided cells and their progeny. Ki67, on the other hand, shows the state of the cell in the moment of time the animal was sacrificed.

Second, cell cycle proteins, Ki67 in particular, can be up regulated in mature cells when they initate caspase related apoptosis (Cernak et al., 2005, Yang and Herrup, 2007), indicating a relationship between cell cycle initiation and cell death. It is possible that encouraging cells to enter the cell cycle at inappropriate stages, via the effects of GA, may result in their failure to complete cell division, leading to their death. Furthermore, Ki67 only labels cells in the cell cycle, it does not give an indication if cells are entering the cell cycle or whether they in fact continue to divide.

Interestingly, this study shows that the application of GA induces cell proliferation in the periphery of the RPE. Subcutaneous injections were given to the animals and so the eye was globally affected and only the periphery appeared to respond. Al-Hussaini et al. (2008) show that peripheral RPE cells in mature rats have the capacity to enter the cell cycle and complete cellular division. This suggests that GA enhances the RPEs natural ability to proliferate. Although the numbers of cells found to be dividing are very small relative to the entire RPE sheet, it indicates that GA may be a beneficial tool for elevating RPE production, particularly in response to specific RPE damage.

Chapter 6

Conclusions

The data presented in this thesis demonstrate that the mature RPE is a dynamic heterogeneous epithelial cell layer. The data in Chapter 2 shows that markers of this tissue demonstrate distinct regional patterns showing RPE cell heterogeneity in both albino and pigmented rats. In addition, immediately adjacent cells also present with differences in the expression of certain proteins. The structural and functional heterogeneity within the RPE mosaic presents a backdrop in which complex changes play out over a lifetime. As neighbouring cells appear to behave differently in terms of gene and protein expression, they may also differentially support their associated photoreceptors. Changes that occur with ageing, notably those induced by oxidative stress, may therefore, differentially reduce the support function in some cells. Thus, cells more susceptible to the effects of ageing may present with a more rapid age-related decline in function, which in turn results in decreased support for the overlying photoreceptors. The fact that the RPE is a mosaic of variable cells rather than a homogenous monolayer is important, especially when finding ways to prevent age related RPE decline as it seems that no preventive measure can be universally effective for all cells.

Chapter 3 highlights the variability of the ageing process and the role that melanin may play in this. Albino and pigmented animals exhibited different ageing phenotypes, with albinos showing the signs of an age-related decline in visual function much sooner than pigmented animals. Recently, a study carried out by Charng et al. (2011) corroborates the findings from my study by showing that pigmented rats appear to be a better model for studying age-related change of the human eye. The differences in the ageing response

between the two pigmentation phenotypes most likely occur as a result of differences in the amount of oxidative stress faced by the animals. Alongside ageing, oxidative stress is one of the key factors believed to contribute to the pathogenesis of many diseases (Liang and Godley, 2003). The central idea of the oxidative stress theory is that the accumulation of molecular damage caused by reactive oxygen species (ROS) contributes significantly to ageing (Gems and Doonan, 2009). The mitochondrial theory appears to be one of the most prevalent theories of ageing whereby it proposes that oxidative damage to the mitochondria can lead to a spiral of confounding effects. This results in damaged mitochondria releasing more ROS, therefore, increasing oxidative damage which in turn leads to eventually defective or dysfunctional mitochondria (Harman, 1981). As mitochondria are essential for the production of ATP, this damage results in reduced energy production and compromised cell function. Gradually with time, these deficits in cellular function become amplified and contribute to the age-related decline in physiological function (Liang and Godley, 2003).

Evidence from a variety of studies suggests that RPE cells are susceptible to oxidative damage as a result of anatomic and physiological factors. Albinos, already lack the protective capacity provided by melanin which has an important role as a cellular antioxidant (Sarna et al., 2003) and is also responsible for reducing the levels of light entering the RPE by acting as a neutral filter. Additionally, the data from this study showed that aged albino rats appeared to have problems with effective phagocytosis of the photoreceptor outer segments. Phagocytosis has evolved as a defence against chronic

oxidative stress to which the photoreceptors are particularly vulnerable (Winkler, 2008). The complete replacement of the outer segments every 10-14 days (Ben-Shabat et al., 2002) is therefore crucial and represents a method of continual self-repair – the oxidised membrane is removed and is compensated by the addition of newly synthesised cellular components, thus maintaining the cell at a constant overall length (Sparrow et al., 2010). Also, as a result of phagocytosis, the RPE synthesises Neuroprotectin 1, a bioactive substance providing protection from oxidative insult (Bazan, 1989, Bazan, 2005, Mukherjee et al., 2004). For this reason, problems with phagocytosis in the aged albinos may contribute to greater oxidative insult to the RPE of these cells causing the enhanced decline in visual function. An interesting experiment would be to evaluate the levels of oxidative stress in the aged albino animals compared to the pigmented. This can be carried out by using QPCR assay in which the formation of oxidative mtDNA damage and repair kinetics in RPE cells can be examined.

Research into albinism is of great interest. Currently, an FDA-approved inhibitor of tyrosine degradation, Nitisinone, has proven to improve eye and skin pigmentation defects in a mouse model of oculocutaneous albinism suggesting that its use in individuals with OCA1 could help to improve their pigmentation and potentially ameliorate vision loss (Onojafe et al., 2011). A pilot clinical study is now being organised to test this hypothesis. Furthermore, it would be interesting to see whether the application of nitisinone to albino rats would prevent the defects seen in Chapter 3.

Chapter 4 demonstrates that individual cells within the RPE monolayer have the ability to migrate in healthy animals. Additionally, after unilateral laser induced damage to the RPE, the number of BrdU positive cells are upregulated in not only the lasered eye, but also in the fellow contralateral non-lasered eye in a quadrant specific manner. The findings from this study are quite interesting and should be considered when future treatments are targeted to just one eye as the paradigm of using the contralateral eye as a control appears to now be inappropriate. The mechanism causing this phenomenon is still unclear, however, more recent experiments being undertaken in our lab have shown that the response to damage in the contralateral eye is immediate. Using ERGs to monitor the response of the fellow eye it has been shown that following bright flashing in one eye, the ERG in the fellow eye can be reduced by 80% within an hour. To investigate the quadrant specific manner in which the fellow eye responds, it would be of interest to use multi-focal ERGs after placing a laser burn in one eye. Such experiments are currently in progress.

Chapter 5 showed that relatively brief exposure to the drug, glatiramer acetate, elevated levels of proliferation in the mature rat RPE suggesting that GA enhances the RPEs natural ability to proliferate. Although the numbers of cells found to be dividing are very small relative to the entire RPE sheet, it indicates that GA may be a beneficial tool for elevating RPE production, particularly in response to specific RPE damage. The animals were only exposed to GA for a period of two weeks in the study, it must however also be questioned whether a more prolonged treatment with GA would pose a potentially detrimental impact on the RPE as excessive cell production could have unfavourable consequences.

The findings from this thesis show the vital role that RPE cells have in maintaining visual function. For this reason RPE cells are not only an attractive target for gene therapy, but also a growing area of research involves cell-based therapies aimed at the replacement of defective RPE. Success in this area could provide a great therapeutic approach in the treatment for many conditions such as AMD. For this reason, an improved understanding of RPE biology is vital.

Appendix

Visual Neuroscience (2011), **28**, Page 1 of 4.

doi:10.1017/S095252381100040X

Glatiramer acetate elevates cell production in the mature retinal pigment epithelium

GOLNAZ SHAHABI AND GLEN JEFFERY

AU2 Institute of Ophthalmology, University College London, London, UK

(RECEIVED May 16, 2011; ACCEPTED September 12, 2011)

Abstract

The retinal-pigmented epithelium (RPE) is critical for visual function. Throughout life, central RPE cells are lost but replenished by peripheral cell production. Glatiramer acetate increases neuronal production in mature brains and is thought to erode age-related deposits in the human retina that are risk factors for macular degeneration. Here, we ask whether this agent also elevates RPE production in mature rat eyes. If so, it may be used to replenish these cells in damaged eyes. Glatiramer acetate was given systemically for 14 days combined with Bromodeoxyuridine (BrdU) to mark cell division. One eye was then processed for the cell cycle marker Ki67 and the other for BrdU. Glatiramer acetate significantly elevated the number of RPE cells in the cell cycle, with more labeled with Ki67. There were also significantly more BrdU-labeled cells over the 14 days, confirming that some cells divided. However, while Ki67 positive cell numbers increased by approximately 100% following examination at one time point, BrdU cell numbers increased by only 3% when averaged per day. Hence, glatiramer acetate induces cells to proliferate, but many may fail either to complete division or to survive. This may have long-term consequences for this tissue.

AU3 **Keywords:** RPE proliferation, AMD

Introduction

AU4 The retinal-pigmented epithelium (RPE) resides adjacent to the outer neural retina and plays a critical role in retinal development and also in the maintenance of photoreceptor function in the mature organism. Throughout life, RPE cell production is maintained in the peripheral retina at a low level, while there is evidence for RPE cell loss centrally (Del Priore et al., 2002; Al-Hussaini et al., 2008). Some newly generated RPE cells migrate centrally to compensate for this age-related loss (Al-Hussaini et al., 2008). Maintenance of the balance between age-related cell loss and cell production is probably an important homeostatic mechanism in the RPE.

The production of RPE cells is partially regulated by melanin because in albino rats, excess RPE cell numbers enter the cell cycle AU5 and many become polyploid without completing cell division (Adams et al., 2010). This leads to progressive ocular pathology AU6 (Shahabi et al., 2011). While the regulators of cell generation in the mature central nervous system are largely unknown, it has been demonstrated that glatiramer acetate induces elevated neuronal production in the adult hippocampus (Butovsky et al., 2006). Glatiramer acetate is a random polymer of four amino acids; glutamic acid, lysine, alanine, and tyrosine that appears to act as an immunomodulator. It has been used in the treatment of multiple AU7 sclerosis, although its exact mode of action is unknown (Carpintero et al., 2010; Van Kaer, 2011). There is a link between this drug and the eye as it has been claimed that glatiramer acetate also reduces age-related deposits behind the human retina (Landa et al., 2008; AU8 Lander et al., 2011). These focal deposits known as drusen are a risk factor for age-related macular degeneration (Sarks, 1976; Green, 1999; Hollyfield, 2010). As glatiramer acetate elevates cell production in the brain and has been linked to a potential ocular therapy for age-related macular degeneration, we ask here whether it impacts on RPE cell production in mature rats. If so, this may represent a therapeutic route for disease states that target the RPE.

Address correspondence and reprint requests to: Glen Jeffery, Institute of Ophthalmology, University College London, 11-43 Bath Street, London EC1V 9EL, UK. E-mail: g.jeffery@ucl.ac.uk

Materials and methods

Ten Listar hooded female rats were used at approximately 8 months old. They were housed with a 12-h light/dark cycle in a temperature- AU9 controlled environment and fed ad libitum. All experimental procedures were carried out under local ethical guidance and the U.K. (Scientific Procedures) Act 1986. Animals were either injected with 0.2 ml phosphate-buffered saline (PBS) ($n = 5$) or 0.2 ml glatiramer acetate ($n = 5500$ μg/rat) followed by 0.8 ml Bromodeoxyuridine AU10 (5-bromo-2-deoxyuridine, BrdU; Sigma, UK, 50 mg/kg). Animals were injected everyday for 14 days and were then sacrificed using CO_2. Their eyes were removed and were fixed in 4% paraformaldehyde in PBS for 1 h.

The RPE and attached choroid were isolated and radial incisions made to produce RPE sheet whole mounts (Al-Hussaini et al., 2008). One eye from each animal was processed for the cell cycle marker Ki67 and one for BrdU, to reveal patterns of cell division. For Ki67, whole mounts were blocked for 2 h in 5% normal donkey serum in PBS with 3% Triton X-100 and incubated overnight in rabbit anti-Ki67 (1:1000; Vector), diluted in 1% normal AU11

donkey serum in PBS with 3% Triton X-100. After PBS washing, eyecups were incubated in the secondary antibody, donkey anti-rabbit Alexa Flour 488, for 2 h in 1% normal donkey serum in PBS with 0.3% Triton X-100. Nuclei were subsequently stained with 4,6-AU12 diamidino-2-phenylindole (DAPI; Sigma-Aldrich, UK). The tissue was then washed in PBS followed by washing in Tris buffer saline AU13 (pH 7.4). They were mounted with Vectashield (Vector Laboratories, UK).

For BrdU, the processing was identical to that of Al-Hussaini et al. (2008). Briefly, whole mounts were stained with a mouse anti-BrdU primary antibody and a donkey antimouse Alexa Flour 568 as the secondary. Before the secondary antibody could be used, antigen retrieval was undertaken by applying 6 M hydrochloric acid diluted in 1% Triton X-100 in PBS for 30 min onto the whole mounts. The tissue was washed and mounted as above. Individual RPE sheets were not double stained for both Ki67 and BrdU because in previous experiments where this was undertaken, some Ki67-labeled cells were ghost like in appearance. This raised the concern that the antigen retrieval process necessary for BrdU label was in some way reducing the quality of the Ki67, undermining the value of double labeling the whole mounts. All cell counts were made at a magnification of 200×. Once a cell was identified, it was examined at 400× on channels for both the cell label and DAPI. Cell counts were made over the entire RPE surface.

To control for potential differences in the area of the RPE whole mounts, they were measured from low power images. Further, the number of cells counted in each whole mount has been normalized for area by dividing the total number of labeled cells present by the area of the RPE surface. Statistical comparisons were made using the nonparametric Mann–Whitney *U* test, which makes no assumptions regarding the normality of the data distribution. Data are plotted as means with standard deviations.

Results and discussion

The RPE whole mounts were approximately 65 mm^2 in area. There was little variation in this area between animals and nonsignificant differences between the animals injected with PBS or glatiramer acetate (Mean experimental group area = 66.85 mm^2, S.D. = 3.93; Mean control group area = 66.75 mm^2, S.D. = 3.93, $P = 1.00$).

Ki67-positive RPE cells were present in allthe eyes examined. There were on average seven positive cells present in the RPE sheets of animals injected with PBS. However, in those injected with glatiramer acetate, the number increased to an average of 16 positive cells. Hence, the number of Ki67-positive cells doubled in the drug-treated animals. This difference was significant (Mean experimental group = 15.4, S.D. = 5.41; Mean control group = 6.8, S.D. = 4.96, $P = 0.0297$). In every case, Ki67-positive cells were confined to the peripheral retina as revealed previously (Al-Hussaini et al., 2008). The difference between the experimental and control groups corrected for area remained statistically significant (Fig. 1A; Mean experimental group = 0.234, S.D. = 0.095; Mean control group = 0.012, S.D. = 0.008, $P = 0.0297$). These data reveal that significantly more RPE cells were in the cell cycle in the peripheral retina in those animals injected with glatiramer acetate than those injected with PBS.

Ki67 labeling of the RPE does not reveal that cells are actually dividing, only that they are in the cell cycle when the animal was killed. Not all cells that enter the cell cycle complete cell division. Cell cycle entry can be a prelude to cell death or to a polyploidy state where the cell is arrested in the cell cycle (Cernak et al., 2005; Yang & Herrup, 2007; Shahabi et al., 2011). To confirm that cell division was taking place, the number of BrdU-labeled RPE cells were counted. The average number of BrdU-positive cells found in PBS-treated animals was 40 per RPE sheet, while in the experimental group, the average increased to 60 per sheet, which represents a 50% increase over the 14-day period. This difference was statistically significant (Mean experimental group = 58.8, S.D. = 8.671; Mean control group = 38.8, S.D. = 10.99, $P = 0.0159$). The number of BrdU cells was again corrected for area, and again, this difference was statistically significant (Fig. 1B; Mean experimental group = 0.876, S.D. = 0.080; Mean control group = 0.576, S.D. = 0.138, $P = 0.0040$). However, Ki67 labeling represents cells in the cell cycle at the time of death, while the BrdU label was cumulative over 14 days. If the percentage increase in BrdU is averaged per day, in glatiramer acetate-injected animals, it is only 3%. While the vast majority of BrdU-labeled cells in both groups were located in the periphery, a small number were present outside this region, consistent with the findings of Al-Hussaini et al. (2008), and the hypothesis that some cells that divide in the periphery may migrate centrally.

This study shows that relatively brief exposure to glatiramer acetate elevates cell production in peripheral RPE cells. The mechanism by which this occurs is unclear; however, as argued by Butovsky et al. (2006), who demonstrated elevated hippocampal neurogenesis following glatiramer acetate administration, the process is likely to depend in part on local immune activity that is associated with microglia production of growth factors such as insulin-like growth factor 1 (IGF1). This may rest on the finding that glatiramer acetate induces a phenotypic switch in microglia in the brain to dendritic cells that produce IGF1 (Butovsky et al., 2006).

There is likely to be a balance between cell production and death over extended periods in the ageing RPE (Del Priore et al., 2002). The data on aging RPE are very mixed with morphological studies providing evidence for both age-related cell loss, age-related cell increase, and for a relatively static state (Gao & Hollyfield, 1992; Panda-Jonas et al., 1996; Harman et al., 1997; Del Priore et al., 2002). However, the spread of data is large in all these studies. It is likely that there are numerous variables impacting on the regulation of RPE cell numbers with age, and that we are only aware of some of these. In spite of such differences, it is clear that RPE cells are generated in the mature peripheral retina in a life-long manner (Al-Hussaini et al., 2008). Further, the only study to mark dying cells in the mature RPE has only been able to demonstrate them at central locations (Del Priore et al., 2002).

The results of this study clearly reveal with two separate markers that glatiramer acetate increases levels of proliferation in the mature RPE. While the numbers we reveal are not large, it is important to note that, particularly for the Ki67 label, this is a snap shot of a dynamic process, in which there is a constant low level of proliferation over life (Al-Hussaini et al., 2008). However, one clear facet of this study is the disparity between the data generated using the cell cycle marker Ki67 and that using the marker of cell division, BrdU. The Ki67 data revealed an approximate 100% increase in the number of cells in the cell cycle at a single time point following drug administration, while 14 sequential daily injections of BrdU elevated cell division by only approximately 50%, which is 3% per day. There are many variables that can lead to discrepancies between positively labeled cell numbers with the two markers, in particular the fact that Ki67 labels all phases of the cell cycle, while BrdU is only incorporated in S phase, which accounts for 10–30% of the cell cycle depending on total DNA load. Given that there was a 100% increases in Ki67

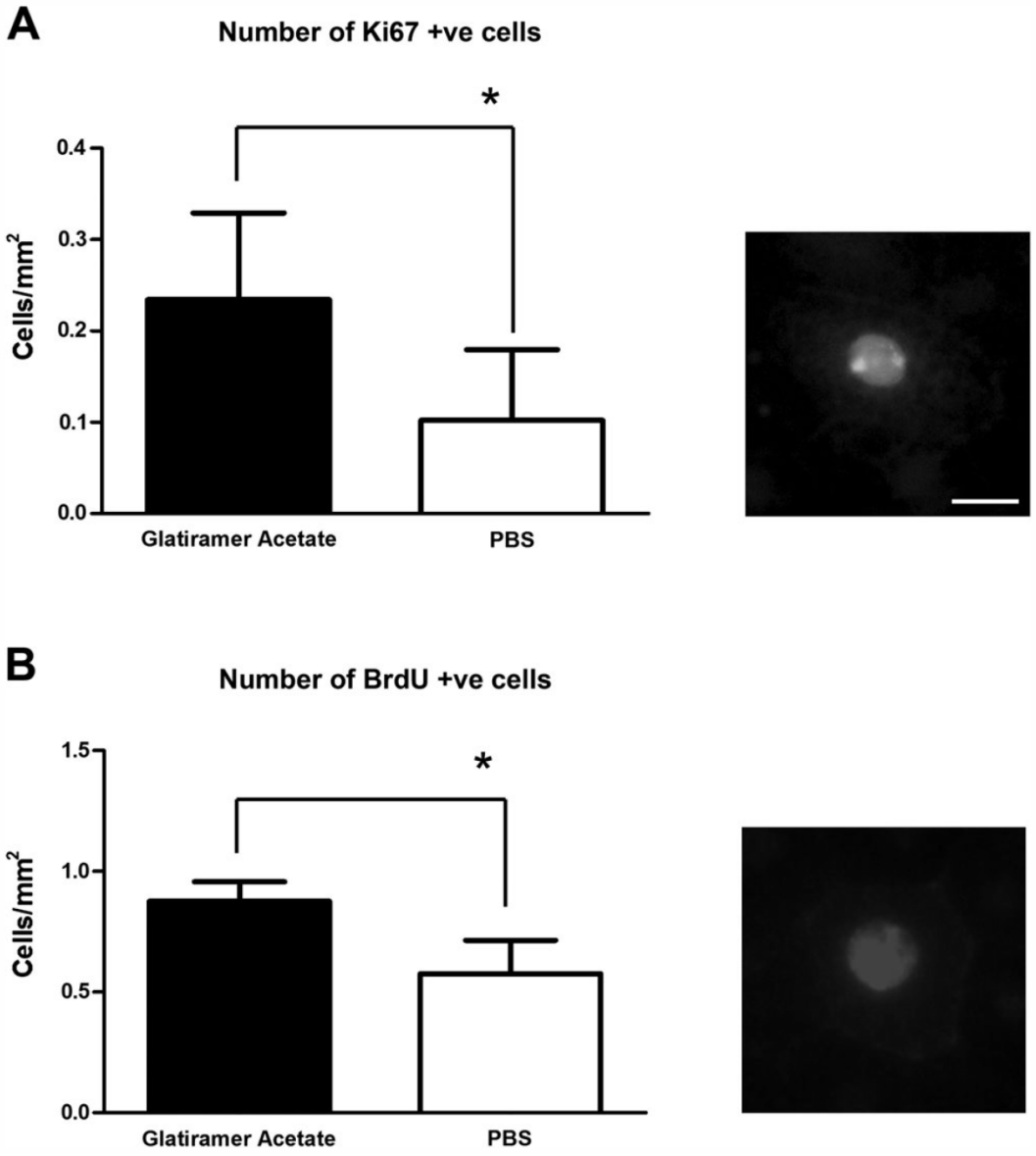

Fig. 1. Ki67 (**A**) and BrdU (**B**) labeling of the RPE corrected for the number of cells (mm^2). Presence of a cell within the cell cycle was assessed with Ki67 at a single time point. BrdU was injected over 14 consecutive days. Significantly elevated levels of Ki67 ($P = 0.0297$) and BrdU ($P = 0.0040$) were found following administration of glatiramer acetate demonstrating that it increases cell proliferation. The photomicrographs show a positively labeled RPE cell for ki67 (Green, A) and BrdU (Red, B). However, while Ki67-positive cell numbers doubled, BrdU-positive cell numbers only increased by approximately 50% following 14 consecutive daily pulses, which represents 3% per day. It is possible that many cells entering the cell cycle, as shown with the Ki67 label, fail to complete appropriate cell division, as revealed by BrdU numbers. These cells may either die or may be arrested in the cell cycle. Graphs for the absolute number of cells in each group were almost identical to those shown corrected for area. Scale bar = 25 μm for both photomicrographs.

on a single day, it might be expected that the elevation in BrdU would be much greater. However, the large difference between the two markers may indicate that many cells in the cell cycle do not progress to full cell division.

The unexpectedly low number of BrdU cells is unlikely to be due to it being diluted out through multiple cell divisions over the 14 days. Separately, we have carried out multiple injections of BrdU and traced the progressive accumulation of labeled RPE

cells. This showed that labeled RPE cells increase in number in a roughly linear manner within the time window used here with no indication of numbers declining or leveling off.

There are two alternative explanations for the discrepancy. First, cell cycle proteins can be up regulated in mature cells when they initiate caspase-related apoptosis (Cernak et al., 2005; Yang & Herrup, 2007). It is possible that encouraging cells into the cell cycle at inappropriate stages may result in their failure to complete cell division and they fail to survive. Second, RPE cells can enter the cell cycle but then may be unable to progress through to full cell division and to become polyploid (Adam et al., 2009: Shahabi et al., 2011). There is a tendency towards this in the rodent RPE where the majority of central RPE cells are binucleated (Ts'o & Friedman, 1967). In human, binucleation is uncommon and associated with pathology, specifically proximity to drusen (Al-Hussaini et al., 2009). However, when pigment is absent, albino RPE cells enter the cell cycle in large numbers as melanin precursors are known to regulate the cell cycle (Illia & Jeffery, 1999; Shahabi et al., 2011). These RPE cells become trapped going through inappropriate nuclear division becoming large and distorted but failing to complete cell division. These cells eventually become dysfunctional, with elevated cell death that impacts on the adjacent neural retina (Shahabi et al., 2011). Whether this is the case with glatiramer acetate is unclear, but the discrepancy between the two markers implies that either cell death or polyploidy may be taking place, although the impact of this may not be apparent until animals age further.

We did not notice any progression towards polyploidy in the tissue examined, although the treatment period may not have been long enough for this to be obvious. The alternative may be cell death. However, repeated attempts to mark dying RPE cells have been unsuccessful, as they are difficult to identify, probably due to their rapid rate of clearance and possibly due to their partial masking by melanin. They can be revealed locally following laser lesions (von Leithner et al., 2010) and have been rarely revealed in aged human RPE whole mounts (Del Priore et al., 2002), but here, the number of RPE cells is vast in comparison with the number present in rodents.

There are likely to be homeostatic mechanisms regulating the size of the RPE population over life. While there may be situations in which it is beneficial to elevate RPE production, particularly in response to specific damage, its elevation generally may not be advantageous. However, any potential detrimental impact may not be apparent until the system has been exposed to glatiramer acetate for a period and the animal progressed through to later maturity.

Acknowledgments

This research was supported by The Rosetrees Trust.

References

Adams, T., Shahabi, G., Hoh-Kam, J. & Jeffery, G. (2010). Held under arrest: Many mature albino RPE cells display polyploidal features consistent with abnormal cell cycle retention. *Experimental Eye Research* **90**, 368–372.

Al-Hussaini, H., Schneiders, M., Lundh, P. & Jeffery, G. (2009). Drusen are associated with local and distant disruptions to human retinal pigment epithelium cells. *Experimental Eye Research* **88**, 610–612.

Al-Hussaini, H., Vugler, A., Semo, M. & Jeffery, G. (2008). Mature mammalian retinal pigment epithelium cells proliferate in vivo. *Molecular Vision* **14**, 1784–1791.

Butovsky, O., Koronyo-Hamaoui, M., Kunis, G., Ophir, E., Landa, G., Cohen, H. & Schwartz, M. (2006). Glatiramer acetate fights against Alzheimer's disease by inducing dendritic-like microglia expressing insulin-like growth factor 1. *Proceedings of the National Academy of Sciences of the United States of America* **103**, 11784–11789.

Cernak, I., Stoica, B., Byrnes, K.R., Di Giovanni, S. & Faden, S. (2005). Role of cell cycle in the pathobiology of central nervous system trauma. *Cell Cycle* **4**, 1286–1293.

Del Priore, L.V., Kuo, Y.H. & Tezel, T.H. (2002). Age-related changes in human RPE cell density and apoptosis proportion in situ. *Investigative Ophthalmology and Visual Science* **43**, 3312–3318.

Gao, H. & Hollyfield, J.G. (1992). Aging of the human retina. Differential loss of neurons and retinal pigment epithelial cells. *Investigative Ophthalmology and Visual Science* **33**, 1–17.

Green, W.R. (1999). Histopathology of age-related macular degeneration. *Molecular Vision* **5**, 27.

Harman, A.M., Fleming, P.A., Hoskins, R.V. & Moore, S.A. (1997). Development and ageing of cell topography in the human retinal pigment epithelium. *Investigative Ophthalmology and Visual Science* **38**, 2016–2026.

Hollyfield, J.G. (2010). Age-related macular degeneration: the molecular link between oxidative damage, tissue specific inflammation and outer retinal disease: The Proctor lecture. *Investigative Ophthalmology and Visual Science* **51**, 1275–1281.

Illia, M. & Jeffery, G. (1999). Retinal mitosis is regulated by dopa, a melanin precursor that may influence the time at which cells exit the cell cycle: analysis of patterns of cell production in pigmented and albino retinae. *The Journal of Comparative Neurology* **405**, 394–405.

Landa, G., Butovsky, O., Shoshani, J., Schwartz, M. & Pollack, A. (2008). Weekly vaccination with Copaxone (glatiramer acetate) as a potential therapy for dry age-related macular degeneration. *Current Eye Research* **33**, 1011–1013.

Landa, G., Rosen, R.B., Patel, A., Lima, V.C., Tai, K.W., Perez, V.R., Aizman, A. & Garcia, P.M. (2011). Qualitative spectral OCT/SLO analysis of dursen change in dry age-related macular degeneration patients treated with copaxone. *Journal of Ocular Pharmacology and Therapeutics* **27**, 77–82.

Panda-Jonas, S., Jonas, J.B. & Jackobczyk-Zmija, M. (1996). Retinal pigment epithelial cell count, distribution and correlations in normal human eyes. *American Journal of Ophthalmology* **212**, 181–189.

Sarks, S.H. (1976). Ageing and degeneration in the macular region: A clinico-pathological study. *The British Journal of Ophthalmology* **60**, 324–341.

Shahabi, G., Lenassi, E. & Jeffery, G., (2011). *Distorting the Mosaic: The Effect of Melanin on Ageing RPE.* ARVO Meeting Presentation 3208/A456.

Ts'o, M.O.M. & Friedman, E. (1967). The retinal pigmented epithelium. I. Comparative histology. *Archives of Ophthalmology* **78**, 641–649.

von Leithner, P.L., Ciurtin, C. & Jeffery, G. (2010). Microscopic mammalian retinal pigment epithelium lesions induce widespread proliferation with different magnitudes between centre and periphery. *Molecular Vision* **16**, 570–581.

Yang, Y. & Herrup, K. (2007). Cell division in the CNS: Protective response or lethal event in post-mitotic neurons. *Biochimica et Biophysica Acta* **1772**, 457–466.

References

ADAMIS, A. P., SHIMA, D. T., YEO, K. T., YEO, T. K., BROWN, L. F., BERSE, B., D'AMORE, P. A. & FOLKMAN, J. 1993. Synthesis and secretion of vascular permeability factor/vascular endothelial growth factor by human retinal pigment epithelial cells. *Biochem Biophys Res Commun,* 193**,** 631-8.

AHARONI, R., ARNON, R. & EILAM, R. 2005. Neurogenesis and neuroprotection induced by peripheral immunomodulatory treatment of experimental autoimmune encephalomyelitis. *J Neurosci,* 25**,** 8217-28.

AHARONI, R., KAYHAN, B., EILAM, R., SELA, M. & ARNON, R. 2003. Glatiramer acetate-specific T cells in the brain express T helper 2/3 cytokines and brain-derived neurotrophic factor in situ. *Proc Natl Acad Sci U S A,* 100**,** 14157-62.

AHARONI, R., TEITELBAUM, D., LEITNER, O., MESHORER, A., SELA, M. & ARNON, R. 2000. Specific Th2 cells accumulate in the central nervous system of mice protected against experimental autoimmune encephalomyelitis by copolymer 1. *Proc Natl Acad Sci U S A,* 97**,** 11472-7.

AKEO, K., TANAKA, Y. & OKISAKA, S. 1994. A comparison between melanotic and amelanotic retinal pigment epithelial cells in vitro concerning the effects of L-dopa and oxygen on cell cycle. *Pigment Cell Res,* 7**,** 145-51.

AL-HUSSAINI, H., KAM, J. H., VUGLER, A., SEMO, M. & JEFFERY, G. 2008. Mature retinal pigment epithelium cells are retained in the cell cycle and proliferate in vivo. *Mol Vis,* 14**,** 1784-91.

AL-HUSSAINI, H., SCHNEIDERS, M., LUNDH, P. & JEFFERY, G. 2009. Drusen are associated with local and distant disruptions to human retinal pigment epithelium cells. *Exp Eye Res,* 88**,** 610-2.

ALBERT, D. M. & DIAZ-ROHENA, R. 1989. A historical review of sympathetic ophthalmia and its epidemiology. *Surv Ophthalmol,* 34**,** 1-14.

ANDERSON, D. H., STERN, W. H., FISHER, S. K., ERICKSON, P. A. & BORGULA, G. A. 1981. The onset of pigment epithelial proliferation after retinal detachment. *Invest Ophthalmol Vis Sci,* 21**,** 10-6.

ANGELOV, D. N., WAIBEL, S., GUNTINAS-LICHIUS, O., LENZEN, M., NEISS, W. F., TOMOV, T. L., YOLES, E., KIPNIS, J., SCHORI, H., REUTER, A., LUDOLPH, A. & SCHWARTZ, M. 2003. Therapeutic vaccine for acute and chronic motor neuron diseases: implications for amyotrophic lateral sclerosis. *Proc Natl Acad Sci U S A,* 100**,** 4790-5.

ARNON, R. & AHARONI, R. 2007. Neurogenesis and neuroprotection in the CNS--fundamental elements in the effect of Glatiramer acetate on treatment of autoimmune neurological disorders. *Mol Neurobiol,* 36**,** 245-53.

AVIDAN, H., KIPNIS, J., BUTOVSKY, O., CASPI, R. R. & SCHWARTZ, M. 2004. Vaccination with autoantigen protects against aggregated beta-amyloid and glutamate toxicity by controlling microglia: effect of CD4+CD25+ T cells. *Eur J Immunol,* 34**,** 3434-45.

BAEHR, W., WU, S. M., BIRD, A. C. & PALCZEWSKI, K. 2003. The retinoid cycle and retina disease. *Vision Res,* 43**,** 2957-8.

BAKALASH, S., SHLOMO, G. B., ALONI, E., SHAKED, I., WHEELER, L., OFRI, R. & SCHWARTZ, M. 2005. T-cell-based vaccination for morphological and functional neuroprotection in a rat model of chronically elevated intraocular pressure. *J Mol Med (Berl),* 83**,** 904-16.

BALDA, M. S., GARRETT, M. D. & MATTER, K. 2003. The ZO-1-associated Y-box factor ZONAB regulates epithelial cell proliferation and cell density. *J Cell Biol,* 160**,** 423-32.

BAN, Y. & RIZZOLO, L. J. 2000a. Differential regulation of tight junction permeability during development of the retinal pigment epithelium. *Am J Physiol Cell Physiol,* 279**,** C744-50.

BAN, Y. & RIZZOLO, L. J. 2000b. Regulation of glucose transporters during development of the retinal pigment epithelium. *Brain Res Dev Brain Res,* 121**,** 89-95.

BAZAN, N. G. 1989. The metabolism of omega-3 polyunsaturated fatty acids in the eye: the possible role of docosahexaenoic acid and docosanoids in retinal physiology and ocular pathology. *Prog Clin Biol Res,* 312**,** 95-112.

BAZAN, N. G. 2005. Neuroprotectin D1 (NPD1): a DHA-derived mediator that protects brain and retina against cell injury-induced oxidative stress. *Brain Pathol,* 15**,** 159-66.

BAZZONI, G., MARTINEZ-ESTRADA, O. M., ORSENIGO, F., CORDENONSI, M., CITI, S. & DEJANA, E. 2000. Interaction of junctional adhesion molecule with the tight junction components ZO-1, cingulin, and occludin. *J Biol Chem,* 275**,** 20520-6.

BEATTY, S., KOH, H., PHIL, M., HENSON, D. & BOULTON, M. 2000. The role of oxidative stress in the pathogenesis of age-related macular degeneration. *Surv Ophthalmol,* 45**,** 115-34.

BELOKOPYTOV, M., BELKIN, M., DUBINSKY, G., EPSTEIN, Y. & ROSNER, M. 2010. Development and recovery of laser-induced retinal lesion in rats. *Retina,* 30**,** 662-70.

BELOKOPYTOV, M., BEN-SHLOMO, G., ROSNER, M., BELKIN, M., DUBINSKI, G., EPSTEIN, Y. & OFRI, R. 2008. Functional efficacy of glatiramer acetate treatment for laser-induced retinal damage in rats. *Lasers Surg Med,* 40**,** 196-201.

BEN-SHABAT, S., PARISH, C. A., HASHIMOTO, M., LIU, J., NAKANISHI, K. & SPARROW, J. R. 2001. Fluorescent pigments of the retinal pigment epithelium and age-related macular degeneration. *Bioorg Med Chem Lett,* 11**,** 1533-40.

BEN-SHABAT, S., PARISH, C. A., VOLLMER, H. R., ITAGAKI, Y., FISHKIN, N., NAKANISHI, K. & SPARROW, J. R. 2002. Biosynthetic studies of A2E, a major fluorophore of retinal pigment epithelial lipofuscin. *J Biol Chem,* 277**,** 7183-90.

BHARTI, K., NGUYEN, M. T., SKUNTZ, S., BERTUZZI, S. & ARNHEITER, H. 2006. The other pigment cell: specification and development of the pigmented epithelium of the vertebrate eye. *Pigment Cell Res,* 19**,** 380-94.

BINDER, S., STANZEL, B. V., KREBS, I. & GLITTENBERG, C. 2007. Transplantation of the RPE in AMD. *Prog Retin Eye Res,* 26**,** 516-54.

BIRNGRUBER, R., HILLENKAMP, F. & GABEL, V. P. 1985. Theoretical investigations of laser thermal retinal injury. *Health Phys,* 48**,** 781-96.

BLANCHETTE, F. & NEUHAUS, O. 2008. Glatiramer acetate: evidence for a dual mechanism of action. *J Neurol,* 255 Suppl 1**,** 26-36.

BLASZCZYK, W. M., STRAUB, H. & DISTLER, C. 2004. GABA content in the retina of pigmented and albino rats. *Neuroreport,* 15**,** 1141-4.

BOK, D. 1993. The retinal pigment epithelium: a versatile partner in vision. *J Cell Sci Suppl,* 17**,** 189-95.

BONILHA, V. L. 2008. Age and disease-related structural changes in the retinal pigment epithelium. *Clin Ophthalmol,* 2**,** 413-24.

BONNEL, S., MOHAND-SAID, S. & SAHEL, J. A. 2003. The aging of the retina. *Exp Gerontol,* 38**,** 825-31.

BOOTH, C. M. & BROWN, M. C. 1993. Expression of GAP-43 mRNA in mouse spinal cord following unilateral peripheral nerve damage: is there a contralateral effect? *Eur J Neurosci,* 5**,** 1663-76.

BORISY, G. G. & SVITKINA, T. M. 2000. Actin machinery: pushing the envelope. *Curr Opin Cell Biol,* 12**,** 104-12.

BOST, L. M., AOTAKI-KEEN, A. E. & HJELMELAND, L. M. 1992. Coexpression of FGF-5 and bFGF by the retinal pigment epithelium in vitro. *Exp Eye Res,* 55**,** 727-34.

BOULTON, M. & DAYHAW-BARKER, P. 2001. The role of the retinal pigment epithelium: topographical variation and ageing changes. *Eye (Lond),* 15**,** 384-9.

BOULTON, M., DONTSOV, A., JARVIS-EVANS, J., OSTROVSKY, M. & SVISTUNENKO, D. 1993. Lipofuscin is a photoinducible free radical generator. *J Photochem Photobiol B,* 19**,** 201-4.

BOULTON, M., MORIARTY, P., JARVIS-EVANS, J. & MARCYNIUK, B. 1994. Regional variation and age-related changes of lysosomal enzymes in the human retinal pigment epithelium. *Br J Ophthalmol,* 78**,** 125-9.

BOULTON, M., ROANOWSKA, M. & WESS, T. 2004. Ageing of the retinal pigment epithelium: implications for transplantation. *Graefes Arch Clin Exp Ophthalmol,* 242**,** 76-84.

BOVOLENTA, P., MALLAMACI, A., BRIATA, P., CORTE, G. & BONCINELLI, E. 1997. Implication of OTX2 in pigment epithelium determination and neural retina differentiation. *J Neurosci,* 17**,** 4243-52.

BOWES RICKMAN, C., EBRIGHT, J. N., ZAVODNI, Z. J., YU, L., WANG, T., DAIGER, S. P., WISTOW, G., BOON, K. & HAUSER, M. A. 2006. Defining the human macula transcriptome and candidate retinal disease genes using EyeSAGE. *Invest Ophthalmol Vis Sci,* 47**,** 2305-16.

BRINKMANN, R., HUTTMANN, G., ROGENER, J., ROIDER, J., BIRNGRUBER, R. & LIN, C. P. 2000. Origin of retinal pigment epithelium cell damage by pulsed laser irradiance in the nanosecond to microsecond time regimen. *Lasers Surg Med,* 27**,** 451-64.

BROWN, D. C. & GATTER, K. C. 2002. Ki67 protein: the immaculate deception? *Histopathology,* 40**,** 2-11.

BUI, B. V., SINCLAIR, A. J. & VINGRYS, A. J. 1998. Electroretinograms of albino and pigmented guinea-pigs (Cavia porcellus). *Aust N Z J Ophthalmol,* 26 Suppl 1**,** S98-100.

BUNZ, F., DUTRIAUX, A., LENGAUER, C., WALDMAN, T., ZHOU, S., BROWN, J. P., SEDIVY, J. M., KINZLER, K. W. & VOGELSTEIN, B. 1998. Requirement for p53 and p21 to sustain G2 arrest after DNA damage. *Science,* 282**,** 1497-501.

BURKE, J. M. 1993. Cytochrome oxidase activity in bovine and human retinal pigment epithelium: topographical and age-related differences. *Curr Eye Res,* 12**,** 1073-9.

BURKE, J. M., CAO, F. & IRVING, P. E. 2000. High levels of E-/P-cadherin: correlation with decreased apical polarity of Na/K ATPase in bovine RPE cells in situ. *Invest Ophthalmol Vis Sci,* 41**,** 1945-52.

BURKE, J. M. & HJELMELAND, L. M. 2005. Mosaicism of the retinal pigment epithelium: seeing the small picture. *Mol Interv,* 5**,** 241-9.

BURKE, J. M., MCKAY, B. S. & JAFFE, G. J. 1991. Retinal pigment epithelial cells of the posterior pole have fewer Na/K adenosine triphosphatase pumps than peripheral cells. *Invest Ophthalmol Vis Sci,* 32**,** 2042-6.

BURKE, J. M., SKUMATZ, C. M., IRVING, P. E. & MCKAY, B. S. 1996. Phenotypic heterogeneity of retinal pigment epithelial cells in vitro and in situ. *Exp Eye Res,* 62**,** 63-73.

BURKE, J. M. & SOREF, C. 1988. Topographical variation in growth in cultured bovine retinal pigment epithelium. *Invest Ophthalmol Vis Sci,* 29**,** 1784-8.

BURNS, M. S. & HARTZ, M. J. 1992. The retinal pigment epithelium induces fenestration of endothelial cells in vivo. *Curr Eye Res,* 11**,** 863-73.

BUTOVSKY, O., HAUBEN, E. & SCHWARTZ, M. 2001. Morphological aspects of spinal cord autoimmune neuroprotection: colocalization of T cells with B7--2 (CD86) and prevention of cyst formation. *FASEB J,* 15**,** 1065-7.

BUTOVSKY, O., TALPALAR, A. E., BEN-YAAKOV, K. & SCHWARTZ, M. 2005. Activation of microglia by aggregated beta-amyloid or lipopolysaccharide impairs MHC-II expression and renders them cytotoxic whereas IFN-gamma and IL-4 render them protective. *Mol Cell Neurosci,* 29**,** 381-93.

BYLSMA, G. W. & GUYMER, R. H. 2005. Treatment of age-related macular degeneration. *Clin Exp Optom,* 88**,** 322-34.

CAI, J., NELSON, K. C., WU, M., STERNBERG, P., JR. & JONES, D. P. 2000. Oxidative damage and protection of the RPE. *Prog Retin Eye Res,* 19**,** 205-21.

CAMPOCHIARO, P. A. 2000. Retinal and choroidal neovascularization. *J Cell Physiol,* 184**,** 301-10.

CAO, W., TOMBRAN-TINK, J., CHEN, W., MRAZEK, D., ELIAS, R. & MCGINNIS, J. F. 1999. Pigment epithelium-derived factor protects cultured retinal neurons against hydrogen peroxide-induced cell death. *J Neurosci Res,* 57**,** 789-800.

CARR, A. J., VUGLER, A. A., YU, L., SEMO, M., COFFEY, P., MOSS, S. E. & GREENWOOD, J. 2011. The expression of retinal cell markers in human retinal pigment epithelial cells and their augmentation by the synthetic retinoid fenretinide. *Mol Vis,* 17**,** 1701-15.

CASTEDO, M., COQUELLE, A., VIVET, S., VITALE, I., KAUFFMANN, A., DESSEN, P., PEQUIGNOT, M. O., CASARES, N., VALENT, A., MOUHAMAD, S., SCHMITT, E., MODJTAHEDI, N., VAINCHENKER, W., ZITVOGEL, L., LAZAR, V., GARRIDO, C. & KROEMER, G. 2006. Apoptosis regulation in tetraploid cancer cells. *EMBO J,* 25**,** 2584-95.

CAYOUETTE, M., WHITMORE, A. V., JEFFERY, G. & RAFF, M. 2001. Asymmetric segregation of Numb in retinal development and the influence of the pigmented epithelium. *J Neurosci,* 21**,** 5643-51.

CEREIJIDO, M., VALDES, J., SHOSHANI, L. & CONTRERAS, R. G. 1998. Role of tight junctions in establishing and maintaining cell polarity. *Annu Rev Physiol,* 60**,** 161-77.

CERNAK, I., STOICA, B., BYRNES, K. R., DI GIOVANNI, S. & FADEN, A. I. 2005. Role of the cell cycle in the pathobiology of central nervous system trauma. *Cell Cycle,* 4**,** 1286-93.

CHAN, C. C., ROBERGE, R. G., WHITCUP, S. M. & NUSSENBLATT, R. B. 1995. 32 cases of sympathetic ophthalmia. A retrospective study at the National Eye Institute, Bethesda, Md., from 1982 to 1992. *Arch Ophthalmol,* 113**,** 597-600.

CHANG, G. C. & YOUNG, L. H. 2011. Sympathetic ophthalmia. *Semin Ophthalmol,* 26**,** 316-20.

CHANG, H. Y. & YANG, X. 2000. Proteases for cell suicide: functions and regulation of caspases. *Microbiol Mol Biol Rev,* 64**,** 821-46.

CHARNG, J., NGUYEN, C. T., BUI, B. V. & VINGRYS, A. J. 2011. Age-related retinal function changes in albino and pigmented rats. *Invest Ophthalmol Vis Sci*.

CHARTERIS, D. G. 1995. Proliferative vitreoretinopathy: pathobiology, surgical management, and adjunctive treatment. *Br J Ophthalmol,* 79**,** 953-60.

CHIBA, C., HOSHINO, A., NAKAMURA, K., SUSAKI, K., YAMANO, Y., KANEKO, Y., KUWATA, O., MARUO, F. & SAITO, T. 2006. Visual cycle protein RPE65 persists in new retinal cells during retinal regeneration of adult newt. *J Comp Neurol,* 495**,** 391-407.

CHOW, R. L. & LANG, R. A. 2001. Early eye development in vertebrates. *Annu Rev Cell Dev Biol,* 17**,** 255-96.

CHUNG, K., KIM, H. J., NA, H. S., PARK, M. J. & CHUNG, J. M. 1993. Abnormalities of sympathetic innervation in the area of an injured peripheral nerve in a rat model of neuropathic pain. *Neurosci Lett,* 162**,** 85-8.

CRABB, J. W., MIYAGI, M., GU, X., SHADRACH, K., WEST, K. A., SAKAGUCHI, H., KAMEI, M., HASAN, A., YAN, L., RAYBORN, M. E., SALOMON, R. G. & HOLLYFIELD, J. G. 2002. Drusen proteome analysis: an approach to the etiology of age-related macular degeneration. *Proc Natl Acad Sci U S A,* 99**,** 14682-7.

CRYNS, V. & YUAN, J. 1998. Proteases to die for. *Genes Dev,* 12**,** 1551-70.

CUNEA, A. & JEFFERY, G. 2007. The ageing photoreceptor. *Vis Neurosci,* 24**,** 151-5.

CUNHA-VAZ, J. G. 1976. The blood-retinal barriers. *Doc Ophthalmol,* 41**,** 287-327.

CURCIO, C. A. & DRUCKER, D. N. 1993. Retinal ganglion cells in Alzheimer's disease and aging. *Ann Neurol,* 33**,** 248-57.

CURCIO, C. A., MILLICAN, C. L., ALLEN, K. A. & KALINA, R. E. 1993. Aging of the human photoreceptor mosaic: evidence for selective vulnerability of rods in central retina. *Invest Ophthalmol Vis Sci,* 34**,** 3278-96.

CURCIO, C. A., OWSLEY, C. & JACKSON, G. R. 2000. Spare the rods, save the cones in aging and age-related maculopathy. *Invest Ophthalmol Vis Sci,* 41**,** 2015-8.

DAMICO, F. M., KISS, S. & YOUNG, L. H. 2005. Sympathetic ophthalmia. *Semin Ophthalmol,* 20**,** 191-7.

DAVSON, H. 1990. *Physiology of the eye*, Macmillan.

DAWSON, D. W., VOLPERT, O. V., GILLIS, P., CRAWFORD, S. E., XU, H., BENEDICT, W. & BOUCK, N. P. 1999. Pigment epithelium-derived factor: a potent inhibitor of angiogenesis. *Science,* 285**,** 245-8.

DE JONG, P. T. 2006. Age-related macular degeneration. *N Engl J Med,* 355**,** 1474-85.

DEEG, C. A., RAITH, A. J., AMANN, B., CRABB, J. W., THURAU, S. R., HAUCK, S. M., UEFFING, M., WILDNER, G. & STANGASSINGER, M. 2007. CRALBP is a highly prevalent autoantigen for human autoimmune uveitis. *Clin Dev Immunol,* 2007**,** 39245.

DEL PRIORE, L. V., KUO, Y. H. & TEZEL, T. H. 2002. Age-related changes in human RPE cell density and apoptosis proportion in situ. *Invest Ophthalmol Vis Sci,* 43**,** 3312-8.

DEL RIO-TSONIS, K. & TSONIS, P. A. 2003. Eye regeneration at the molecular age. *Dev Dyn,* 226**,** 211-24.

DEL VIVA, M. M. & AGOSTINI, R. 2007. Visual spatial integration in the elderly. *Invest Ophthalmol Vis Sci,* 48**,** 2940-6.

DELORI, F. C., GOGER, D. G. & DOREY, C. K. 2001. Age-related accumulation and spatial distribution of lipofuscin in RPE of normal subjects. *Invest Ophthalmol Vis Sci,* 42**,** 1855-66.

DOREY, C. K., WU, G., EBENSTEIN, D., GARSD, A. & WEITER, J. J. 1989. Cell loss in the aging retina. Relationship to lipofuscin accumulation and macular degeneration. *Invest Ophthalmol Vis Sci,* 30**,** 1691-9.

DOXSEY, S. 2001. Re-evaluating centrosome function. *Nat Rev Mol Cell Biol,* 2**,** 688-98.

DRAGER, U. C. 1985. Birth dates of retinal ganglion cells giving rise to the crossed and uncrossed optic projections in the mouse. *Proc R Soc Lond B Biol Sci,* 224**,** 57-77.

DRUBAIX, I., LEGEAIS, J. M., ROBERT, L. & RENARD, G. 1997. Corneal hyaluronan content during post-ablation healing: evidence for a transient depth-dependent contralateral effect. *Exp Eye Res,* 64**,** 301-4.

DRUZHYNA, N. M., WILSON, G. L. & LEDOUX, S. P. 2008. Mitochondrial DNA repair in aging and disease. *Mech Ageing Dev,* 129**,** 383-90.

DRYJA, T. P., MCGEE, T. L., REICHEL, E., HAHN, L. B., COWLEY, G. S., YANDELL, D. W., SANDBERG, M. A. & BERSON, E. L. 1990. A point mutation of the rhodopsin gene in one form of retinitis pigmentosa. *Nature,* 343**,** 364-6.

DUAN, W. R., GARNER, D. S., WILLIAMS, S. D., FUNCKES-SHIPPY, C. L., SPATH, I. S. & BLOMME, E. A. 2003. Comparison of immunohistochemistry for activated caspase-3 and cleaved cytokeratin 18 with the TUNEL method for quantification of apoptosis in histological sections of PC-3 subcutaneous xenografts. *J Pathol,* 199**,** 221-8.

DUDA, P. W., SCHMIED, M. C., COOK, S. L., KRIEGER, J. I. & HAFLER, D. A. 2000. Glatiramer acetate (Copaxone) induces degenerate, Th2-polarized immune responses in patients with multiple sclerosis. *J Clin Invest,* 105**,** 967-76.

DUNCAN, J. L., LAVAIL, M. M., YASUMURA, D., MATTHES, M. T., YANG, H., TRAUTMANN, N., CHAPPELOW, A. V., FENG, W., EARP, H. S., MATSUSHIMA, G. K. & VOLLRATH, D. 2003. An RCS-like retinal dystrophy phenotype in mer knockout mice. *Invest Ophthalmol Vis Sci,* 44**,** 826-38.

EICHLER, W., FRIEDRICHS, U., THIES, A., TRATZ, C. & WIEDEMANN, P. 2002. Modulation of matrix metalloproteinase and TIMP-1 expression by cytokines in human RPE cells. *Invest Ophthalmol Vis Sci,* 43**,** 2767-73.

ELBERGER, A. J. & HONIG, M. G. 1990. Double-labeling of tissue containing the carbocyanine dye DiI for immunocytochemistry. *J Histochem Cytochem,* 38**,** 735-9.

ENDL, E. & GERDES, J. 2000. The Ki-67 protein: fascinating forms and an unknown function. *Exp Cell Res,* 257**,** 231-7.

ERSHOV, A. V. & STROEVA, O. G. 1989. Post-natal pattern of cell proliferation in retinal pigment epithelium of mice studied with tritiated thymidine autoradiography. *Cell Differ Dev,* 28**,** 173-7.

FANNING, A. S., JAMESON, B. J., JESAITIS, L. A. & ANDERSON, J. M. 1998. The tight junction protein ZO-1 establishes a link between the transmembrane protein occludin and the actin cytoskeleton. *J Biol Chem,* 273**,** 29745-53.

FEENEY-BURNS, L., HILDERBRAND, E. S. & ELDRIDGE, S. 1984. Aging human RPE: morphometric analysis of macular, equatorial, and peripheral cells. *Invest Ophthalmol Vis Sci,* 25**,** 195-200.

FENG, W., YASUMURA, D., MATTHES, M. T., LAVAIL, M. M. & VOLLRATH, D. 2002. Mertk triggers uptake of photoreceptor outer segments during phagocytosis by cultured retinal pigment epithelial cells. *J Biol Chem,* 277**,** 17016-22.

FINNEMANN, S. C., BONILHA, V. L., MARMORSTEIN, A. D. & RODRIGUEZ-BOULAN, E. 1997. Phagocytosis of rod outer segments by retinal pigment epithelial cells requires alpha(v)beta5 integrin for binding but not for internalization. *Proc Natl Acad Sci U S A,* 94**,** 12932-7.

FINNEMANN, S. C. & NANDROT, E. F. 2006. MerTK activation during RPE phagocytosis in vivo requires alphaVbeta5 integrin. *Adv Exp Med Biol,* 572**,** 499-503.

FINNEMANN, S. C. & SILVERSTEIN, R. L. 2001. Differential roles of CD36 and alphavbeta5 integrin in photoreceptor phagocytosis by the retinal pigment epithelium. *J Exp Med,* 194**,** 1289-98.

FISCHER, A. J. & REH, T. A. 2001. Transdifferentiation of pigmented epithelial cells: a source of retinal stem cells? *Dev Neurosci,* 23**,** 268-76.

FISHER, J., LEVKOVITCH-VERBIN, H., SCHORI, H., YOLES, E., BUTOVSKY, O., KAYE, J. F., BEN-NUN, A. & SCHWARTZ, M. 2001. Vaccination for neuroprotection in the mouse optic nerve: implications for optic neuropathies. *J Neurosci,* 21**,** 136-42.

FONN, D., DU TOIT, R., SIMPSON, T. L., VEGA, J. A., SITU, P. & CHALMERS, R. L. 1999. Sympathetic swelling response of the control eye to soft lenses in the other eye. *Invest Ophthalmol Vis Sci,* 40**,** 3116-21.

FRANK, R. N. 1997. Growth factors in age-related macular degeneration: pathogenic and therapeutic implications. *Ophthalmic Res,* 29**,** 341-53.

FRENKEL, D., MARON, R., BURT, D. S. & WEINER, H. L. 2005. Nasal vaccination with a proteosome-based adjuvant and glatiramer acetate clears beta-amyloid in a mouse model of Alzheimer disease. *J Clin Invest,* 115**,** 2423-33.

FRIEDMAN, D. S., O'COLMAIN, B. J., MUNOZ, B., TOMANY, S. C., MCCARTY, C., DE JONG, P. T., NEMESURE, B., MITCHELL, P. & KEMPEN, J. 2004. Prevalence of age-related macular degeneration in the United States. *Arch Ophthalmol,* 122**,** 564-72.

FROHLICH, E. & KLESSEN, C. 2001. Enzymatic heterogeneity of bovine retinal pigment epithelial cells in vivo and in vitro. *Graefes Arch Clin Exp Ophthalmol,* 239**,** 25-34.

FUJISAWA, H., MORIOKA, H., WATANABE, K. & NAKAMURA, H. 1976. A decay of gap junctions in association with cell differentiation of neural retina in chick embryonic development. *J Cell Sci,* 22**,** 585-96.

FURUSE, M., ITOH, M., HIRASE, T., NAGAFUCHI, A., YONEMURA, S. & TSUKITA, S. 1994. Direct association of occludin with ZO-1 and its possible involvement in the localization of occludin at tight junctions. *J Cell Biol,* 127**,** 1617-26.

GANEM, N. J. & PELLMAN, D. 2007. Limiting the proliferation of polyploid cells. *Cell,* 131**,** 437-40.

GANEM, N. J., STORCHOVA, Z. & PELLMAN, D. 2007. Tetraploidy, aneuploidy and cancer. *Curr Opin Genet Dev,* 17**,** 157-62.

GAO, H. & HOLLYFIELD, J. G. 1992. Aging of the human retina. Differential loss of neurons and retinal pigment epithelial cells. *Invest Ophthalmol Vis Sci,* 33**,** 1-17.

GEMS, D. & DOONAN, R. 2009. Antioxidant defense and aging in C. elegans: is the oxidative damage theory of aging wrong? *Cell Cycle,* 8**,** 1681-7.

GEORGIADIS, A., TSCHERNUTTER, M., BAINBRIDGE, J. W., BALAGGAN, K. S., MOWAT, F., WEST, E. L., MUNRO, P. M., THRASHER, A. J., MATTER, K., BALDA, M. S. & ALI, R. R. 2010. The tight

junction associated signalling proteins ZO-1 and ZONAB regulate retinal pigment epithelium homeostasis in mice. *PLoS One,* 5**,** e15730.
GODING, C. R. 2000. Mitf from neural crest to melanoma: signal transduction and transcription in the melanocyte lineage. *Genes Dev,* 14**,** 1712-28.
GOLDEN, T. R. & MELOV, S. 2001. Mitochondrial DNA mutations, oxidative stress, and aging. *Mech Ageing Dev,* 122**,** 1577-89.
GOLLAPALLI, D. R. & RANDO, R. R. 2004. The specific binding of retinoic acid to RPE65 and approaches to the treatment of macular degeneration. *Proc Natl Acad Sci U S A,* 101**,** 10030-5.
GOTTARDI, C. J., ARPIN, M., FANNING, A. S. & LOUVARD, D. 1996. The junction-associated protein, zonula occludens-1, localizes to the nucleus before the maturation and during the remodeling of cell-cell contacts. *Proc Natl Acad Sci U S A,* 93**,** 10779-84.
GOYAL, L. 2001. Cell death inhibition: keeping caspases in check. *Cell,* 104**,** 805-8.
GREEN, D. G., HERREROS DE TEJADA, P. & GLOVER, M. J. 1991. Are albino rats night blind? *Invest Ophthalmol Vis Sci,* 32**,** 2366-71.
GREEN, D. G., HERREROS DE TEJADA, P. & GLOVER, M. J. 1994. Electrophysiological estimates of visual sensitivity in albino and pigmented mice. *Vis Neurosci,* 11**,** 919-25.
GRESH, J., GOLETZ, P. W., CROUCH, R. K. & ROHRER, B. 2003. Structure-function analysis of rods and cones in juvenile, adult, and aged C57bl/6 and Balb/c mice. *Vis Neurosci,* 20**,** 211-20.
GRONSKOV, K., EK, J. & BRONDUM-NIELSEN, K. 2007. Oculocutaneous albinism. *Orphanet J Rare Dis,* 2**,** 43.
GU, S. M., THOMPSON, D. A., SRIKUMARI, C. R., LORENZ, B., FINCKH, U., NICOLETTI, A., MURTHY, K. R., RATHMANN, M., KUMARAMANICKAVEL, G., DENTON, M. J. & GAL, A. 1997. Mutations in RPE65 cause autosomal recessive childhood-onset severe retinal dystrophy. *Nat Genet,* 17**,** 194-7.
GUIDOTTI, J. E., BREGERIE, O., ROBERT, A., DEBEY, P., BRECHOT, C. & DESDOUETS, C. 2003. Liver cell polyploidization: a pivotal role for binuclear hepatocytes. *J Biol Chem,* 278**,** 19095-101.
HALL, A. 1998. Rho GTPases and the actin cytoskeleton. *Science,* 279**,** 509-14.
HAMANN, S. 2002. Molecular mechanisms of water transport in the eye. *Int Rev Cytol,* 215**,** 395-431.
HAMILTON, W. D. 1966. The moulding of senescence by natural selection. *J Theor Biol,* 12**,** 12-45.
HAMMOND, B. R., JR. & CARUSO-AVERY, M. 2000. Macular pigment optical density in a Southwestern sample. *Invest Ophthalmol Vis Sci,* 41**,** 1492-7.
HAN, J., YAN, X. L., HAN, Q. H., LI, Y., ZHU, J. & HUI, Y. N. 2009. Electric fields contribute to directed migration of human retinal pigment epithelial cells via interaction between F-actin and beta1 integrin. *Curr Eye Res,* 34**,** 438-46.
HAN, J., YAN, X. L., HAN, Q. H., LI, Y. J., DU, Z. J. & HUI, Y. N. 2011. Integrin beta1 subunit signaling is involved in the directed migration of human retinal pigment epithelial cells following electric field stimulation. *Ophthalmic Res,* 45**,** 15-22.
HAN, M., GIESE, G., SCHMITZ-VALCKENBERG, S., BINDEWALD-WITTICH, A., HOLZ, F. G., YU, J., BILLE, J. F. & NIEMZ, M. H. 2007. Age-related structural abnormalities in the human retina-choroid complex revealed by two-photon excited autofluorescence imaging. *J Biomed Opt,* 12**,** 024012.
HARDY, J. & SELKOE, D. J. 2002. The amyloid hypothesis of Alzheimer's disease: progress and problems on the road to therapeutics. *Science,* 297**,** 353-6.
HARIK, S. I., KALARIA, R. N., WHITNEY, P. M., ANDERSSON, L., LUNDAHL, P., LEDBETTER, S. R. & PERRY, G. 1990. Glucose transporters are abundant in cells with "occluding" junctions at the blood-eye barriers. *Proc Natl Acad Sci U S A,* 87**,** 4261-4.
HARMAN, A. M. & BEAZLEY, L. D. 1989. Generation of retinal cells in the wallaby, Setonix brachyurus (quokka). *Neuroscience,* 28**,** 219-32.

HARMAN, A. M., FLEMING, P. A., HOSKINS, R. V. & MOORE, S. R. 1997. Development and aging of cell topography in the human retinal pigment epithelium. *Invest Ophthalmol Vis Sci,* 38**,** 2016-26.

HARMAN, D. 1981. The aging process. *Proc Natl Acad Sci U S A,* 78**,** 7124-8.

HARPER, J. W., ADAMI, G. R., WEI, N., KEYOMARSI, K. & ELLEDGE, S. J. 1993. The p21 Cdk-interacting protein Cip1 is a potent inhibitor of G1 cyclin-dependent kinases. *Cell,* 75**,** 805-16.

HASKINS, J., GU, L., WITTCHEN, E. S., HIBBARD, J. & STEVENSON, B. R. 1998. ZO-3, a novel member of the MAGUK protein family found at the tight junction, interacts with ZO-1 and occludin. *J Cell Biol,* 141**,** 199-208.

HAUBEN, E., BUTOVSKY, O., NEVO, U., YOLES, E., MOALEM, G., AGRANOV, E., MOR, F., LEIBOWITZ-AMIT, R., PEVSNER, E., AKSELROD, S., NEEMAN, M., COHEN, I. R. & SCHWARTZ, M. 2000. Passive or active immunization with myelin basic protein promotes recovery from spinal cord contusion. *J Neurosci,* 20**,** 6421-30.

HAYES, B. P. 1976. The distribution of intercellular gap junctions in the developing retina and pigment epithelium of Xenopus laevis. *Anat Embryol (Berl),* 150**,** 99-111.

HEIDUSCHKA, P. & SCHRAERMEYER, U. 2008. Comparison of visual function in pigmented and albino rats by electroretinography and visual evoked potentials. *Graefes Arch Clin Exp Ophthalmol,* 246**,** 1559-73.

HEINTZ, N. 1993. Cell death and the cell cycle: a relationship between transformation and neurodegeneration? *Trends Biochem Sci,* 18**,** 157-9.

HERGOTT, G. J., NAGAI, H. & KALNINS, V. I. 1993. Inhibition of retinal pigment epithelial cell migration and proliferation with monoclonal antibodies against the beta 1 integrin subunit during wound healing in organ culture. *Invest Ophthalmol Vis Sci,* 34**,** 2761-8.

HINCHCLIFFE, E. H. & SLUDER, G. 2001. "It takes two to tango": understanding how centrosome duplication is regulated throughout the cell cycle. *Genes Dev,* 15**,** 1167-81.

HINTON, D. R., HE, S., GRAF, K., YANG, D., HSUEH, W. A., RYAN, S. J. & LAW, R. E. 1998. Mitogen-activated protein kinase activation mediates PDGF-directed migration of RPE cells. *Exp Cell Res,* 239**,** 11-5.

HISCOTT, P., SHERIDAN, C., MAGEE, R. M. & GRIERSON, I. 1999. Matrix and the retinal pigment epithelium in proliferative retinal disease. *Prog Retin Eye Res,* 18**,** 167-90.

HOGAN, M. J., ALVARADO, J. A. & WEDDELL, J. E. 1971. *Histology of the human eye : an atlas and textbook,* Philadelphia, London, Saunders.

HOH KAM, J., LENASSI, E. & JEFFERY, G. 2010. Viewing ageing eyes: diverse sites of amyloid Beta accumulation in the ageing mouse retina and the up-regulation of macrophages. *PLoS One,* 5.

HOOPER, C. Y. & GUYMER, R. H. 2003. New treatments in age-related macular degeneration. *Clin Experiment Ophthalmol,* 31**,** 376-91.

HORWITZ, A. R. & PARSONS, J. T. 1999. Cell migration--movin' on. *Science,* 286**,** 1102-3.

HUANG, J., POSSIN, D. E. & SAARI, J. C. 2009. Localizations of visual cycle components in retinal pigment epithelium. *Mol Vis,* 15**,** 223-34.

HUTTENLOCHER, A., PALECEK, S. P., LU, Q., ZHANG, W., MELLGREN, R. L., LAUFFENBURGER, D. A., GINSBERG, M. H. & HORWITZ, A. F. 1997. Regulation of cell migration by the calcium-dependent protease calpain. *J Biol Chem,* 272**,** 32719-22.

HYNES, R. O. & LANDER, A. D. 1992. Contact and adhesive specificities in the associations, migrations, and targeting of cells and axons. *Cell,* 68**,** 303-22.

IANNACCONE, P. M. 1987. The study of mammalian organogenesis by mosaic pattern analysis. *Cell Differ,* 21**,** 79-91.

ILIA, M. & JEFFERY, G. 1996. Delayed neurogenesis in the albino retina: evidence of a role for melanin in regulating the pace of cell generation. *Brain Res Dev Brain Res,* 95**,** 176-83.

ILIA, M. & JEFFERY, G. 1999. Retinal mitosis is regulated by dopa, a melanin precursor that may influence the time at which cells exit the cell cycle: analysis of patterns of cell production in pigmented and albino retinae. *J Comp Neurol,* 405**,** 394-405.

ILIA, M. & JEFFERY, G. 2000. Retinal cell addition and rod production depend on early stages of ocular melanin synthesis. *J Comp Neurol,* 420**,** 437-44.

ISHIBASHI, K., TIAN, J. & HANDA, J. T. 2004. Similarity of mRNA phenotypes of morphologically normal macular and peripheral retinal pigment epithelial cells in older human eyes. *Invest Ophthalmol Vis Sci,* 45**,** 3291-301.

ITOH, M., NAGAFUCHI, A., YONEMURA, S., KITANI-YASUDA, T. & TSUKITA, S. 1993. The 220-kD protein colocalizing with cadherins in non-epithelial cells is identical to ZO-1, a tight junction-associated protein in epithelial cells: cDNA cloning and immunoelectron microscopy. *J Cell Biol,* 121**,** 491-502.

JACKSON, G. R., OWSLEY, C. & CURCIO, C. A. 2002. Photoreceptor degeneration and dysfunction in aging and age-related maculopathy. *Ageing Res Rev,* 1**,** 381-96.

JARRETT, S. G., LIN, H., GODLEY, B. F. & BOULTON, M. E. 2008. Mitochondrial DNA damage and its potential role in retinal degeneration. *Prog Retin Eye Res,* 27**,** 596-607.

JEFFERY, G. 1997. The albino retina: an abnormality that provides insight into normal retinal development. *Trends Neurosci,* 20**,** 165-9.

JEFFERY, G., DARLING, K. & WHITMORE, A. 1994a. Melanin and the regulation of mammalian photoreceptor topography. *Eur J Neurosci,* 6**,** 657-67.

JEFFERY, G. & KINSELLA, B. 1992. Translaminar deficits in the retinae of albinos. *J Comp Neurol,* 326**,** 637-44.

JEFFERY, G., SCHUTZ, G. & MONTOLIU, L. 1994b. Correction of abnormal retinal pathways found with albinism by introduction of a functional tyrosinase gene in transgenic mice. *Dev Biol,* 166**,** 460-4.

JEFFERY, G. & WILLIAMS, A. 1994. Is abnormal retinal development in albinism only a mammalian problem? Normality of a hypopigmented avian retina. *Exp Brain Res,* 100**,** 47-57.

JENSEN, A. M., WALKER, C. & WESTERFIELD, M. 2001. mosaic eyes: a zebrafish gene required in pigmented epithelium for apical localization of retinal cell division and lamination. *Development,* 128**,** 95-105.

JOHNSON, D. A., FIELDS, C., FALLON, A., FITZGERALD, M. E., VIAR, M. J. & JOHNSON, L. R. 2002. Polyamine-dependent migration of retinal pigment epithelial cells. *Invest Ophthalmol Vis Sci,* 43**,** 1228-33.

JOHNSON, K. P., BROOKS, B. R., COHEN, J. A., FORD, C. C., GOLDSTEIN, J., LISAK, R. P., MYERS, L. W., PANITCH, H. S., ROSE, J. W. & SCHIFFER, R. B. 1995. Copolymer 1 reduces relapse rate and improves disability in relapsing-remitting multiple sclerosis: results of a phase III multicenter, double-blind placebo-controlled trial. The Copolymer 1 Multiple Sclerosis Study Group. *Neurology,* 45**,** 1268-76.

KALA, M., MIRAVALLE, A. & VOLLMER, T. 2011. Recent insights into the mechanism of action of glatiramer acetate. *J Neuroimmunol,* 235**,** 9-17.

KAM, J. H., LENASSI, E. & JEFFERY, G. 2010. Viewing Ageing Eyes: Diverse Sites of Amyloid Beta Accumulation in the Ageing Mouse Retina and the Up-Regulation of Macrophages. *PLoS One,* 5.

KATSUNO, T., UMEDA, K., MATSUI, T., HATA, M., TAMURA, A., ITOH, M., TAKEUCHI, K., FUJIMORI, T., NABESHIMA, Y., NODA, T. & TSUKITA, S. 2008. Deficiency of zonula occludens-1 causes embryonic lethal phenotype associated with defected yolk sac angiogenesis and apoptosis of embryonic cells. *Mol Biol Cell,* 19**,** 2465-75.

KATZ, M. L. & ROBISON, W. G., JR. 1986. Evidence of cell loss from the rat retina during senescence. *Exp Eye Res,* 42**,** 293-304.

KAWAMURA, S. & TACHIBANAKI, S. 2008. Rod and cone photoreceptors: molecular basis of the difference in their physiology. *Comp Biochem Physiol A Mol Integr Physiol,* 150**,** 369-77.
KEE, N., SIVALINGAM, S., BOONSTRA, R. & WOJTOWICZ, J. M. 2002. The utility of Ki-67 and BrdU as proliferative markers of adult neurogenesis. *J Neurosci Methods,* 115**,** 97-105.
KEVANY, B. M. & PALCZEWSKI, K. 2010. Phagocytosis of retinal rod and cone photoreceptors. *Physiology (Bethesda),* 25**,** 8-15.
KIILGAARD, J. F., PRAUSE, J. U., PRAUSE, M., SCHERFIG, E., NISSEN, M. H. & LA COUR, M. 2007. Subretinal posterior pole injury induces selective proliferation of RPE cells in the periphery in in vivo studies in pigs. *Invest Ophthalmol Vis Sci,* 48**,** 355-60.
KIM, I. B., LEE, M. Y., OH, S., KIM, K. Y. & CHUN, M. 1998. Double-labeling techniques demonstrate that rod bipolar cells are under GABAergic control in the inner plexiform layer of the rat retina. *Cell Tissue Res,* 292**,** 17-25.
KING, G. L. & SUZUMA, K. 2000. Pigment-epithelium-derived factor--a key coordinator of retinal neuronal and vascular functions. *N Engl J Med,* 342**,** 349-51.
KINNEAR, P. E., JAY, B. & WITKOP, C. J., JR. 1985. Albinism. *Surv Ophthalmol,* 30**,** 75-101.
KIPNIS, J. & SCHWARTZ, M. 2002. Dual action of glatiramer acetate (Cop-1) in the treatment of CNS autoimmune and neurodegenerative disorders. *Trends Mol Med,* 8**,** 319-23.
KIPNIS, J., YOLES, E., PORAT, Z., COHEN, A., MOR, F., SELA, M., COHEN, I. R. & SCHWARTZ, M. 2000. T cell immunity to copolymer 1 confers neuroprotection on the damaged optic nerve: possible therapy for optic neuropathies. *Proc Natl Acad Sci U S A,* 97**,** 7446-51.
KIPNIS, J., YOLES, E., SCHORI, H., HAUBEN, E., SHAKED, I. & SCHWARTZ, M. 2001. Neuronal survival after CNS insult is determined by a genetically encoded autoimmune response. *J Neurosci,* 21**,** 4564-71.
KLINGHOFFER, R. A., SACHSENMAIER, C., COOPER, J. A. & SORIANO, P. 1999. Src family kinases are required for integrin but not PDGFR signal transduction. *EMBO J,* 18**,** 2459-71.
KNIESEL, U. & WOLBURG, H. 1993. Tight junction complexity in the retinal pigment epithelium of the chicken during development. *Neurosci Lett,* 149**,** 71-4.
KOHLER, C., ORRENIUS, S. & ZHIVOTOVSKY, B. 2002. Evaluation of caspase activity in apoptotic cells. *J Immunol Methods,* 265**,** 97-110.
KOKKINOPOULOS, I., SHAHABI, G., COLMAN, A. & JEFFERY, G. 2011. Mature peripheral RPE cells have an intrinsic capacity to proliferate; a potential regulatory mechanism for age-related cell loss. *PLoS One,* 6**,** e18921.
KOLESNIKOV, A. V., FAN, J., CROUCH, R. K. & KEFALOV, V. J. 2010. Age-related deterioration of rod vision in mice. *J Neurosci,* 30**,** 11222-31.
KOLTZENBURG, M., WALL, P. D. & MCMAHON, S. B. 1999. Does the right side know what the left is doing? *Trends Neurosci,* 22**,** 122-7.
KONARI, K., SAWADA, N., ZHONG, Y., ISOMURA, H., NAKAGAWA, T. & MORI, M. 1995. Development of the blood-retinal barrier in vitro: formation of tight junctions as revealed by occludin and ZO-1 correlates with the barrier function of chick retinal pigment epithelial cells. *Exp Eye Res,* 61**,** 99-108.
KORNZWEIG, A. L., FELDSTEIN, M. & SCHNEIDER, J. 1957. The eye in old age. IV. Ocular survey of over one thousand aged persons with special reference to normal and disturbed visual function. *Am J Ophthalmol,* 44**,** 29-37.
KRALJ-HANS, I., TIBBER, M., JEFFERY, G. & MOBBS, P. 2006. Differential effect of dopamine on mitosis in early postnatal albino and pigmented rat retinae. *J Neurobiol,* 66**,** 47-55.
KRILL, A. E. & LEE, G. B. 1963. The electroretinogram in albinos and carriers of the ocular albino trait. *Arch Ophthalmol,* 69**,** 32-8.
KRISS, A., RUSSELL-EGGITT, I., HARRIS, C. M., LLOYD, I. C. & TAYLOR, D. 1992. Aspects of albinism. *Ophthalmic Paediatr Genet,* 13**,** 89-100.

KRISS, J. P., MARUYAMA, Y., TUNG, L. A., BOND, S. B. & REVESZ, L. 1963. The fate of 5-bromodeoxyuridine, 5-bromodeoxycytidine, and 5-iododeoxycytidine in man. *Cancer Res,* 23**,** 260-8.

KRITCHEVSKY, S. B. & MULDOON, M. F. 1996. Oxidative stress and aging: still a hypothesis. *J Am Geriatr Soc,* 44**,** 873-5.

KVANTA, A. 1994. Expression and secretion of transforming growth factor-beta in transformed and nontransformed retinal pigment epithelial cells. *Ophthalmic Res,* 26**,** 361-7.

LAGNADO, L. 1998. Retinal processing: amacrine cells keep it short and sweet. *Curr Biol,* 8**,** R598-600.

LANDA, G., BUTOVSKY, O., SHOSHANI, J., SCHWARTZ, M. & POLLACK, A. 2008. Weekly vaccination with Copaxone (glatiramer acetate) as a potential therapy for dry age-related macular degeneration. *Curr Eye Res,* 33**,** 1011-3.

LANDA, G., ROSEN, R. B., PATEL, A., LIMA, V. C., TAI, K. W., PEREZ, V. R., AIZMAN, A. & GARCIA, P. M. 2011. Qualitative spectral OCT/SLO analysis of drusen change in dry age-related macular degeneration patients treated with Copaxone. *J Ocul Pharmacol Ther,* 27**,** 77-82.

LAVADO, A., JEFFERY, G., TOVAR, V., DE LA VILLA, P. & MONTOLIU, L. 2006. Ectopic expression of tyrosine hydroxylase in the pigmented epithelium rescues the retinal abnormalities and visual function common in albinos in the absence of melanin. *J Neurochem,* 96**,** 1201-11.

LAVALLEE, C. R., CHALIFOUX, J. R., MOOSALLY, A. J. & BALKEMA, G. W. 2003. Elevated free calcium levels in the subretinal space elevate the absolute dark-adapted threshold in hypopigmented mice. *J Neurophysiol,* 90**,** 3654-62.

LENGAUER, C., KINZLER, K. W. & VOGELSTEIN, B. 1998. Genetic instabilities in human cancers. *Nature,* 396**,** 643-9.

LI, X. & KOLEGA, J. 2002. Effects of direct current electric fields on cell migration and actin filament distribution in bovine vascular endothelial cells. *J Vasc Res,* 39**,** 391-404.

LIANG, F. Q. & GODLEY, B. F. 2003. Oxidative stress-induced mitochondrial DNA damage in human retinal pigment epithelial cells: a possible mechanism for RPE aging and age-related macular degeneration. *Exp Eye Res,* 76**,** 397-403.

LINDA, H., PIEHL, F., DAGERLIND, A., VERGE, V. M., ARVIDSSON, U., CULLHEIM, S., RISLING, M., ULFHAKE, B. & HOKFELT, T. 1992. Expression of GAP-43 mRNA in the adult mammalian spinal cord under normal conditions and after different types of lesions, with special reference to motoneurons. *Exp Brain Res,* 91**,** 284-95.

LU, L., HACKETT, S. F., MINCEY, A., LAI, H. & CAMPOCHIARO, P. A. 2006. Effects of different types of oxidative stress in RPE cells. *J Cell Physiol,* 206**,** 119-25.

LUHMANN, U. F., ROBBIE, S., MUNRO, P. M., BARKER, S. E., DURAN, Y., LUONG, V., FITZKE, F. W., BAINBRIDGE, J. W., ALI, R. R. & MACLAREN, R. E. 2009. The drusenlike phenotype in aging Ccl2-knockout mice is caused by an accelerated accumulation of swollen autofluorescent subretinal macrophages. *Invest Ophthalmol Vis Sci,* 50**,** 5934-43.

LUND, R. D. 1965. Uncrossed Visual Pathways of Hooded and Albino Rats. *Science,* 149**,** 1506-7.

MACHEMER, R. & LAQUA, H. 1975. Pigment epithelium proliferation in retinal detachment (massive periretinal proliferation). *Am J Ophthalmol,* 80**,** 1-23.

MANES, G., LEDUCQ, R., KUCHARCZAK, J., PAGES, A., SCHMITT-BERNARD, C. F. & HAMEL, C. P. 1998. Rat messenger RNA for the retinal pigment epithelium-specific protein RPE65 gradually accumulates in two weeks from late embryonic days. *FEBS Lett,* 423**,** 133-7.

MARGOLIS, R. L., LOHEZ, O. D. & ANDREASSEN, P. R. 2003. G1 tetraploidy checkpoint and the suppression of tumorigenesis. *J Cell Biochem,* 88**,** 673-83.

MARKS, M. S. & SEABRA, M. C. 2001. The melanosome: membrane dynamics in black and white. *Nat Rev Mol Cell Biol,* 2**,** 738-48.

MARLHENS, F., BAREIL, C., GRIFFOIN, J. M., ZRENNER, E., AMALRIC, P., ELIAOU, C., LIU, S. Y., HARRIS, E., REDMOND, T. M., ARNAUD, B., CLAUSTRES, M. & HAMEL, C. P. 1997. Mutations in RPE65 cause Leber's congenital amaurosis. *Nat Genet,* 17**,** 139-41.

MARMOR, M. F. 1999. Mechanisms of fluid accumulation in retinal edema. *Doc Ophthalmol,* 97**,** 239-49.

MARMOR, M. F. & WOLFENSBERGER, T. J. 1998. *The retinal pigment epithelium : function and disease,* New York ; Oxford, Oxford University Press.

MARSHALL, J. 1987. The ageing retina: physiology or pathology. *Eye (Lond),* 1 (Pt 2)**,** 282-95.

MARSHALL, J., GRINDLE, J., ANSELL, P. L. & BORWEIN, B. 1979. Convolution in human rods: an ageing process. *Br J Ophthalmol,* 63**,** 181-7.

MARTIN, D. M., YEE, D., CARLSON, R. O. & FELDMAN, E. L. 1992. Gene expression of the insulin-like growth factors and their receptors in human neuroblastoma cell lines. *Brain Res Mol Brain Res,* 15**,** 241-6.

MARTINEZ-MORALES, J. R., DOLEZ, V., RODRIGO, I., ZACCARINI, R., LECONTE, L., BOVOLENTA, P. & SAULE, S. 2003. OTX2 activates the molecular network underlying retina pigment epithelium differentiation. *J Biol Chem,* 278**,** 21721-31.

MARTINEZ-MORALES, J. R., RODRIGO, I. & BOVOLENTA, P. 2004. Eye development: a view from the retina pigmented epithelium. *Bioessays,* 26**,** 766-77.

MARTINEZ-MORALES, J. R., SIGNORE, M., ACAMPORA, D., SIMEONE, A. & BOVOLENTA, P. 2001. Otx genes are required for tissue specification in the developing eye. *Development,* 128**,** 2019-30.

MATSUMOTO, K. & WOLFFE, A. P. 1998. Gene regulation by Y-box proteins: coupling control of transcription and translation. *Trends Cell Biol,* 8**,** 318-23.

MATTER, K., AIJAZ, S., TSAPARA, A. & BALDA, M. S. 2005. Mammalian tight junctions in the regulation of epithelial differentiation and proliferation. *Curr Opin Cell Biol,* 17**,** 453-8.

MATTHEWS, P. B. 1991. The human stretch reflex and the motor cortex. *Trends Neurosci,* 14**,** 87-91.

MAZZORANA, M., MONTOYA, G. & MORTUZA, G. B. 2011. The centrosome: a target for cancer therapy. *Curr Cancer Drug Targets,* 11**,** 600-12.

MCLACHLAN, E. M., JANIG, W., DEVOR, M. & MICHAELIS, M. 1993. Peripheral nerve injury triggers noradrenergic sprouting within dorsal root ganglia. *Nature,* 363**,** 543-6.

MELZACK, R. 1990. Phantom limbs and the concept of a neuromatrix. *Trends Neurosci,* 13**,** 88-92.

MERIN, S. & AUERBACH, E. 1976. Retinitis pigmentosa. *Surv Ophthalmol,* 20**,** 303-46.

MICELI, M. V., LILES, M. R. & NEWSOME, D. A. 1994. Evaluation of oxidative processes in human pigment epithelial cells associated with retinal outer segment phagocytosis. *Exp Cell Res,* 214**,** 242-9.

MILLER, H., MILLER, B. & RYAN, S. J. 1986. The role of retinal pigment epithelium in the involution of subretinal neovascularization. *Invest Ophthalmol Vis Sci,* 27**,** 1644-52.

MIYAMURA, N., OGAWA, T., BOYLAN, S., MORSE, L. S., HANDA, J. T. & HJELMELAND, L. M. 2004. Topographic and age-dependent expression of heme oxygenase-1 and catalase in the human retinal pigment epithelium. *Invest Ophthalmol Vis Sci,* 45**,** 1562-5.

MOCHII, M., ONO, T., MATSUBARA, Y. & EGUCHI, G. 1998. Spontaneous transdifferentiation of quail pigmented epithelial cell is accompanied by a mutation in the Mitf gene. *Dev Biol,* 196**,** 145-59.

MOSHIRI, A., CLOSE, J. & REH, T. A. 2004. Retinal stem cells and regeneration. *Int J Dev Biol,* 48**,** 1003-14.

MUKHERJEE, P. K., MARCHESELLI, V. L., SERHAN, C. N. & BAZAN, N. G. 2004. Neuroprotectin D1: a docosahexaenoic acid-derived docosatriene protects human retinal pigment epithelial cells from oxidative stress. *Proc Natl Acad Sci U S A,* 101**,** 8491-6.

MURPHY, T. L., SAKAMOTO, T., HINTON, D. R., SPEE, C., GUNDIMEDA, U., SORIANO, D., GOPALAKRISHNA, R. & RYAN, S. J. 1995. Migration of retinal pigment epithelium cells in vitro is regulated by protein kinase C. *Exp Eye Res,* 60**,** 683-95.

MUSARELLA, M. A. 2001. Molecular genetics of macular degeneration. *Doc Ophthalmol,* 102**,** 165-77.

MUSTAFI, D., ENGEL, A. H. & PALCZEWSKI, K. 2009. Structure of cone photoreceptors. *Prog Retin Eye Res,* 28**,** 289-302.

NAGAI, H. & KALNINS, V. I. 1996. Normally occurring loss of single cells and repair of resulting defects in retinal pigment epithelium in situ. *Exp Eye Res,* 62**,** 55-61.

NAGINENI, C. N., KUTTY, V., DETRICK, B. & HOOKS, J. J. 2005. Expression of PDGF and their receptors in human retinal pigment epithelial cells and fibroblasts: regulation by TGF-beta. *J Cell Physiol,* 203**,** 35-43.

NAKAYAMA, A., NGUYEN, M. T., CHEN, C. C., OPDECAMP, K., HODGKINSON, C. A. & ARNHEITER, H. 1998. Mutations in microphthalmia, the mouse homolog of the human deafness gene MITF, affect neuroepithelial and neural crest-derived melanocytes differently. *Mech Dev,* 70**,** 155-66.

NANDROT, E. F., KIM, Y., BRODIE, S. E., HUANG, X., SHEPPARD, D. & FINNEMANN, S. C. 2004. Loss of synchronized retinal phagocytosis and age-related blindness in mice lacking alphavbeta5 integrin. *J Exp Med,* 200**,** 1539-45.

NEUHAUS, O., FARINA, C., YASSOURIDIS, A., WIENDL, H., THEN BERGH, F., DOSE, T., WEKERLE, H. & HOHLFELD, R. 2000. Multiple sclerosis: comparison of copolymer-1- reactive T cell lines from treated and untreated subjects reveals cytokine shift from T helper 1 to T helper 2 cells. *Proc Natl Acad Sci U S A,* 97**,** 7452-7.

NEVES, G. & LAGNADO, L. 1999. The retina. *Curr Biol,* 9**,** R674-7.

NEVEU, M. M., HOLDER, G. E., SLOPER, J. J. & JEFFERY, G. 2005. Optic chiasm formation in humans is independent of foveal development. *Eur J Neurosci,* 22**,** 1825-9.

NGUYEN, M. & ARNHEITER, H. 2000. Signaling and transcriptional regulation in early mammalian eye development: a link between FGF and MITF. *Development,* 127**,** 3581-91.

NIGG, E. A. 2002. Centrosome aberrations: cause or consequence of cancer progression? *Nat Rev Cancer,* 2**,** 815-25.

NIGG, E. A. 2007. Centrosome duplication: of rules and licenses. *Trends Cell Biol,* 17**,** 215-21.

NUCCITELLI, R. 2003. A role for endogenous electric fields in wound healing. *Curr Top Dev Biol,* 58**,** 1-26.

O'STEEN, W. K., ANDERSON, K. V. & SHEAR, C. R. 1974. Photoreceptor degeneration in albino rats: dependency on age. *Invest Ophthalmol,* 13**,** 334-9.

OETTING, W. S. 2000. The tyrosinase gene and oculocutaneous albinism type 1 (OCA1): A model for understanding the molecular biology of melanin formation. *Pigment Cell Res,* 13**,** 320-5.

OETTING, W. S. & KING, R. A. 1999. Molecular basis of albinism: mutations and polymorphisms of pigmentation genes associated with albinism. *Hum Mutat,* 13**,** 99-115.

OHNO-MATSUI, K. 2011. Parallel findings in age-related macular degeneration and Alzheimer's disease. *Prog Retin Eye Res,* 30**,** 217-38.

ONOJAFE, I. F., ADAMS, D. R., SIMEONOV, D. R., ZHANG, J., CHAN, C. C., BERNARDINI, I. M., SERGEEV, Y. V., DOLINSKA, M. B., ALUR, R. P., BRILLIANT, M. H., GAHL, W. A. & BROOKS, B. P. 2011. Nitisinone improves eye and skin pigmentation defects in a mouse model of oculocutaneous albinism. *J Clin Invest*.

OYSTER, C. W. 1999. *The human eye : structure and function,* Sunderland, Mass., Sinauer Associates ; [Basingstoke : MacMillan, distributor].

PAGE, J. W. & CROGNALE, M. A. 2005. Differential aging of chromatic and achromatic visual pathways: behavior and electrophysiology. *Vision Res,* 45**,** 1481-9.

PANDA-JONAS, S., JONAS, J. B. & JAKOBCZYK-ZMIJA, M. 1996. Retinal pigment epithelial cell count, distribution, and correlations in normal human eyes. *Am J Ophthalmol,* 121**,** 181-9.

PAOLISSO, G., TAGLIAMONTE, M. R., RIZZO, M. R., MANZELLA, D., GAMBARDELLA, A. & VARRICCHIO, M. 1998. Oxidative stress and advancing age: results in healthy centenarians. *J Am Geriatr Soc,* 46**,** 833-8.

PARAPURAM, S. K., COJOCARU, R. I., CHANG, J. R., KHANNA, R., BROOKS, M., OTHMAN, M., ZAREPARSI, S., KHAN, N. W., GOTOH, N., COGLIATI, T. & SWAROOP, A. 2010. Distinct signature of altered homeostasis in aging rod photoreceptors: implications for retinal diseases. *PLoS One,* 5**,** e13885.

PEIRSON, S. N., BUTLER, J. N. & FOSTER, R. G. 2003. Experimental validation of novel and conventional approaches to quantitative real-time PCR data analysis. *Nucleic Acids Res,* 31**,** e73.

PIEHL, F., ARVIDSSON, U., JOHNSON, H., CULLHEIM, S., VILLAR, M., DAGERLIND, A., TERENIUS, L., HOKFELT, T. & ULFHAKE, B. 1991. Calcitonin Gene-related Peptide (CGRP)-like Immunoreactivity and CGRP mRNA in Rat Spinal Cord Motoneurons after Different Types of Lesions. *Eur J Neurosci,* 3**,** 737-757.

POLLACK, A. & KORTE, G. E. 1990. Repair of retinal pigment epithelium and its relationship with capillary endothelium after krypton laser photocoagulation. *Invest Ophthalmol Vis Sci,* 31**,** 890-8.

RACKE, M. K., LOVETT-RACKE, A. E. & KARANDIKAR, N. J. 2010. The mechanism of action of glatiramer acetate treatment in multiple sclerosis. *Neurology,* 74 Suppl 1**,** S25-30.

RASK, R. & JENSEN, P. K. 1995. Corneal Abrasion Stimulates Epithelial Healing in the Other Eye. *Investigative Ophthalmology & Visual Science,* 36**,** S576-S576.

RATH, M. F., MORIN, F., SHI, Q., KLEIN, D. C. & MOLLER, M. 2007. Ontogenetic expression of the Otx2 and Crx homeobox genes in the retina of the rat. *Exp Eye Res,* 85**,** 65-73.

RAVID, K., LU, J., ZIMMET, J. M. & JONES, M. R. 2002. Roads to polyploidy: the megakaryocyte example. *J Cell Physiol,* 190**,** 7-20.

RAYMOND, S. M. & JACKSON, I. J. 1995. The retinal pigmented epithelium is required for development and maintenance of the mouse neural retina. *Curr Biol,* 5**,** 1286-95.

REDMOND, T. M., YU, S., LEE, E., BOK, D., HAMASAKI, D., CHEN, N., GOLETZ, P., MA, J. X., CROUCH, R. K. & PFEIFER, K. 1998. Rpe65 is necessary for production of 11-cis-vitamin A in the retinal visual cycle. *Nat Genet,* 20**,** 344-51.

REESE, B. E. & COLELLO, R. J. 1992. Neurogenesis in the retinal ganglion cell layer of the rat. *Neuroscience,* 46**,** 419-29.

RIEDER, C. L. & MAIATO, H. 2004. Stuck in division or passing through: what happens when cells cannot satisfy the spindle assembly checkpoint. *Dev Cell,* 7**,** 637-51.

RILEY, P. A. & BOROVANSKY, J. 2011. *Melanins and melanosomes : biosynthesis, biogenesis, physiological, and pathological functions,* Weinheim, Wiley-VCH ; Chichester : John Wiley [distributor].

RIZZOLO, L. J. 1997. Polarity and the development of the outer blood-retinal barrier. *Histol Histopathol,* 12**,** 1057-67.

RODIECK, R. W. 1998. *The first steps in seeing,* Sunderland, Mass., Sinauer.

ROIDER, J., HILLENKAMP, F., FLOTTE, T. & BIRNGRUBER, R. 1993. Microphotocoagulation: selective effects of repetitive short laser pulses. *Proc Natl Acad Sci U S A,* 90**,** 8643-7.

ROIDER, J., MICHAUD, N. A., FLOTTE, T. J. & BIRNGRUBER, R. 1992. Response of the retinal pigment epithelium to selective photocoagulation. *Arch Ophthalmol,* 110**,** 1786-92.

RONDANELLI, M., MELZI D'ERIL, G. V., ANESI, A. & FERRARI, E. 1997. Altered oxidative stress in healthy old subjects. *Aging (Milano),* 9**,** 221-3.

ROSENBLATT, J., RAFF, M. C. & CRAMER, L. P. 2001. An epithelial cell destined for apoptosis signals its neighbors to extrude it by an actin- and myosin-dependent mechanism. *Curr Biol,* 11**,** 1847-57.

ROTSHENKER, S. 1979. Synapse formation in intact innervated cutaneous-pectoris muscles of the frog following denervation of the opposite muscle. *J Physiol,* 292**,** 535-47.

ROZANOWSKA, M., JARVIS-EVANS, J., KORYTOWSKI, W., BOULTON, M. E., BURKE, J. M. & SARNA, T. 1995. Blue light-induced reactivity of retinal age pigment. In vitro generation of oxygen-reactive species. *J Biol Chem,* 270**,** 18825-30.

ROZANOWSKA, M., SARNA, T., LAND, E. J. & TRUSCOTT, T. G. 1999. Free radical scavenging properties of melanin interaction of eu- and pheo-melanin models with reducing and oxidising radicals. *Free Radic Biol Med,* 26**,** 518-25.

RUGGIERI, M., AVOLIO, C., LIVREA, P. & TROJANO, M. 2007. Glatiramer acetate in multiple sclerosis: a review. *CNS Drug Rev,* 13**,** 178-91.

RUSSELL-EGGITT, I., KRISS, A. & TAYLOR, D. S. 1990. Albinism in childhood: a flash VEP and ERG study. *Br J Ophthalmol,* 74**,** 136-40.

RYEOM, S. W., SPARROW, J. R. & SILVERSTEIN, R. L. 1996. CD36 participates in the phagocytosis of rod outer segments by retinal pigment epithelium. *J Cell Sci,* 109 (Pt 2)**,** 387-95.

SAARI, J. C. & CRABB, J. W. 2005. Focus on molecules: cellular retinaldehyde-binding protein (CRALBP). *Exp Eye Res,* 81**,** 245-6.

SAARI, J. C., NAWROT, M., KENNEDY, B. N., GARWIN, G. G., HURLEY, J. B., HUANG, J., POSSIN, D. E. & CRABB, J. W. 2001. Visual cycle impairment in cellular retinaldehyde binding protein (CRALBP) knockout mice results in delayed dark adaptation. *Neuron,* 29**,** 739-48.

SARKS, S. H. 1975. The aging eye. *Med J Aust,* 2**,** 602-4.

SARNA, T., BURKE, J. M., KORYTOWSKI, W., ROZANOWSKA, M., SKUMATZ, C. M., ZAREBA, A. & ZAREBA, M. 2003. Loss of melanin from human RPE with aging: possible role of melanin photooxidation. *Exp Eye Res,* 76**,** 89-98.

SARNA, T., MENON, I. A. & SEALY, R. C. 1985. Photosensitization of melanins: a comparative study. *Photochem Photobiol,* 42**,** 529-32.

SASTRE, J., PALLARDO, F. V. & VINA, J. 2000. Mitochondrial oxidative stress plays a key role in aging and apoptosis. *IUBMB Life,* 49**,** 427-35.

SCHIAFFINO, M. V. 2010. Signaling pathways in melanosome biogenesis and pathology. *Int J Biochem Cell Biol,* 42**,** 1094-104.

SCHIAFFINO, M. V., BASCHIROTTO, C., PELLEGRINI, G., MONTALTI, S., TACCHETTI, C., DE LUCA, M. & BALLABIO, A. 1996. The ocular albinism type 1 gene product is a membrane glycoprotein localized to melanosomes. *Proc Natl Acad Sci U S A,* 93**,** 9055-60.

SCHORI, H., KIPNIS, J., YOLES, E., WOLDEMUSSIE, E., RUIZ, G., WHEELER, L. A. & SCHWARTZ, M. 2001. Vaccination for protection of retinal ganglion cells against death from glutamate cytotoxicity and ocular hypertension: implications for glaucoma. *Proc Natl Acad Sci U S A,* 98**,** 3398-403.

SCHRAERMEYER, U. & HEIMANN, K. 1999. Current understanding on the role of retinal pigment epithelium and its pigmentation. *Pigment Cell Res,* 12**,** 219-36.

SCHREMPF, W. & ZIEMSSEN, T. 2007. Glatiramer acetate: mechanisms of action in multiple sclerosis. *Autoimmun Rev,* 6**,** 469-75.

SCHUELE, G., RUMOHR, M., HUETTMANN, G. & BRINKMANN, R. 2005. RPE damage thresholds and mechanisms for laser exposure in the microsecond-to-millisecond time regimen. *Invest Ophthalmol Vis Sci,* 46**,** 714-9.

SELA, M. & TEITELBAUM, D. 2001. Glatiramer acetate in the treatment of multiple sclerosis. *Expert Opin Pharmacother,* 2**,** 1149-65.

SELKOE, D. J. 1991. The molecular pathology of Alzheimer's disease. *Neuron,* 6**,** 487-98.

SHAMSI, F. A. & BOULTON, M. 2001. Inhibition of RPE lysosomal and antioxidant activity by the age pigment lipofuscin. *Invest Ophthalmol Vis Sci,* 42**,** 3041-6.
SIEG, D. J., HAUCK, C. R. & SCHLAEPFER, D. D. 1999. Required role of focal adhesion kinase (FAK) for integrin-stimulated cell migration. *J Cell Sci,* 112 (Pt 16)**,** 2677-91.
SIMEONE, A., PUELLES, E. & ACAMPORA, D. 2002. The Otx family. *Curr Opin Genet Dev,* 12**,** 409-15.
SIMO, R., VILLARROEL, M., CORRALIZA, L., HERNANDEZ, C. & GARCIA-RAMIREZ, M. 2010. The retinal pigment epithelium: something more than a constituent of the blood-retinal barrier--implications for the pathogenesis of diabetic retinopathy. *J Biomed Biotechnol,* 2010**,** 190724.
SLEE, E. A., ADRAIN, C. & MARTIN, S. J. 2001. Executioner caspase-3, -6, and -7 perform distinct, non-redundant roles during the demolition phase of apoptosis. *Journal of Biological Chemistry,* 276**,** 7320-6.
SPARROW, J. R. & BOULTON, M. 2005. RPE lipofuscin and its role in retinal pathobiology. *Exp Eye Res,* 80**,** 595-606.
SPARROW, J. R. & CAI, B. 2001. Blue light-induced apoptosis of A2E-containing RPE: involvement of caspase-3 and protection by Bcl-2. *Invest Ophthalmol Vis Sci,* 42**,** 1356-62.
SPARROW, J. R., FISHKIN, N., ZHOU, J., CAI, B., JANG, Y. P., KRANE, S., ITAGAKI, Y. & NAKANISHI, K. 2003. A2E, a byproduct of the visual cycle. *Vision Res,* 43**,** 2983-90.
SPARROW, J. R., HICKS, D. & HAMEL, C. P. 2010. The retinal pigment epithelium in health and disease. *Curr Mol Med,* 10**,** 802-23.
SPRAUL, C. W., KAVEN, C., LANG, G. K. & LANG, G. E. 2004. Effect of growth factors on bovine retinal pigment epithelial cell migration and proliferation. *Ophthalmic Res,* 36**,** 166-71.
STALMANS, P. & HIMPENS, B. 1997. Effect of increasing glucose concentrations and protein phosphorylation on intercellular communication in cultured rat retinal pigment epithelial cells. *Invest Ophthalmol Vis Sci,* 38**,** 1598-609.
STEELE, F. R., CHADER, G. J., JOHNSON, L. V. & TOMBRAN-TINK, J. 1993. Pigment epithelium-derived factor: neurotrophic activity and identification as a member of the serine protease inhibitor gene family. *Proc Natl Acad Sci U S A,* 90**,** 1526-30.
STEINBERG, R. H., FISHER, S. K. & ANDERSON, D. H. 1980. Disc morphogenesis in vertebrate photoreceptors. *J Comp Neurol,* 190**,** 501-8.
STEINBERG, R. H., WOOD, I. & HOGAN, M. J. 1977. Pigment epithelial ensheathment and phagocytosis of extrafoveal cones in human retina. *Philos Trans R Soc Lond B Biol Sci,* 277**,** 459-74.
STEINMETZ, R. L., HAIMOVICI, R., JUBB, C., FITZKE, F. W. & BIRD, A. C. 1993. Symptomatic abnormalities of dark adaptation in patients with age-related Bruch's membrane change. *Br J Ophthalmol,* 77**,** 549-54.
STEVENSON, B. R., SILICIANO, J. D., MOOSEKER, M. S. & GOODENOUGH, D. A. 1986. Identification of ZO-1: a high molecular weight polypeptide associated with the tight junction (zonula occludens) in a variety of epithelia. *J Cell Biol,* 103**,** 755-66.
STONE, J., CAMPION, J. E. & LEICESTER, J. 1978a. The nasotemporal division of retina in the Siamese cat. *J Comp Neurol,* 180**,** 783-98.
STONE, J., ROWE, M. H. & CAMPION, J. E. 1978b. Retinal abnormalities in the Siamese cat. *J Comp Neurol,* 180**,** 773-82.
STRAUSS, O. 2005. The retinal pigment epithelium in visual function. *Physiol Rev,* 85**,** 845-81.
STREETEN, B. W. 1969. Development of the human retinal pigment epithelium and the posterior segment. *Arch Ophthalmol,* 81**,** 383-94.
STREIT, W. J., DUMOULIN, F. L., RAIVICH, G. & KREUTZBERG, G. W. 1989. Calcitonin gene-related peptide increases in rat facial motoneurons after peripheral nerve transection. *Neurosci Lett,* 101**,** 143-8.

STROEVA, O. G. & MITASHOV, V. I. 1983. Retinal pigment epithelium: proliferation and differentiation during development and regeneration. *Int Rev Cytol,* 83**,** 221-93.
STROEVA, O. G. & PANOVA, I. G. 1983. Retinal pigment epithelium: pattern of proliferative activity and its regulation by intraocular pressure in postnatal rats. *J Embryol Exp Morphol,* 75**,** 271-91.
SULIK, G. L., SOONG, H. K., CHANG, P. C., PARKINSON, W. C., ELNER, S. G. & ELNER, V. M. 1992. Effects of steady electric fields on human retinal pigment epithelial cell orientation and migration in culture. *Acta Ophthalmol (Copenh),* 70**,** 115-22.
SUMMERS, C. G. 1996. Vision in albinism. *Trans Am Ophthalmol Soc,* 94**,** 1095-155.
SUMMERS, C. G. 2009. Albinism: classification, clinical characteristics, and recent findings. *Optom Vis Sci,* 86**,** 659-62.
THOMPSON, D. A. & GAL, A. 2003. Vitamin A metabolism in the retinal pigment epithelium: genes, mutations, and diseases. *Prog Retin Eye Res,* 22**,** 683-703.
THORNBERRY, N. A. 1999. Caspases: a decade of death research. *Cell Death Differ,* 6**,** 1023-7.
THORNBERRY, N. A. & LAZEBNIK, Y. 1998. Caspases: enemies within. *Science,* 281**,** 1312-6.
TIBBER, M. S., BECKER, D. & JEFFERY, G. 2007. Levels of transient gap junctions between the retinal pigment epithelium and the neuroblastic retina are influenced by catecholamines and correlate with patterns of cell production. *J Comp Neurol,* 503**,** 128-34.
TIBBER, M. S., WHITMORE, A. V. & JEFFERY, G. 2006. Cell division and cleavage orientation in the developing retina are regulated by L-DOPA. *J Comp Neurol,* 496**,** 369-81.
TS'O, M. O. & FRIEDMAN, E. 1967. The retinal pigment epithelium. I. Comparative histology. *Arch Ophthalmol,* 78**,** 641-9.
TSOU, M. F. & STEARNS, T. 2006. Controlling centrosome number: licenses and blocks. *Curr Opin Cell Biol,* 18**,** 74-8.
TSUKITA, S., YAMAZAKI, Y., KATSUNO, T. & TAMURA, A. 2008. Tight junction-based epithelial microenvironment and cell proliferation. *Oncogene,* 27**,** 6930-8.
VAN SOEST, S. S., DE WIT, G. M., ESSING, A. H., TEN BRINK, J. B., KAMPHUIS, W., DE JONG, P. T. & BERGEN, A. A. 2007. Comparison of human retinal pigment epithelium gene expression in macula and periphery highlights potential topographic differences in Bruch's membrane. *Mol Vis,* 13**,** 1608-17.
VANEY, D. I. 1994. Patterns of Neuronal Coupling in the Retina. *Progress in Retinal and Eye Research,* 13**,** 301-355.
VARGA, Z. M., WEGNER, J. & WESTERFIELD, M. 1999. Anterior movement of ventral diencephalic precursors separates the primordial eye field in the neural plate and requires cyclops. *Development,* 126**,** 5533-46.
VARKONY, H., WEINSTEIN, V., KLINGER, E., STERLING, J., COOPERMAN, H., KOMLOSH, T., LADKANI, D. & SCHWARTZ, R. 2009. The glatiramoid class of immunomodulator drugs. *Expert Opin Pharmacother,* 10**,** 657-68.
VERSTRAETEN, T. C., BUZNEY, S. M., MACDONALD, S. G. & NEUFELD, A. H. 1990. Retinal pigment epithelium wound closure in vitro. Pharmacologic inhibition. *Invest Ophthalmol Vis Sci,* 31**,** 481-8.
VIDAL-SANZ, M., VILLEGAS-PEREZ, M. P., BRAY, G. M. & AGUAYO, A. J. 1988. Persistent retrograde labeling of adult rat retinal ganglion cells with the carbocyanine dye dil. *Exp Neurol,* 102**,** 92-101.
VON LEITHNER, P. L., CIURTIN, C. & JEFFERY, G. 2010. Microscopic mammalian retinal pigment epithelium lesions induce widespread proliferation with differences in magnitude between center and periphery. *Mol Vis,* 16**,** 570-81.
WANG, A. L., LUKAS, T. J., YUAN, M. & NEUFELD, A. H. 2008. Increased mitochondrial DNA damage and down-regulation of DNA repair enzymes in aged rodent retinal pigment epithelium and choroid. *Mol Vis,* 14**,** 644-51.

WANG, K. C., LEE, C. L., CHEN, S. Y., LIN, K. H. & TSAI, C. P. 2011. Glatiramer acetate could be a hypothetical therapeutic agent for neuromyelitis optica. *Med Hypotheses,* 76**,** 820-2.
WANG, Z., DILLON, J. & GAILLARD, E. R. 2006. Antioxidant properties of melanin in retinal pigment epithelial cells. *Photochem Photobiol,* 82**,** 474-9.
WASSELL, J., DAVIES, S., BARDSLEY, W. & BOULTON, M. 1999. The photoreactivity of the retinal age pigment lipofuscin. *J Biol Chem,* 274**,** 23828-32.
WATZKE, R. C., SOLDEVILLA, J. D. & TRUNE, D. R. 1993. Morphometric analysis of human retinal pigment epithelium: correlation with age and location. *Curr Eye Res,* 12**,** 133-42.
WEALE, R. A. 1975. Senile changes in visual acuity. *Trans Ophthalmol Soc U K,* 95**,** 36-8.
WEBSTER, M. J. & ROWE, M. H. 1991. Disruption of developmental timing in the albino rat retina. *J Comp Neurol,* 307**,** 460-74.
WEITER, J. J., DELORI, F. C., WING, G. L. & FITCH, K. A. 1986. Retinal pigment epithelial lipofuscin and melanin and choroidal melanin in human eyes. *Invest Ophthalmol Vis Sci,* 27**,** 145-52.
WERNER, J. S. 2005. Night vision in the elderly: consequences for seeing through a "blue filtering" intraocular lens. *Br J Ophthalmol,* 89**,** 1518-21.
WESTENSKOW, P., PICCOLO, S. & FUHRMANN, S. 2009. Beta-catenin controls differentiation of the retinal pigment epithelium in the mouse optic cup by regulating Mitf and Otx2 expression. *Development,* 136**,** 2505-10.
WILLOTT, E., BALDA, M. S., FANNING, A. S., JAMESON, B., VAN ITALLIE, C. & ANDERSON, J. M. 1993. The tight junction protein ZO-1 is homologous to the Drosophila discs-large tumor suppressor protein of septate junctions. *Proc Natl Acad Sci U S A,* 90**,** 7834-8.
WIMMERS, S., KARL, M. O. & STRAUSS, O. 2007. Ion channels in the RPE. *Prog Retin Eye Res,* 26**,** 263-301.
WINEY, M. 1999. Cell cycle: driving the centrosome cycle. *Curr Biol,* 9**,** R449-52.
WING, G. L., BLANCHARD, G. C. & WEITER, J. J. 1978. The topography and age relationship of lipofuscin concentration in the retinal pigment epithelium. *Invest Ophthalmol Vis Sci,* 17**,** 601-7.
WINKLER, B. S. 2008. An hypothesis to account for the renewal of outer segments in rod and cone photoreceptor cells: renewal as a surrogate antioxidant. *Invest Ophthalmol Vis Sci,* 49**,** 3259-61.
WITMER, A. N., VRENSEN, G. F., VAN NOORDEN, C. J. & SCHLINGEMANN, R. O. 2003. Vascular endothelial growth factors and angiogenesis in eye disease. *Prog Retin Eye Res,* 22**,** 1-29.
WOJTOWICZ, J. M. & KEE, N. 2006. BrdU assay for neurogenesis in rodents. *Nat Protoc,* 1**,** 1399-405.
WU, Z., HASAN, A., LIU, T., TELLER, D. C. & CRABB, J. W. 2004. Identification of CRALBP ligand interactions by photoaffinity labeling, hydrogen/deuterium exchange, and structural modeling. *Journal of Biological Chemistry,* 279**,** 27357-64.
YANG, Y. & HERRUP, K. 2007. Cell division in the CNS: protective response or lethal event in post-mitotic neurons? *Biochim Biophys Acta,* 1772**,** 457-66.
YAU, K. W. 1994. Phototransduction mechanism in retinal rods and cones. The Friedenwald Lecture. *Invest Ophthalmol Vis Sci,* 35**,** 9-32.
YOU, X., ZHENG, X., BERGMANSON, J., AQUAVELLA, J. V., MACKENZIE, I., DEPAOLIS, M. & BOLTZ, R. 1993. Corneal Response and Recovery to Photorefractive Keratectomy in Rabbits. *Investigative Ophthalmology & Visual Science,* 34**,** 801-801.
YOUNG, R. W. 1983. The ninth Frederick H. Verhoeff lecture. The life history of retinal cells. *Trans Am Ophthalmol Soc,* 81**,** 193-228.
ZAHN, J. M., POOSALA, S., OWEN, A. B., INGRAM, D. K., LUSTIG, A., CARTER, A., WEERARATNA, A. T., TAUB, D. D., GOROSPE, M., MAZAN-MAMCZARZ, K., LAKATTA, E. G., BOHELER, K. R., XU, X., MATTSON, M. P., FALCO, G., KO, M. S., SCHLESSINGER, D., FIRMAN, J., KUMMERFELD, S.

K., WOOD, W. H., 3RD, ZONDERMAN, A. B., KIM, S. K. & BECKER, K. G. 2007. AGEMAP: a gene expression database for aging in mice. *PLoS Genet,* 3**,** e201.

ZAREBA, M., BOBER, A., KORYTOWSKI, W., ZECCA, L. & SARNA, T. 1995. The effect of a synthetic neuromelanin on yield of free hydroxyl radicals generated in model systems. *Biochim Biophys Acta,* 1271**,** 343-8.

ZHAO, M., SONG, B., PU, J., WADA, T., REID, B., TAI, G., WANG, F., GUO, A., WALCZYSKO, P., GU, Y., SASAKI, T., SUZUKI, A., FORRESTER, J. V., BOURNE, H. R., DEVREOTES, P. N., MCCAIG, C. D. & PENNINGER, J. M. 2006. Electrical signals control wound healing through phosphatidylinositol-3-OH kinase-gamma and PTEN. *Nature,* 442**,** 457-60.

ZHENG, T. S. & FLAVELL, R. A. 2000. Divinations and surprises: genetic analysis of caspase function in mice. *Exp Cell Res,* 256**,** 67-73.

References from websites:

WEBVISION http://webvision.med.utah.edu/